



Universidad  
de Alcalá

**Programa de Doctorado en Química**

**Innovative miniaturized  
electroanalytical approaches  
for the analysis of clinically  
relevant glycoproteins**

**Tesis Doctoral**

**Tania Sierra Gómez**

**Directores:**

Dr. Agustín González Crevillén

Dr. Jesús Alberto Escarpa Miguel

Alcalá de Henares, Julio 2021









## Agradecimientos / Acknowledgments

Qué difícil resulta condensar cuatro años de tu vida en apenas unas palabras. Y qué difícil es mostrar lo agradecida que estoy con todos aquellos que han contribuido, de una manera u otra, a que hoy esté tan cerca de terminar esta etapa. Aun así, intentaré expresar con palabras mi gratitud hacia todas aquellas personas e instituciones, que me han brindado orientación, ayuda y apoyo durante estos años.

En primer lugar, me gustaría agradecer a la Universidad de Alcalá y a todas y cada una de las personas que forman parte de ella. Llevo diez años siendo parte de su equipo; primero como estudiante de Grado, después como estudiante de Máster, y, por último, como doctoranda con un contrato de Formación de Personal Investigador de su programa propio. Además, me ha ayudado a completar mi formación con su programa para la financiación de estancias de investigación en el extranjero. Me han formado como científica y como persona, y no puedo estar más agradecida.

En segundo lugar, me gustaría agradecer a Alberto Escarpa y Agustín González, mis directores de Tesis y los principales responsables de que esta Tesis haya salido adelante. Alberto, nunca olvidaré cómo cuando todavía era una estudiante, me mencionaste la idea del doctorado y me diste la oportunidad de formar parte en tu increíble grupo de investigación. Gracias por la oportunidad, por la confianza, por el ánimo, por mostrarme que la tenacidad da sus frutos y que siempre hay que dar lo mejor de uno mismo. Agustín, creo que hemos hecho el tándem perfecto y sería imposible imaginarme estos años sin ti como director. Gracias por los ánimos constantes, por la ayuda y el apoyo. Gracias a ambos por todo lo que me habéis enseñado.

Agradecer también a la Prof. Cristina González por sus consejos y ánimos, y al Prof. Miguel Ángel López por su buen humor siempre.

## Acknowledgments

---

*Finally, thank you to Professor Charles Henry for giving me the opportunity to join his amazing group in my research stay in Colorado State University and making me feel comfortable and integrated into his group. I learned so much at the professional and personal level.*

Me gustaría agradecer a la Dr. Celia Pérez-Cerdá por su ayuda desinteresada con las muestras reales.

Mary Shelley escribió: “Quien no haya experimentado la irresistible atracción de la ciencia, no podrá comprender su tiranía”. Y no sabe cuán cierto era. No todos son buenos momentos, no todo es exitoso y no todo es de color rosa. Sin embargo, la clave es quién está a tu lado cuando el barco empieza a tambalearse. Y yo he tenido la inmensa suerte de trabajar durante estos años en el 2L2, y parecerá una tontería, pero ir a trabajar con una sonrisa, te hace las cosas más fáciles. No tengo suficientes palabras para expresar lo que os quiero. Gracias a todos y cada uno de mis compañeros de MINYNANOTECH.

Laura, compañera de gym, fuiste la primera persona que conocí en el laboratorio (¡cuánto tiempo ya eh!), siempre contenta y con una sonrisa. Siempre dispuesta a ayudar y a echarme una mano. Águeda, qué decir de mi compañera de trastadas. Posiblemente una de las tías más inteligentes que pueda conocer en mi vida. Sobrevivirás y brillarás sin ayuda de nadie, hazme caso. Roberto, gracias por las risas, por los buenos momentos y por siempre estar ahí. MariMore, ha sido un placer compartir estos años contigo. Gracias por la ayuda prestada en muchos momentos. Marta, “you are my person”, qué hubiera sido de mí, sin ti a mi lado. Empezamos y terminamos juntas, y el camino ha sido maravilloso. Víctor, llegaste para encajar en el grupo, aunque te dejáramos encerrado en el primer viaje. Eres genial y ha sido un placer compartir laboratorio contigo. Silvia, Silvia, no hago carrera contigo. Sí me hubieran preguntado a quién quería para compartir directores, creo que te hubiera descrito a ti, aun sin conocerte. Siempre contenta, siempre amable, trabajadora y siempre dispuesta a ayudar. Muchas gracias por la ayuda experimental prestada, el karma te debe mucho. Y como me voy a olvidar de mi *lisiada* favorita, Anabela. Qué placer fue compartir con vos esos seis meses. Juanfran y Dani (yo os pongo en pack aquí). Ha sido un lujo compartir tiempo con vosotros, en el lab y fuera de él.

Javi, Carmen y José, sois la nueva generación y además se os ve majos. Continudad con el espíritu del 2L2, os mejorará la vida.

Agradecer también a Beatriz, Juan Víctor e Irene porque siempre han sido muy agradables conmigo y ha sido un placer coincidir con vosotros.

Gracias a tantas otras personas que han pasado por el laboratorio y con quien he compartido muchas experiencias: Carlos (que es uno más de nuestro grupo), Kaisong, Karsten, Flavio, Katharina, Pepe...

Gracias también a mis compis de los laboratorios vecinos, ha sido un placer compartir comidas, quedadas y risas con vosotros (los que estáis ahora y los que ya os habéis marchado). ¡Gracias de verdad!

*Thanks to the people I met during my stay in Fort Collins. It was a difficult time away from home and a pandemic in between, but I felt very integrated into Chuck's group. Special thanks to Eka and Ilhoon, for their scientific help. Also thank Ana, Isabelle, Juanvi and Leah for the group of half-Spanish that we had there. Thanks guys for the moments and the trips.*

Gracias a mis Chicas C por su apoyo y sus momentos divertidos, porque si no, no seríamos nosotras. Ana, pocas cosas más que decirte. Sé que siempre te voy a tener a mi lado, para lo bueno y para lo malo. Sabes que más que amiga, eres familia. Mireia, que ejemplo has sido siempre para mí. ¡Qué grande eres! Mónica, sobre todo en este último tiempo hemos compartido las frustraciones que tiene la tesis, y siempre he podido contar con tu apoyo y tus palabras de ánimo, espero haberte devuelto esto, aunque fuese sólo un poquito. Rocío, ha sido un placer que continuáramos juntas más allá de la carrera y que compartiéramos laboratorio y momentos vividos. Paula, aunque las dos seamos muy despegadas, sabemos que siempre podremos contar con la otra.

Nunca me podría olvidar de mis *quejistas* favoritas: Leyre, Sara y Alejandra. ¿“Cualquier tiempo pasado siempre fue mejor”?, no sé si será verdad, pero me siento muy contenta y afortunada de seguir creciendo y superando etapas a vuestro lado.



## **Acknowledgments**

---

Por último, quiero agradecer a mi familia. Del primero al último, porque son los mejores. Porque sé que se sienten orgullosos de mí, pero lo que no saben es lo orgullosa que yo me siento de ellos. Gracias especialmente a mi hermano Sergio y a mis padres, Miguel y M<sup>a</sup> Carmen, porque soy lo soy, gracias a ellos.





**“Son los problemas sin resolver, no los resueltos, los que  
mantienen activa la mente”**

**Erwin Guido Kolbenheyer**

**“Be the change you want to see in the world”**

**Mahatma Gandhi**



## Resumen

La búsqueda de nuevos biomarcadores clínicos resulta de extraordinario interés para la comunidad científica, lo que ha generado el desarrollo de nuevas aproximaciones analíticas capaces de identificar, detectar y monitorizar estos biomarcadores que, en muchos casos, están asociados a enfermedades autoinmunes, inflamatorias o cáncer. En muchas de estas enfermedades, un diagnóstico precoz y la posibilidad de iniciar una terapia apropiada en un corto periodo de tiempo resultan esenciales, mejorándose el pronóstico de los pacientes.

Las modificaciones postraduccionales (PTMs), entre las cuales se encuentran procesos tan importantes como la glicosilación, fosforilación o la acetilación, son modificaciones o alteraciones químicas reversibles o irreversibles que se dan en la cadena peptídica de las proteínas eucariotas durante o después de su traducción. Estas modificaciones pueden incrementar la especificidad de biomarcadores existentes o permitir el descubrimiento de nuevos biomarcadores con gran precisión hacia determinadas enfermedades, debido a que estas modificaciones juegan un papel trascendental en procesos biológicos, tales como respuestas inmunes, regulación del plegado adecuado de proteínas o procesos inflamatorios.

Entre estas PTMs, cobra especial interés la glicosilación, la cual, a pesar de no ser la modificación más abundante, sí es una de las más importantes. Estas proteínas glicosiladas representan más del 70 % de las proteínas presentes en los seres humanos, y se encuentran en casi todos los tejidos y fluidos de animales, plantas y microorganismos. Hay una gran cantidad de ejemplos de glicoproteínas en la naturaleza; incluyendo hormonas, anticuerpos, determinadas enzimas, proteínas plasmáticas en la sangre o factores de crecimiento.

Entre las funciones que presentan estas macromoléculas se encuentran procesos tan variados como el reconocimiento intercelular, debido a que muchos receptores en la superficie celular son capaces de reconocer secuencias específicas de oligosacáridos, y el reconocimiento de patógenos, ya que muchos de ellos presentan glicoproteínas en su superficie que les

permiten adherirse a la pared celular de las células parasitadas. Además, se ha comprobado que alteraciones del perfil de glicosilación a menudo se asocian con diversas enfermedades, incluyendo el cáncer, la artritis reumatoide u otros tipos de alteraciones inflamatorias.

Todo ello abre la posibilidad de utilizar estas proteínas como biomarcadores para el diagnóstico, pronóstico y seguimiento de enfermedades, así como dianas terapéuticas para el diseño de métodos de diagnóstico, en terapias de próxima generación e incluso para el diseño de vacunas.

En consecuencia, resulta pertinente el desarrollo de nuevas herramientas analíticas que permitan la determinación de glicoproteínas. En muchos casos, se debe llevar a cabo el análisis de la concentración total de una glicoproteína, como ocurre con la  $\alpha_1$ -ácido glicoproteína (AGP) durante procesos inflamatorios. En otros casos, es el perfil de glicofomas el que sufre modificaciones durante un estado patológico o defecto genético. Así, por ejemplo, las glicofomas con menos cantidad de glicanos en la transferrina (Tf) se incrementan respecto a la glicofoma principal, denominándose a este biomarcador transferrina deficiente en carbohidratos (CDT), siendo uno de los principales biomarcadores de los defectos congénitos de la glicosilación (CDG). Estos son un grupo de enfermedades genéticas de rara prevalencia, que se deben a defectos en la síntesis de glicoproteínas.

Por todo ello, y debido al enorme interés que estas macromoléculas han despertado en el campo científico, muchas técnicas analíticas se han utilizado para el análisis de glicoproteínas, tales como la cromatografía líquida (LC), la electroforesis capilar (CE) y la espectrometría de masas (MS). Además, la determinación de las glicoproteínas se puede llevar a cabo mediante inmunoensayos enzimáticos o usando lectinas como agentes de reconocimiento molecular.

Sin embargo, las técnicas anteriormente citadas, consumen mucho tiempo y/o son costosas. En general, estas aproximaciones requieren equipos sofisticados, personal con formación previa, tiempos de análisis largos, grandes volúmenes de muestra y reactivos costosos, lo que limita o

dificulta su uso para el análisis rutinario en la determinación de estos biomarcadores. Además, actualmente, los sistemas de salud están demandando dispositivos analíticos sencillos y eficaces para la determinación de estos biomarcadores en el punto de necesidad o, en su caso, de atención al paciente. Estas aproximaciones analíticas innovadoras se denominan pruebas o ensayos en el punto de atención (POCT) y proporcionan información diagnóstica fiable en un corto periodo de tiempo, lo que permite la toma de decisiones más rápidas y mejor (in)formadas para el diagnóstico y tratamiento de enfermedades.

En este sentido y dentro del marco de la Química Analítica contemporánea, los sensores electroquímicos serigrafiados y las plataformas microfluídicas con detección electroquímica, constituyen excelentes herramientas analíticas que cumplen con los requerimientos de selectividad, sensibilidad y miniaturización inherente exigibles para el desarrollo de tecnología analítica tipo POCT.

Por una parte, los sensores electroquímicos serigrafiados presentan un enfoque exitoso para el desarrollo de dispositivos de bajo coste. Además, esta tecnología permite reducir los volúmenes de muestra requeridos para cada análisis y (bio)-funcionalizar la superficie con diferentes (nano)-materiales que permiten mejorar la sensibilidad, la selectividad y la reproducibilidad de los análisis.

Por otra parte, las plataformas microfluídicas permiten integrar en un solo dispositivo miniaturizado todas las etapas (bio)-analíticas necesarias para llevar a cabo una prueba de diagnóstico mediante un control preciso de los fluidos en la microescala. En estos sistemas, la detección electroquímica constituye una valiosa herramienta, debido a su inherente miniaturización y su alta compatibilidad con las técnicas de micro y nano fabricación requeridas en el desarrollo de los mencionados sistemas microfluídicos y sensóricos, sin detrimento de su sensibilidad.

Por todo ello, el objetivo principal de esta Tesis Doctoral ha sido el diseño y el desarrollo de nuevas herramientas y estrategias analíticas electroquímicas (ultra)-miniaturizadas basadas en sensores serigrafiados y en sistemas microfluídicos para la determinación de biomarcadores



glicoproteicos (AGP y Tf) en muestras clínicas relevantes para el diagnóstico de enfermedades.

Este objetivo central, la selección y la definición de los objetivos y de los hitos específicos de esta Tesis Doctoral, se recogen en el **Capítulo I**. En este capítulo, también se recoge la Hipótesis de partida. En efecto, el diseño de esta Tesis Doctoral tiene como punto de partida la propuesta pertinente del desarrollo de herramientas electroquímicas (ultra)-miniaturizadas que permitieran la determinación rápida, *in situ*, y de bajo coste de glicoproteínas como biomarcadores de enfermedades relevantes. Todo ello para avanzar hacia la descentralización del análisis clínico con la consecuente reducción del tiempo entre la toma de muestra y la obtención de los resultados analíticos, buscado la generación de diagnósticos más rápidos sin pérdida de fiabilidad.

En el **Capítulo II**, en primer lugar, se discute el desafío que supone la búsqueda de biomarcadores glicoproteicos, así como la necesidad del desarrollo de nuevos dispositivos POCT en este ámbito. A continuación, se introducen y describen las complejidades relacionadas con la detección electroquímica en el campo de las glicoproteínas. Finalmente, se describen las tecnologías utilizadas en esta Tesis Doctoral para el desarrollo de POCT: sensores electroquímicos serigrafiados y plataformas microfluídicas electroquímicas.

Los resultados obtenidos en esta Tesis Doctoral se presentan y se discuten en los siguientes tres capítulos (**Capítulos III-V**).

En el **Capítulo III**, se recogen los resultados obtenidos durante el diseño y desarrollo de aproximaciones electroanalíticas basadas en la construcción de sensores electroquímicos de base serigrafiada para la detección de los dos biomarcadores glicoproteicos de alta relevancia clínica seleccionados e indicados con anterioridad: AGP y Tf.

Como primera aproximación, se desarrolló un sensor electroquímico basado en electrodos serigrafiados de carbono (SPCE) para la determinación total de AGP en muestras de suero. La metodología incluyó la precipitación ácida selectiva del resto de proteínas para lograr una determinación sensible, precisa y fiable en una muestra de suero comercial.

En este caso, la detección electroquímica se llevó a cabo mediante el marcaje de la glicoproteína con un complejo de osmio (VI), el cual se unió a los grupos dioles de los sacáridos presentes en la glicoproteína, formando un éster que produjo dos señales electroquímicas. El límite de detección obtenido ( $1.6 \text{ mg L}^{-1}$ ) fue adecuado para la determinación de AGP en las muestras ensayadas. Sin embargo, el elevado tiempo invertido en el proceso de marcaje ( $t = 16 \text{ h}$ ), impidió, conceptualmente, su implementación como POCT.

En aras de paliar este inconveniente, en una segunda aproximación, se llevó a cabo el marcaje de esta glicoproteína usando una aproximación química basada en un intercambio de ligandos, consiguiéndose reducir drásticamente el tiempo necesario en el proceso de marcaje a 15 min. Además, se emplearon nanomateriales de carbono para mejorar la sensibilidad y, en mayor medida, reducir el ensuciamiento y la pasivación de la superficie del electrodo. Estos electrodos fueron fabricados mediante la filtración del nanomaterial sobre un filtro de Teflón, con los diseños y geometrías adecuados para su empleo como transductores electroquímicos. Los transductores de nanotubos de carbono de pared múltiple fueron los que exhibieron las mejores características analíticas con un límite de detección mejorado en comparación con la aproximación analítica anterior ( $\text{LOD} = 0.6 \text{ mg L}^{-1}$ ).

Seguidamente, se desarrolló un sensor electroquímico serigrafado de carbono para la determinación de CDT, un biomarcador, como se ha indicado anteriormente, de una enfermedad rara denominada CDG. La CDT se basa en un cambio en la concentración a la que se encuentra cada una de las glicofomas de la Tf. Así cuando el estado patológico aparece, las formas con menos glicanos de la Tf ven incrementadas su porcentaje, mientras que la glicofoma mayoritaria ve reducida su presencia. En esta aproximación y aprovechando que la glicoproteína presenta dos señales electroquímicas sobre carbono; una debida al osmio unido a sus carbohidratos, y otra debida a los aminoácidos presentes en su estructura, se utilizó la relación existente entre ambas (señal carbohidratos/señal proteína) como indicador del grado de glicosilación. Este nuevo parámetro se denominó índice electroquímico de la glicosilación (EIG) y mostró una excelente correlación con el

parámetro oficial de medida del % CDT. Con esta nueva aproximación se determinó el nivel de CDT en muestras de suero, obteniéndose diferencias significativas entre muestras de enfermos de CDG y de sanos.

En aras de avanzar hacia el desarrollo de POCTs que cumplieran con las prestaciones requeridas de miniaturización, portabilidad, sencillez y fiabilidad para el diagnóstico y monitorización de enfermedades, en el **Capítulo IV** se exploraron nuevas herramientas analíticas basadas en dispositivos microfluídicos de separación, en concreto, microchips de electroforesis (ME) con detección electroquímica (ED), para la determinación simultánea de las glicoproteínas estudiadas anteriormente: AGP y Tf. Debido a la baja sensibilidad que en muchos casos presentan para su detección electroquímica directa, estas fueron marcadas, también como se ha indicado anteriormente, por un complejo de osmio (VI), incrementando de esta manera la señal electroquímica. Además, el potencial de oxidación obtenido para la glicoproteína marcada con el complejo de osmio a +0.50 V, permitió la medida analítica selectiva de las de las glicoproteínas, evitando interferencias del resto de las proteínas. El método se aplicó al análisis de un material de referencia certificado, obteniéndose una excelente exactitud ( $E_r \leq 4 \%$ ) y una separación de las dos glicoproteínas en menos de 400 s.

En el **Capítulo V** se presenta una aproximación microfluídica electroquímica más disruptiva, en la cual, el dispositivo se diseñó y fabricó utilizando materiales poliméricos de bajo coste, para llevar a cabo de forma integrada tanto el marcaje de las glicoproteínas con el complejo de osmio (VI) como la detección electroquímica de estas en el mismo dispositivo. En estos dispositivos microfluídicos accionados por capilaridad, también llamados métodos microfluídicos de control pasivo, en lugar de utilizar una bomba externa para inducir el flujo, como ocurre en los métodos de control activo, se utiliza la tensión superficial de un fluido que actúa sobre la pared del canal (o fibras en el caso del papel) para la generación del flujo.

En los trabajos presentados en este capítulo de la Tesis Doctoral, los dispositivos se fabricaron utilizando un adhesivo de doble cara y capas transparentes de plástico. Dichos materiales fueron alternativamente

apilados formando canales de varias capas. Esta nueva aproximación permitió diseñar y desarrollar un sistema microfluídico electroquímico donde se integraron las etapas analíticas requeridas para la determinación de las glicoproteínas estudiadas en esta Tesis Doctoral (AGP y Tf).

Ambas aproximaciones basadas en el empleo de sistemas microfluídicos como herramientas analíticas (ME y dispositivos accionados por capilaridad, abordadas en los capítulos IV y V, respectivamente), permitieron avanzar en las prestaciones analíticas requeridas para el desarrollo futuro de dispositivos tipo POCT.

Por último, aunque las conclusiones obtenidas se han ido recogiendo específicamente en cada uno de los artículos científicos que configuran los capítulos de esta Tesis Doctoral, se ha creído conveniente recopilar las conclusiones generales en el **Capítulo VI**.

No obstante, y a modo de conclusión general, durante la Tesis Doctoral se desarrollaron exitosamente diferentes aproximaciones analíticas dirigidas y compatibles con el desarrollo de sistemas de diagnóstico de nueva generación tipo POCT. Estas aproximaciones se abordaron a través del diseño y el desarrollo de una sensorica electroquímica (ultra)-miniaturizada, tanto serigrafiada como microfluídica, para la detección y determinación fiables de dos glicoproteínas de elevada relevancia clínica: AGP y Tf. Estas nuevas aproximaciones constituyen por sí mismas una excelente alternativa de mejora a los métodos de rutina llevados a cabo en los laboratorios clínicos para el análisis de estos biomarcadores, no sólo en términos de sensibilidad, fiabilidad y simplicidad, sino también en lo que se refiere a las ventajas que comporta en el ámbito clínico la disminución del consumo de reactivos y muestras, tiempos de análisis y costes, todo ello conducente a un diagnóstico mejorado.

Asimismo, un valor añadido y de conjunto que aportan los resultados obtenidos en esta Tesis Doctoral puede descansar en el avance conseguido hacia la descentralización y la simplificación de los análisis que supondría la implementación de estas tecnologías tipo POCT; estableciéndose estas como herramientas analíticas innovadoras y prometedoras en los ámbitos del diagnóstico y del seguimiento clínico.



# Summary

The research of new clinical biomarkers is of relevant interest to the scientific community, which has generated the development of new analytical approaches capable of identifying, detecting and monitoring these biomarkers, which, in many cases, are associated with autoimmune, inflammatory diseases or cancer. In many of these diseases, an early diagnosis, and the possibility of initiating an appropriate therapy in a short period of time would be essential, improving the prognosis of the patients.

Post-translational modifications (PTMs), among which are important processes such as glycosylation, phosphorylation, or acetylation, are reversible or irreversible chemical modifications or alterations that occur in the peptide chain of eukaryotic proteins during or after their translation. These modifications can increase the specificity of existing biomarkers or allow the discovery of new biomarkers with great precision towards certain diseases, because these modifications play a transcendental role in biological processes, such as immune responses, regulation of the proper folding of proteins or inflammatory processes.

Among these PTMs, glycosylation is of particular interest, which, despite not being the most abundant modification, is one of the most important. These glycosylated proteins represent more than 70 % of the proteins present in humans and are found in almost all tissues and fluids of animals, plants, and microorganisms. There are many examples of glycoproteins in nature, including hormones, antibodies, certain enzymes, plasma proteins in the blood or growth factors.

Among the functions that these macromolecules present are processes as variable as intercellular recognition, due to the fact that many receptors on the cell surface are capable of recognizing specific oligosaccharide sequences, and the recognition of pathogens, since many of them present glycoproteins in their surface that allow them to adhere to the cell wall of the parasitized cells. In addition, it has been found that alterations in the

## Summary

---

glycosylation profile are often associated with various diseases, including cancer, rheumatoid arthritis, or other types of inflammation disorders.

All this opens the possibility of using these proteins not only as biomarkers for the diagnosis, prognosis, and monitoring of diseases, but also as therapeutic targets for the design of diagnostic methods, next generation therapies and even for the design of vaccines.

Consequently, the development of new analytical tools that allow the determination of glycoprotein biomarkers is relevant. In many cases, analysis of the total concentration of a glycoprotein must be carried out, as is the case with  $\alpha_1$ -acid glycoprotein (AGP) during inflammatory processes. In other cases, it is the glycoform profile that undergoes modifications during a pathological state or genetic defect. Thus, for example, glycoforms with less amount of glycans in transferrin (Tf) are increased with respect to the main glycoform, calling this biomarker carbohydrate deficient transferrin (CDT), being one of the main biomarkers of congenital disorders of glycosylation (CDG), which are a group of diseases, of rare prevalence, that are due to defects in the synthesis of glycoproteins.

Therefore, and due to the enormous interest, that these macromolecules have aroused in the scientific field, many analytical techniques have been used for the analysis of glycoproteins such as liquid chromatography (LC), capillary electrophoresis (CE) and mass spectrometry (MS). Furthermore, the determination of glycoproteins can be carried out by enzyme immunoassays or by using lectins as molecular recognition agents.

However, the aforementioned techniques are time consuming and/or expensive. In general, these approaches require sophisticated equipment, trained personnel, long analysis times, large sample volumes, and expensive reagents, which limits or hinders their use for routine analysis of these biomarkers. In addition, currently, health systems are demanding simple and efficient analytical devices for the determination of these biomarkers at the point of need or, where appropriate, patient care. These innovative analytical approaches are called point-of-care tests or assays (POCTs), and they provide reliable diagnostic information in a short period of time,

allowing for faster and better (in)formed decisions for diagnosis and treatment of diseases.

In this sense, and within the framework of contemporary Analytical Chemistry, electrochemical sensors screen-printed based and microfluidics platforms with electrochemical detection constitute excellent analytical tools that meet these selectivity, sensitivity, and inherent miniaturization requirements required for the development of POCT devices.

On one hand, electrochemical sensors screen-printed based present a successful approach to developing low-cost devices. In addition, this technology allows to reduce the sample volumes required for each analysis and (bio)-functionalize the surface with different (nano)-materials that allow to improve the sensitivity, the selectivity, and the reproducibility of the analysis.

On the other hand, microfluidics platforms make it possible to integrate in a single miniaturized device all the (bio)-analytical stages necessary to carry out a diagnostic test through precise control of fluids at the microscale. In these systems, electrochemical detection constitutes a valuable tool, due to its inherent miniaturization and its high compatibility with the micro and nano fabrication techniques required in the development of the aforementioned microfluidic and sensory systems, without detriment to its sensitivity.

Therefore, the main objective of this Doctoral Thesis has been the design and development of new electrochemical (ultra)-miniaturized analytical tools and strategies (electrochemical sensors screen-printed based and microfluidics systems) for the determination of glycoprotein biomarkers (AGP and Tf) in relevant clinical samples for the diagnosis of diseases.

This central objective, the selection and definition of the objectives and specific milestones of this Doctoral Thesis, are included in **Chapter I**. In this chapter, the starting hypothesis is also included. Indeed, the design of this Doctoral Thesis has as its starting point the pertinent proposal and the development of (ultra)-miniaturized electrochemical tools that allow the rapid, in situ, and low-cost determination of glycoproteins as biomarkers of relevant diseases. All this to advance towards the decentralization of the



clinical analysis with the consequent reduction of the time between taking the sample and obtaining the analytical results, seeking the generation of faster diagnoses without loss of reliability.

In **Chapter II**, in the first place, the challenge posed by the search for glycoprotein biomarkers is discussed, as well as the need for the development of new POCT devices in this area. In the following, the complexities related to electrochemical detection in the field of glycoproteins are introduced and described. Finally, the technologies used in this Doctoral Thesis for the development of POCT (electrochemical sensors screen-printed based and electrochemical microfluidics platforms) are described.

The results obtained in this Doctoral Thesis are presented and discussed in the following three chapters (**Chapters III-V**).

In **Chapter III**, the results obtained during the design and development of electroanalytical approaches based in the construction of electrochemical sensors for the detection of the two glycoprotein biomarkers of high clinical relevance selected and indicated above are collected: AGP and Tf.

As a first approach, an electrochemical sensor based on screen-printed carbon electrodes (SPCE) was developed for the total determination of AGP in serum samples. The methodology included the selective acid precipitation of the rest of the proteins to achieve a sensitive, precise, and reliable determination in a commercial serum sample. In this case, the electrochemical detection was performed by labeling the glycoprotein with an osmium (VI) complex, which labeled the diol groups of the saccharides present in the glycoprotein, forming an ester that produced two electrochemical signals. The limit of detection obtained ( $1.6 \text{ mg L}^{-1}$ ) was adequate for the determination of AGP in the samples tested. However, the high time invested in the labeling process ( $t = 16 \text{ h}$ ), conceptually prevented its implementation as POCT.

In order to solve this drawback, in a second approach, the glycoprotein labeling was carried out using a chemical approach based on a ligand exchange, achieving a drastic reduction of the time required in the marking process to 15 min. In addition, carbon nanomaterials were used to improve

sensitivity and further reduce fouling and passivation of the electrode surface. These electrodes were manufactured by filtering the nanomaterial on a Teflon filter with suitable designs and geometries for use as electrochemical transducers. Multi-walled carbon nanotube transducers exhibited the best analytical characteristics with an improved detection limit compared to the previous analytical approach (LOD = 0.6 mg L<sup>-1</sup>).

Next, an electrochemical sensor screen-printed based was developed for the determination of CDT, a biomarker, as indicated above, of a rare disease called CDG. The CDT is based on a change in the concentration at which each of the Tf glycoforms is found. Thus, when the pathological state appears, the forms with less glycans of Tf see their percentage increased, while the majority glycoform sees its presence reduced. In this approach and taking advantage of the fact that the glycoprotein presents two electrochemical signals on carbon; one due to the osmium attached to its carbohydrates, and the other due to the amino acids present in its structure, the relationship between both (carbohydrate signal/protein signal) was used as an indicator of the degree of glycosylation. This new parameter was called electrochemical index of glycosylation (EIG) and it showed an excellent correlation with the official measurement parameter % CDT. With this new approach, the level of CDT present in serum samples was determined, obtaining significant differences between samples of CDG patients and healthy ones.

In order to advance towards the development of POCTs that meet the required features of miniaturization, portability, simplicity, and reliability for the diagnosis and monitoring of diseases, in **Chapter IV** new analytical tools based on microfluidics separation devices were explored, specifically, microchips electrophoresis (ME) with electrochemical detection (ED), for the simultaneous determination of the previously studied glycoproteins: AGP and Tf. Due to the low sensitivity that in many cases they present for their direct electrochemical detection, they were labeled, also as previously indicated, by an osmium (VI) complex, thus increasing the electrochemical signal. Furthermore, the oxidation potential obtained for the glycoprotein labeled with the osmium complex at +0.50 V, allowed the selective analytical measurement of those of the glycoproteins, avoiding interference

from the rest of the proteins. The method was applied to the analysis of a certified reference material, obtaining excellent accuracy ( $E_r \leq 4\%$ ) and a separation of the two glycoproteins in less than 400 s.

In **Chapter V**, a more disruptive electrochemical microfluidic approach is presented, in which the device was designed and manufactured using low-cost polymeric materials to carry out the labeling of glycoproteins with the osmium (VI) complex as the electrochemical detection of these in the same device. In these capillary-driven microfluidics devices, also called passive control microfluidics methods, instead of using an external pump to induce flow as in active control methods, the surface tension of a fluid acting on the wall of the tube is used (or fibers in the case of paper) to drive flow.

In the papers presented in this chapter of the Doctoral Thesis, the devices were manufactured using double-sided adhesive and transparent plastic layers. Both materials were alternately stacked forming multi-layered channels. This new approach allowed the design and development of an electrochemical microfluidic system where the analytical stages required for the determination of the glycoproteins studied in this Doctoral Thesis (AGP and Tf) were integrated.

Both approaches based on the use of microfluidics systems as analytical tools (ME and capillary-driven electrochemical microfluidics devices, discussed in Chapters IV and V, respectively), allowed progress in the analytical performance required for the future development of POCT devices.

Finally, although the obtained conclusions have been specifically collected in each of the scientific articles that make up the chapters of this Doctoral Thesis, it has been deemed appropriate to list the general conclusions in **Chapter VI**.

However, and as a general conclusion, during the Doctoral Thesis different analytical approaches directed and compatible with the future development of new diagnostic systems and POCT were successfully developed. These approaches are addressed through the design and the development of a (ultra)-miniaturized electrochemical sensor, both screen-printed and microfluidics, for the reliable detection and determination of

two glycoproteins of high clinical relevance: AGP and Tf. These new approaches constitute by themselves an excellent alternative for improvement to the routine methods carried out in clinical laboratories for the analysis of these biomarkers, not only in terms of sensitivity, reliability, and simplicity, but also in terms of the advantages it entails in the clinical field, the reduction of the consumption of reagents and samples, analysis times, and costs, all leading to an improved diagnosis.

Likewise, an added and overall value provided by the results obtained in this Doctoral Thesis can rest on the progress made towards decentralization and the simplification of the analysis that the implementation of these technologies would entail; establishing these as innovative and promising analytical tools in the fields of diagnosis and clinical follow-up.



---

---

# Table of contents

<b>I.</b>	<b>Hypothesis, motivation, and milestones</b>	<b>1</b>
<b>II.</b>	<b>Introduction</b>	<b>9</b>
<b>II.1.</b>	<b>Glycoproteins as clinical biomarkers: state of the art</b>	<b>9</b>
II.1.1.	$\alpha_1$ -acid glycoprotein	21
II.1.2.	Transferrin	23
<b>II.2.</b>	<b>Electroanalysis of glycoproteins. Point-of-care testing devices based on electrochemical detection</b>	<b>28</b>
II.2.1.	Methods for glycoprotein determination	28
II.2.2.	Direct electroanalysis of glycoproteins	36
II.2.2.1.	Nanomaterials in the electroanalysis of glycoproteins	43
II.2.3.	Point-of-care testing devices based on electrochemical detection	46
II.2.3.1.	Screen-printed technology	50
II.2.3.2.	Microfluidics technology	50
<b>II.3.</b>	<b>References</b>	<b>54</b>
<b>III.</b>	<b>Electrochemical sensors screen-printed based for glycoprotein determination</b>	<b>69</b>
<b>III.1.</b>	<b>Introduction and objectives</b>	<b>71</b>
III.1.1.	References	77
<b>III.2.</b>	<b>Results and discussion</b>	<b>79</b>
III.2.1.	<b>Article 1:</b> $\alpha_1$ -acid glycoprotein determination using disposable carbon screen-printed electrodes	81
III.2.2.	<b>Article 2:</b> $\alpha_1$ -acid glycoprotein determination using carbon nanomaterial-based electrodes	101
III.2.3.	<b>Article 3:</b> Rapid screening of carbohydrate deficient transferrin for congenital disorders of glycosylation diagnosis	123
<b>IV.</b>	<b>Microchip electrophoresis with electrochemical detection for analysis of glycoproteins</b>	<b>147</b>
<b>IV.1.</b>	<b>Introduction and objectives</b>	<b>149</b>
IV.1.1.	References	156
<b>IV.2.</b>	<b>Results and discussion</b>	<b>158</b>
IV.2.1.	<b>Article 4:</b> Determination of glycoproteins by microchip electrophoresis using Os(VI)-based selective electrochemical tag	159

<b>V.</b>	<b>Capillary-driven electrochemical microfluidics for analysis of glycoproteins</b>	<b>181</b>
<b>V.1.</b>	<b>Introduction and objectives</b>	<b>183</b>
V.1.1.	References	189
<b>V.2.</b>	<b>Results and discussion</b>	<b>191</b>
V.2.1.	<b>Article 5:</b> Pump-free microfluidic device for the electrochemical detection of $\alpha_1$ -acid glycoprotein	193
V.2.2.	<b>Article 6:</b> Low-cost and passive electrochemical microfluidic device for diagnosis of congenital disorders of glycosylation	217
<b>VI.</b>	<b>General Conclusions</b>	<b>243</b>
<b>VII.</b>	<b>Appendices</b>	<b>251</b>
	Acronyms	253
	List of Figures and Tables	255
<b>VIII.</b>	<b>Publications, patents, and conferences</b>	<b>267</b>







# CHAPTER I

**Hypothesis,  
motivation,  
and milestones**



# I. Hypothesis, motivation, and milestones

Glycoproteins, which are molecules formed by oligosaccharides covalently attached to proteins, represent more than 70 % of proteins in the humans. Due to the abundance and the diversity of these macromolecules in biological fluids (serum, saliva, and urine), as well as the unique changes that may occur in some diseases, glycoproteins become as relevant biomarkers. For that reason, glycoproteins have been investigated by scientists for decades, not only for the large number of functions, but also because they have been associated with various congenital, metabolic, and immune diseases, and cancer.

Consequently, the development of new analytical tools that allow the determination of glycoproteins biomarkers is highly needed. Due to the attention that these macromolecules have aroused in the scientific field, many analytical techniques have been used for the analysis of glycoproteins, commonly liquid chromatography, capillary electrophoresis, and mass spectrometry.

However, the aforementioned techniques are time consuming and/or expensive. In general, these methods require sophisticated equipment, trained personnel, long analysis times, large sample volumes, and expensive reagents.

All these drawbacks highlight the need to develop new analytical approaches for the glycoprotein determination, which can provide physicians and patients with simple, fast, and easy-to-use diagnosis/prognosis tests. Furthermore, these techniques must require a small amount of clinical sample as additional value. These analytical features meet the point-of-care testing (POCT) standards, which are simple, effective, and fully decentralized analytical devices that can be used anywhere and provided reliable diagnostic information in a short period of

time, allowing for faster and better formed decisions in the diagnosis and treatment of diseases.

In this sense, our starting **hypothesis** that has motivated this Doctoral Thesis, is that selected (ultra)-miniaturized analytical tools, such as screen-printed based electrochemical sensors and electrochemical microfluidics devices, can jointly offer solutions for POCT-based diagnostics allowing an improvement in the glycoprotein biomarkers determination in terms of speed, simplicity, and costs.

Electrochemical detection configures a very suitable alternative for POCT-based diagnostics due to its selectivity, sensitivity, simplicity, inherent miniaturization, and portability as well as due its high compatibility with micro and nanotechnologies, requiring low volumes of clinical samples. Glycoproteins have a poor electroactivity due to, in near-physiological conditions, their carbohydrates components (glycans) are electrochemically inactive. To solve this problem, the use of Os(VI) complexes as electrochemical probe was proposed.

On the one hand, screen-printing electrodes (SPEs) have emerged as miniaturized tools that respond to the growing need for rapid *in situ* analysis, and as a choice for mass production of disposable POCT. SPEs are suitable to make effective, high versatile, and low-cost miniaturized devices. Furthermore, one of their main advantages is that the surface of electrodes can be tailored modified by selected (bio) and (nano)-materials.

On the other hand, the miniaturization of laboratories, which finds its greatest exponent in the lab-on-a-chip (LOC) technology also provides a great opportunity to create devices capable of outperforming analysis in an incredible variety of applications. In this field, electrochemical microfluidics is also a strong candidate for providing all the required characteristics for *in situ* clinical analysis and for fabricating truly POCT devices, due to the possibility of integration of multiple analytical steps in the same device. This technology presents several advantages such as accurate liquid handling, short analysis times, low-sample and reagent consumption, and low-waste generation in line with green chemistry standards.

Specifically, microchip electrophoresis (ME) is a mature microfluidics technology with a wide range of possibilities in LOC applications. In recent years, the scientists have looked for several ways to create low-cost, ease-to-manufacture, flexible, and disposable microfluidics devices. In this sense, capillary-driven microfluidics devices are an alternative approach for miniaturized fluid handling in which liquid samples are passively pumped by capillarity. This technology represents a great advance towards the development of simple and easy-to-use POCT.

Under these considerations, the **general objective** of this Doctoral Thesis has been focused on the design, development and evaluation of (ultra)-miniaturized analytical approaches (electrochemical sensors screen-printed based, microchip electrophoresis with electrochemical detection (ED) and capillary-driven electrochemical microfluidics) for fast and reliable analysis of glycoproteins with high significance in clinical diagnosis:  $\alpha_1$ -acid glycoprotein (AGP) in inflammatory diseases and transferrin (Tf) in congenital disorders of glycosylation (CDG)), in order to achieve POCT devices for these diseases.

To reach the general objective stated before, three **specific objectives** have also been defined:

- 1.** To develop screen-printed based electrochemical sensors for selective and sensitive determination of the target glycoprotein biomarkers (AGP and Tf) in clinical samples.
- 2.** To develop an approach based on microchip electrophoresis with electrochemical detection (ME-ED) for the separation and analysis of AGP and Tf in serum samples.
- 3.** To design and fabricate low-cost capillary-driven electrochemical microfluidics devices for the labeling and analysis of AGP and Tf in clinical samples.

According to the objectives exposed above, the following **milestones** have been identified related with the main goals of this Doctoral Thesis:

**1.1.** Development of an electrochemical sensor using disposable screen-printed carbon electrodes (SPCEs) and Os(VI) complex as electrochemical tag for the determination of AGP in serum samples.

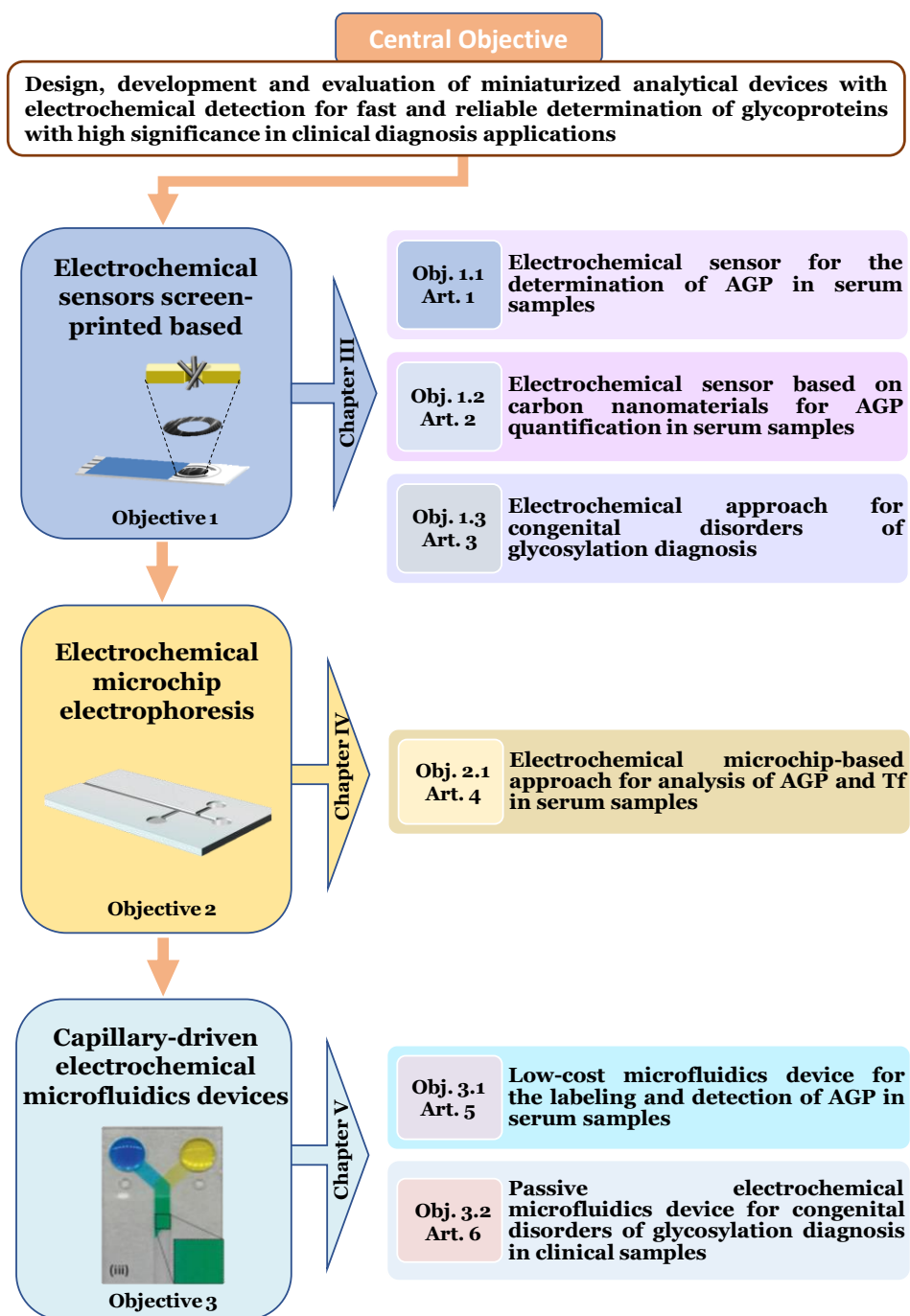
**1.2.** Fabrication of a disposable SPCEs based on carbon nanomaterials with improved analytical performance for AGP quantification in serum samples.

**1.3.** Proposal and evaluation of a novel electrochemical index of glycosylation (EIG) for the assessment of carbohydrate deficient transferrin as biomarker of CDG on board on (magneto) SPCEs-based electrochemical sensors.

**2.1.** Optimization of a ME-ED approach for the separation and analysis of AGP and Tf in serum samples.

**3.1.** Design and development of a passive low-cost electrochemical microfluidics for the labeling and detection of AGP in serum samples.

**3.2.** Design and development of a passive low-cost electrochemical microfluidics for EIG assessment in clinical samples.



**Scheme I.1.** Schematics to achieve the central objective of this Doctoral Thesis.





# CHAPTER II

## **Introduction**



## II. Introduction

### II.1. Glycoproteins as clinical biomarkers: state of the art

Glycoproteins are a group of proteins which suffer a post-translational process in which oligosaccharide chains are covalently attached to them. This type of proteins is present in almost all tissues and fluids of animals, including humans (where more than 70 % of proteins are glycosylated), in plants and in microorganisms (1,2). There are a lot of examples of glycoproteins in the nature: hormones (thyrotropin and the follicle stimulating hormone), antibodies, some enzymes (pancreatic ribonuclease B), blood plasma proteins (ceruloplasmin,  $\alpha_1$ -acid glycoprotein, transferrin, prothrombin) or growth factors, among others (3).

The molecular weight of glycoproteins ranges from tens of thousands to several millions of Da and hydrocarbon content ranges from fractions of 1 to 80 %. Depending to the amino content, you can find two types of glycoproteins: (a) those containing the usual assortment of amino acids and small amounts of carbohydrates (3 to 40 %); (b) those containing a specific variety of amino acids with predominant of serine and threonine and a high carbohydrate content (60 to 80 %).

With the aim of advancing in disease diagnosis, drug development, and personalized medicine, researchers have put all their efforts into discovering new biomarkers, which are indications of medical state observed from outside the patient and can be measured accurately and reproducibly. In this sense, the common post-translational modifications (PTMs), which include but are not limited to glycosylation, phosphorylation, sulfation, and acetylation (**Figure II.1.1**), may increase the specificity of existing biomarkers or lead to the discovery of new biomarkers with greater accuracy for detecting human diseases, due to these PTMs play important roles in biological processes, including regulation of proper protein folding, host pathogen interactions, immune responses, and also inflammation (4–6).

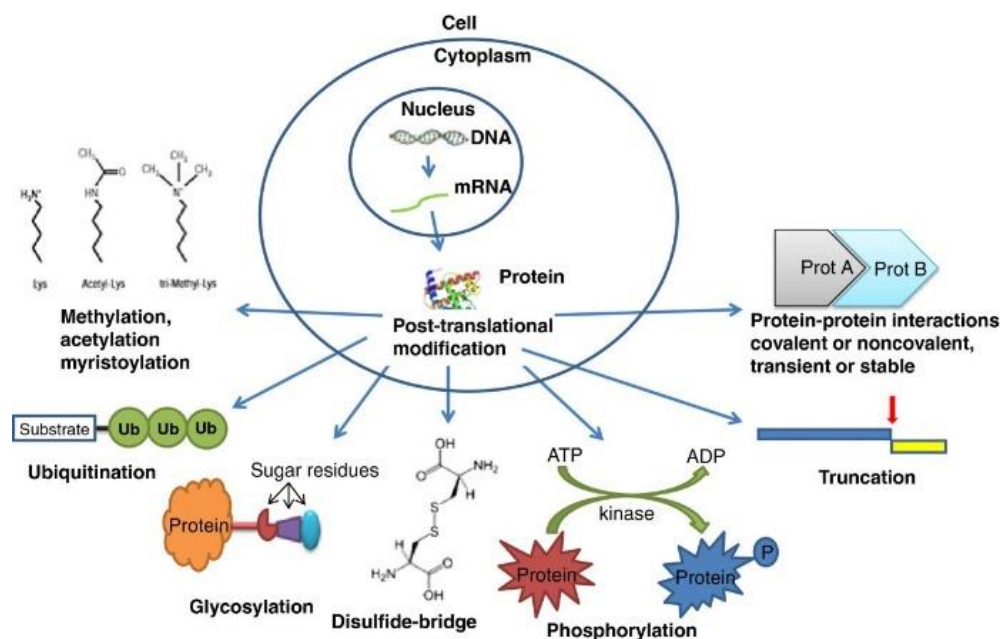


**Figure II.1.1.** Different protein post-translational modifications (7).

Although other PTMs have a higher percentage of incidence as shown in **Figure II.1.2**, glycosylation is one of the most important and complex post-translational process, which has been found in almost all known organisms and has been widely studied by scientists.

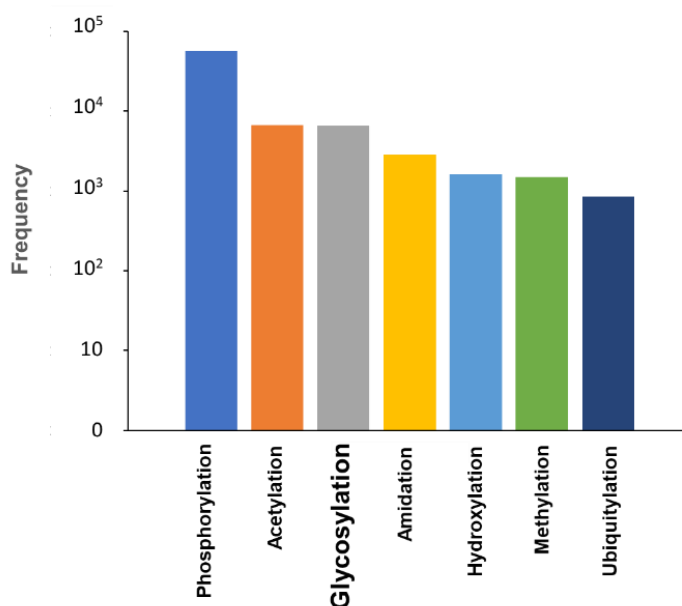


**Figure II.1.2.** Summary of the top experimental post-translational modifications carried out. The data shown were obtained from reference (8), which used Swiss-Prot database.

## II.1. Glycoproteins as clinical biomarkers: state of the art

In this process, covalent attachment to the peptide is via glycosidic bonding to the side chain of serine, threonine, or asparagine residues. Depending on which amino acid is involved in the sugar bonding, we can find two different types of glycosylation: when the oligosaccharide group is attached to the -OH group of serine and threonine are called "O-linked", whereas those attached to the -NH<sub>2</sub> amide group of asparagine are called "N-linked" (the most common interaction) (**Figure II.1.3**) (3,9).

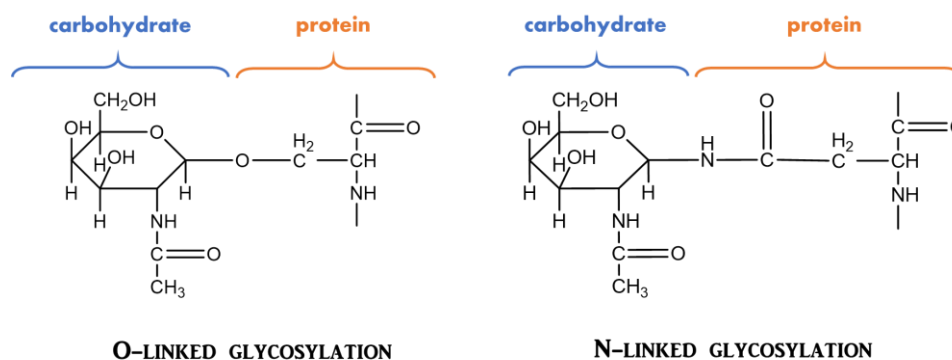


**Figure II.1.3.** Different types of glycoprotein depending where the sugar bond with the protein occurs.

In the case of N-glycoprotein biosynthesis, this takes place through a metabolic via in three different compartments of the cell: the cytosol, the endoplasmic reticulum (ER) and Golgi apparatus.

Unlike the protein sequence, which is determined by DNA template, sugars are linked to proteins by the catalysis of highly specific enzymes that recognize the adequate site to bind sugar (10). The first step consists in adding, one by one and in a determinate order, different monosaccharides to a lipid molecule, which is in the membrane, with the help of glycosyltransferases (enzymes that transfer sugars). Then, new changes in glycan composition are performed progressively (assembly), in the cytosol and subsequently in the ER. In this step, the glycan chain is transferred to the target proteins. When the process is finished, the glycoprotein continues to Golgi apparatus, where it is produced the remodeling of the glycans chains, until it acquires its definitive composition (processing). Once the bond between protein and glycan has occurred, glycoprotein is ready to perform its function (2,11) (**Figure II.1.4**).

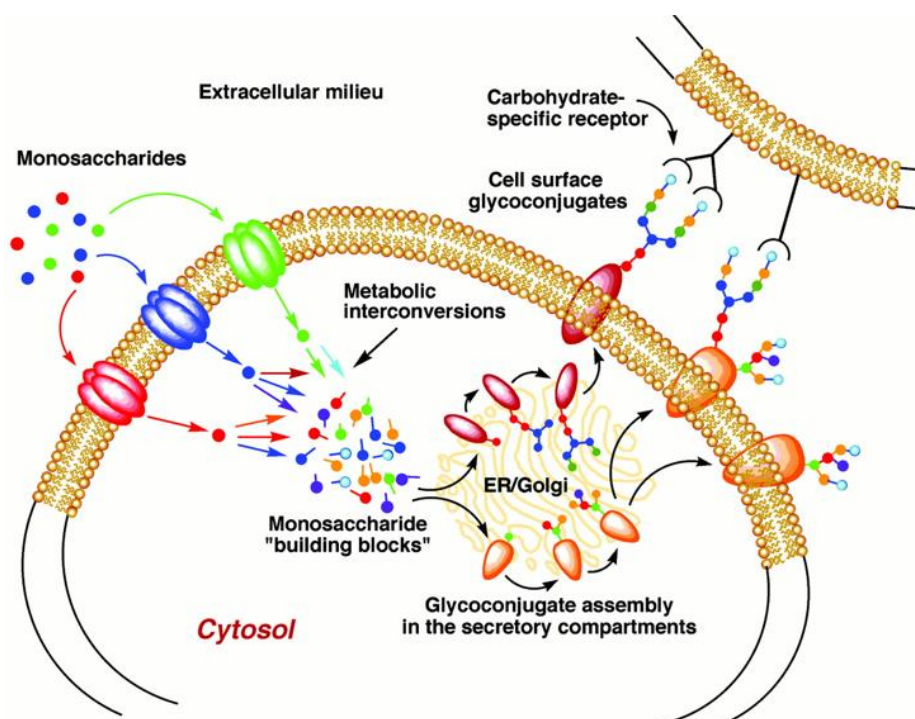


**Figure II.1.4.** Glycoconjugate biosynthesis process and cell surface recognition. The process starts with exogenous monosaccharides which are converted to monosaccharides "building blocks" inside the cell. In the case of N-linked glycoproteins, a core oligosaccharide is assembled in the cytosol and then transported into the ER where it is processed (glycosidases) and then transported into the Golgi apparatus where it is produced a finish remodulation (glycosyltransferases). Finally, the glycoconjugate is fully mature form and is ready to carry out its functions (11).

The expression of glycans is specific to each tissue and cell and also depends on the presence of pathological states. An abnormal expression of a single enzyme participating in that process can alter the following steps and cause aberrant oligosaccharides structures. The types of cells that contained these biomolecules, determine the enzymes expressed and therefore, the variation of glycans reflects both cellular or tissue origin and (bio)-chemical and physiological conditions at that time (12).

Furthermore, due to the great variety of sugars, which contain a great quantity of functional groups in diverse conformations, it is possible to find a diverse potential binding sites, which means that glycoproteins present an enormously variety and complexity in their structure (13). In addition, there

## II.1. Glycoproteins as clinical biomarkers: state of the art

---

are many factors that can influence in the glycan complexity, including 1) different specific expression of glycosyltransferases and glycosidases; 2) availability of monosaccharides; 3) age; 4) gender; 5) environment (health, diet, smoking or alcohol consumption); 6) disease processes. Therefore, glycoproteins synthesized by cells usually exist as complex mixtures of up to hundreds of glycoforms (or glycosylated variants, glyco-variants). These variants differ in glycosylation site occupancy and glycan structures (giving rise to macroheterogeneity and microheterogeneity, respectively) (10,14,15).

The presence of carbohydrate part in protein is a chemical label that helps to differentiate between proteins that must be kept in the cytoplasm (non-glycosylated proteins) and those that must leave the cell (glycosylated proteins). Furthermore, the covalent attachment of large hydrophilic carbohydrates modulates protein stability, as well as determine its conformation and help in the interaction with other proteins. In addition, this carbohydrate part protects the protein against intracellular proteolysis during biosynthesis and transport (16,17).

Protein glycosylation is a costly process for the organism in terms of energy and materials, it is estimated that the cell allocates 1 % of its genome to glycosylation machinery, but despite this, the process continues to move forward what it is a reflection of the relevance of these units. In fact, glycans have important biological functions, such as cell signaling, cell-cell interaction, immune recognition, cell proliferation and differentiation, among others (14,18).

Glycoproteins perform transcendental functions as sites of intercell recognition, since many receptors on the cell surface are able to recognize specific sequences of oligosaccharides. In the nature, we can find two well-known examples of recognitions that occur through oligosaccharides chains: one of them is the recognition between egg cells and sperm cells, necessary for the phenomenon of fertilization to occur in pluricellular organisms with sexual reproduction (19,20). Another, it is found in the blood groups, because these depend on the type of glycoprotein that contains the membrane of erythrocytes. So, blood group A has N-



## Chapter II. Introduction

---

acetylgalactosamine as oligosaccharide, while blood group B has a chain of galactose, and therefore the blood group AB presents the two types of glycoproteins and blood group O lacks both. To determine the blood group, antibodies that recognize a certain type of membrane glycoprotein are used. Knowledge of the blood group not only is it important for transfusions, but also for preventing the formation of clots that cause fatal heart attacks and thrombosis (21).

On the other hand, some viruses, which can be potentially dangerous for many mammals, including humans, present glycoproteins in their surface that work in the processes of adhesion of the viral particle to parasitizing cells (22). Such is the case of the GP120 protein of the Human Immunodeficiency Virus or HIV, which interacts with a surface protein of human cells known as GP41 and which contributes to the entry of the virus into the cell (23,24).

Glycoprotein levels, structures, and locations are different depending on the stage of the disease development. Glycoproteins can be also affected by environmental factors such as nutrition status and chemotherapy. Furthermore, the alterations of glycosylation profile are often associated with diverse diseases, including cancer, rheumatoid arthritis, and other kinds of inflammation stages. All of this opens up the possibility to use these proteins as biomarkers for disease diagnosis, prognosis, and monitoring (25). Furthermore, these can be used as therapeutic targets for the design of diagnostic methods, next-generation therapies, and even for the design of vaccines (26).

There are a great number of glycoproteins which can be used as biomarkers of several cancers (ovarian, breast, prostate, etc.), because glycosylation plays an important role in cancer development, progression, and metastasis (27,28). For example, P-glycoprotein has been identified to be closely associated with carcinogenesis and functional processes in the tumor (29–31). Besides the US Food and Drug Administration (FDA) have approved several glycoprotein based biomarkers such as CA125 (mucin 16) for ovarian cancer and prostate-specific antigen (PSA) for prostate cancer (32).

In addition, recent studies have reported the relevance of glycoproteins in pathogen recognition, inflammation, innate immune responses, and the development of autoimmune diseases, which are a chronic inflammatory disorder arising from a wide range of abnormalities of the immune system. The P-glycoprotein over-expression can be proposed as mechanism of drug resistance in patients with these autoimmune diseases. Aberrant protein glycosylated have been confirmed as biomarkers of human neurodegenerative diseases, such as Creutzfeldt-Jakob disease, Alzheimer's disease, and Parkinson's disease (33,34). These diseases are characterized by the progressive degeneration of the structure and function of the central nervous system.

Due to the abundance and the diversity of glycoproteins in biological fluids such as serum, saliva, or urine, as well as the unique changes that may occur in some diseases and not others, glycoproteins can be perfect biomarkers. In **Table II.1.1**, we can see different biological fluids use for the detection of glycoprotein biomarkers. Although serum is considered a primary source of biomarkers; urine and saliva are increasingly being explored and used as rapidly accessible samples, because they are non-invasive biofluids, which requiring minimal sample processing and posing fewer biohazard risks.

## Chapter II. Introduction

**Table II.1.1.** Examples of glycosylation studies for various clinically relevant biological fluids (5).

Body Fluid	Disease	Description
<b>Serum</b>	Alzheimer's disease	Increased O-GlcNAcylation levels and decreased global glycosylation
	Hepatocellular Carcinoma	Increase in the levels of Golgi glycoprotein GP73 in HCC patient serum
	Ovarian cancer	Changes in serum glycome profile of ovarian cancer patients
	Breast cancer	Abundant fucosylation in metastatic breast cancer patient sera
	Inflammatory diseases, such as neonatal sepsis or Crohn disease	Levels of $\alpha_1$ -acid glycoprotein can increase two or three times during disease or injury
	Inflammatory disorders	Levels of transferrin decrease when disease appear
	Congenital disorders of glycosylation and chronic alcohol abuse	The amount of glycans in serum transferrin is lower than normal
<b>Saliva</b>	Oral ulcer	Proteomic and N-glycoproteomic quantification reveal aberrant changes in the human saliva of oral ulcer patients
	Control	Analysis of age and gender associated N-glycoproteome in human whole saliva
	Control	Identification of N-Linked Glycoproteins in Human Saliva
<b>Cerebrospinal fluid</b>	Alzheimer's disease	Unusually glycosylated acetylcholinesterase in CSF samples of AD patients as a diagnostic molecule
	Schizophrenia	Identification of N-glycosylation changes in the CSF and serum in patients with schizophrenia
<b>Urine</b>	Prostate cancer	Characterization of glycoproteins from urine samples of prostate cancer patients with different Gleason scores
	Prostate cancer	Investigation of glycoproteome to discriminate prostate cancer from benign prostatic hyperplasia

HCC: Hepatocellular carcinoma; CSF: Cerebrospinal fluid; AD: Alzheimer disease.

## II.1. Glycoproteins as clinical biomarkers: state of the art

---

As mentioned above, glycoproteins also play important roles in inflammatory process, which is the response to infections as well as the pathogenesis of metabolic and cardiovascular diseases. Because it is not possible to determine the level of inflammation in apparently healthy people with the use of clinical signs or symptoms, the World Health Organization (WHO) has recommended measuring several proteins in order to determine these processes. During the inflammation, the post-translational modifications in glycan include changes in the number of antennary branches, increased sialylation and fucosylation and decreased galactosylation, among others process. Inflammation is the basis for many autoimmune and chronic low-grade inflammatory diseases such as cardiovascular disease (CVD), type 2 diabetes (T2DM) and cancer. Furthermore, inflammation is associated with altered metabolism of both micro- and macronutrients. As a result, many clinical tests used glycoproteins as biomarkers for diagnostic and/or prognostic purposes or for monitoring response to therapy.

Inflammatory glycoproteins are predominantly synthesized and secreted by hepatocytes but can be produced by activated macrophages and neutrophils in the periphery. As it can see in **Table II.1.2**, there a lot of glycoproteins which can be used as biomarkers in inflammatory problems.

## Chapter II. Introduction

**Table II.1.2.** Human inflammatory glycoproteins modified during an acute phase response.

Category	Positive and negative acute phase proteins	Molecular weight (KDa)	Glycosylation sites	Adult concentration in serum
<b>Binding or transport proteins</b>	$\alpha_1$ -Acid glycoprotein	41-43	5	0.2 - 1.0 mg mL <sup>-1</sup>
	Haptoglobin	100	4	0.3 - 3.0 mg mL <sup>-1</sup>
	Ceruloplasmin	151	6	0.2 - 0.6 mg mL <sup>-1</sup>
<b>Antiproteases</b>	$\alpha_1$ -Antitrypsin	52	3	0.9 - 2.0 mg mL <sup>-1</sup>
	$\alpha_2$ -Macroglobulin	179	8	1.3 - 3.0 mg mL <sup>-1</sup>
<b>Coagulation system</b>	Fibrinogen $\alpha$ , $\beta$ , $\gamma$	340	5 N-, 2 O-linked	1.5 - 4.0 mg mL <sup>-1</sup>
	Plasminogen	92	1 N-, 2 O-linked	plasma 120 - 200 $\mu$ g mL <sup>-1</sup>
	Vitronectin	140	3	plasma 110 -140 $\mu$ g mL <sup>-1</sup>
<b>Miscellaneous</b>	Fibronectin	220-440	7 N-, 3 O-linked	0.3 mg mL <sup>-1</sup>
	C-reactive protein (CRP)	115-120	1	hsCRP < 1.0 $\mu$ g mL <sup>-1</sup> $\geq$ 3.0 $\mu$ g mL <sup>-1</sup> risk for CVD
	Transferrin	76-81	3 N-, 1 O-linked	1.7 - 3.7 mg mL <sup>-1</sup>
	Transthyretin	55	1	0.2 - 0.4 mg mL <sup>-1</sup>
	$\alpha$ -Fetoprotein (AFP)	70	1	< 15 ng mL <sup>-1</sup>

### II.1.1. $\alpha_1$ -acid glycoprotein

Among these proteins,  $\alpha_1$ -acid glycoprotein (AGP) is typically used in conjunction with C-reactive protein (CRP) to establish the time course and severity of infections. CRP is an acute protein primarily expressed and secreted by the liver; whose concentrations can increase from baseline levels of less than  $1 \mu\text{g mL}^{-1}$  within 48 h. Although CRP is widely used in clinical practice, and there are papers in which do not find evidence that AGP would be a better biomarker of mortality risk for inflammatory diseases, the WHO has recommended measuring AGP and CRP as co-biomarkers in inflammatory process because they reflect different stages of the acute-phase response (35–37). AGP has some properties that is important take them into account: 1) a longer half-life than CRP (60-120 *vs* 19 h), AGP rises more slowly and stays elevated longer than CRP, so that it can better reflect long-term chronic inflammation; 2) typically higher prevalence in population due to these kinetics; and 3) higher concentrations in serum, urine and saliva.

AGP, also known as orosomucoid, is a serum glycoprotein which was first described in 1950 by Karl Schmid and Richard J. Winzler. AGP contains a single chain of 183 amino acids with two disulfide bridges. The carbohydrate content represents 45 % of the molecular weight (41-43 KDa) attached in the form of five to six highly sialylated complex-type-N-linked glycans (**Figure II.1.5**). The protein, which belongs to a group of acute phase proteins, presents a low isoelectric point (pI = 2.8-3.8) (38,39). 12-20 glycoforms of AGP can be detected in normal human serum and this micro-heterogeneity is strongly dependent on the pathophysiological conditions (40).

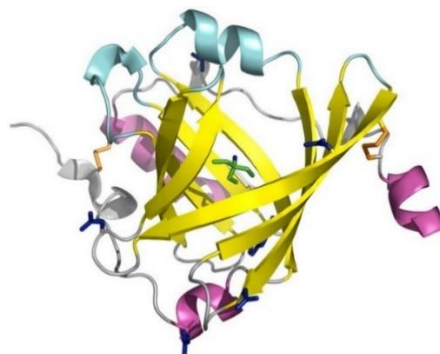


**Figure II.1.5.** Crystal structure of human AGP at 1.8 Å resolution. Secondary structure is colored yellow ( $\beta$ -strands), pink ( $\alpha$ -helix), and gray (coils), while the two disulphide bridges (connecting Cys residues 5-147 and 72-165) are shown in orange. Loop 1 (A/B), loop 2 (C/D), loop 3 (E/F), and loop 4 (G/H) at the open end of the  $\beta$ -barrel are highlighted in cyan. The bound Tris molecule inside the cavity is shown as a stick model in green, with the amino nitrogen is colored blue. The Asn side chains of the five N-linked glycosylation sites (Asn15, Asn38, Asn54, Asn75, and Asn85) in the native protein (41).

AGP is a major plasma protein with diverse physiological roles such as immune modulation, binding and transporting basic or neutral compounds including drugs, capillary barrier function maintenance, and metabolic regulation (38,42).

This glycoprotein is expressed by the liver and secreted in a monomeric form into the circulation, where it is observed in concentrations between 0.2-1 mg mL<sup>-1</sup>. However, its serum concentration rises in response to systemic tissue injury, inflammation or infection, potentially increasing the concentration two- to four-fold (43). In fact, AGP levels have been evaluated as serum biomarker for inflammatory bowel diseases, and even for early diagnosis of neonatal sepsis (44), yielding excellent results in prognosis of Crohn disease. Changes in glycosylation of AGP are not restricted to acute inflammatory conditions, but also occur in a wide variety of other pathophysiological conditions like pregnancy, severe rheumatoid arthritis, alcoholic liver cirrhosis, and hepatitis.

Interestingly, AGP glycan modification appears to occur in some inflammatory diseases, but not others. For example, increased AGP glycan

branching has been observed in patients with asthma and rheumatoid arthritis, but not in patients with ulcerative colitis. The regulation of AGP activity is complex: the inflammation induces not only an increase in AGP serum concentration, but also a qualitative change in its carbohydrate moiety, generating a multitude of glycoforms, each of them with different, and sometimes opposite and contradictory activities (45).

### II.1.2. Transferrin

In the context of glycoprotein biomarkers, transferrin (Tf) has received a lot of attention. In this case, Tf, which contains 679 amino acid residues, has a higher point isoelectric and molecular weight than AGP (pI = 5.2-5.6 and molecular weight = 70-95 KDa). This glycoprotein exhibits only two N-linked disialylated biantennary oligosaccharide chains (Asn413 and Asn611) and an average glycosylation content of about 6 % <sub>w/w</sub> (**Figure II.1.6**) (46,47). Furthermore, it is mainly produced in the liver and has a half-life of approximately 8 days in the serum. Tf has been detected in various body fluids including serum, plasma, bile, amniotic, cerebrospinal, lymph, and breast milk. Tf is the most important and abundant iron glycoprotein in serum, and it well-known for its function in the transport and metabolism of iron in the body (48).

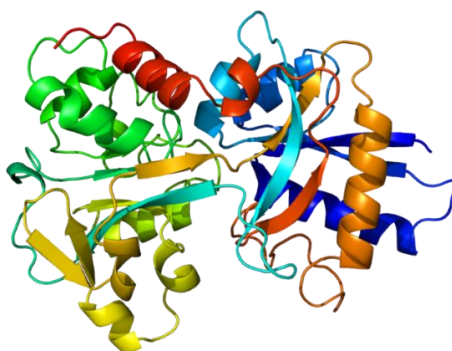


**Figure II.1.6.** Crystal structure of transferrin. The Tf molecule is divided into two evolutionary related lobes, designated the N-lobe (336 amino acids) and C-lobe (343 amino acids), which are linked by a short spacer sequence. Each lobe contains two domains comprising a series of  $\alpha$ -helices, which overlay a central  $\beta$ -sheet backbone (49).



## Chapter II. Introduction

---

Iron circulates in the plasma until it attaches to a Tf receptor. This can be supposing a problem, due to free iron can be toxic, promoting free radical formation via the Fenton and Haber–Weiss reactions, thus resulting in oxidative damage to tissues. For example, levels of Tf tend to decrease during radiotherapy treatment, and they promote oxidative stress by increasing the levels of redox reactive iron in the circulation. For these reasons, it is vital that iron is transported in a redox-inactive form (Tf promotes auto-oxidation reactions involving CHO aldehyde groups and protein amino groups leading to the formation of glycated products). Tf has the capacity to bind two atoms of iron and thus prevents the participation of iron in redox reactions with ensuing formation of toxic reactive oxygen species (ROS). Once iron is bound to Tf, it is transported for all biological tissues. In this sense, Tf level testing is used to determine the cause of anemia (high level circulation of Tf iron-free in the body signifies low iron and revealing a possible iron deficiency), examine iron metabolism and determine the iron-carrying capacity of the blood (50,51).

Although the primary role of Tf is to transport iron safely around the body to supply growing cells, Tf has other different functions. For example, it plays a critical role in host defense, by depriving iron from invading pathogens or the binding of Tf to iron impedes bacterial survival. Tf also has the ability to modulate differentiation and growth of cells, being important in different activities including myotrophic, embryo-morphogenic proliferative, mitogenic, neurotropic, chemotactic, and angiogenic activities (46,51).

Furthermore, Tf is negative acute phase protein, so a concentration decrease is observed during inflammation processes. For example, Tf levels in Type I diabetes patients are typically 10 % lower than those in normal individuals (52,53).

As we mentioned before, the main Tf glycoform contains two N-biantennary glycans with a total number of four sialic acids (tetrasialo-Tf, pI = 5.4). However, there are other minority glycoforms with two (disialo-Tf, pI = 5.7), three (trisialo-Tf, pI = 5.6), five (pentasialo-Tf, pI = 5.2) and six (hexasialo-Tf, pI = 5.0) sialic acids (**Figure II.1.7**). Under certain

## II.1. Glycoproteins as clinical biomarkers: state of the art

pathological states or due to genetic defects, the profile of glycoforms can suffer modifications and minority glycoforms with lower amount of glycans (asialo-, disialo- and trisialo-Tf) are increased respect to the main glycoform (tetrasialo-Tf). This low glycosylated Tf is called carbohydrate deficient transferrin (CDT) and it is the clinically used biomarker for the detection of congenital disorders of glycosylation (CDG), chronic alcohol abuse and cerebrospinal fluid loss (54,55).

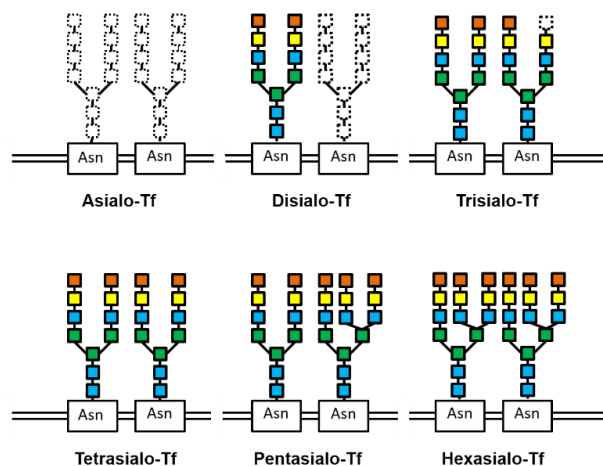


**Figure II.1.7.** Different glycoforms of transferrin depending on the number of sialic acids present in the glycoprotein. Asialo-Tf with any sialic acids; diasialo-Tf with two sialic acids; trisialo-Tf with three sialic acids; tetrasialo-Tf with four sialic acids; pentasialo-Tf with five sialic acids; and hexasialo-Tf with six sialic acids.

CDG, which were first reported in 1980, are a group clinically and genetically diverse of metabolic disorders, which are due to defects in the synthesis of glycoproteins (mutation in any of the many genes specifying enzymes or proteins involved in their synthesis) and/or in the attachment of glycans to proteins and lipids. Inheritance mode in most types is autosomal recessive but subtypes linked to the X chromosome and with inheritance autosomal dominant have been described. Over 150 types have currently been described, most of which involve defects of N-glycosylation, but this family of metabolic diseases is still growing since about 17 % of the actual number have been reported in the last three years (56–58). The

## Chapter II. Introduction

---

Orphanet database reports a collective prevalence at birth of 1.5/100000 (59).

Most CDG patients have dysmorphic facial features, abnormal fat distribution, and variable coagulation and endocrine defects. However, in other patients, it can be found neurologic, cardiac, gastrointestinal, hepatic, renal, hematologic, and/or immunologic problems (we recommended to see the review “Therapeutic approaches in Congenital Disorders of Glycosylation (CDG) involving N-linked glycosylation: an update” *Genetics in Medicine*, 2019 about the different symptoms present in CDG).

The analysis of this rare disease is still a challenge by the fact that most analysis are based on small groups of patients where an extreme phenotype is identified, skewing our appreciation of the disease (60,61). The clinical presentation of these defects is very variable and, therefore, any patient with unexplained multisystemic disease should be selected for differential diagnosis CDG. So, there are not unique and precise symptoms which can be relate with these diseases (62). However, it seems clear that, due to the extremely severe symptoms, early and accurate diagnosis of CDG is crucial for timely implementation of appropriate therapies and improving clinical outcomes (63). Diagnosis is suspected for these clinical manifestations and confirmed by laboratory test, including biomarker such as abnormal serum Tf profiles. The diagnosis is also supported by genetic study that identifies the gene responsible for the defect (64).

CDG due to a modification in N-glycosylation are the most abundant and are classified into two types depending on what stage of the glycosylation process the defects occur: CDG-I and CDG-II (65). CDG-I are referring to defects in the assembly of the lipid-bound oligosaccharide chain and their transfer to the protein. In this case, the defects are characterized by unoccupied glycosylation points in proteins, so they are completely free of N-glycans. On the other hand, CDG-II are referring to defects during the subsequent process of binding glycans to the protein that occur in the cytoplasm and Golgi apparatus and are characterized in the truncated or incomplete N-glycan chains (66). Different profile of Tf glycoform appears depending on what type of CDG occurs. In CDG-I glycoforms asialo- and

## II.1. Glycoproteins as clinical biomarkers: state of the art

---

diasialo-Tf are increased, whereas in CDG-II monosialo- and trisialo-Tf are increased.

As for therapies used against this pathology, CDG is still a poorly treatable family of disorders. On one hand, we can find better known and conservative therapies, such as nutritional therapies and transplantation. On the other hand, a few emerging therapy options are under preclinical investigation with promising preliminary results: enzyme therapy, the use of pharmacological chaperones, or gene therapy. We recommend reading two new reviews on current and future therapies used against this pathology: “Therapeutic approaches in Congenital Disorders of Glycosylation (CDG) involving N-linked glycosylation: an update” *Genetics in Medicine*, 2019 and “Congenital disorders of glycosylation: Still “hot” in 2020” *BBA - General Subjects*, 2021.

In sum, glycoproteins are considered perfect candidates as biomarkers, which assist in the diagnosis and follow-up of different diseases, such as inflammation process or genetic diseases, among others.

## **II.2. Electroanalysis of glycoproteins. Point-of-care testing devices based on electrochemical detection**

### **II.2.1. Methods for glycoprotein determination**

The development of techniques and methods for the separation, purification, and detection of biological macromolecules, such as proteins and glycoproteins, has been an important prerequisite for many of the advancements made in (bio)-science and (bio)-technology. Among other macromolecules, proteins and glycoproteins has been being investigated by scientists for decades, not only for the large number of functions that these molecules have, but also they have been associated with various congenital, metabolic, neurodegenerative, and immune diseases and cancer.

The development of methodologies to detect and quantify proteins, specifically protein biomarkers, has increasingly become essential for detection and treatment of certain diseases, which can be correlated with changes in concentration of a protein biomarker in biological fluids. In many cases, proteins must be detected in very low concentrations, so researchers have developed several strategies to carry out accurate and simple diagnosis methodologies, using different recognition elements (e.g., antibodies, aptamers) and different sensing principles and techniques (e.g., optical, electrochemical). For total quantification of proteins, we find different methods which include, but are not limited to Biuret method ( $\text{Cu}^{2+}$  binds to the peptide binding of proteins and produces a purple color; proteins are quantified spectrophotometrically), Lowry method (depends on the concentration of tyrosine (Tyr) and tryptophan (Trp) sample), turbidimetry (depends on protein precipitation) and UV absorption (absorption at 270 nm of the aromatic rings of Tyr and Trp). Analytical techniques such as 2D-gel electrophoresis, high-performance liquid chromatography (HPLC), capillary electrophoresis (CE) coupled with mass spectrometry (MS), and laser-induced fluorescence detection (LIF) are also employed in proteomics (67,68).

However, chemical and biochemical analysis are often impeded by the small amounts of sample available and, in the case of glycoproteins, the vast

structural heterogeneity of glycans. As it was aforementioned, multiple sites of glycosylation are present in a protein, and the site occupancy can vary under different conditions, both leads to glycosylation macroheterogeneity. But also, glycans occupying a glycosylation site are complex and can vary significantly in terms of size, charge state, glycosidic linkage, and branching pattern. This leads to another level of heterogeneity, namely microheterogeneity (69). The combination of two levels of heterogeneity results in complex mixtures (70). Even for a single protein sequence, these mixtures can contain more than one hundred differently glycosylated isoforms (glycoforms). It is for the extreme complexity and diversity of glycoprotein structures that grow the necessity of highly sensitive and efficient methods for separation, detection, and structural investigation.

In the case of glycoprotein-based biomarkers, the total concentration of these glycoproteins in biological fluids is sometimes used (for example, PSA for prostate cancer follow-up) and, in other cases, the presence of a certain glycoform or the profile of glycans of glycoprotein (for example, MUC1 for monitoring the breast cancer treatment).

In this sense, there are different ways to characterize their glycosylation profile depending on the goal (glycan profiles, glycan structures and heterogeneity, glycosylation site(s), content of specific glycans...). In general, there are two general strategies for glycoprotein analysis. One is the “top-down” strategy in which the intact glycoproteins are detected without extensive separation or digestion. This methodology provide the protein sequencing ladders and *in situ* localization of complex glycans (71). The other is the “bottom-up” strategy, which is the most widely applied to analysis of glycoproteins. It includes two common analytical approaches. One approach is to the release of glycans from the glycoproteins by chemical or enzymatic methods, and then the carbohydrates and proteins are purified and analyzed, respectively. In this methodology the structures of glycans and sequences of proteins can be obtained. But unfortunately, the information of binding sites of carbohydrates on proteins could be lost. The other approach is to directly digest glycoproteins with endoproteases (trypsin is the most commonly used protease in shotgun proteomics studies because of its high cleavage specificity to the carboxyl side of arginine and

## Chapter II. Introduction

lysine), and then digested glycopeptides are characterized. The glycosylation sites can be determined.

Ideally, glycoprotein analysis should involve simpler procedures which modified minimally the test samples. For example, glycan release from the glycoprotein can hamper the elucidation of the structural–functional role that glycans may play on the protein and vice versa. However, there are occasions that released N-glycans is necessary for different reasons, although this means including more steps. In these cases, the first step was a cleavage of glycan moiety from a protein or a peptide backbone either enzymatically or chemically. The second step was the separation of carbohydrates released from the glycan by chromatographic, electrophoretic, and other techniques. The final step was the detection of separated carbohydrates by MS, fluorescent or electrochemical detection.

In order to release intact glycans from the protein or peptide backbone, either enzymatic or chemical methods can be employed (72). Each of these procedures has certain advantages and disadvantages. Enzymatic release yields intact oligosaccharides and peptides or proteins but depending on the substrate specificity of the enzyme employed. It is for that reason that not all types of glycans are liberated. N-glycosidase F (PNGase F) is the most commonly used enzyme, because it liberates a great variety of N-linked glycans (73) (**Figure II.2.1**). On the other hand, chemical procedures may lead to partial or complete destruction of non-carbohydrate substituents and of the polypeptide backbone.

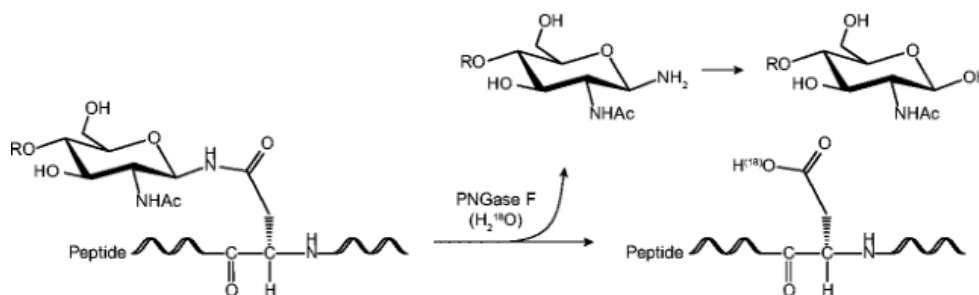


**Figure II.2.1.** Schematic representation showing mechanism of glycan release from proteins of N-glycans by PNGase F (74).

Following their release from the glycoprotein, free glycans are usually found in a solution that contains salts, detergents, proteins, peptides, amino acids, and so forth. Before further analysis, these contaminants must be removed. There are several methods for glycan desalting and purification. For example, the graphitized carbon desalting method is based on the ability of oligosaccharides to bind to carbon beads, while unbound simple monosaccharides, salts, and detergents can be washed away with water (75).

As mentioned above, sometimes efforts are directed, not so much to the total quantification of glycoproteins, but to the separation and identification of glycoforms present in the glycoproteins. In this aspect, a series of techniques used in these cases will be discussed below.

Mass spectrometry (MS) has become a powerful tool to determine glycoproteins due to its sensitivity, stoichiometry, specificity and speed, which facilitates the identification of the glycoproteins, glycosylation sites, and structures of glycans (71,76). Instrumental improvements and the availability of reliable commercial instrumentation to numerous laboratories have also driven new developments in terms of ionization and fragmentation techniques and of selective ion monitoring. Electrospray ionization (ESI) and matrix-assisted laser desorption ionization (MALDI) are two soft ionization technologies which are widely applied to the analysis of glycoproteins and glycans (77). Since most carbohydrates do not possess any chromophores, spectroscopic labels must be introduced through derivatization, usually at the reducing end, being this technique not only useful for separation but also as detection method of glycoproteins. Although there is no universal method for comprehensive identification of glycoproteins, MS has the great advantages in structural analysis of glycoproteins.

Liquid Chromatography (LC) continues to play a very important role in glycomic and glycoproteomic research with its different retention modes, column dimensions, and formats and its use as either an analytical profiling technique or a micropreparatory tool (78). The use of fluorescence derivatization has become routine in conjunction with conventional HPLC columns and increasingly with the UHPLC (ultrahigh performance liquid



## Chapter II. Introduction

---

chromatography) columns packed with particles smaller than 2  $\mu\text{m}$  in diameter (79). Due to the wide range of adsorbents and solvent systems available as well as the speed and reproducibility of separation HPLC has proved to be of great value in profiling and separation of glycans (73). Different chromatographic separation techniques have been applied to glycan analysis, including reversed-phase (80), normal phase (hydrophilic interaction) (81), and porous graphitized carbon (PGC) chromatography (82).

Another high-resolution separation technique, which is used for achieving an unequivocal identification and a comprehensive characterization of glycoprotein, is capillary electrophoresis (CE) and, in a lesser extent, microchip electrophoresis (ME) (83). In CE charged analytes are separated according to their migration velocity in an electric field placed across the ends of a capillary column. The benefits of CE are high separation efficiency and speed of analysis (84). Whereas the high resolving power of CE is undoubtedly very useful for comparative monitoring the glycoform populations of, for example, recombinant glycoproteins, it does not allow *per se* any conclusions on the nature of glycan chains attached (85).

Last but not least, as one of the most efficient protein separation techniques, SDS-PAGE and, more recently, 2-dimensional (2D) gel electrophoresis is often employed as the first step for isolation or analysis of glycoproteins. Fractionation by gel electrophoresis is based on sizes, shapes, and net charges of macromolecules. In 2D-gels, glycoproteins often produce characteristic “trains” of protein spots reflecting different isoelectric points and/or molecular masses of the glycoforms (86). A significant drawback of this technique, however, is the frequent under-representation of membrane (glyco)proteins in common 2D-gel electrophoresis due to a low solubilizing power of the non-ionic and zwitterionic detergents generally used in isoelectric focusing for hydrophobic proteins (73). In addition, many of them are only weakly stained by conventional dyes due to the high carbohydrate content. Therefore, alternative approaches have to be applied for isolation, purification and/or characterization of membrane (glyco)proteins including blue native electrophoresis, 2D benzyldimethyl-n-hexadecylammoniumchloride/SDS-PAGE or SDS-PAGE in conjunction

with nano-HPLC after solubilization of the membrane proteins with ionic/non-ionic detergents and chaotropic agents. Additional information on the type of glycans attached can be obtained by combining gel electrophoretic separation and/or lectin probing.

To obtain a comprehensive picture of a glycoprotein in terms of its structure, conformation and stability, numerous analytical strategies with different principles are needed and, in many cases, it is necessary the use of intact glycoproteins. The analysis of intact glycoproteins has the advantage of providing access to the complete protein sequence and the ability to locate and characterize post-translational modifications. In addition, application of enzymes in glycan cleavage can be expensive, when extensive characterization of glycans has to be performed, and thus cost-effective methods are continuously evolving.

Many of the separation techniques discussed above can be used to measure intact glycoprotein (87). However, it is found diverse problems. For example, the extensive microheterogeneity of the glycoproteins makes that MS characterization of intact glycoproteins more difficult than MS analysis of proteins. Furthermore, glycoproteins are less efficiently ionized. Although matrix-assisted laser desorption/ionization time-of-flight mass spectrometry (MALDI-TOF-MS) is in principle capable of recording spectra of intact glycoproteins, resolution of individual glycoforms can only be achieved for small proteins ( $\cong$  40 KDa) (73).

On the other hand, laser-induced fluorescence (LIF) is the most used detector coupled to separation techniques in proteomics and clinical analysis. The sensitivity shows by LIF detection is high but, in general, proteins, peptides, and amino acids are not fluorescent and need the use of fluorescence tags, making this method more laborious and expensive. Regarding glycoproteins, a high number of chemical derivatization procedures involving the reducing end-aldehyde group of glycans have been developed. Using reductive amination, chromogenic, or fluorescent groups can be introduced which enable highly sensitive detection during chromatographic separation, whereas incorporation of ionizable functional groups may mediate a uniform charge thus allowing a highly efficient

electrophoretic separation (73). In addition, the peptidic part can be also labeled through terminal amine groups, using fluorescence tags such as fluorescein isothiocyanate (FITC), aminopyrene trisulfonic acid (APTS), 4,4-difluoro-4-bora-3a,4a-diaza-s-indacene (BODIPY), mnaphthalene-2,3-dicarboxaldehyde (NDA), *o*-phthaldialdehyde (OPA), 3-(2-furoyl)quinoline-2-carboxaldehyde (FQ) (88,89). Native LIF of proteins and glycopeptides at 275 nM has shown to be feasible (90), but it is difficult to achieve good sensitivity because of the intense background produced by fluorescent impurities that are usually present in real-world samples (91).

Regarding the determination of total concentration of glycoprotein biomarkers, the techniques more commonly employed are (bio)-sensors, enzyme-linked immunosorbent assay (ELISA) or lectin assay, which will be briefly discussed below.

(Bio)-sensors based on electrochemical transduction mechanisms have recently made advances into the field of glycan analysis. These glycoprotein (bio)-sensors offer simple, rapid, sensitive, and economical approaches to the measurement of biomarkers related to cancer and disease diagnostics, and bioprocess monitoring of therapeutic glycoproteins (92). The most common types of glycobiosensor design are presented in **Figure II.2.2**. All of them use selective binding agents; the most common of which are lectins (carbohydrate binding proteins), which will be discussed below, and a redox probe combined with one of the electrochemical transduction techniques, being the most common electrochemical impedance spectroscopy (EIS) and differential pulse voltammetry (DPV). Typically, when EIS is used (**Figure II.2.2 A**), the electrode (bare or modified with a nanomaterial coating) is modified with a glycan-binding agent (lectin), which imparts selectivity and affinity. In the case of a lectin biosensor sandwich assay (**Figure II.2.2 B**), a surface-bound lectin selectively attracts a glycan target to the electrode surface, and a second redox active lectin conjugate binds to the captured target. Lastly, in the case of cell surface carbohydrate analysis, the cell is often captured at an electrode surface (bare or modified with a nanomaterial coating), and a lectin-enzyme conjugate in the presence of substrate selectively binds to cell surface carbohydrates and provides the electrochemical signature (**Figure II.2.2 C**).

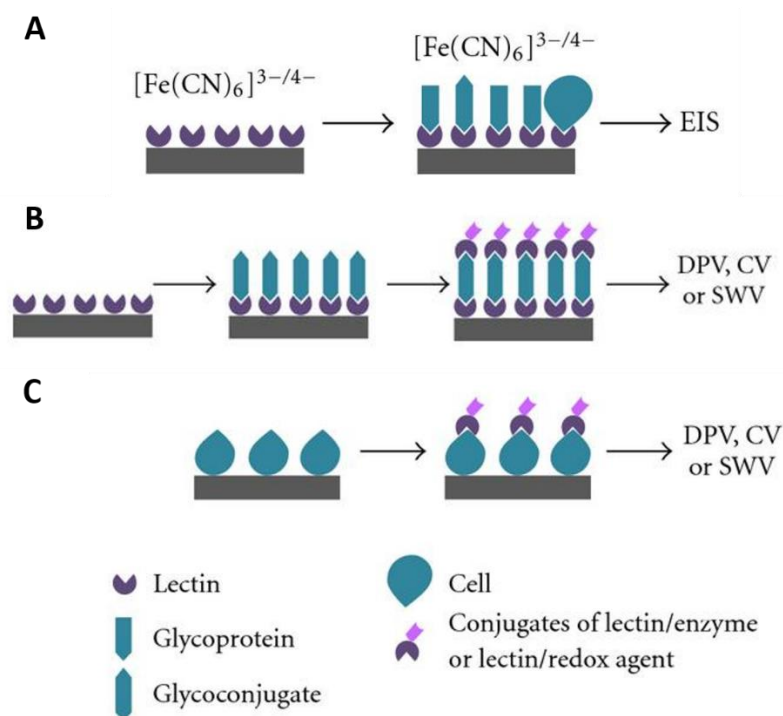


**Figure II.2.2.** Schematic showing the most common types of electrochemical (bio)-sensors for glycan analysis: (A) electrochemical impedance spectroscopy-(EIS) based assay; (B) a lectin biosensor sandwich assay; (C) surface cell carbohydrate assay using a binding lectin/enzyme conjugate to provide the electrochemical signature (93).

Talking about selective binding agents, a very efficient tool to characterize glycoprotein-glycans is offered by lectin affinity chromatography (LAC), in which labeled or non-labeled carbohydrates can be used. Due to their ability to specifically recognize distinct oligosaccharide epitopes, lectins bound to appropriate matrices like agarose, membranes, or magnetic beads, lectins allow the isolation, fractionation as well as the characterization of glycoproteins on the basis of their different glycan structures (73,94). In conjunction with other separation techniques, LAC can help to separate structural isomers and provides substantial information on their structural features.

On the other hand, ELISA is the most widely used type of immunoassay for detecting or quantifying due to its simplicity and sensitivity. Lectin-ELISA assays have been developed to analyze glycosylation changes of proteins from serum samples (95,96).

As we can see, current methods such as mass spectrometry (MS), liquid chromatography (LC), capillary electrophoresis (CE), and liquid chromatography coupled to mass spectrometry (LC-MS) have been routinely applied for glycoproteins analysis (97). Furthermore, biosensor, ELISA method and lectin assay, are commonly employed to determinate the total concentration of glycoproteins. However, these methods have adequate sensitivity but usually suffer from high cost, time-consuming procedure, and professional operation. It is for that reason, that throughout this research contained in this Doctoral Thesis, efforts will focus on electrochemical detection for glycoproteins.

### **II.2.2. Direct electroanalysis of glycoproteins**

Direct electrochemical detection (ED) of glycoproteins can be a simple and cheap strategy for glycoprotein biomarker determination, because it avoids the use of bio-reagents such as enzymes, lectins, etc., and it offers intrinsic advantages such as high sensitivity, fast response time, simple instrumentation, and low-cost. In addition, ED is among the most flexible analytical tools with instrumentation that can be miniaturized and integrated with microfluidics separation techniques, such as microchip electrophoresis (ME). However, finding a review on electrochemical techniques for protein analysis is rather difficult, and the use of ED for glycoprotein determination is extremely scarce. Nevertheless, ED of saccharides, amino acids, and peptides has been successfully implemented and this experience could be transferred to glycoprotein analysis.

Regarding carbohydrates, one of the main advantage of using ED is the possibility of direct detection (without any labeling step), and thus a simpler, faster, and more efficient carbohydrate analysis is possible compared to fluorescent/optical reading (98-100). However, there are intrinsic limitations of this approach including possible epimerization and

degradation of carbohydrates at elevated pH needed for ED and a need to know molar response for each carbohydrate to be assayed. Moreover, the method requires quite pure carbohydrates free from amino acids residues, peptides, and organic acids, to avoid interference with ED. Another problem, which was a challenge for some time, was unwanted adsorption of products of carbohydrate oxidation on the electrode surface (radical intermediates, formed through interfacial electrode reaction with carbohydrates, can rapidly foul the electrode) (99). This problem was effectively solved in 1981, when Hughes and Johnson first introduced a pulsed amperometric detection (PAD) of carbohydrates at Pt electrodes using a triple-pulse potential wave form allowing detection of carbohydrates with frequency of at least 1 Hz (101,102). Then, with the passing years, ED of carbohydrates was also performed on electrodes made from transition metals (Cu, Ni, Co, and Ru) at a constant potential. These transition metal electrodes require strongly alkaline conditions which produce oxide or hydroxide surfaces that provide electrocatalytic properties against carbohydrate oxidation (103,104). In the case of Cu and Ni electrodes, their high oxidative states (NiO(OH) and CuO(OH)) act as redox mediator for carbohydrate oxidation (105). These types of electrodes decrease the risk for surface poisoning by carbohydrate oxidation by products (103,106–108) and have contributed to the growth of carbohydrates electroanalysis.

Electrochemistry of proteins has focused on the electroactivity of non-protein redox centers (such as metal ions). At the beginning of the 1980s, it was shown that tyrosine (Tyr) and tryptophan (Trp) residues produced voltammetric oxidation signals at carbon electrodes (not only as free amino acids, but also Tyr and Trp residues yield oxidation signals in proteins) at positive potentials far from zero (**Figure II.2.3**), while other amino acids did not produce any oxidation signal at these electrodes in a pH range 4–10 (109–111). In the first decade after this discovery, the oxidation signals of proteins exhibited low sensitivity, but later by using different carbon electrodes and ED techniques (constant current chronopotentiometry stripping (CPS)), these signals became more useful tools in electrochemical protein analysis and were applied in biomedical research (112). Moreover, it was found that proteins are strongly adsorbed at carbon electrodes, which

made it possible to prepare protein-modified electrodes without covalent binding of the protein to the surface. Furthermore, it was found that using adsorptive transfer stripping voltammetry (AdTSV), which are two-step electrochemical technique (first, analytes are accumulated on an electrode and then, the amount of an accumulated species is measured by voltammetry (113)), microliter volumes of proteins were sufficient for the analysis at carbon electrodes (99).

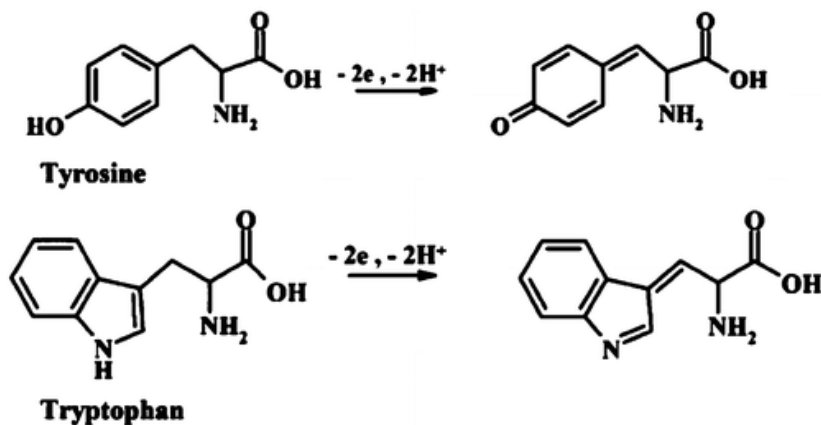


**Figure II.2.3.** Schemes of electrochemical oxidation of tyrosine (Tyr) and tryptophan (Trp) (114).

More efficient direct electron transfer (DET) can be obtained for proteins by introducing a redox center into more hydrophobic regions far from aqueous environment, thus lowering the reorganization energy (99). In this sense, there are several derivatization agents (label-based detection) that can help in the protein determination, because, covalent and non-covalent labeling of proteins can improve the selectivity and sensitivity of the method.

For example, a derivatization step is needed for amino acids and peptides detection. The family of dialdehyde compounds (NDA and OPA) combined with a nucleophile ( $CN^-$ , sulfur derivatives) are clearly the most used, but other electrochemical tags such as 6-aminoquinolyl-N-hydroxysuccinimidyl carbamate (6-AQC) and naphthalene-2,3-dicarboxaldehyde (NDTE) have been also explored (115). These compounds react with primary amines to form an electroactive and fluorescence derivative (**Figure II.2.4**).

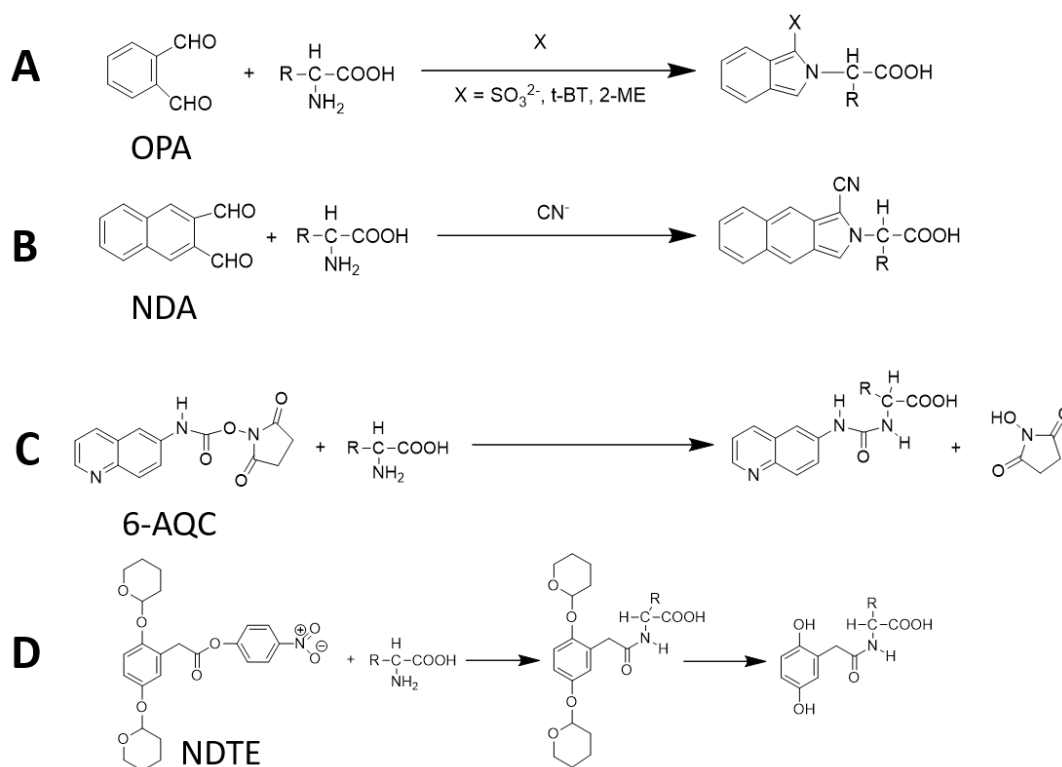


**Figure II.2.4.** Reactions of electrochemical derivatization reagents with amino acids.

On the other hand, Palecek's group explored the use of osmium complexes as electrochemical tag for the ED of carbohydrates, peptides, proteins, and glycoproteins. In the first work published by this group, they demonstrated that complex of osmium tetroxide with 2,2'-bipyridine (Os(VIII)-bipy) can be used for the modification and ED of peptides at neutral pH (116). This complex form adducts with Trp residues (**Figure II.2.5 A**), which yields a catalytic peak at  $-1.2$  V (*vs* Ag/AgCl) using differential pulse adsorptive stripping voltammetry (DPAdTSV) at a hanging mercury drop electrodes. By this technique, two peptide hormones (salmon luteinizing hormone and human luteinizing hormone) were detected at  $1 \text{ ng mL}^{-1}$  concentration. Authors extended this methodology to Trp containing proteins (avidin, streptavidin, lysozyme) (117). Again, DPAdTSV technique was employed along with a pyrolytic graphite electrode (PGE) instead of a mercury electrode. Os(VIII)-bipy-protein adduct yielded a specific signal at  $-0.54$  V at a PGE. Using this signal, a limit of detection (LOD) of tens of nanomolars were achieved for the studied proteins.



## Chapter II. Introduction

Later, the same group demonstrated that the Os(VI) complexes react with diol groups from saccharides to form osmate ester, which yields two redox couples in carbon electrodes (118,119). In another work, they modified glycoproteins with Os(VI) complexes (bipy and N,N,N,N-tetramethylethylenediamine (TEMED)) (120). Furthermore, they demonstrated that Os(VI) complexes selectively bind to the carbohydrate part and not to the polypeptidic backbone (120). Os(VI) complex reacts with hydroxyl groups from glycans to form a stable adduct (**Figure II.2.5 B**), which generates two peaks at a PGE using adsorptive transfer stripping square wave voltammetry (AdTSWV). Depending on the complex agent linked to Os(VI), the oxidation potentials of both peaks varied (-0.84 and -0.35 V for Os(VI)TEMED, -0.43 and -0.1 V for Os(VI)-bipy *vs* Ag/AgCl). This method was applied to the detection of RNaseB and avidin achieving LODs ranging from 25 to 50 nM.

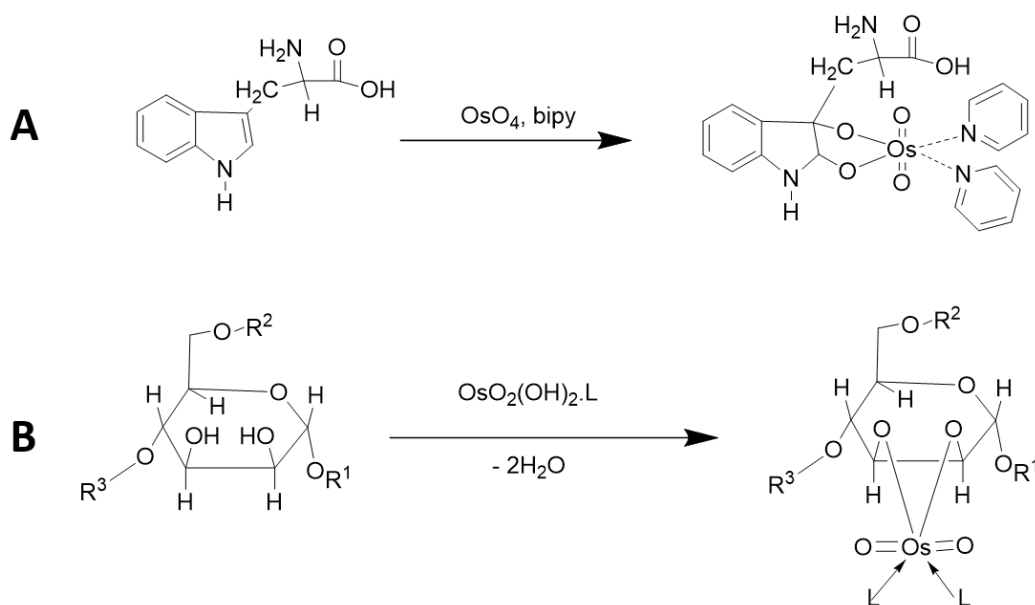


**Figure II.2.5.** Reaction of electrochemical derivatization reagents with proteins (**A**) and glycoproteins (**B**).

Additionally, it is worth mentioning that this electrochemical tag was devised by Palecek's group for carbohydrate sensing and they developed excellent applications in glycomics and transcriptomics (121,122).

## II.2. Electroanalysis of glycoproteins

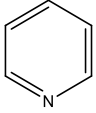
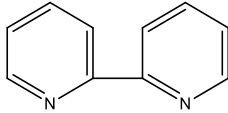
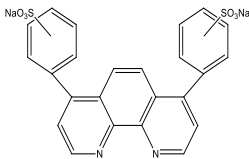
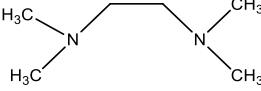
---

Other advantages of using Os(VI)L (L=ligand) are that they did not produce any electroactive adducts with DNA and proteins, suggesting high specificity in the glycoprotein measurements. Furthermore, the reaction is very simple and does not require any special equipment. The complex can be only mixed with the carbohydrate at room temperature, and the adduct is formed within hours. Using a ligand exchange process or elevated temperature (75 °C), the reaction can proceed in about 15 min (119,123). Another advantage of this labeling protocol is that a complex with a redox label can be formed after biorecognition, not disturbing the binding event.

Properties and ED behavior of Os(VI)L adduct can be significantly influenced by the nature of the chosen ligand. **Table II.2.1** shows some ligands that are useful in ED using Os(VI)L adduct. For example, by using Os(VI)bpds (bpds = bathophenanthrolinedisulfonic acid), negative charges can be introduced in the adduct. Using Os(VI)bipy, electrocatalytic peaks can be obtained allowing the determination at the picomolar level (124). The reaction of Os(VI)TEMED produces adducts particularly interesting, because these adducts can be determined using adsorptive stripping methods, without any purification step (125).

## Chapter II. Introduction

**Table II.2.1.** Nitrogenous ligands (L) applied in Os(VI)L complexes.

Ligand	Abbreviations	Appreciable catalytic peak	Structure
Pyridine	py	no	
2,2'-bipyridine	bipy	yes	
bathophenanthroline disulfonic acid	bpds	yes	
N,N,N',N'-tetramethylethylenediamine	TEMED	yes	

Excess of the reagent may interfere with the ED determination, and mostly a purification step, such as dialysis or separation on a chromatographic column or membrane, is necessary. This step can be omitted when the adsorptive transfer stripping (*ex situ*) method (125) is used with carbon electrodes (126). In adsorptive transfer stripping experiments, the electrode with strongly adsorbed adduct is washed to remove the weakly adsorbed Os(VI)L complex. The modified electrode is then transferred to the electrolytic cell containing blank background electrolyte followed by voltammetric measurement. In this way, the purification step is avoided, and the adsorption can be performed from a small analyte drop (e.g., 3–10  $\mu\text{L}$ , depending on the electrode size). Using adsorptive transfer stripping, an abundance of monomeric carbohydrates (e.g., glucose) does not interfere in the determination as it can be easily washed away from the electrode (127,128).

### II.2.2.1. Nanomaterials in the electroanalysis of glycoproteins

Considering the importance of selectivity and sensitivity toward the efficiency of detection approach, it is important create economical and stable synthetic receptors. In this sense, the choice of electrode material is nearly always a critical one. In the case of glycoproteins is not an exception and in many cases a popular approach to ultrasensitive detection is driving the enhancement of sensitivity with signal amplification. One of the earliest efforts to describe the beneficial properties of nanomaterials in the field of glycomics was published by Reichardt *et al.* in 2013, applying nanomaterials as support for the delivery of vaccines, cellular imaging, (bio)-sensors/diagnostics, glycan isolation, and enrichment (129). Since this review was published, there has been an explosion of papers focusing on the integration of nanomaterials in the field of glycomics.

Nanomaterials are often incorporated into sensor designs either to increase the surface area and subsequently the signal generated at the electrode, or as a redox agent. In general, nanomaterials-based electrochemical immunosensors amplify the sensitivity by facilitating greater loading of biorecognition molecules due to the larger sensing surface as well as by improving the electrochemical properties of the transducer (130,131).

Carbon-based nanostructures (CNMs) (carbon nanotubes, graphene, nanospheres) (132) and magnetic/metallic nanoparticles (nanowires made of inorganic materials (mainly metal oxides and metals)) (133) have been successfully applied as carriers/tracers to develop amplified electrochemical bioassays. Not only as support for the fabrication of sensitive and selective sensors, but also as materials for the preparation of stationary phases (134).

The appearance of nanomaterials revolutionized the electrochemistry, in general, and the electroanalysis, in particular. A large number of electrochemical sensors was developed using carbon and metallic nanoparticles, nanotubes, nanohorns, nanowires, and graphene (135,136). Recently, graphene like 2D nanostructures such as transition metal

dichalcogenides and phosphorene were joined to this group (137,138). In addition, the analytical performance of electrochemical detectors coupled to flow systems were dramatically improved due to these nanomaterials (139–141). Among the properties of these materials, the high active surface, high conductivity, high passivation resistance, and the electrocatalytic properties (142,143) should be noted. But the most important feature of these materials is the ability to control and shape their size and structure and, therefore, the properties of such materials opening up great possibilities when designing new sensors and bioanalytical tests. The use of nanomaterials yields an improvement of electrochemical methods in terms of sensitivity, selectivity, and reproducibility (144,145).

The choice of electrode not only affects the cost of the assay or biosensor, but also the sensitivity of the detection method. Therefore, the electrode material and design must be optimized for each application.

Nanomaterials can be classified based on their geometric shape into **(Figure II.2.6)**:

- Nanoparticles; spheres 1-50 nm in size.
- Nanowires: cylinders with diameters on the nanometer scale and lengths up to several microns.
- Nanotubes: hollow cylinders with sizes similar to nanowires, carbon nanotubes being the most representative structures.
- Nanobelts or nanorods: cone trunks with shapes similar to a cane or bell.

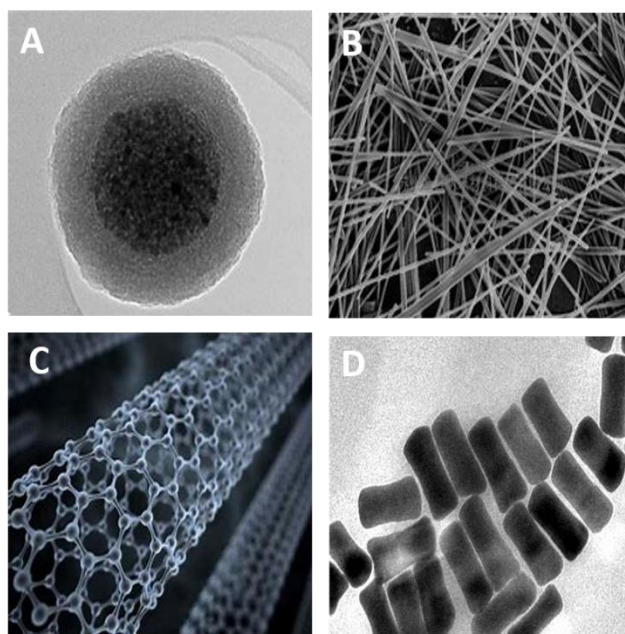


**Figure II.2.6.** Types of nanomaterials depending on their geometric shape (A) nanoparticles; (B) nanowires; (C) nanotubes; (D) nanorods.

In the case of the determination of glycoproteins, it is found in the bibliography various interesting reviews about the topic (146–148).

We will focus on carbon nanotubes (CNTs), one of the most widely used nanomaterials. CNTs were rediscovered by Iijima in 1991 (149,150) and these can be classified into two large groups based on their structure: single-walled carbon nanotubes (SWCNT) consisting of a simple sheet of graphite rolled over itself forming a hollow cylinder; and multi-walled carbon nanotubes (MWCNT) that are concentrically grouped as if it were the trunk of a tree (**Figure II.2.7**).

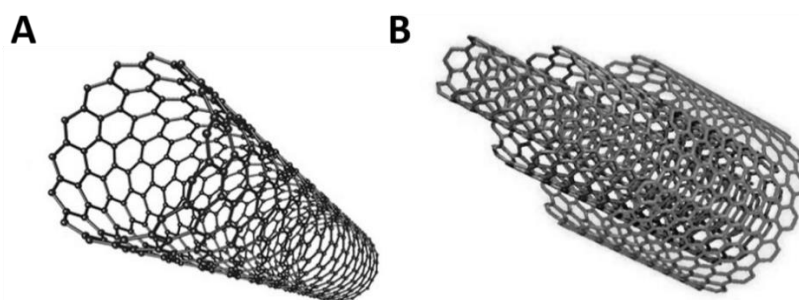


**Figure II.2.7.** Types of carbon nanotubes (A) SWCNT; (B) MWCNT.

Due to the unique and extraordinary catalytic, geometric, mechanical, electronic, and chemical properties of CNTs, these structures are the subject of extensive study in many scientific areas and taking advantage of these properties new devices have been developed. The properties that make CNTs an interesting electrodic material are the improvement of electron transfer (electrocatalytic properties) and their enormous adsorption capacity. Its large active surface area, which generates an increase in the electrochemical signal and its anti-fouling properties that improves the stability of the electrode, are other characteristics that make CNTs a very attractive material (151–153).

The properties of CNTs, such as their high electronic conductivity and mechanical resistance and their ability to catalyze redox reactions of certain compounds have revolutionized electroanalytical chemistry, generating, in recent years, a huge number of publications based on these nanomaterials (154–157).

### **II.2.3. Point-of-care testing devices based on electrochemical detection**

Traditionally, and still today, diagnostic tests are usually performed at central laboratories equipped with bench-top equipment and operated by trained personnel. Most of the analytical methods depend largely on laboratory-based analytical techniques, including LC–MS, gas chromatography coupled to mass spectrometry (GC–MS), and other techniques. The employment of these analytical instruments in clinical diagnosis incurs costly tests. Moreover, they require relatively time-consuming and complicated sample pretreatment processes (e.g., digestion or clean-up steps), complicated equipment operations, trained personnel, and specific consumables, finally lengthen the detection process, and lead to the potential loss of the target analyte. Additionally, sample transports are also needed, as experiments cannot be performed outside specialized laboratories. Furthermore, patients and physicians usually have to wait for days to receive the test results and therefore, physician can spend a lot of time to make a treatment decision, which in many cases is too late.

## II.2. Electroanalysis of glycoproteins

---

In contrast to the centralization and increased efficiency in laboratory diagnostics, there has been a recent trend towards a more decentralized diagnostic analysis, called point-of-care testing (POCT), which is commonly described as bedside, near-patient, remote, and decentralized laboratory testing. This can be performed in a hospital, emergency department, in a physician's office, or at home. The number of analytes (e.g., metabolites, proteins, microorganisms, physical and chemical parameters) that can be detected by POCT is enormous. POCT systems have made it possible to have different diagnostic tests near the patient that improve response time to care and speed up decision-making (158–160).

**Table II.2.2** shows the main differences between carry out the analysis in central laboratories or using a POCT.

**Table II.2.2.** Comparison of laboratory-based blood testing and point-of-care system (161).

Laboratory based system	Point-of-care system
1. Test is ordered	1. Test is ordered
2. Test request is processed	2. Nurse draws blood sample
3. Nurse draws blood sample	3. Sample is analyzed
4. Sample is transported to the lab	4. Results are reviewed by a nurse
5. Sample is labelled and stored	5. Clinician acts on results
6. Sample is centrifuged	
7. Serum sample is sorted to analysts	
8. Sample is analyzed	
9. Results are reviewed by the lab staff	
10. Results are reported to the department	
11. Clinician acts on results	

The foundation of today's POCT began in the late 20th century with portable glucose meters. At that time, its future seemed uncertain. Now POCT is an integral component of healthcare delivery due to real and perceived benefits including expanded access beyond traditional healthcare



## Chapter II. Introduction

---

settings, less blood required, improved patient and clinician communication and satisfaction. The global POCT market is anticipated to reach USD 35.3 billion by 2024 from 18.6 billion in 2016 (162). In this sense, Spanish Society of Laboratory Medicine (SEQCML) has launched the first POCT Test Database in Spain, called POCT ONLINE, with more than 1200 registrations and available on Internet (163). Likewise, the affordability of POCT devices is an opportunity to improve health technology in developing countries, democratizing access to diagnostic tests.

It offers the advantages of widening accessibility to diagnosis, minimal sample volumes, reduced costs, and rapid analysis times. Ideally, POCT devices must provide first results within minutes using a simple protocol with one or two steps for the analysis of whole blood, urine, or other biological samples. They are equipped with single-use test cartridges or strips that provide qualitative or quantitative results with in-built readers, while others are designed for multiple-use cartridges with quantification conducted on bench-top readers.

POCT has the potential to provide a faster result, but whether that faster result translates into improved patient care is another question. While some of the tests are important for patient care, others are sometimes unnecessary and duplicate pre-existing methods. POCT without quality control can give false results, to the patient's detriment, and increasing the overall cost of care. Therefore, it is important to develop new point-of-care platforms, which show real advantages over pre-existing methods. In this sense, the guidelines generally required for developing efficient POCT devices are provided by the WHO and are very clear. These guidelines are known as ASSURED, in which the acronym ASSURED stands for affordable, sensitive, specific, user-friendly, rapid/robust, equipment-free or minimal, and delivered to the greatest need (164). Recently, they extend the criteria: real-time connectivity and ease of sample collection (REASSURED).

Rigorous requirements are set for POCT diagnostic systems in order to satisfy the needs for POCT as follows: (a) rapid test results to allow patients to receive follow-up treatment at the point-of-care; (b) accurate, quantitative results that could be comparable to the ones from bench-top

analyzers at central laboratories, in order to avoid false diagnostics; and (c) easy-to-use systems that could be run by a non-expert, with minimum user interventions. In that sense, a “sample-to-answer” system is a desirable format because users only need to load a sample to the systems and then obtain the test results after pushing a start button (159).

The advantages and disadvantages of POCT over core laboratory testing are summarized in **Table II.2.3**.

**Table II.2.3.** Advantages and disadvantages of point-of-care testing.

Advantages	Disadvantages
Portable	Quality of results
Rapid results	Clinically focused operators
Small sample volume	Inappropriate and overutilization
Unprocessed samples	Regulatory compliance
Ease of use	Costs

The growth of POCT is supported by new analytical technologies (e.g., miniaturization, nanoparticle techniques, multiplexing, wireless connectivity, and novel biomarkers) (165). Electrochemical devices have traditionally received the major share of the attention in biosensor development producing simple and yet accurate and sensitive platforms for patient diagnosis and have been a promising approach for POCT diagnosis, mainly due to its inexpensive instrumentation and easy miniaturization.

In the next chapters of this Doctoral Thesis, three different technologies related to POCT for glycoprotein electrochemical detection, will be discussed. These technologies are screen-printed electrodes and two kind of microfluidics techniques: microchip electrophoresis and capillary-driven microfluidics devices.

### II.2.3.1. Screen-printed technology

The screen-printed technology provides a cheap and easy means to fabricate disposable electrochemical devices in bulk quantities which are used for rapid, low-cost, on-site, real-time, and recurrent industrial, pharmaceutical, or environmental analysis.

Specifically, screen-printed electrodes (SPEs), which was first introduced in the 1990s, thanks to their ability to be functionalized and customized for the detection of different analytes (e.g., DNA, proteins), have acquired a predominant importance in the last decade. Specially, when we talk about miniaturization of electrochemical analytical systems (166).

SPEs represent a successful approach to develop low-cost solutions, with the possibility to increase the level of standardization. In addition, this technology allows analysts to reduce sample volumes required for each analysis and to customize the surface for a more efficient functionalization, due to the surface of SPEs can be easily modified with various materials to fit multiple purposes related to each analyte and to achieve a variety of improvements in their sensitivity, selectivity and stability (167,168).

Literature reports different studies based on SPEs to realize electrochemical sensors addressing the sensitive and specific quantification of different proteins and biomolecules.

### II.2.3.2. Microfluidics technology

Lab-on-chip (LOC) technology is basically defined as a miniature chemistry laboratory that can perform various laboratory operations on a miniaturized scale including sampling, preparation, preconcentration, filtration, derivatization, reaction, isolation, and detection. In other words, LOC is a device which is capable of scaling the single or multiple laboratory functions down to chip-format (169–171).

One of the pillars of LOC systems is microfluidics, which is defined as the science and technology that process or manipulate small amounts of fluid (from  $10^{-9}$  to  $10^{-18}$  L) using channels measuring from tens to hundreds of micrometers (172). The technology was popularized in the early 1990s for

applications related to chemical separations, but in the intervening years it has been applied to an incredible array of applications, ranging from genomics to synthesis.

Microfluidics-based devices use channels to transport small amounts of fluid precisely by actuation forces. Multiple approaches to fluidic transport have been developed, and these fall into two categories: passive (e.g., gravity, surface tension, capillary force) and active (e.g., micropump, electric force, centrifugal force) approaches. A particularly attractive vision for the microfluidics community has been the development of integrated LOC systems that reproduce laboratory-scale processes with reduced cost, less time, and with substantially smaller footprints than their conventional counterparts.

Microfluidics diagnostic devices can analyze diverse clinical samples, including blood, oral fluid/saliva, and urine. Disposable devices can be produced, eliminating the need for washing processes between sample separations and making them easy-to-use even in remote regions. Several materials are available for constructing effective microfluidics-based devices. These materials fall into three broad categories: inorganic materials (silicon, glass, ceramics), polymeric materials (elastomers, thermoplastics), and paper. The choice of material depends on the function(s) the device will execute, the processing cost, and its compatibility with bulk manufacturing techniques.

On one hand, ME is not only the miniaturized format of CE but also a technology that provides additional functionalities such as parallelization (higher throughput), integration of multiple analytical steps and portability, and also several advantages such as shorter analysis times, lower sample and reagent consumption, and lower waste generation (green chemistry). In consequence, ME has become a good alternative to more conventional methods, which are time-consuming and expensive (173,174). Moreover, ME is a mature technology with a wide range of possibilities in LOC applications (175). ED is an excellent approach for ME due to its easy miniaturization without losing analytical performance (unlike optical

methods), and good sensitivity and moderate selectivity. Also, derivatization step is not widely needed (176,177).

On the other hand, capillary-driven microfluidics devices are an alternative scheme for miniaturized fluid handling in which liquid samples are passively wicked (or “pumped”) by lateral flow through paper substrates. Instead of using an external pump to induce flow, capillary-driven devices use the surface tension of a fluid acting on the channel wall (or fibers in the case of paper) to drive flow. Whitesides’ group popularized this phenomenon as being a member of the “microfluidics” family in 2007 (178,179), but similar ideas have been used for many decades and indeed, products relying on lateral flow are widely available to consumers in the form of pregnancy tests.

These devices are implemented by forming hydrophobic/hydrophilic patterns to guide fluid movement through paper. A variety of creative techniques have been developed to form such patterns including wax printing, inkjet printing, photolithography, flexographic printing and many others; paper can also be cut to a specific geometry to guide fluid movement (180,181) and in others cases, it can be used as pump.

Furthermore, several ways to create pump-free microfluidics have become popular due to its very low-cost, ease-to-fabrication, flexibility, disposability, and the convenience of liquid transport without applying an external driving force. For these reasons, there is great enthusiasm for using microfluidics for POCT diagnostic assays, with particular interest in their use as a low-cost platform for delivering medical diagnostics in resource-limited settings (182,183).

As explained in the review “Electrochemistry, biosensors and microfluidics: a convergence of fields” (184), electrochemistry, biosensors, and microfluidics have become increasingly linked together, making it difficult to conceive of them as separate entities.

As shown in the Venn diagram in **Figure II.2.8**, these intersections can be sub-divided into four application areas: (A) electrochemistry and microfluidics, (B) electrochemical biosensors, (C) microfluidics biosensors, and (D) microfluidics electrochemical biosensors.

Throughout the papers presented, an attempt will be made to combine these three technologies with an emphasis on how they are combining to form new application areas, including so-called “point-of-care” diagnostics, in which measurements traditionally performed in a laboratory are moved into the field. Microfluidics electrochemical biosensors, is a particularly attractive subject, with great promise for point-of-care diagnostics and other advances that are shaping the world that we live in.

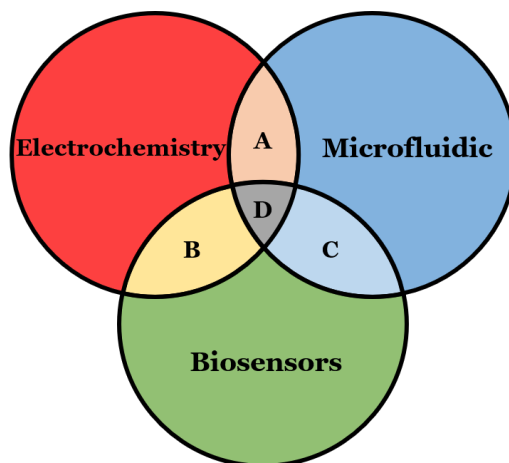


**Figure II.2.8.** Ven diagram,: electrochemistry, biosensors, and microfluidics (A) electrochemistry & microfluidics; (B) electrochemical biosensing; (C) microfluidics biosensing; (D) microfluidics electrochemical biosensing (184).

In each of the following chapters of this Doctoral Thesis, three POCT technologies (SPE, ME and capillary-driven microfluidics) have been explored for the electrochemical determination of two relevant glycoprotein biomarkers: AGP and Tf. In addition, the suitability of developed methodologies has been demonstrated in real samples (plasma and serum) and applied to the diagnosis of diseases (congenital disorders of glycosylation).

## II.3. References

1. Marth JD, Grewal PK. Mammalian glycosylation in immunity. *Nat Rev.* **2008**, 8, 874–887.
2. Merry T, Astrautsova S. Glycoproteins. In: *Encyclopedia of life sciences.* **2010.** 1–13.
3. Fairbanks AJ. The ENGases : versatile biocatalysts for the production of homogeneous N-linked glycopeptides and glycoproteins. *Chem Soc Rev.* **2017**, 46, 5128–5146.
4. Pagel O, Loroch S, Sickmann A, Zahedi RP. Current strategies and findings in clinically relevant post-translational modification-specific proteomics. *Expert Rev Proteomics.* **2015**, 12, 235–253.
5. Pascovici D, Wu JX, Mckay MJ, Joseph C, Noor Z, Kamath K, Wu Y, Ranganathan S, Gupta V, Mirzaei M. Clinically Relevant Post-Translational Modification Analyses—Maturing Workflows and Bioinformatics Tools. *Int J Mol Sci.* **2019**, 20, 16.
6. Audagnotto M, Peraro MD. Protein post-translational modifications : In silico prediction tools and molecular modeling. *Comput Struct Biotechnol J.* **2017**, 15, 307–319.
7. Woods AG, Wetie AGN, Sokolowska I, Russell S, Ryan JP, Michel TM, Thome J, Darie CC. Mass spectrometry as a tool for studying autism spectrum disorder. *J Mol Psychiatry.* **2013**, 1, 1–10.
8. Khoury GA, Baliban RC, Floudas CA. Proteome-wide post-translational modification statistics: frequency analysis and curation of the swiss-prot database. *Sci Rep.* **2011**, 1, 1–5.
9. Payne RJ, Wong C. Advances in chemical ligation strategies for the synthesis of glycopeptides and glycoproteins. *Chem Commun.* **2010**, 46, 21–43.
10. Hart GW, Copeland RJ. Glycomics Hits the Big Time. *Cell.* **2010**, 143, 672–676.
11. Bertozzi CR, Kiessling LL. Chemical Glycobiology. *Carbohydrates Glycobiol.* **2001**, 291, 2357–2365.
12. Dijk W Van, Turner GA, Mackiewicz A. Changes in glycosylation of acute-phase proteins in health and disease: occurrence, regulation and function. *Glycosylation Dis.* **1994**, 1, 5–14.
13. Li Y, Tran AH, Danishefsky SJ, Tan Z. Chemical biology of glycoproteins: From chemical synthesis to biological impact. 1st ed. Vol. 621, *Chemical and Synthetic Biology Approaches To Understand Cellular Functions - Part A.* Elsevier Inc.; **2019.** 213–229.

14. Almeida A, Kolarich D. The promise of protein glycosylation for personalised medicine. *Biochim Biophys Acta - Gen Subj.* **2016**, 1860, 1583–1595.
15. Connelly MA, Gruppen EG, Otvos JD, Dullaart RPF. Inflammatory glycoproteins in cardiometabolic disorders, autoimmune diseases and cancer. *Clin Chim Acta.* **2016**, 459, 177–186.
16. Lyons JJ, Milner JD, Rosenzweig SD. Glycans instructing immunity: the emerging role of altered glycosylation in clinical immunology. *Front Pediatr.* **2015**, 3, 54.
17. Lauc G, Walker JM. Ubiquitous Importance of Protein Glycosylation. *Methods Mol Biol.* **2017**, 1503, 1–13.
18. Gamblin DP, Scanlan EM, Davis BG. Glycoprotein Synthesis: An Update. *Chem Rev.* **2009**, 109, 131–163.
19. Raj I, Al Hosseini SH, Dioguardi E, Nishimura K, Han L, Villa A, Sanctis D, Jovine L. Structural Basis of Egg Coat-Sperm Recognition at Fertilization. *Cell.* **2017**, 169, 1315–1326.
20. López-Salguero JB, Fierro R, Michalski J, Jiménez-Morales I, Lefebvre T, Mondragón-Payne O, Baldini SF, Vercoutter-Edouart AS, González-Márquez H. Identification of lipid raft glycoproteins obtained from boar spermatozoa. *Glycoconj J.* **2020**, 37, 499–509.
21. Aoki T. A Comprehensive Review of Our Current Understanding of Red Blood Cell (RBC) Glycoproteins. *Membranes (Basel).* **2017**, 7, 1–19.
22. Spiegel M, Plegge T, Pöhlmann S. The Role of Phlebovirus Glycoproteins in Viral Entry, Assembly and Release. *Viruses.* **2016**, 8, 1–20.
23. Pu J, Wang Q, Xu W, Lu L, Jiang S. Development of Protein- and Peptide-Based HIV Entry Inhibitors Targeting gp120 or gp41. *Viruses.* **2019**, 11, 1–35.
24. Parajuli B, Acharya K, Yu R, Ngo B, Rashad AA, Abrams CF, Chaiken IM. Lytic Inactivation of Human Immunodeficiency Virus by Dual Engagement of gp120 and gp41 Domains in the Virus Env Protein Trimer. *Biochemistry.* **2016**, 55, 6100–6114.
25. Komaromy A, Reider B, Jarvas G, Guttman A. Glycoprotein biomarkers and analysis in chronic obstructive pulmonary disease and lung cancer with special focus on serum immunoglobulin G. *Clin Chim Acta.* **2020**, 506, 204–213.
26. Margolin E, Chapman R, Williamson A, Rybicki EP, Meyers AE. Production of complex viral glycoproteins in plants as vaccine immunogens. *Plant Biotechnol J.* **2018**, 16, 1531–1545.



27. Hu M, Lan Y, Lu A, Ma X, Zhang L. Glycan-based biomarkers for diagnosis of cancers and other diseases: Past, present, and future. In: *Progress in Molecular Biology and Translational Science*. 1st ed. Elsevier Inc.; **2019**, 1–24.
28. Silsirivanit A. Glycosylation markers in cancer. In: *Advances in Clinical Chemistry*. 1st ed. Elsevier Inc.; **2019**, 189–213.
29. Pan S, Brentnall TA, Chen R. Glycoproteins and glycoproteomics in pancreatic cancer. *J Gastroenterol*. **2016**, 22, 9288–9299.
30. Kailemia MJ, Park D, Lebrilla CB. Glycans and glycoproteins as specific biomarkers for cancer. *Anal Bioanal Chem*. **2017**, 409, 395–410.
31. Sajic T, Liu Y, Arvaniti E, Surinova S, Williams E, Schiess R, Hüttenhain R, Sethi A, Pan S, Brentnall TA, Chen R, Blattmann P, Friedrich B, Niméus E, Malander S, Omlin A, Gillessen S, Claassen M, Aebbersol R. Similarities and Differences of Blood N- Glycoproteins in Five Solid Carcinomas at Localized Similarities and Differences of Blood N-Glycoproteins in Five Solid Carcinomas at Localized Clinical Stage Analyzed by SWATH-MS. *Cell Rep*. **2018**, 29, 2819–2831.
32. Scott E, Munkley J. Glycans as Biomarkers in Prostate Cancer. *Int J Mol Sci*. **2019**, 20, 1–20.
33. Haran J, Bhattarai S, Foley S, Dutta P, Ward DV, Bucci V, McCormick BA. Alzheimer's Disease Microbiome Is Associated with Dysregulation of the Anti-Inflammatory P-glycoprotein Pathway. *MBio*. **2019**, 10, 1–14.
34. Hayes AJ, Melrose J. Glycans and glycosaminoglycans in neurobiology: key regulators of neuronal cell function and fate. *Biochem J*. **2018**, 475, 2511–2545.
35. WHO. C-reactive protein concentrations as a marker of inflammation or infection for interpreting biomarkers of micronutrient status. *World Health Organization*. **2014**, 1–4.
36. Suchdev PS, Williams AM, Mei Z, Flores-Ayala R, Pasricha S, Rogers LM, Namaste SML. Assessment of iron status in settings of inflammation: challenges and potential approaches. *Am J Clin Nutr*. **2017**, 106, 1626–1633.
37. Gannon BM, Glesby MJ, Finkelstein JL, Raj T, Erickson D, Mehta S. A point-of-care assay for alpha-1-acid glycoprotein as a diagnostic tool for rapid, mobile-based determination of inflammation. *Curr Res Biotechnol*. **2019**, 1, 41–48.
38. Hocheplied T, Berger FG, Baumann H, Libert C. Alpha1 -Acid glycoprotein: an acute phase protein with inflammatory and immunomodulating properties. *Cytokine Growth Factor Rev*. **2003**, 14, 25–34.

39. Puerta A, Díez-Masa JC, Martín-Álvarez PJ, Martín-Ventura JL, Barbas C, Tuñón J, Egido J, De Frutos M. Study of the capillary electrophoresis profile of intact  $\alpha$ -1-acid glycoprotein isoforms as a biomarker of atherothrombosis. *Analyst*. **2011**, 136, 816–822.
40. Lacunza I, Sanz J, Díez-Masa JC, de Frutos M. CZE of human alpha-1-acid glycoprotein for qualitative and quantitative comparison of samples from different pathological conditions. *Electrophoresis*. **2006**, 27, 4205–4214.
41. Schönfeld DL, Ravelli RBG, Mueller U, Skerra A. The 1.8-Å Crystal Structure of  $\alpha$ 1 -Acid Glycoprotein (Orosomucoid) Solved by UV RIP Reveals the Broad Drug-Binding Activity of This Human Plasma Lipocalin. *J Mol Biol*. **2008**, 384, 393–405.
42. Fournier T, Medjoubi-n N, Porquet D. Alpha-1-acid glycoprotein. *Biochim Biophys Acta*. **2000**, 1482, 157–171.
43. Clerc F, Reiding KR, Jansen BC, Kammeijer GSM, Bondt A, Wuhrer M. Human plasma protein N -glycosylation. *Glycoconj J*. **2016**, 33, 309–343.
44. İpek İÖ, Saracoglu M, Bozaykut A.  $\alpha$ 1 -Acid glycoprotein for the early diagnosis of neonatal sepsis. *J Matern Neonatal Med*. **2010**, 23, 617–621.
45. Gannon BM, Glesby MJ, Finkelstein JL, Raj T. A point-of-care assay for alpha-1-acid glycoprotein as a diagnostic tool for rapid, mobile-based determination of inflammation. *Curr Res Biotechnol*. **2019**, 1, 41–48.
46. Gomme PT, Mccann KB. Transferrin: structure, function and potential therapeutic actions applications of this protein. *Drug Discov Today*. **2005**, 10, 267–273.
47. Kawabata H. Transferrin and transferrin receptors update. *Free Radic Biol Med*. **2019**, 133, 46–54.
48. Xiao G, Liu Z, Zhao M, Wang H, Zhou B. Transferrin 1 Functions in Iron Trafficking and Genetically Interacts with Ferritin in *Drosophila melanogaster*. *Cell Rep*. **2019**, 26, 748–758.
49. Macgillivray RTA, Moore SA, Chen J, Anderson BF, Baker H, Luo Y., et al. Biological Macromolecular Structures Enabling Breakthroughs in Research and Education. *Protein Data Bank*. **1998**, p. <https://www.rcsb.org/structure/1a8e>.
50. Szőke D, Panteghini M. Diagnostic value of transferrin. *Clin Chim Acta*. **2012**, 413, 1184–1189.
51. Elsayed ME, Sharif MU, Stack AG. Transferrin Saturation : A Body Iron Biomarker. 1st ed. Vol. 75, *Advances in Clinical Chemistry*. Elsevier Inc.; **2016**, 71–97.

52. Kami T, Szczygie J, Jurecka P, Irnazarow I. The many faces of transferrin: Does genotype modulate immune response? *Fish Shellfish Immunol.* **2020**, 102, 511–518.
53. Nam Y, Kim Y, Chang J, Kho H. Salivary biomarkers of inflammation and oxidative stress in healthy adults. *Arch Oral Biol.* **2019**, 97, 215–222.
54. Bortolotti F, Paoli G De, Tagliaro F. Carbohydrate-deficient transferrin (CDT) as a marker of alcohol abuse: A critical review of the literature 2001 – 2005. *J Chromatogr B.* **2006**, 841, 96–109.
55. Scherpenzeel M Van, Willems E, Lefeber DJ. Clinical diagnostics and therapy monitoring in the congenital disorders of glycosylation. *Glycoconj J.* **2016**, 33, 345–358.
56. Jaeken J. Congenital disorders of glycosylation. *Ann N Y Acad Sci.* **2010**, 1214, 190–198.
57. Verheijen J, Tahata S, Kozicz T, Witters P, Morava E. Therapeutic approaches in Congenital Disorders of Glycosylation (CDG) involving N-linked glycosylation: an update. *Genet Med.* **2019**, 1–12.
58. Ondruskova N, Cechova A, Hansikova H, Honzik T. BBA - General Subjects Congenital disorders of glycosylation: Still “ hot ” in 2020. *BBA - Gen Subj.* **2021**, 1865, 129751.
59. Orphanet Report Series - Prevalence of rare diseases: Bibliographic data. Jan, **2021**. [http://www.orpha.net/orphacom/cahiers/docs/GB/Prevalence\\_of\\_rare\\_diseases\\_by\\_decreasing\\_prevalence\\_or\\_cases.pdf](http://www.orpha.net/orphacom/cahiers/docs/GB/Prevalence_of_rare_diseases_by_decreasing_prevalence_or_cases.pdf).
60. Gilfix BM. Congenital disorders of glycosylation and the challenge of rare diseases. *Hum Mutat.* **2019**, 40, 1010-1012.
61. Scott K, Gadomski T, Kozicz T, Morava E. Congenital disorders of glycosylation: new defects and still counting. *J Inherit Metab Dis.* **2014**, 37, 609–617.
62. Chang IJ, He M, Lam CT. Congenital disorders of glycosylation. *Ann Transl Med.* **2018**, 6, 1–13.
63. Wolthuis DFGJ, Janssen MC, Cassiman D, Lefeber DJ, Morava-Kozicz E. Defining the phenotype and diagnostic considerations in adults with congenital disorders of N-linked glycosylation. *Expert Rev Mol Diagn.* **2014**, 14, 217–224.
64. Pérez-Cerdá C, Girós M, Serrano M, Pérez Dueñas B. Trastornos de la glicosilación. *XI Congreso Nacional de Errores Congénitos del Metabolismo.* **2015**, 13–27.
65. Al Teneiji A, Bruun TUJ, Sidky S, Cordeiro D, Cohn RD, Mendoza-Londono R, Mahendranath M, Raiman J, Siriwardena K, Kyriakopoulou L, Mercimek-Mahmutoglu S. Phenotypic and genotypic spectrum of congenital disorders of glycosylation type I and type II. *Mol Genet Metab.* **2017**, 120, 235–242.

66. Jaeken J. Congenital disorders of glycosylation. 1st ed. Vol. 113, Chapter 179, *Handbook of Clinical Neurology. Pediatric Neurology, Part III*. Elsevier B.V. **2013**, 1737-1743.
67. Bantscheff M, Lemeer S, Savitski MM, Kuster B. Quantitative mass spectrometry in proteomics: critical review update from 2007 to the present. *Anal Bioanal Chem*. **2012**, 404, 939–965.
68. Sapan C V, Lundblad RL. Review of methods for determination of total protein and peptide concentration in biological samples. *Proteomics Clin Appl*. **2015**, 9, 268–276.
69. Wu D, Li J, Struwe WB, Robinson C V. Probing N-glycoprotein microheterogeneity by lectin affinity purification-mass spectrometry analysis. *Chemical Science*. **2019**, 10, 5146-5155.
70. Kolarich D, Jensen PH, Altmann F, Packer NH. Determination of site-specific glycan heterogeneity on glycoproteins. *Nat Protoc*. **2012**, 7, 7–9.
71. Ruhaak LR, Xu G, Li Q, Goonatileke E, Lebrilla CB. Mass Spectrometry Approaches to Glycomic and Glycoproteomic Analyses. *Chem Rev*. **2018**, 118, 7886–7930.
72. Gaunitz S, Nagy G, Pohl NLB, Novotny M V. Recent Advances in the Analysis of Complex Glycoproteins. *Anal Chem*. **2017**, 89, 389–413.
73. Geyer H, Geyer R. Strategies for analysis of glycoprotein glycosylation. *Biochim Biophys Acta*. **2006**, 1764, 1853–1869.
74. Shajahan A, Heiss C, Ishihara M, Azadi P. Glycomic and glycoproteomic analysis of glycoproteins—a tutorial. *Anal Bioanal Chem*. **2017**, 409, 4483–4505.
75. Roth Z, Yehezkel G, Khalaila I. Identification and Quantification of Protein Glycosylation. *Int J Carbohydr Chem*. **2012**, 2012, 1–10.
76. Kailemia MJ, Xu G, Wong M, Li Q, Goonatileke E, Leon F, Lebrilla CB. Recent Advances in the Mass Spectrometry Methods for Glycomics and Cancer. *Anal Chem*. **2018**, 90, 208–224.
77. Dong X, Huang Y, Gwan Cho B, Zhong J, Gautam S, Peng W, Williamson SD, Banazadeh A, Torres-Ulloa KY, Mechref Y. Advances in mass spectrometry-based glycomics. *Electrophoresis*. **2018**, 39, 3063–3081.
78. Hajba L, Csanky E, Guttman A. Liquid phase separation methods for N-glycosylation analysis of glycoproteins of biomedical and biopharmaceutical interest . A critical review. *Anal Chim Acta*. **2016**, 943, 8–16.
79. Stumpe M, Miller C, Morton NS, Bell G, Watson DG. High-performance liquid chromatography determination of  $\alpha$ 1-acid glycoprotein in small volumes of plasma from neonates. *J Chromatogr B Anal Technol Biomed Life Sci*. **2006**, 831, 81–84.

80. Vreeker GCM, Wuhrer M. Reversed-phase separation methods for glycan analysis. *Anal Bioanal Chem.* **2017**, 409, 359–378.
81. Pedrali A, Tengattini S, Marrubini G, Bavaro T, Hemström P, Massolini G, Terreni M, Temporini C. Characterization of Intact Neoglycoproteins by hydrophilic interaction liquid chromatography. *Molecules.* **2014**, 19, 9070–9088.
82. Stavenhagen K, Kolarich D, Wuhrer M. Clinical Glycomics Employing Graphitized Carbon Liquid Chromatography–Mass Spectrometry. *Chromatographia.* **2015**, 78, 307–320.
83. Yang X, Bartlett MG. Glycan analysis for protein therapeutics. *J Chromatogr B.* **2019**, 1120, 29–40.
84. Lu G, Crihfield CL, Gattu S, Veltri LM, Holland LA. Capillary Electrophoresis Separations of Glycans. *Chem Rev.* **2018**, 118, 7867–7885.
85. Zhang C, Bi C, Clarke W, Hage DS. Glycoform analysis of alpha-1-acid glycoprotein based on capillary electrophoresis and electrophoretic injection. *J Chromatogr A.* **2017**, 1523, 114–122.
86. Tang L, De Seta F, Odreman F, Venge P, Piva C, Guaschino S, García RC. Proteomic Analysis of Human Cervical-Vaginal Fluids. *J Proteome Res.* **2007**, 6, 2874–2883.
87. Staub A, Guillarme D, Schappler J, Veuthey J, Rudaz S. Intact protein analysis in the biopharmaceutical field. *J Pharm Biomed Anal.* **2011**, 55, 810–822.
88. Wuethrich A, Quirino JP. Derivatization for separation and detection in capillary electrophoresis (2012 – 2015). *Electrophoresis.* **2016**, 37, 45–55.
89. Rigas PG. Post-column labeling techniques in amino acid analysis by liquid chromatography. *Anal Bioanal Chem.* **2013**, 405, 7957–7992.
90. Lee TT, Yeung ES. Quantitative Determination of Native Proteins in Individual Human Erythrocytes by Capillary Zone Electrophoresis with Laser-Induced Fluorescence Detection. *Anal Chem.* **1992**, 64, 3045–3051.
91. Garrido-Medina R, Puerta A, Rivera-Monroy Z, Frutos M De, Guttman A, Diez-Masa C. Analysis of alpha-1-acid glycoprotein isoforms using CE-LIF with fluorescent thiol derivatization. *Electrophoresis.* **2012**, 33, 1113–1119.
92. Marcelino P, Cassandra L, Barroso B. Electrochemical Biosensing Strategies to Detect Serum Glycobiomarkers. *Adv Res.* **2016**, 6, 1–17.
93. Sánchez-Pomales G, Zangmeister RA. Recent Advances in Electrochemical Glycobiosensing. *Int J Electrochem.* **2011**, 2011, 1–11.
94. Clark D, Mao L. Cancer biomarker discovery: Lectin-based strategies targeting glycoproteins. *Dis Markers.* **2012**, 33, 1–10.

95. Wu J, Xie X, Liu Y, He J, Benitez R, Buckanovich RJ, Lubman, DM. Identification and Confirmation of Differentially Expressed Fucosylated Glycoproteins in the Serum of Ovarian Cancer Patients Using a Lectin Array and LC–MS/MS. *J Proteome Res.* **2012**, 11, 4541–4552.
96. Wu J, Zhu J, Yin H, Buckanovich RJ, Lubman DM. Analysis of Glycan Variation on Glycoproteins from Serum by the Reverse Lectin-Based ELISA Assay. *J Proteome Res.* **2014**, 13, 2197–2204.
97. Alley WR, Mann BF, Novotny M V. High-sensitivity Analytical Approaches for the Structural Characterization of Glycoproteins. *Chem Rev.* **2013**, 113, 2668–2732.
98. Baldwi RP. Electrochemical Detection of Carbohydrates at Constant Potential after HPLC and CE Separations (Chapter 26). *Carbohydrate Analysis by Modern Chromatography and Electrophoresis.* **2002**, 947-959.
99. Paleček E, Tkac J, Bartosik M, Bertok T, Ostatná V, Paleček J. Electrochemistry of Nonconjugated Proteins and Glycoproteins. Toward Sensors for Biomedicine and Glycomics. *Chem Rev.* **2015**, 115, 2045–2108.
100. Dorte S, Sierra T, Crevillen AG, Escarpa A. Chapter 14: CE/microchip electrophoresis of carbohydrates and glycoconjugates with electrochemical detection. In: *Carbohydrate Analysis by Modern Liquid Phase Separation Techniques.* **2021**.
101. Corradini C, Cavazza A, Bignardi C. Coupled with Pulsed Electrochemical Detection as a Powerful Tool to Evaluate Carbohydrates of Food Interest: Principles and Applications. *Int J Carbohydr Chem.* **2012**, 2012,1–13.
102. Hughes S, Johson DC. Amperometric detection of simple carbohydrates at platinum electrodes in alkaline solutions by application of a triple-pulse potential waveform. *Anal Chim Acta.* **1981**, 132, 11–22.
103. García M, Escarpa A. Disposable electrochemical detectors based on nickel nanowires for carbohydrate sensing. *Biosens Bioelectron.* **2011**, 26, 2527–2533.
104. Torto N. Recent progress in electrochemical oxidation of saccharides at gold and copper electrodes in alkaline solutions. *Bioelectrochemistry.* **2009**, 76, 195–200.
105. Toghil K, Xiao L, Phillips M, Compton R. The non-enzymatic determination of glucose using an electrolytically fabricated nickel microparticle modified boron-doped diamond electrode or nickel foil electrode. *Sensors Actuators B Chem.* **2010**, 147, 642–652.

106. Fu Y, Zhang L, Chen G. Preparation of a carbon nanotube-copper nanoparticle hybrid by chemical reduction for use in the electrochemical sensing of carbohydrates. *Carbon*. **2012**, 50, 2563–2570.
107. Male KB, Hrapovic S, Liu Y, Wang D, Luong JHT. Electrochemical detection of carbohydrates using copper nanoparticles and carbon nanotubes. *Anal Chim Acta*. **2004**, 516, 35–41.
108. Zhang W, Zhang X, Zhang L, Chen G. Fabrication of carbon nanotube-nickel nanoparticle hybrid paste electrodes for electrochemical sensing of carbohydrates. *Sensors Actuators B Chem*. **2014**, 192, 459–466.
109. Brabec V, Mornstein V. Electrochemical behaviour of proteins at graphite electrodes I. Electrooxidation of proteins as a new probe of protein structure and reactions. *Biochim Biophys Acta*. **1980**, 625, 43–50.
110. Brabec V, Mornstein V. Electrochemical behaviour of proteins at graphite electrodes II. Electrooxidation of amino acids. *Biophys Chem*. **1980**, 12, 159–165.
111. Malfoy B, Reynaud J. Electrochemical investigations of amino acids at solid electrodes: Part II. Amino acids containing no sulfur atoms: Tryptophan, tyrosine, histidine and derivatives. *J Electroanal Chem Interfacial Electrochem*. **1980**, 114, 213–223.
112. Paleček E, Bartosik M, Ostatná V, Trefulka M. Electrocatalysis in Proteins, Nucleic Acids and Carbohydrates. *Chem Rec*. **2012**, 12, 27–45.
113. Pingarrón JM, Labuda J, Barek J, Brett CMA, Camoes MF, Fojta M, Hibbert B. Terminology of electrochemical methods of analysis (IUPAC Recommendations 2019). *Pure Appl Chem*. **2020**, 92, 641–694.
114. Suprun E V, Zharkova MS, Morozevich GE, Veselovsky A V, Shumyantseva V V, Archakov AI. Analysis of Redox Activity of Proteins on the Carbon Screen Printed Electrodes. *Electroanalysis*. **2013**, 25, 2109–1216.
115. Sierra T, Crevillen AG, Escarpa A. Derivatization agents for electrochemical detection in amino acid, peptide and protein separations: The hidden electrochemistry? *Electrophoresis*. **2017**, 38, 2695–2703.
116. Billova S, Kizek R, Paleček E. Differential pulse adsorptive stripping voltammetry of osmium-modified peptides. *Bioelectrochemistry*. **2002**, 56, 63–66.
117. Fojta M, Billová S, Havran L, Pivonková H, Cernocká H, Horáková P, Paleček E. Osmium Tetroxide, 2,2'-Bipyridine: Electroactive Marker for Probing Accessibility of Tryptophan Residues in Proteins. *Anal Chem*. **2008**, 80, 4598–4605.

118. Trefulka M, Paleček E. Voltammetry of Os(VI)-Modified Polysaccharides at Carbon Electrodes. *Electroanalysis*. **2009**, 21, 1763–1766.
119. Trefulka M, Paleček E. Modification of poly- and oligosaccharides with Os(VI)pyridine. Voltammetry of the Os(VI) adducts obtained by ligand exchange. *Electroanalysis*. **2013**, 25, 1813–1817.
120. Trefulka M, Paleček E. Direct chemical modification and voltammetric detection of glycans in glycoproteins. *Electrochem commun*. **2014**, 48, 52–55.
121. Strmecki S, Trefulka M, Zatloukalová P, Durech M, Vojtesek B, Paleček E. Immunoassays of chemically modified polysaccharides, glycans in glycoproteins and ribose in nucleic acids. *Anal Chim Acta*. **2017**, 955, 108–115.
122. Bartosik M, Trefulka M, Hrstka R, Vojtesek B, Palecek E. Os (VI) bipy-based electrochemical assay for detection of specific microRNAs as potential cancer biomarkers. *Electrochem commun*. **2013**, 33, 55–58.
123. Trefulka M, Paleček E. Voltammetric determination of Os (VI)-modified oligosaccharides at nanomolar level. *Bioelectrochemistry*. **2012**, 88, 8–14.
124. Paleček E, Trefulka M. Electrocatalytic detection of polysaccharides at picomolar concentrations. *Analyst*. **2011**, 136, 321–326.
125. Trefulka M, Paleček E. Voltammetry of Os(VI)-Modified Polysaccharides. *Electroanalysis*. **2010**, 22, 1837–1845.
126. Bartosik M, Hrstka R, Palecek E, Vojtesek B. Adsorptive Transfer Stripping for Quick Electrochemical Determination of microRNAs in Total RNA Samples. *Electroanalysis*. **2014**, 26, 2558–2562.
127. Krizkova S, Fabrik I, Adam V, Kukacka J, Prusa R, Chavis G, Trnkova L, Strnadel J, Horak V, Kizek R. Utilizing of Adsorptive Transfer Stripping Technique Brdicka Reaction for Determination of Metallothioneins Level in Melanoma Cells, Blood Serum and Tissues. *Sensors*. **2008**, 8, 3106–3122.
128. Stremecki S, Plavsic M. Adsorptive transfer chronopotentiometric stripping of sulphated polysaccharides. *Electrochem commun*. **2012**, 18, 100–103.
129. Reichardt NC, Martín-Lomas M, Penadés S. Glyconanotechnology. *Chem Soc Rev*. **2013**, 42, 4358–4376.
130. Tiwari JN, Vij V, Kemp KC, Kim KS. Engineered Carbon-Nanomaterial-Based Electrochemical Sensors for Biomolecules. *ACS Nano*. **2016**, 10, 46–80.
131. Wang Y, Qu K, Tang L, Li Z, Moore E, Zeng X, Liu Y, Li J. Nanomaterials in carbohydrate biosensors. *Trends Anal Chem*. **2014**, 58, 54–70.



132. Gao C, Guo Z, Liu J, Huang X. The new age of carbon nanotubes: An updated review of functionalized carbon nanotubes in electrochemical sensors. *Nanoscale*. **2012**, 4, 1948–1963.
133. Kokkinos C, Economou A. Emerging trends in biosensing using stripping voltammetric detection of metal-containing nanolabels- A review. *Anal Chim Acta*. **2017**, 961, 12–32.
134. Crevillén AG, Escarpa A, García CD. Chapter 1: Carbon-based Nanomaterials in Analytical Chemistry. In: *Carbon-based Nanomaterials in Analytical Chemistry*. **2018**. p. 1–36. Detection Science Series. Editorial: Royal Society of Chemistry
135. Pingarrón JM, Yáñez-Sedeño P, González-Cortés A. Gold nanoparticle-based electrochemical biosensors. *Electrochim Acta*. **2008**, 53, 5848–5866.
136. Yang W, Ratinac KR, Ringer SP, Thordarson P, Gooding JJ, Braet F. Carbon Nanomaterials in Biosensors: Should You Use Nanotubes or Graphene? *Angew Chem Int Ed*. **2010**, 49, 2114–2138.
137. Sajedi-Moghaddam A, Saievar-Iranizad E, Pumera M. Two-dimensional transition metal dichalcogenide/conducting polymer composites: synthesis and applications. *Nanoscale*. **2017**, 9, 8052–8065.
138. Pumera M. Phosphorene and black phosphorus for sensing and biosensing. *Trends Anal Chem*. **2017**, 93, 1–6.
139. Martín A, López MÁ, Gonzalez MC, Escarpa A. Multidimensional carbon allotropes as electrochemical detectors in capillary and microchip electrophoresis. *Electrophoresis*. **2015**, 36, 179–194.
139. Pumera M, Escarpa A. Nanomaterials as electrochemical detectors in microfluidics and CE: Fundamentals, designs, and applications. *Electrophoresis*. **2009**, 30, 3315–3323.
141. Moreno M, Sánchez A, Bermejo E, Zapardiel A, Chicharro M. Carbon nanotubes as analytical tools in capillary electromigration methods. *Appl Mater Today*. **2017**, 9, 456–481.
142. Scida K, Stege PW, Haby G, Messina GA, García CD. Recent applications of carbon-based nanomaterials in analytical chemistry: Critical review. *Anal Chim Acta*. **2011**, 691, 6–17.
143. Pérez-López B, Merkoçi A. Carbon nanotubes and graphene in analytical sciences. *Microchim Acta*. **2012**, 179, 1–16.
144. García M, Batalla P, Escarpa A. Metallic and polymeric nanowires for electrochemical sensing and biosensing. *Trends Anal Chem*. **2014**, 57, 6–22.
145. Agüí L, Yáñez-Sedeño P, Pingarrón JM. Role of carbon nanotubes in electroanalytical chemistry. A review. *Anal Chim Acta*. **2008**, 622, 11–47.

146. Dosekova E, Filip J, Bertok T, Both P, Kasak P, Tkac J. Nanotechnology in Glycomics: Applications in Diagnostics, Therapy, Imaging, and Separation Processes. *Med Res Rev.* **2016**, 37, 514–626.
147. Sun N, Wu H, Chen H, Shen X, Deng C. Advances in hydrophilic nanomaterials for glycoproteomics. *Chem Commun.* **2019**, 55, 10359–10375.
148. Sun N, Wu H, Shen X, Deng C. Nanomaterials in Proteomics. *Adv Funct Mater.* **2019**, 29, 1900253.
149. Iijima S. Helical microtubes of graphitic carbon. *Nature.* **1991**, 354, 56–58.
150. Iijima S, Ichihashi T. Single-shell carbon nanotubes of 1-nm diameter. *Nature.* **1993**, 363, 603–605.
151. Anzar N, Hasan R, Tyagi M, Yadav N, Narang J. Carbon nanotube - A review on Synthesis, Properties and plethora of applications in the field of biomedical science. *Sensors Int.* **2020**, 1, 100003.
152. Beitollahi H, Movahedifar F, Tajik S, Jahani S. A Review on the Effects of Introducing CNTs in the Modification Process of Electrochemical Sensors. *Electroanalysis.* **2019**, 31, 1195–1203.
153. Armenta S, Esteve-Turrillas FA. Chapter 11: Carbon-based nanomaterials in Analytical Chemistry. In: *Handbook of Smart Materials in Analytical Chemistry.* **2019**.
154. Moretto L, Metelka R, Scopece P. Chapter 5: Carbon nanomaterials in electrochemical detection. In: *Carbon-based Nanomaterials in Analytical Chemistry.* **2019**.
155. Quesada-Gonzalez D, Merkoci A. Nanomaterial-based devices for point-of-care diagnostic applications. *Chem Soc Rev.* **2018**, 47, 4697–4709.
156. Loh KP, Ho D, Chee Chiu GN, Leong DT, Pastorin G, Chow EKH. Clinical Applications of Carbon Nanomaterials in Diagnostics and Therapy. *Adv Mater.* **2018**, 1802368, 1–21.
157. Baby R, Saifullah B, Zobir Hussein M. Carbon Nanomaterials for the Treatment of Heavy Metal-Contaminated Water and Environmental Remediation. *Nanoscale Res Lett.* **2019**, 14, 1–17.
158. Warsinke A. Point-of-care testing of proteins. *Anal Bioanal Chem.* **2009**, 393, 1393–1405.
159. Jung W, Han J, Choi J, Ahn CH. Point-of-care testing (POCT) diagnostic systems using microfluidic lab-on-a-chip technologies. *Microelectron Eng.* **2015**, 132, 46–57.
160. Nichols JH. Point-of-care testing. In *Contemporary Practice in Clinical Chemistry (Fourth Edition).* **2020**, 323–336.
161. Tüdos AJ, Besselink AJ, Schasfoort RBM. Trends in miniaturized total analysis systems for point-of-care testing in clinical chemistry. *Lab Chip.* **2001**, 1, 83–95.

162. Marketers MEDIA. Point-Of-Care Testing (POCT) Market Outlook 2017 To 2024: Blood Glucose Testing Kits Is Driving The Market – According To New Research Study. **2019**.
163. Laboratorio SE de M de. POCT ONLINE. **2018**. Available from: <https://www.seqc.es/es/poctonline/>.
164. Martinez AW, Phillips ST, Whitesides GM. Diagnostics for the Developing World: Microfluidic Paper-Based Analytical Devices. *Anal Chem*. **2010**, 82, 3–10.
165. Luppá PB, Müller C, Schlichtiger A, Schlebusch H. Point-of-care testing (POCT): Current techniques and future perspectives. *Trends Anal Chem*. **2011**, 30, 887–898.
166. Beitollahi H, Mohammadi ZS, Safaei M, Tajik S. Applications of electrochemical sensors and biosensors based on modified screen-printed electrodes: a review. *Anal Methods*. **2020**, 12, 1547–1560.
167. Li M, Li D, Xiu G, Long Y. Applications of screen-printed electrodes in current environmental analysis. *Curr Opin Electrochem*. **2012**, 3, 137–143.
168. Economou A. Screen-Printed Electrodes Modified with “Green” Metals for Electrochemical Stripping Analysis of Toxic Elements. *Sensors*. **2018**, 18, 1032.
169. Khalid N, Kobayashi I, Nakajima M. Recent lab-on-chip developments for novel drug discovery. *WIREs Syst Biol Med*. **2017**, 9, 1–17.
170. Gupta S, Ramesh K, Ahmed S, Kakkar V. Lab-on-Chip Technology: A Review on Design Trends and Future Scope in Biomedical Applications. *Int J Bio-Science Bio-Technology*. **2016**, 8, 311–322.
171. Büyüktiryaki S, Sümbelli Y, Kecili R, Mustansar Hussain C. Lab-On-Chip Platforms for Environmental Analysis. In: *Encyclopedia of Analytical Science*. **2018**. 267–273.
172. Whitesides GM. The origins and the future of microfluidics. *Nature*. **2006**, 442, 368–373.
173. Atalay YT, Vermeir S, Witters D, Vergauwe N, Verbruggen B, Verboven P, Nicolai BM, Lammertyn J. Microfluidic analytical systems for food analysis. *Trends Food Sci Technol*. **2011**, 22, 386–404.
174. Ou X, Chen P, Huang X, Shunji L, Liu B. Microfluidic chip electrophoresis for biochemical analysis. *J Sep Sci*. **2020**, 43, 258–270.
175. Escarpa A. Lights and shadows on Food Microfluidics. *Lab Chip*. **2014**, 14, 3213–3224.

176. Garcia-Carmona L, Martin A, Sierra T, Gonzalez MC, Escarpa A. Electrochemical detectors based on carbon and metallic nanostructures in capillary and microchip electrophoresis. *Electrophoresis*. **2016**, 38, 1–15.
177. Nuchtavorn N, Suntornsuk W, Lunte SM, Suntornsuk L. Recent applications of microchip electrophoresis to biomedical analysis. *J Pharm Biomed Anal*. **2015**, 113, 72–96.
178. Martinez AW, Phillips ST, Butte MJ, Whitesides GM. Patterned Paper as a Platform for Inexpensive, Low-Volume, Portable Bioassays. *Angew Chem*. **2010**, 119, 1340–1342.
179. Martinez AW, Phillips ST, Whitesides GM. Three-dimensional microfluidic devices fabricated in layered paper and tape. *PNAS*. **2008**, 105, 19606–19611.
180. Pal A, Cuellar HE, Kuang R, Caurin HFN, Goswami D, Martínez R V. Self-Powered, Paper-Based Electrochemical Devices for Sensitive Point-of-Care Testing. *Adv Mater Technol*. **2017**, 2, 1700130–1700140.
181. Sachdeva S, Davis RW, Saha AK. Microfluidic Point-of-Care Testing: Commercial Landscape and Future Directions. *Front Bioeng Biotechnol*. **2021**, 8, 1–14.
182. Li Y, He R, Niu Y, Li F. Paper-Based Electrochemical Biosensors for Point-of-Care Testing of Neurotransmitters. *J Anal Test*. **2019**, 3, 19–36.
183. Tian T, Bi Y, Xu X, Zhu Z, Yang C. Integrated paper-based microfluidic devices for point-of-care testing. *Anal Methods*. **2018**, 10, 3567–3581.
184. Rackus DG, Shamsi H, Wheeler AR. Electrochemistry, biosensors and microfluidics: a convergence of fields. *Chem Soc Rev*. **2015**, 44, 5320–5340.



# CHAPTER III

## **Electrochemical sensors screen- printed based for glycoprotein determination**



# III. Electrochemical sensors screen-printed based for glycoprotein determination

## III.1. Introduction and objectives

Since years ago, the Analytical Chemistry must face one of the main challenges, which is the development of methods that respond to the growing need to perform rapid *in situ* analysis. Furthermore, these methods must be sensitive and accurate. In recent years, many of the methods developed with this end have been based on the use of electrochemical techniques due to their high sensitivity and selectivity, low-cost and portable size (1,2).

Traditionally, conventional solid electrodes (glassy carbon electrode (GCE), carbon paste electrode, etc.) have been used for multiple electroanalytical works. They are very attractive due to their characteristics and properties such as their high chemical stability, wide potential window, and low background current, among others (3). However, nowadays when scientists are focused on developing POCT devices, these electrodes have several drawbacks, such as high cathodic residual current, low resistance towards mechanical damage, and electrochemical polymerization of analytes (electrode passivation). Furthermore, the modifiers in these sensors are in loose association or physical contact with the electrode (4,5).

For that reason, the use of screen-printed technology, which consists of layer-by-layer depositions of ink upon a solid substrate, for electrode fabrication has received a lot of attention by the researchers. This technology has advantages of design flexibility, process automation, good reproducibility, and a wide choice of material. For this, since the 1990s screen-printed electrodes (SPE) has made a breakthrough and has recently become very popular in many applications (6). In the past few years, innovative SPEs implemented in sensors and biosensors have experienced a remarkable progression with a large number of scientific papers published on this issue (7). Recently, considerable advancement has been made



towards integration of SPEs and fluid-handling and/or sample-processing tools to ensure portable POCT devices. Consequently, screen-printing technology has emerged as the method of choice for mass production of POCT disposable (bio)-sensors. SPEs are suitable to make effective, versatile, and low-cost miniaturized devices, capable of giving reproducible results with high sensitivity in (bio)-chemical detection.

The substitution of more conventional electrodes for new disposable tests is an alternative that presents many advantages for these determinations. Electrodes with these dimensions (in many case microelectrodes and ultramicroelectrodes) offer advantages such as the ability to measure small currents in the range of picoamperes to nanoamperes (pA-nA), rapid response to changes in applied potential, low ohmic reduction in electric potential, efficient diffusional mass transport, and steady-state response at diffusion-controlled potential. Furthermore, screen-printed technology allows to carry out the mass production in a highly reproducible way with a reduced costs (7,8). An additional advantage of screen-printed is that it enables the implementation of a variety of configurations (single working electrodes, arrays of working electrodes, 3-electrode configurations, etc.) with different electrode geometries and sizes, opening a great field of applications for these electrodes (9). In addition, SPEs are disposable devices. This advantage avoids the tedious polishing (or electrochemical treatment) step to reuse the working electrode that is required for most solid electrodes to overcome passivation and/or contamination on their surfaces.

SPEs usually contain three electrodes: working (WE), counter/auxiliar (CE/AE) and reference (RE). WE is the main one on which the electrochemical reactions take place. RE and AE electrodes are also employed to complete the electronic circuit. Screen-printed technology consists of layer-by-layer depositions of ink upon a solid substrate, using screen or mesh, defining the geometry of the sensor. During the printing process of SPEs (**Figure III.1.1 A**), the most commonly used pastes are silver and carbon ink. Silver ink is printed as a conductive track while the working electrodes are often printed using carbon-based inks (10,11). This technology has advantages of design flexibility, process automation, good reproducibility, and a wide choice of materials (7).

SPEs can be produced in-house using commercial screen-printing equipment by printing different inks on various types of plastic or ceramic holdings. Alternatively, a large variety of carbon or modified SPEs is commercially available from different manufacturers (e.g., Dropsens, PalmSens, Micrux Technologies, etc.) (**Figure III.1.1 B and C**).

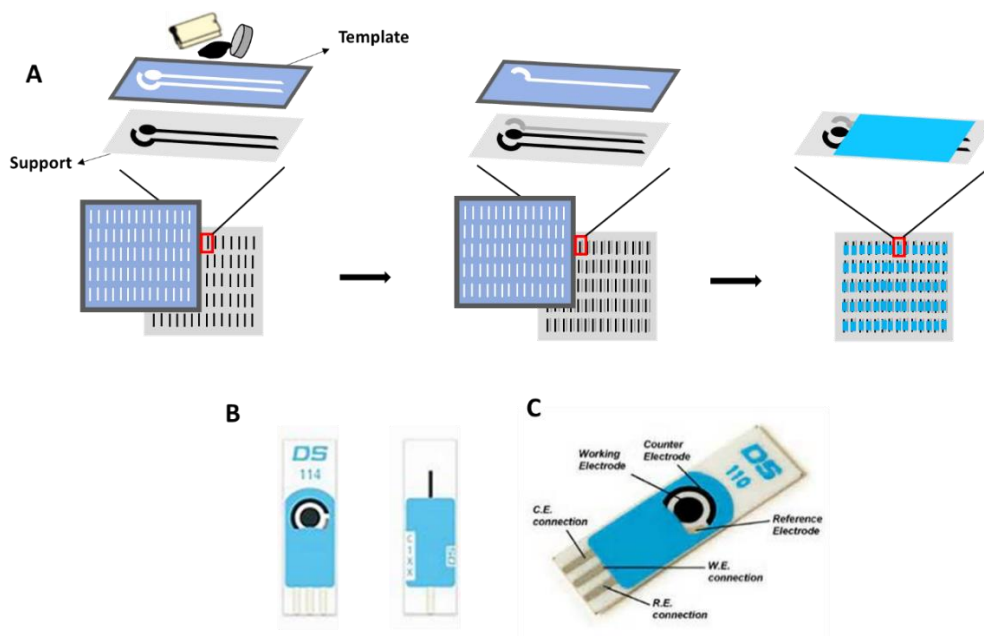


**Figure III.1.1.** (A) Manufacturing process of SPEs. First, a template was used to fabricate working and counter electrodes with carbon ink. Second, reference electrode was printed with silver paint. (B) Commercial SPEs used for microchip electrophoresis in this Doctoral Thesis. (C) Commercial SPEs with working, counter and reference electrodes and minimal cell volume (50  $\mu\text{L}$ ).

One of the main advantages of SPEs is their high versatility. This feature is largely due to the wide range of ways in which the surface of electrodes can be modified by changing the ink composition or depositing various substances on the electrodes surface such as metal films, polymers, enzymes, etc (11–13). The bulk modification of SPEs is very simple compared with ordinary GCE, which need several preparation and refreshment steps (14,15).

Besides, major development has been accomplished in the fabrication of SPEs by employing nanostructures materials. More recently, metallic

nanoparticles, nanowires, carbon nanotubes, and graphene, and their nanocomposites have also been included either in these pastes or as a later stage on the working electrode (15). These materials are used to enhance the immobilization efficiency of biological molecules and accelerate the charge transfer rate on the electrode surface. Furthermore, they can increase the electrochemical mediation to amplify signals from SPEs.

These disposable sensors can be easily modified in various ways and are also suitable for measuring multiple biological samples, as only a small sample volume is required. However, the selection of the different materials as inks of SPEs is very important according to the specific purpose of the electrochemical sensor (14).

The well-known electrochemistry of carbon nanomaterials (CNM) has opened an opportunity for the customization of the sensors. Several approaches to the fabrication of modified SPEs have been applied, such as drop casting, ink-printed, electrodeposition, among other manufacturing strategies (16).

Commonly, the building of CNM-based detectors has been carried out using thin film coating (drop casting approach). The design of CNM thin film electrodes is very simple and a wide range of underlying electrodes can be chosen (17). Although this approach has widely been used with satisfactory results, it has some limitations. Mainly, nanomaterial distribution on the electrode surface leads to a fragile modification and the analytical response is still dependent on both the nanomaterial and the electrode substrate (18,19).

As alternative to casting approach, our group has recently proposed a novel methodology that enables the manufacture of electrodes in which the transduction is based exclusively on CNM (18,20). To this end, the transducers were fabricated by filtering carbon nanomaterials solutions through a Teflon filter, and then they were retained on the filter, creating a conductive film over the non-conductive filter (carbon nanotubes scaffold films (CNSFs)) (**Figure III.1.2**). In this approach, the electronic transfer occurs directly on the target nanomaterial so that it is the only transducer

in the electrochemical sensing and, consequently, the analytical advantage of these nanomaterials is directly exploited.

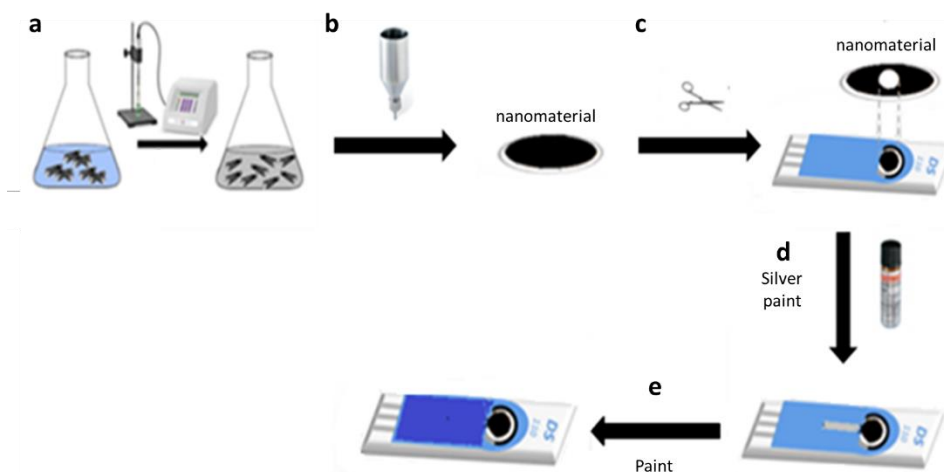


**Figure III.1.2.** Strategy to make carbon nanotubes scaffold films (CNSFs). (a) Nanomaterial were dispersed in N,N-dimethylformamide. (b) Dispersion was filtered using a 0.1  $\mu\text{m}$  Teflon filter. (c) The membrane, which contains the nanomaterial, was cut, and stuck in double-sided adhesive tape and put in the electrode. (d) Conductive silver paint was used to create the electric contact. (e) Finally, epoxy protective overcoat was used for the isolation.

On the other hand, and as it is mentioned in the introduction Chapter, adsorptive transfer stripping voltammetry (AdTSV) is one of the more sensitive electroanalytical techniques using in glycoprotein detection. This technique consists of two steps. First a pre-accumulation step of the analyte on the working electrode surface by an adsorption process (physical or chemical) followed by an electrochemical detection step, which can be performed using different voltammetry modes for oxidation or reduction of the accumulated substance (21) (**Figure III.1.3**).

AdTSV using SPEs benefits from the simplicity of application as reported in many electroanalytical methods (22,23), for example, allowing a good performance for determination of substances in biological samples as urine and serum.

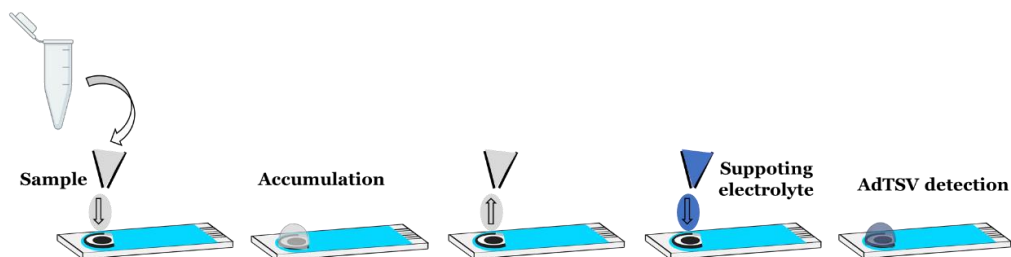


**Figure III.1.3.** Analysis by the AdTSV technique using a SPEs.

Taking into account all stated before, this **Chapter III** was focused on two main objectives. On one hand, the development and optimization of a derivatization protocol of glycoproteins with an Os(VI) complex (electrochemical tag), which allows the electrochemical measurement of these macromolecules by AdTSWV. On the other hand, the analytical possibilities offered by SPEs for the determination of glycoproteins will be explored. In addition, the analytical behavior of these glycoproteins will be evaluated using different CNMs.

### III.1.1. References

1. Beitollahi H, Mohammadi ZS, Safaei M, Tajik S. Applications of electrochemical sensors and biosensors based on modified screen-printed electrodes: a review. *Anal Methods*. **2020**, 12, 1547–1560.
2. Arduini F, Cinti S, Scognamiglio V, Moscone D, Palleschi G. How Cutting-edge Technologies Impact the Design of Electrochemical (Bio)sensors for Environmental Analysis. A Review. *Anal Chim Acta*. **2017**, 959, 15–42.
3. Fanjul-Bolado P, Hernández-Santos D, Lamas-Ardisana PJ, Martín-Pernía A, Costa-García A. Electrochemical characterization of screen-printed and conventional carbon paste electrodes. *Electrochimica Acta*. **2008**, 53, 3635–3642.
4. Rodríguez IN, Leyva JM, Hidalgo de Cisneros J. Use of a Bentonite-modified Carbon Paste Electrode for the Determination of Some Phenols in a Flow System by differential-pulse voltammetry. *Analyst*. **1997**, 122, 601–604.
5. Shams E, Babaei A, Reza A, Kooshki M. Voltammetric determination of dopamine at a zirconium phosphated silica gel modified carbon paste electrode. *Bioelectrochemistry*. **2009**, 75, 83–88.
6. Li M, Li D, Xiu G, Long Y. Applications of screen-printed electrodes in current environmental analysis. *Curr Opin Electrochem*. **2012**, 3, 137–143.
7. Taleat Z, Khoshroo A, Mazloun-Ardakani M. Screen-printed electrodes for biosensing: A review (2008-2013). *Microchim Acta*. **2014**, 181, 865–891.
8. Renedo OD, Alonso-Lomillo MA, Martínez MJA. Recent developments in the field of screen-printed electrodes and their related applications. *Talanta*. **2007**, 73, 202–219.
9. Economou A. Screen-Printed Electrodes Modified with “Green” Metals for Electrochemical Stripping Analysis of Toxic Elements. *Sensors*. **2018**, 18, 1032.
10. Jaiswal N, Tiwari I. Recent build outs in electroanalytical biosensors based on carbon-nanomaterial modified screen printed electrode platforms. *Anal Methods*. **2017**, 9, 3895–3907.
11. Chu Z, Peng J, Jin W. Advanced nanomaterial inks for screen-printed chemical sensors. *Sensors Actuators B Chem*. **2017**, 243, 919–926.
12. Arduini F, Micheli L, Moscone D, Palleschi G, Piermarini S, Ricci F, Volpe G. Electrochemical biosensors based on nanomodified screen-printed electrodes: Recent applications in clinical analysis. *Trends Anal Chem*. **2016**, 79, 114–126.
13. Armenta S, Esteve-Turrillas FA. Chapter 11: Carbon-based nanomaterials in Analytical Chemistry. In: *Handbook of Smart Materials in Analytical Chemistry*. **2019**.
14. Syedmoradi L, Daneshpour M, Alvandipour M, Gomez FA, Hajghassem H, Omidfar K. Point of care testing: The impact of nanotechnology. *Biosens Bioelectron*. **2017**, 87, 373–387.
15. Trojanowicz M. Impact of nanotechnology on design of advanced screen-printed electrodes for different analytical applications. *Trends Anal Chem*. **2016**, 84, 22–47.

16. Moretto L, Metelka R, Scopece P. Chapter 5: Carbon nanomaterials in electrochemical detection. In: *Carbon-based Nanomaterials in Analytical Chemistry*. **2019**.
17. Gomez FJV, Martin A, Silva MF, Escarpa A. Microchip electrophoresis-single wall carbon nanotube press-transferred electrodes for fast and reliable electrochemical sensing of melatonin and its precursors. *Electrophoresis*. **2015**, 36, 1880–1885.
18. Martín A, Vázquez L, Escarpa A. Carbon nanomaterial scaffold films with conductivity at micro and sub-micron levels. *J Mater Chem A*. **2016**, 4, 13142–13147.
19. Pumera M, Escarpa A. Nanomaterials as electrochemical detectors in microfluidics and CE: Fundamentals, designs, and applications. *Electrophoresis*. **2009**, 30, 3315–3323.
20. Martín A, Escarpa A. Tailor designed exclusive carbon nanomaterial electrodes for off-chip and on-chip electrochemical detection. *Microchim Acta*. **2017**, 184, 307–313.
21. dos Santos WTP, Compton RG. A simple method to detect the stimulant modafinil in authentic saliva using a carbon-nanotube screen-printed electrode with adsorptive stripping voltammetry. *Sensors Actuators B Chem*. **2019**, 285, 137–144.
22. Fanjul-bolado P, Santos H, Montoya M, Costa- A. Uric Acid Determination by Adsorptive Stripping Voltammetry on Multiwall Carbon Nanotubes Based Screen-Printed Electrodes. *Electroanalysis*. **2015**, 27, 1276–1281.
23. Ahmar H, Tabani H, Koruni MH, Saeed S, Davarani H, Fakhari AR. A new platform for sensing urinary morphine based on carrier assisted electromembrane extraction followed by adsorptive stripping voltammetric detection on screen-printed electrode. *Biosens Bioelectron*. **2014**, 54, 189–194.

## **III.2. Results and discussion**

This Chapter has been focused on the use of electrochemical sensors screen-printed based for glycoprotein determination, in concrete  $\alpha_1$ -acid glycoprotein (AGP) and transferrin (Tf), both related to inflammatory diseases, among other applications. Firstly, these glycoproteins are labeled with an electrochemical tag (Os(VI) complex), which help in the electrochemical detection, and then they are quantified by adsorptive transfer stripping square wave voltammetry (AdTSWV).

The combination of screen-printed technology and electrochemical detection, in order to develop suitable electrochemical methods for these target analytes, constitutes the core of this Chapter. Furthermore, we prove that the inherent advantages of screen-printed electrodes technology (low sample consumption, low-cost and point-of-care testing) make this methodology very attractive in this field and can be very helpful in determining glycoproteic biomarkers.

Taking these aspects in mind, a simple and cheap electrochemical method for total AGP determination using disposable screen-printed carbon electrodes (SPCEs) and using a selective acidic precipitation of the rest of proteins has been developed to achieve sensitive, accurate, and reliable determination in a commercial serum sample (**III.2.1**).

In the next section (**III.2.2**), the great advantages provided by carbon nanomaterials in screen-printed technology, specifically in increasing analytical signal, as well as an improvement in electrode passivation will be demonstrated. Different carbon nanotubes scaffold films (CNSFs) were applied to AGP determination in serum samples, being multi-walled carbon nanotubes scaffold films (MWSFs) those that yielded the best analytical performance in terms of sensitivity.

Finally, a new way to measure carbohydrate deficient transferrin (CDT) using SPCEs will be showed (**III.2.3**). Labeled Tf with Os(VI) complex generates two voltammetric signals: one from carbohydrates (electrochemical signal of Os(VI) complex at -0.9 V/Ag) and one from the amino acids present in glycoprotein (intrinsic electrochemical signal of



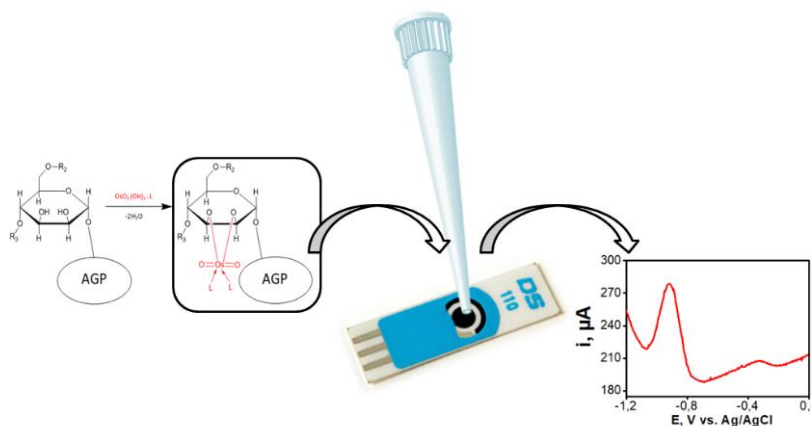
glycoprotein at +0.8 V/Ag). The relationship between the two analytical signals (carbohydrate signal/protein signal) is an indicator of the degree of glycosylation (electrochemical index of glycosylation (EIG)). A new approach to measure the level of CDT was proposed, relied on the Os(VI) signal/protein signal ratio (EIG). In addition, the suitability of the proposed electrochemical sensor was evaluated by analyzing serum samples from congenital disorders of glycosylation (CDG) patients.

### III.2.1. Article 1: Total $\alpha_1$ -acid glycoprotein determination in serum samples using disposable screen-printed electrodes and osmium (VI) as electrochemical tag

Tania Sierra, María Cristina González, Begoña Moreno, Agustín G. Crevillén, Alberto Escarpa

Talanta 180 (2018) 206–210

**Abstract:**  $\alpha_1$ -acid glycoprotein (AGP) or orosomucoid is a serum glycoprotein which belongs to the group of acute phase proteins. It is a potential biomarker for inflammatory bowel diseases. In this sense, there is a need for developing fast and cheap analytical methods for diagnosis, prognosis, and follow-up of these diseases. In this work, we propose a simple and cheap electrochemical method for total AGP determination using disposable screen-printed carbon electrodes (SPCEs) and using a selective acidic precipitation of the rest of proteins. This method avoids the use of biological components, decreasing dramatically the analysis cost. Firstly, AGP is labeled with an electrochemical tag (osmium (VI) complex) and then the total amount of AGP is quantified by adsorptive transfer stripping square wave voltammetry. The method optimized showed a good linear correlation ( $r = 0.9992$ ) and limit of detection of  $1.6 \text{ mg L}^{-1}$ . The methodology was successfully applied to quantify AGP in a commercial serum sample. This methodology could be useful in clinical diagnosis because of AGP levels increase two or three times when inflammatory processes happen. Moreover, the inherent advantages of SPCE technology (low sample consumption, low-cost. and point-of-care testing) make this methodology very attractive in this field.





## 1. Introduction

$\alpha_1$ -acid glycoprotein (AGP) or orosomucoid is a serum glycoprotein with a molecular weight between 41-43 KDa. Human AGP presents five N-linked glycans attached to the protein structure. It is also negatively charged (pI = 2.7-3.2) due to the presence of sialic acids (1,2). Additionally, AGP belongs to a group of acute phase proteins that may play a role in the modulation of the immune system in response to stress, along with many other functions such as drug binder and carrier (1,2). AGP concentration in healthy humans is 0.2-1 g L<sup>-1</sup>, whereas during disease or injury it can increase two to three times (3). In this sense, total AGP content has been studied as serum biomarker for inflammatory bowel diseases (4) and for early diagnosis of neonatal sepsis (5); specifically, it showed excellent results in prognosis of Crohn disease (6) and good correlation with endoscopic activity (occurrence of aphthous lesions, nodularity, erythema, ulcerations, stenosis in bowel wall) (7). The follow-up of Crohn disease patients is carried out by colonoscopy and cross-sectional imaging, but both techniques are time consuming and expensive and, also, colonoscopy is an invasive procedure. For these reasons, there is a great interest in finding reliable biomarkers and in developing fast and cheap analytical methods for detecting them (8).

In this way, screen-printed electrode (SPE) technology offers disposable, low sample consumption and cheap electrochemical platforms for *in situ* analysis and/or point-of-care testing (9). These features make SPE an attractive tool for clinical analysis (10,11). With respect to protein biomarkers detection, all developed methods employ a recognizing element (aptamer, antibody, molecular imprinted polymer) and, the majority of them, a signal transducer (usually, an enzyme) which detects the binding of the complementary species (11). In the case of AGP, there are several commercial kits for its total amount determination based on a turbidimetric immunoassay (12). These biomolecules (enzymes, antibodies, and aptamers) increase the analysis cost.

On the other hand, direct electrooxidation of proteins is possible thanks to the presence of electroactive amino acids; mainly, cysteine, tyrosine, and

tryptophan. In fact, limits of detection in nanomolar level can be obtained for proteins employing square wave voltammetry (SWV) and chronopotentiometric stripping analysis (CPS) (13,14). But, in the case of glycoproteins, the electrochemical detection is less sensible because their carbohydrate parts (glycans) are electrochemically inactive under conditions close to physiological (15).

Intact glycoproteins can be electrochemically detected by two strategies: label-free and label-based detection. The usual electrochemical techniques employed for a label-free analysis include electrochemical impedance spectroscopy (EIS) and capacitance (14). These methods employ lectins as recognizing element but their application in complex and real samples is scarce although there is one interesting example in human serum (16). Respect to label-based detection, there are several works in which nanomaterials were used as electrochemical tags for glycoproteins. For example, chicken ovomucoid was labeled with ZnO quantum dots (17) and an IgGs with black phosphorus nanoparticles (18) and MoSe<sub>2</sub> nanoparticles (19). But real samples were not analyzed in these works. Recently, Palecek's group proposed the use of osmium (VI) complexes as electrochemical probe for oligo- and polysaccharide detection (20). The osmium (VI) complexes react with diol groups from saccharides to form osmate ester which yields two redox couples in carbon electrodes (21). Later, this group extended its application to glycoproteins detection demonstrating Os(VI) complexes selectively bind to the carbohydrate part and not to the polypeptidic backbone (15). It is worth to mention that glycan isomers can be distinguished using this electrochemical tag (22,23).

In this work, we propose a simple and cheap electrochemical method for total AGP determination using disposable SPCEs and using a selective acidic precipitation of the rest of proteins to avoid interferences (24). To achieve the electrochemical detection of AGP, the protein was labeled with an osmium (VI) complex. An adsorptive transfer stripping square wave voltammetry (AdTSWV) was chosen as electrochemical technique. Several parameters such as frequency, amplitude, and accumulation time were optimized. Additionally, precision and accuracy of the method were studied. Finally, the developed method was applied to serum samples.

## 2. Material and methods

### 2.1. Reagents

$\alpha_1$ -acid glycoprotein (AGP), potassium osmate (VI) dihydrate, N,N,N',N'-tetramethylethylenediamine (TEMED), and human serum were acquired from Sigma-Aldrich (Darmstadt, Germany). Perchloric acid, hydrochloric acid, acetic acid, disodium hydrogen phosphate, and sodium dihydrogen phosphate were purchased from Panreac (Barcelona, Spain). Sodium acetate and borax were purchased from Merck (Darmstadt, Germany). Boric acid was acquired from Fluka (Darmstadt, Germany). All solutions were prepared in Milli-Q water (Merck Millipore, Darmstadt, Germany).

### 2.2. Instrumentation

Potentiostat Autolab PGSTAT101 (Methrom-Autolab, Utrecht, The Netherlands) was used for all electrochemical measurement. This instrument was controlled by the software Nova 1.6.

Screen-printed carbon electrodes (SPCE) (DRP-110, Dropsens, Oviedo, Spain) were employed for electrochemical detection (single use). They consist of carbon working electrode (4 mm diameter), carbon counter electrode, and silver reference electrode. This kind of SPCEs works as an electrochemical cell which needs a minimum volume of 50  $\mu$ L. Centrifuge Multifuge Heraeus3 L-R (Thermo Fischer Scientific, Waltham, MA, USA) was employed for sample ultrafiltration by Amicon<sup>®</sup> Ultra-2 mL centrifugal filters (cutoff 10 KDa) (Merck Millipore, Darmstadt, Germany).

Mass spectrometry analysis were carried out in an Ultraflex III (Bruker, Billerica, MA, USA) using positive linear mode, 2,5-dihydroxyacetophenone (DHAP) as matrix in presence of ammonium citrate and 2 % TFA in water.

### 2.3. Procedures

#### 2.3.1. Preparation of Os(VI)O<sub>2</sub>(OH)<sub>2</sub>TEMED complex

The preparation of Os(VI)O<sub>2</sub>(OH)<sub>2</sub>TEMED complex was carried out according to bibliography (20). Briefly, 18.4 mg of potassium osmate (VI) dihydrate (50  $\mu$ mol) were suspended in 1.22 mL of water. Then, 5.8 mg of

TEMED (50  $\mu\text{mols}$ ) and 0.41 mL of a 0.2 M sodium phosphate pH = 7.0 solution were poured into the previous solution. Finally, 10  $\mu\text{L}$  of 10 M HCl solution were added. The solution was shaken for one hour to allow the formation of  $\text{Os(VI)O}_2(\text{OH})_2\text{TEMED}$  complex (reddish color) and finally, the solution was filtered using a syringe Nylon filter 0.22  $\mu\text{m}$  (Tecno-Air, Barcelona, Spain). The final concentration of Os(VI) complex obtained was 30.3 mM.

#### 2.3.2. AGP labeling with $\text{Os(VI)O}_2(\text{OH})_2\text{TEMED}$ complex

AGP-Os(VI) adduct was prepared as follow: 1.02 mg of AGP ( $2.5 \times 10^{-8}$  mols) were dissolved into 234  $\mu\text{L}$  of 50 mM sodium phosphate pH = 7.0 buffer using a “protein low bind” Eppendorf tube (Hamburg, Germany). Then, 16.5  $\mu\text{L}$  of  $\text{Os(VI)O}_2(\text{OH})_2\text{TEMED}$  solution were added in the previous solution (mol ratio 1/20 between AGP and Os(VI)) and it was kept under agitation 16 h at 37 °C and 950 r.p.m. using a thermo shaker (Biosan TS-100C, Riga, Latvia). The final concentration of AGP-Os(VI) adduct obtained was 100  $\mu\text{M}$ . Then, this solution was filtered through Amicon® Ultra-2 mL centrifugal filters (cut-off 10 KDa) in order to remove the non-reacted  $\text{Os(VI)O}_2(\text{OH})_2\text{TEMED}$  complex (centrifugal parameters: 4 °C, for 40 min at 4500g). The filters were washed twice with 250  $\mu\text{L}$  of 50 mM sodium phosphate pH = 7.0 solution to ensure the complete removal of  $\text{Os(VI)O}_2(\text{OH})_2\text{TEMED}$  complex. The Amicon filters were inverted and centrifuged (5 min at 2000g) to recovery the AGP-Os(VI)TEMED adduct solution (final volume 250  $\mu\text{L}$ , stock solution). The stock solution was stored at -16 °C for a maximum of four days (stability was studied). Finally, working solutions were prepared by dilution of stock solution (previously thawed) in Britton-Robinson buffer (BR) or 50 mM sodium phosphate buffer pH = 7.0.

The labeling protocol of AGP was modified when serum samples were analyzed due to the high concentration of glucose and other carbohydrates in these samples. For ensuring the labeling of AGP with the electrochemical tag, the concentration of  $\text{Os(VI)O}_2(\text{OH})_2\text{TEMED}$  complex in the solution was increased from 2 mM (as in the standard protocol) to 6 mM. The protocol was as follow; 200.5  $\mu\text{L}$  of serum sample were mixed with 49.5  $\mu\text{L}$

of Os(VI)O<sub>2</sub>(OH)<sub>2</sub>TEMED solution and it was kept under agitation 16 h at 37 °C and 950 r.p.m. using a thermo shaker (Biosan TS-100C, Riga, Latvia). Then, the solution was filtered using Amicon filters for removing not only the excess of reagent but also the glucose and other small carbohydrates labeled with Os(VI) present in serum. Later, AGP-Os(VI)TEMED adduct was isolated from the rest of proteins by a selective acidic precipitation (18). Briefly, 50 µL of serum labeled with the electrochemical tag Os(VI) and 100 µL of 0.5 M perchloric acid were vortex mixed in a “protein low bind” Eppendorf tube for 20 s. The acidified serum was then centrifuged at 3000g for 20 min at room temperature (Microcentrifuge Mini Spin® Eppendorf, Hamburg, Germany). Finally, the supernatant was adequately diluted in Britton-Robinson (BR) buffer at pH = 3.0 buffer before the AdTSWV analysis.

#### 2.3.3. Electrochemical measurements

Os(VI)O<sub>2</sub>(OH)<sub>2</sub>TEMED complex dissolved in 50 mM sodium phosphate pH = 7.0 buffer was electrochemically characterized by cyclic voltammetry: start potential -1.4 V, switching potential +0.4 V, and scan rate 1 V s<sup>-1</sup>. Nitrogen was used for oxygen removal (10 min). Electrochemical detection was performed using adsorptive transfer stripping square wave voltammetry (AdTSWV). In this case, 10 µL of sample were dropped onto the working electrode and, then, the analyte was adsorbed for accumulation time 5 min at open circuit potential. Then, the electrode was washed with water and finally, 50 µL of background electrolyte (0.2 M Britton-Robinson buffer pH = 3 or 50 mM sodium phosphate pH = 7.0 buffer) were dropped on the SPCE for voltammogram recording. Square wave voltammetry (SWV) parameters: start potential -1.4 V, end potential +0.1 V, step potential 5 mV, amplitude 50 mV, and frequency 100 Hz, if not stated otherwise.

### 3. Results and discussion

#### 3.1. Characterization of Os(VI)O<sub>2</sub>(OH)<sub>2</sub>TEMED complex and AGP-Os(VI) adduct

Firstly, 10 mM Os(VI)O<sub>2</sub>(OH)<sub>2</sub>TEMED solution prepared in 50 mM phosphate buffer at pH 7.0 was electrochemically characterized by cyclic



voltammetry using SPCE (see **Figure III.2.1.1**). As can be observed in this figure, the electrochemical tag  $\text{Os(VI)O}_2(\text{OH})_2\text{TEMED}$  showed one quasi reversible redox couple at about  $-1$  V (peaks 1 and 3) and one anodic peak at  $-0.2$  V (peak 2). In addition, there are other minor anodic peaks between  $-1$  V and  $-0.2$  V.

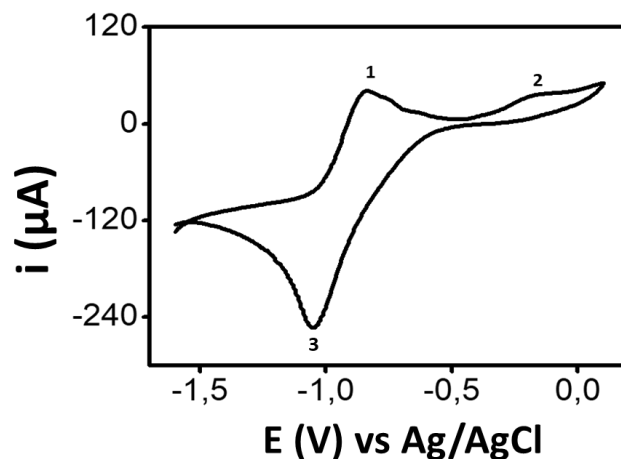


**Figure III.2.1.1.** Cyclic voltammogram of 10 mM  $\text{Os(VI)O}_2(\text{OH})_2\text{TEMED}$  complex in 50 mM phosphate buffer pH 7. Scan rate  $1 \text{ V s}^{-1}$ .

Next, AGP standard was labeled with the electrochemical tag  $\text{Os(VI)O}_2(\text{OH})_2\text{TEMED}$  (see **Section 2.3.2**) obtaining the corresponding adduct, hereinafter, AGP- $\text{Os(VI)}$ . A ratio 1/20 (protein/tag) was used to ensure the maximum labeling. To estimate the amount of  $\text{Os(VI)}$  complex molecules per protein, non-labeled AGP and AGP- $\text{Os(VI)}$  adduct were studied by MALDI-TOF mass spectrometry in order to know the molecular weight (Supplementary information, **Figure III.2.1.S1**). Unexpectedly, the labeling with  $\text{Os(VI)}$  complex just generated a mass increase of approximately 789 Da in the protein corresponding to two molecules of this tag ( $M_w [\text{Os(VI)O}_2(\text{OH})_2\text{TEMED}] = 372.4 \text{ Da}$ ). In spite of the tag excess added in the reaction and the five N-linked glycans present in the AGP, two electrochemical tags were just bonded to the protein. Maybe, there was some kind of steric impediments in the reaction.

AGP- $\text{Os(VI)}$  adduct was electrochemically studied using adsorptive transfer stripping square wave voltammetry (AdTSWV) employing standard

conditions (start potential  $-1.4$  V, end potential  $+0.1$  V, step potential  $5$  mV, amplitude  $50$  mV, frequency  $100$  Hz, accumulation time  $1$  min). **Figure III.2.1.2** shows voltammograms of  $50$  mM phosphate buffer at pH  $7.0$  (blank) (**Figure III.2.1.2**, red line),  $400$  mg  $L^{-1}$  AGP in phosphate buffer (control) (**Figure III.2.1.2**, blue line) and  $400$  mg  $L^{-1}$  AGP-Os(VI) in phosphate buffer (**Figure III.2.1.2**, black line). Clearly, a new peak rise from the background at  $-0.8$  V corresponding to the AGP-Os(VI) signal. In fact, the potential is close to the free tag ( $-1$  V). Apparently, this result is not in concordance with previous characterization of this tag (20) where two redox couples were obtained at about  $-0.70$  and  $-0.25$  V. However, it is important to underline that, in the work previously mentioned, a pyrolytic graphite electrode was employed instead of SPCE electrode and the osmium complex was dissolved in  $0.2$  M sodium acetate at pH  $5.0$  instead of  $50$  mM phosphate buffer at pH  $7.0$ .

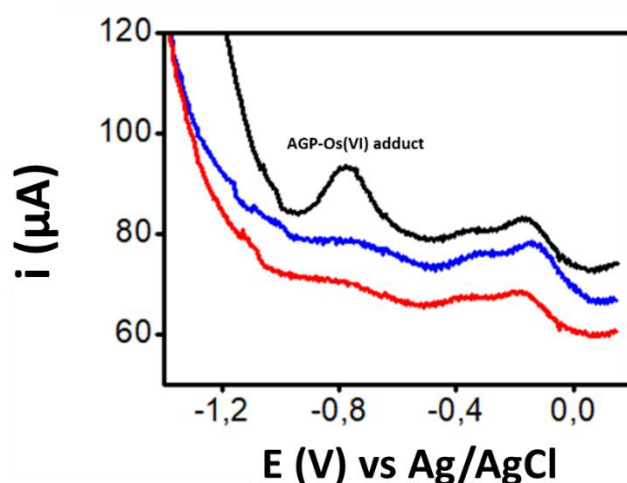


**Figure III.2.1.2.** Voltammograms obtained by AdTSWV of  $50$  mM phosphate buffer at pH  $7.0$  (blank) (red line),  $400$  mg  $L^{-1}$  AGP in phosphate buffer (control) (blue line) and  $400$  mg  $L^{-1}$  AGP-Os(VI) in phosphate buffer (black line). Conditions: start potential  $-1.4$  V, end potential  $+0.1$  V, step potential  $5$  mV, amplitude  $50$  mV, frequency  $100$  Hz, accumulation time  $1$  min.

### 3.2. Optimization and analytical performance of AdTSWV method for AGP detection. Application to serum samples analysis

In order to find the best voltammetric signals for detecting AGP-Os(VI), pH studies were carried out. For this study, 400 mg L<sup>-1</sup> AGP-Os(VI) was prepared in 0.2 M Britton-Robinson buffer ranging from pH 7.0 to pH 2.0. As can be observed in **Figure III.2.1.3**, a new peak ranging from -1.05 V to -0.85 V (named as 2) appeared in the voltammograms at pHs equal or lower than 5. This peak is presented too at pH 7.0 but it is difficult to notice because it is a shoulder in the current dropping zone. This finding is in concordance with the bibliography wherein detected other glycoprotein-Os(VI) adducts (20). Additionally, a displacement of anodic peaks (1 y 2) towards more positive potentials when pH is decreased was also noticed. It means the redox reaction of the electrochemical tag is pH dependent as it was reported previously (25).

As it is also shown in **Figure III.2.1.3**, the lower the pH the higher the signal (see peak 2). To explain this effect, two aspects should be taken into account; first, in AdTSWV only adsorbed protein is measured, and second, the main interaction between proteins and untreated carbon material is hydrophobic type (26), so the interaction is stronger at pH close to protein isoelectric point. As AGP isoelectric point is around 3, a decreasing of the pH value from 7.0 to 2.0 means an increasing of the protein adsorption and, therefore, the electrochemical signal obtained is higher. Between pH 2.0 and 3.0 there is not significant difference in the signal, so pH = 3.0 was selected as optimum pH value. Peak 2 ( $E_p = -0.9$  V) was chosen for quantitative purposes because it was clearly defined than peak 1 ( $E_p = -0.3$  V).

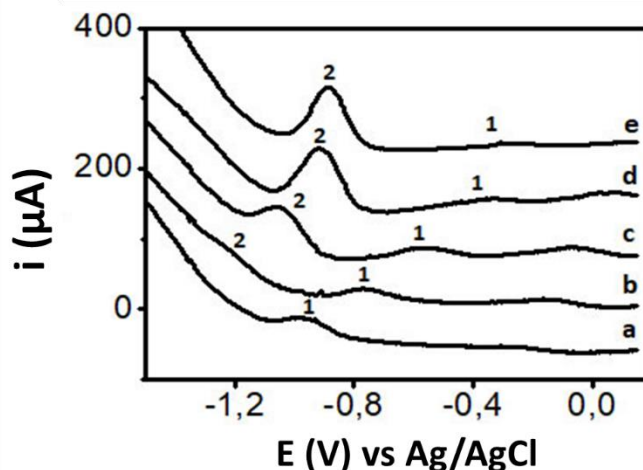


**Figure III.2.1.3.** Voltammograms obtained for AGP-Os(VI) (AGP 400 mg L<sup>-1</sup>) in BR buffer at different pHs; 9 (**a**), 7 (**b**), 5 (**c**), 3 (**d**) and 2 (**e**). Conditions: as in **Figure III.2.1.2**. Peaks 1 and 2 belong to AGP-Os(VI) adduct.

Several AdTSWV parameters were also optimized. Amplitude pulse was studied from 25 mV to 100 mV (accumulation time 1 min, frequency 100 Hz) and frequency from 25 Hz to 200 Hz (accumulation time 1 min, pulse 50 mV). The optimal values found were 50 mV and 100 Hz, respectively. Finally, the accumulation time was also optimized (0, 2 and 5 min) and 5 min was chosen as optimal. Longer times were not studied because it is not considered useful from practical point of view.

On the other hand, the capability of AdTSWV for sensing AGP in serum samples was carefully evaluated. In this way, calibration studies were carried out in the experimental conditions previously optimized. The linearity of the method was studied from 8 mg L<sup>-1</sup> to 400 mg L<sup>-1</sup> using the peak area. As it is expected in adsorptive methods (15), two different zones were observed. First, a linear dependence from 4.0 mg L<sup>-1</sup> to 40.0 mg L<sup>-1</sup> is found and then a quasi-plateau is reached (from 40 mg L<sup>-1</sup> to 400 mg L<sup>-1</sup>) (results are not shown). At 40 mg L<sup>-1</sup> protein concentration, the electrode surface is almost completely covered by protein and no more protein can be adsorbed on it. A good correlation coefficient was obtained from 4.0 mg L<sup>-1</sup> to 40.0 mg L<sup>-1</sup> ( $r = 0.9992$ ). The calibration curve slope was  $(1.07 \pm 0.02) \times 10^{-7}$  A L mg<sup>-1</sup> and the intercept  $(-4.0 \pm 6.1) \times 10^{-8}$  A ( $n = 3$ ). The limit of detection obtained from the calibration curve was 1.6 mg L<sup>-1</sup> (3 S/N

criterion). This LOD is similar to those obtained from turbidimetric immunoassay methods (about  $1.2 \text{ mg L}^{-1}$ ) (12). The analytical characteristics obtained show that AdTSWV method is adequate for AGP determination in serum samples in which AGP concentration in healthy humans ranged between  $200\text{--}1000 \text{ mg L}^{-1}$  (3).

As it is well-known, one of the handicaps of labeling reaction is to label analytes at very low concentration (27). Keeping this in mind, a AGP standard solution prepared at concentration of  $1.6 \text{ mg L}^{-1}$  was labeled with Os(VI) complex and then analyzed by AdTSWV. As it is shown in **Figure III.2.1.4**, a small peak of AGP was obtained demonstrating that LOD of overall method (or concentration limit of detection as other authors stated) is  $1.6 \text{ mg L}^{-1}$ .

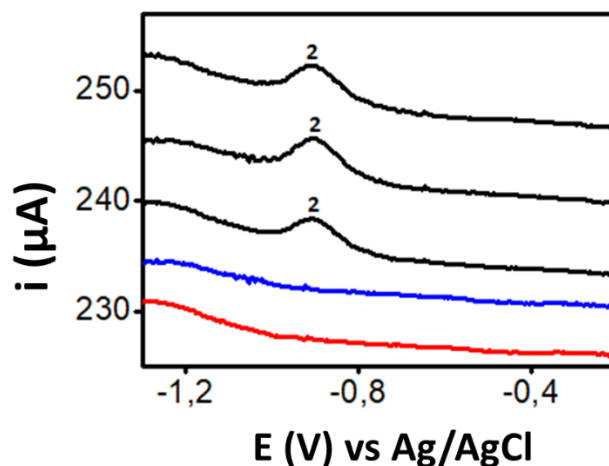


**Figure III.2.1.4.** Voltammograms obtained by AdTSWV of AGP solution labeled and analyzed at concentration  $1.6 \text{ mg L}^{-1}$ . Controls: BR buffer at pH 3.0 (blank) (red line),  $1.6 \text{ mg L}^{-1}$  non-labeled AGP in BR buffer (control) (blue line). Conditions: BR buffer pH 3, start potential  $-1.4 \text{ V}$ , end potential  $+0.1 \text{ V}$ , step potential  $5 \text{ mV}$ , amplitude  $50 \text{ mV}$ , frequency  $100 \text{ Hz}$ , accumulation time  $5 \text{ min}$ . Peak 2 belongs to AGP-Os(VI) adduct.

Precision was also carefully studied using a AGP-Os(VI) solution ( $40 \text{ mg L}^{-1}$  AGP) prepared in BR buffer at pH 3.0. RSD = 11 % ( $n = 4$ ) was obtained using the same batch and employing different SPCEs. Batch-to-batch

solutions reproducibility was also evaluated yielding a RSD value of 21 % ( $n = 4$ ). The origin of this variability using the same batch could be related with differences in active surface between SPCEs. Reproducibility values obtained are acceptable for AGP determination because, as it is well-known, AGP levels in serum can increase two or three times during disease or injury (3). Therefore, it is important to underline that this method could discriminate between healthy and sick individuals.

Recovery studies were performed to evaluate the method accuracy. A serum sample was diluted ten times in BR pH 3 to minimize the signal of the endogenous AGP and then, a known amount of AGP standard was added to this solution to reach a final AGP concentration of  $4 \text{ g L}^{-1}$ . Next, this sample was treated following the protocol showed in **Section 2.3.2** (serum samples).

The sample was adequately diluted and analyzed by AdTSWV obtaining a recovery of  $81 \pm 6 \%$  ( $n = 5$ ) using external calibration. This result was similar to those obtained by Stumpe *et al.* (79.1 %) employing the same sample treatment (acidic precipitation) for AGP isolation in plasma samples (24). Finally, a commercial serum sample was also analyzed (sample was adequately diluted after derivatization protocol) obtaining a value of  $0.48 \pm 0.09 \text{ g L}^{-1}$  for AGP ( $n = 5$ ), which is within the normal physiological range.

Finally, a simplification of the developed method was explored by eliminating the ultrafiltration step which is a long and expensive methodology. It basically consisted in replacing ultrafiltration by a washing step in which the SPCE was immersed in water for 1 min after AGP deposition step. This strategy was previously employed in the bibliography for eliminating the reagent excess (15,20) but we were worried about the glucose and other carbohydrates present in serum which could be adsorbed on SPCE. The serum sample was analyzed employing both methodologies (water washing and ultrafiltration steps) and also without any cleaning step. These new methodologies were compared with ultracentrifugation ones using a t-test at 95 % confidence level ( $P \geq 0.05$ ) (see **Table III.2.1.1**). It was not found significant differences between water washing and ultrafiltration methodologies ( $P = 0.14$ ), so water washing step could replace

### Chapter III. Electrochemical sensors screen-printed based

---

ultracentrifugation ones. Moreover, there was significant differences between ultracentrifugation and no cleaning methodology ( $P = 0.01$ ). This means that there are other labeled compounds and/or rests of reagent in the sample which have to be eliminated before electrochemical readout.

**Table III.2.1.1.** Comparison between cleaning methodologies in serum samples.

	Ultrafiltration	Water washing	No cleaning
Average area (a.u.)	$5.0 \times 10^{-7}$	$4.3 \times 10^{-7}$	$12.2 \times 10^{-7}$
Standard deviation	$0.4 \times 10^{-7}$	$0.4 \times 10^{-7}$	$1.2 \times 10^{-7}$
Probability of null hypothesis ( $H_0$ )*	-	0.14	0.01

\*  $H_0$ : average area from ultrafiltration = average area from other methodology, t-test at 95 % confidence level,  $P=0.05$ .

## 4. Conclusions

In this work, a simple and cheap electrochemical method (AdTSWV) was developed for the determination of AGP in serum samples using disposable screen-printed carbon electrodes (SPCEs). Thanks to the selective acidic precipitation, AGP was isolated from the rest of proteins avoiding the use of biomolecules. Moreover, the methodology was simplified replacing ultrafiltration step by a water washing protocol which is faster, simpler, and cheaper. Taking into account overall mentioned before, the analysis cost could be practically reduced to the price of one SPCE. The main drawback of the method proposed is the long derivatization protocol (16 h) but we are working on it considering different ligands for Os(VI) as other authors did it. Finally, this methodology was successfully applied to quantify AGP in a commercial serum sample. In spite of batch-to-batch reproducibility (RSD = 21 %) and recovery (81 %) were not excellent, this methodology could be useful in clinical diagnosis (inflammatory bowel diseases and neonatal sepsis) because AGP levels increase two or three times when inflammatory processes happen. Moreover, the inherent advantages of SPE technology (low sample consumption, low-cost and point-of-care testing) make this methodology very attractive in this field.



### Acknowledgments

This work has been financially supported by the NANOAVANSENS program from the Community of Madrid (S2013/MIT-3029), the Spanish Ministry of Economy, and Competitiveness CTQ 2014-58643-R. T.S. acknowledges the FPI fellowship from the University of Alcalá.

### Associated content

#### Supporting Information

**Figure III.2.1.S1.** MALDI-TOF mass spectra of unlabeled AGP and AGP-Os(VI) adduct.

### Author information

#### Corresponding Authors

Alberto Escarpa – Department of Analytical Chemistry, Physical Chemistry and Chemical Engineering, University of Alcalá, Madrid, Spain. Chemical Research Institute “Andrés M. del Río” (IQAR), University of Alcalá, Madrid, Spain; [orcid.org/0000-0002-7302-0948](https://orcid.org/0000-0002-7302-0948); Email: [alberto.escarpa@uah.es](mailto:alberto.escarpa@uah.es)

Agustín G. Crevillen – Department of Analytical Sciences, Faculty of Sciences, Universidad Nacional de Educación a Distancia (UNED), Madrid, Spain; Email: [agustingcrevillen@ccia.uned.es](mailto:agustingcrevillen@ccia.uned.es)

#### Other Authors

Tania Sierra - Department of Analytical Chemistry, Physical Chemistry and Chemical Engineering, University of Alcalá, Madrid, Spain.

María Cristina González - Department of Analytical Chemistry, Physical Chemistry and Chemical Engineering, University of Alcalá, Madrid, Spain. Chemical Research Institute “Andrés M. del Río” (IQAR), University of Alcalá, Madrid, Spain.

Begoña Moreno - Department of Analytical Chemistry, Physical Chemistry and Chemical Engineering, University of Alcalá, Madrid, Spain.

### Authors Contribution

The manuscript was written through contributions of all the authors. All the authors have given approval to the final version of the manuscript.

## Supporting Information

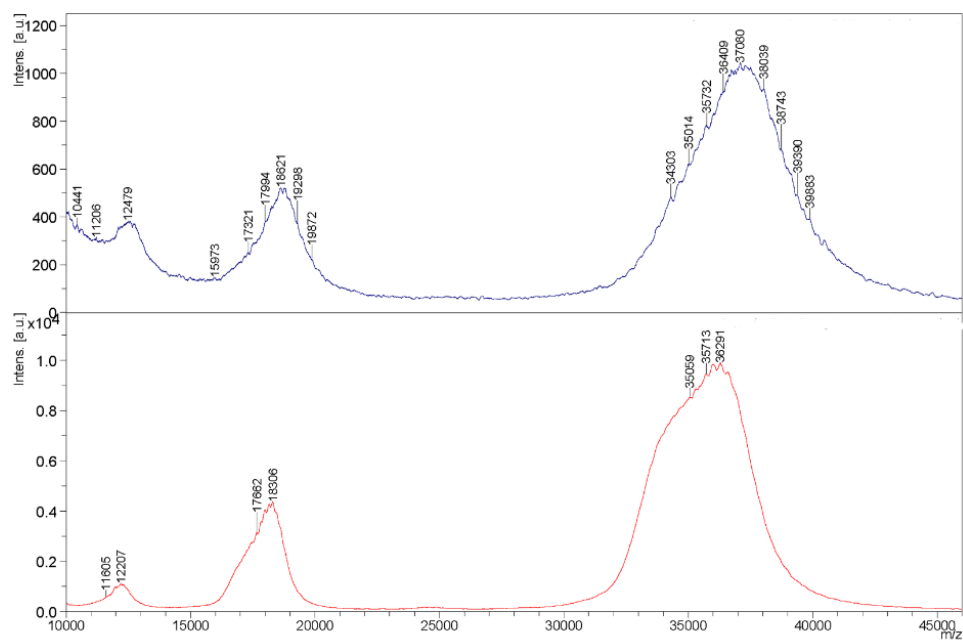


**Figure III.2.1.S1.** MALDI-TOF mass spectra of unlabeled AGP (red line) and AGP-Os(VI) adduct (blue line).

#### References

1. Hocheplied T, Berger FG, Baumann H, Libert C.  $\alpha_1$ -Acid glycoprotein: an acute phase protein with inflammatory and immunomodulating properties. *Cytokine Growth Factor Rev.* **2003**, 14, 25–34.
2. Fournier T, Medjoubi N, Porquet D. Alpha-1-acid glycoprotein. *Biochim. Biophys. Acta.* **2000**, 1482, 157–171.
3. Shiyan SD, Bovin NV. Carbohydrate composition and immunomodulatory activity of different glycoforms of  $\alpha$  1-acid glycoprotein. *Glycoconj. J.* **1997**, 14, 631–638.
4. Vermeire S, Van Assche F, Rutgeerts P. Oratory markers in IBD: magic, or unnecessary toys? *Gut.* **2006**, 55, 426–431.
5. Ipek IO, Saracoglu M, Bozaykut A.  $\alpha_1$ -acid glycoprotein for the early diagnosis of neonatal sepsis. *J. Matern. Fetal Neonatal. Med.* **2010**, 23, 617–621.
6. Brignola C, Campieri M, Bazzocchi G, Farruggia P, Tragnone A, Assuero Lanfranchi G. A laboratory index for predicting relapse in asymptomatic patients with Crohn's disease. *Gastroenterology.* **1986**, 91, 1490–1494.
7. Miranda-García P, Chaparro M, Gisbert JP. Correlation between serological biomarkers and endoscopic activity in patients with inflammatory bowel disease. *Gastroenterol. Hepatol.* **2016**, 39, 508–515.
8. Benitez JM, Meuwis MA, Reenaers C, Van Kemseke C, Meunier P, Louis E. Role of endoscopy, cross-sectional imaging, and biomarkers in Crohn's disease monitoring. *Gut.* **2013**, 62, 1806–1816.
9. Dominguez Renedo O, Alonso-Lomillo MA, Arcos Martinez MJ. Recent developments in the field of screen-printed electrodes and their related applications. *Talanta.* **2007**, 73, 202–219.
10. Taleat Z, Khoshroo A, Mazloum-Ardakani M. Screen-printed electrodes for biosensing: a review (2008–2013). *Microchim. Acta.* **2014**, 181, 865–891.
11. Costa-Rama E, Costa-Garcia A. Screen-printed electrochemical Immunosensors for the detection of cancer and cardiovascular biomarkers. *Electroanalysis.* **2016**, 28, 1700–1715.
12. Christiansen MS, Blirup-Jensen S, Foged L, Larsen M, Magid E. A particle-enhanced turbidimetric immunoassay for quantitative determination of orosomucoid in urine: development, validation, and reference values. *Clin. Chem. Lab. Med.* **2004**, 42, 1168–1177.
13. Suprun EV, Zharkova MS, Morozevich GE, Veselovsky AV, Shumyantseva VV, Archakov AI. Analysis of redox activity of proteins on the carbon screen printed electrodes. *Electroanalysis.* **2013**, 25, 2109–2116.
14. Paleček E, Tkac J, Bartosik M, Bertok T, Ostatna V, Paleček J. Electrochemistry of Nonconjugated Proteins and Glycoproteins. Toward Sensors for Biomedicine and Glycomics. *Chem. Rev.* **2015**, 115, 2045–2108.
15. Trefulka M, Paleček E. Direct chemical modification and voltammetric detection of glycansin glycoproteins. *Electrochem. Commun.* **2014**, 48, 52–55.

16. Bertok T, Klukova L, Sediva A, Kasak P, Semak V, Micusik M, Omastova M, Chovanova L, Vlcek M, Imrich R, Vikartovska A, Tkac J. *Anal. Chem.* **2013**, 85, 7324–7332.
17. Yang C, Gu B, Xu C, Xu X. Self-assembled ZnO quantum dot bioconjugates for direct electrochemical determination of allergen. *J. Electroanal. Chem.* **2011**, 660, 97–100.
18. Mayorga-Martinez CC, Latiff NM, Sheng Eng AY, Sofer Z, Pumera M. Black phosphorus nanoparticle labels for immunoassays via hydrogen evolution reaction mediation. *Anal. Chem.* **2016**, 88, 10074–10079.
19. Toh RJ, Mayorga-Martinez CC, Sofer Z, Pumera M. MoSe<sub>2</sub> nanolabels for electrochemical immunoassays. *Anal. Chem.* **2016**, 88, 12204–12209.
20. Trefulka M, Paleček E. Voltammetry of Os(VI)-modified polysaccharides at carbon electrodes. *Electroanalysis*. **2009**, 21, 1763–1766.
21. Trefulka M, Paleček E. Modification of poly- and oligosaccharides with Os(VI) pyridine. Voltammetry of the Os(VI) adducts obtained by ligand exchange. *Electroanalysis*. **2013**, 25, 1813–1817.
22. Trefulka M, Paleček E. Can voltammetry distinguish glycan isomers? *Chem. Pap.* **2015**, 69, 241–244.
23. Trefulka M, Paleček E. Distinguishing glycan isomers by voltammetry. Modification of 2,3-sialyllactose and 2,6-sialyllactose by osmium(VI) complexes. *Electrochem. Commun.* **2017**, 85, 19–22.
24. Stumpe M, Miller C, Morton NS, Bell G, Watson DG. High-performance liquid chromatography determination of  $\alpha_1$ -acid glycoprotein in small volumes of plasma from neonates. *J. Chromatogr. B.* **2006**, 831, 81–84.
25. Trefulka M, Paleček E. Voltammetry of Os(VI)-modified polysaccharides. *Electroanalysis*. **2010**, 22, 1837–1845.
26. Nagy B, Toth A, Savina I, Mikhalovsky S, Mikhalovska L, Geissler E, Laszlo K. Double probe approach to protein adsorption on porous carbon surfaces. *Carbon.* **2017**, 112, 103–110.
27. Sierra T, Crevillén AG, Escarpa A. Derivatization agents for electrochemical detection in amino acid, peptide, and protein separations: the hidden electrochemistry? *Electrophoresis*. **2017**, 38, 2695–2703.

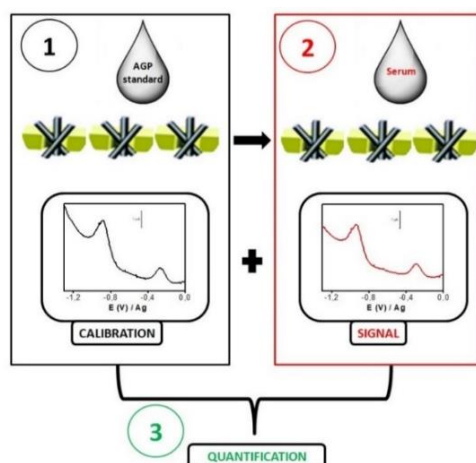


## III.2.2. Article 2: Disposable carbon nanotube scaffold films for fast and reliable assessment of $\alpha_1$ -acid glycoprotein in human serum using adsorptive transfer stripping square wave voltammetry

Tania Sierra, Silvia Dorte, María Cristina González, F. Javier Palomares, Agustín G. Crevillén, Alberto Escarpa

Analytical and Bioanalytical Chemistry 411 (2019) 1887-1894

**Abstract:**  $\alpha_1$ -acid glycoprotein (AGP) is a serum glycoprotein whose levels are increased two or three times during disease or injury. This makes it a potential biomarker for inflammatory bowel diseases and sepsis. Consequently, fast, simple, and cheap analytical methods for prognosis, diagnosis, and follow-up of these diseases are demanded. In this work, we propose a simple electrochemical approach based on carbon nanotubes scaffold films (CNSFs) for total AGP determination in serum samples. Firstly, AGP is labeled with an electrochemical tag (osmium (VI) complex), and then the total amount of AGP is quantified by adsorptive transfer stripping square wave voltammetry (AdTSWV). Multi-walled carbon nanotubes scaffold films (MWSFs) yielded the best analytical performance in terms of sensitivity with a good limit of detection of  $0.6 \text{ mg L}^{-1}$  for AGP determination in serum samples, in less than 20 min. A simplified AGP calibration and its sequential serum sample analysis strategy with good accuracy (81 %) and excellent reproducibility ( $\text{RSD} < 1 \%$ ) was additionally proposed to meet the point-of-care/needs requirements.





#### 1. Introduction

$\alpha_1$ -acid glycoprotein (AGP), also named orosomucoid, is a serum glycoprotein with a low isoelectric point ( $pI = 2.8-3.8$ ), a molecular weight around 41-43 KDa, and a high carbohydrate content (40 % w/w) (1,2). The function of AGP is still not well-known, but it is considered as an anti-inflammatory and immunomodulatory protein (3). AGP concentration in serum of healthy individuals is 0.2-1.0 g L<sup>-1</sup> (4), but serum concentration can rise up to three or fourfold because of infection, rheumatic disorders, surgery, myocardial infarction, or nephritis (5). In fact, AGP levels have been evaluated as serum biomarker for inflammatory bowel diseases (6) and even for early diagnosis of neonatal sepsis (7), yielding excellent results in prognosis of Crohn disease (8) and endoscopic activity (occurrence of aphthous lesions, nodularity, erythema, ulcerations, stenosis in the bowel wall) (9). Typically, colonoscopy and cross-sectional imaging are employed for Crohn disease follow-up. However, both techniques are time consuming and expensive and, also, colonoscopy is invasive, so there is a high demand in finding reliable biomarkers and alternative methodologies for Crohn disease monitoring (10).

In this sense, AGP determination is commonly carried out by separation techniques (1-3,11,12) and enzyme immunoassays (13). In addition, there are several commercial kits for its total amount determination based on a turbidimetric immunoassay (14). However, these techniques are time consuming and/or expensive.

Electrochemical methods are an interesting alternative because of its low-cost, easy miniaturization (point-of-care testing), and high sensitivity (15,16). In fact, electrochemical detection of glycoproteins can be performed by two strategies: label-free and label-based detection. The most employed electrochemical techniques for label-free analysis are electrochemical impedance spectroscopy (EIS) and capacitance (17,18). These methods employ recognizing elements such as lectins or antibodies but their application in complex and real samples is scarce. With respect to label-based detection, nanomaterials have been used as electrochemical tags for



glycoproteins in several works (19–21). However, real samples were not analyzed in these works.

In this sense, Palecek's group successfully employed osmium(VI) complexes as electrochemical probe for oligo- and polysaccharide detection (22) and then, they expanded its use to glycoproteins, demonstrating Os(VI) complexes specifically link to the carbohydrate part and not to the polypeptide backbone (23). The osmium (VI) complexes react with diol groups from saccharides to produce osmate esters, which generate two electrochemical signals in carbon electrodes (24). Recently, our group developed a simple and cheap electrochemical method for total AGP determination in serum using this electrochemical probe and disposable screen-printed carbon electrodes (SPCEs). However, the labeling protocol was too long (16 h), hindering its application as point-of-care testing (POCT) (25).

Carbon nanomaterials (CNMs), such as graphene (26–31) or carbon nanotubes (CNTs) (32–35), have been used as electrochemical transducers in order to improve the analytical signal due to their unique physical and chemical properties. CNMs exhibit superior electrical and mechanical properties, thermal stability, electrochemical activity, ease-to-modify, chemical diversity, and biocompatibility, ensuring their wide applications in electrochemical (bio)sensors (36–38). They enhance the analytical performance in terms of selectivity, sensitivity, and reproducibility. Also, CNM based electrodes yield lower detection potentials for several compounds, while faradaic currents are increased and surface fouling is reduced (28,35,39).

Commonly, the building of CNM-based detectors has been carried out using thin film coating (drop casting approach). The design of CNM thin film electrodes is very simple and a wide range of underlying electrodes can be chosen (40). Although this approach has widely been used with satisfactory results, however, it has some limitations. Mainly, nanomaterial distribution on the electrode surface leads to a fragile modification and the analytical response is still dependent on both the nanomaterial and the electrode substrate (41,42).

### **III.2.2. AGP determination using carbon nanomaterial electrodes**

---

As alternative to casting approach and in order to exploit the advantages of the use of the CNMs, our group has recently proposed a novel technology which the transduction is based exclusively on them (41,43). To this end, the transducers were fabricated by filtering CNMs solutions through a Teflon filter, and then they were retained on the filter, creating a conductive film over the non-conductive filter. In this approach, the electronic transfer occurs directly on the target nanomaterial so that it is the only transducer in the electrochemical sensing and, consequently, the analytical advantage of these nanomaterials is directly exploited. This approach was successfully applied to the determination of neurotransmitters and uric acid (43) and L-tyrosine in plasma and blood samples (44).

On the other hand, one of the main drawbacks in electrochemical detection of proteins is that when proteins are oxidized on solid electrodes, these are easily poisoned by the strong adsorption ability of proteins. Furthermore, glycoproteins yield poor sensitivity in direct oxidation because their carbohydrate part is not electroactive in physiological conditions. In this sense, the use of CNMs can be a pertinent approach to overcome these problems.

In the following sections, the analytical potency of disposable carbon nanotube scaffold film electrodes (CNSFs) for fast, simple, and cheap total AGP determination will be demonstrated. A future utility of these CNSFs for POCT is also envisioned. To our best knowledge, this is the first time that this technology is applied for glycoprotein detection.

## **2. Material and methods**

### **2.1. Reagents**

$\alpha_1$ -acid glycoprotein (AGP), potassium osmate (VI) dihydrate, N,N,N',N'-tetramethylethylenediamine (TEMED), boric acid, pyridine, N,N-dimethylformamide, certified human serum reference material (ERM-DA470K/IFCC),  $[\text{Ru}(\text{NH}_3)_6]\text{Cl}_3$ ,  $\text{K}_4\text{Fe}(\text{CN})_6 \cdot 3\text{H}_2\text{O}$ ,  $\text{K}_3\text{Fe}(\text{CN})_6$ , multi-walled carbon nanotubes (MWCNTs, ref. 659258), and single-walled carbon nanotubes (SWCNTs, ref. 704113) were purchased from Sigma–Aldrich (Darmstadt, Germany). Perchloric acid, hydrochloric acid, acetic acid,

disodium hydrogen phosphate, and sodium dihydrogen phosphate were purchased from Panreac (Barcelona, Spain). Sodium acetate was purchased from Merck (Darmstadt, Germany). Phosphoric acid was acquired from Scharlab (Barcelona, Spain).

All solutions were prepared in Milli-Q water (Merck Millipore, Darmstadt, Germany).

Teflon filters with a pore size of 0.1  $\mu\text{m}$  (JVWP01300, Millipore Omnipore), double-sided cello tape (Fixo, Spain), silver conductive paint (Electrolube, UK), and epoxy protective overcoat (242-SB, ESL Europe) were used to build SPCEs.

### 2.2. Instrumentation

Potentiostat Autolab PGSTAT204 (Methrom-Autolab, Utrecht, The Netherlands) was used for all electrochemical and impedance measurements. This instrument was controlled by the software Nova 1.10.

Screen-printed carbon electrodes (SPCEs) (DRP-110, Dropsens, Oviedo, Spain) were employed. They consist of carbon working electrode (4 mm diameter), carbon counter electrode, and silver reference electrode. This kind of SPCEs works as an electrochemical cell, which needs a minimum volume of 50  $\mu\text{L}$ .

Microcentrifuge MiniSpin<sup>®</sup> (Eppendorf, Hamburg, Germany) was employed for centrifugation.

### 2.3. Procedures

#### 2.3.1. Electrode design and fabrication

CNSFs consist of a working electrode (4 mm diameter), a carbon counter electrode, and a silver reference electrode. Two kinds of CNSFs were prepared using SWCNT (SWSFs) and MWCNT (MWSFs).

The working electrode was fabricated as follows. Firstly, the carbon nanotubes were dispersed in N,N-dimethylformamide (0.5 mg/100 mL concentration). Dispersions were sonicated in ultrasonic bath for 1 h and then, a tip sonicator VCX130 (Sonics, Newtown, USA) was used for 15 min

### **III.2.2. AGP determination using carbon nanomaterial electrodes**

---

at 100 % (130 W), to assure the maximum dispersion of CNMs. Then, MWCNT and SWCNT dispersions (5.0 mL) were separately filtered using a steel funnel on a 0.1  $\mu\text{m}$  Teflon filter. This membrane was cut with a biopsy punch (circle of 4 mm diameter, Biopunch, Redding, USA) and stuck in a double-sided adhesive tape. This membrane was set on a ceramic slab and the adequate electric contacts were created with conductive silver paint. These electric contacts were isolated by using epoxy protective over coat (44).

#### **2.3.2. Preparation of Os(VI)O<sub>2</sub>(OH)<sub>2</sub>py complex**

The preparation of Os(VI)O<sub>2</sub>(OH)<sub>2</sub>py complex was carried out according to bibliography (24). 18.4 mg (50  $\mu\text{mol}$ ) of potassium osmate dihydrate were suspended in 4.97 mL water, then 8.9  $\mu\text{L}$  (8.7 mg, 110  $\mu\text{mol}$ ) pyridine were added and followed by the addition of 10  $\mu\text{L}$  10 M HCl. The pH level was adjusted to 6.5–7.5 and the solution was filtered through a 0.45  $\mu\text{m}$  membrane (Tecno-Air, Barcelona, Spain). The final concentration of Os(VI)py complex obtained was 10 mM.

#### **2.3.3. AGP labeling with Os(VI)O<sub>2</sub>(OH)<sub>2</sub>py complex and ligand exchange**

Briefly, AGP-Os(VI)py complexes were prepared as follows: 0.57 mg of AGP ( $1.40 \times 10^{-8}$  mol) were dissolved into 225  $\mu\text{L}$  of 50 mM sodium phosphate buffer at pH = 7 using a "protein low bind" Eppendorf tube (Hamburg, Germany) (24). Then, 25  $\mu\text{L}$  of 10 mM Os(VI)O<sub>2</sub>(OH)<sub>2</sub>py solution were added in the previous solution and it was kept under agitation 4 min at 25 °C and 950 r.p.m. using a thermo shaker (Biosan TS-100C, Riga, Latvia). For ligand exchange, four-fold molar excess of TEMED with respect to Os(VI)py was added (10  $\mu\text{L}$  of 0.1 M TEMED solution prepared in 0.2 M acetate buffer pH 5.0) and agitated 8 min at 25 °C and 950 r.p.m. The final concentration of AGP-Os(VI) adduct obtained was 2.18 g L<sup>-1</sup>. Finally, working solutions were prepared by dilution of stock solution in Britton–Robinson (BR) buffer.

The labeling protocol of AGP was modified when serum samples were analyzed due to the high concentration of glucose and other carbohydrates in these samples, according to our previously published work (25). The

protocol was as follows: 200.5  $\mu\text{L}$  of serum sample was mixed with 49.5  $\mu\text{L}$  of  $\text{Os(VI)O}_2(\text{OH})_2\text{py}$  solution and it was kept under agitation 4 min at 25  $^\circ\text{C}$  and 950 r.p.m. using a thermo shaker (Biosan TS-100  $^\circ\text{C}$ , Riga, Latvia). Twenty microliters of TEMED (0.1 M TEMED solution prepared in 0.2 M acetate buffer pH 5.0) was added and agitated 8 min at 25  $^\circ\text{C}$  and 950 r.p.m. Later, AGP-Os(VI)TEMED adduct was isolated from the rest of proteins by a selective acidic precipitation (45). Briefly, 50  $\mu\text{L}$  of serum labeled with the electrochemical tag Os(VI) and 100  $\mu\text{L}$  of 0.5 M perchloric acid were vortex mixed in a "protein low bind" Eppendorf tube for 20 s. The acidified serum was then centrifuged at 7400 r.p.m. for 20 min at room temperature. Finally, the supernatant was adequately diluted in BR buffer pH = 3 before the AdTSWV analysis.

#### 2.3.4. Electrochemical measurements

Electrochemical detection was performed using adsorptive transfer stripping square wave voltammetry (AdTSWV). In this case, 10  $\mu\text{L}$  of sample was dropped onto the working electrode and the analyte was adsorbed for accumulation time 5 min at open circuit potential. Then, the electrode was washed with water during 1 min and finally, 50  $\mu\text{L}$  of background electrolyte (0.2 M BR buffer pH 3) was dropped on the SPCE for voltammogram recording. Square wave voltammetry (SWV) parameters were start potential  $-1.4$  V, end potential  $+0.1$  V, step potential 5 mV, amplitude 50 mV, and frequency 100 Hz, if not stated otherwise. The buffer and the optimal electrochemical conditions were established from our previously published work (25).

Electrochemical impedance spectroscopy (EIS) was performed using 5 mM  $\text{K}_4\text{Fe(CN)}_6/\text{K}_3\text{Fe(CN)}_6$  in 0.1 M KCl electrolyte as redox probe. The frequencies ranged from 100,000 to 0.01 Hz.

#### 2.3.5. Measurements of electrode surface area by using Randles–Sevcik equation

In cyclic voltammetry, a reversible process follows the Randles–Sevcik equation (at 25  $^\circ\text{C}$ ):

$$I_p = 2.69 \times 10^5 n^{\frac{3}{2}} A C_o D_0^{\frac{1}{2}} v^{\frac{1}{2}}$$

### III.2.2. AGP determination using carbon nanomaterial electrodes

---

where  $i_p$  refers to the anodic peak current,  $n$  is the electron transfer number,  $A$  is the electrode surface area,  $D_o$  is the diffusion coefficient of redox probe,  $C_o$  is the concentration of redox probe, and  $v$  is the scan rate.

Using a reversible redox probe, it is possible to measure the electrode surface area by calculating the slope of  $i_p$  vs  $v^{1/2}$  plot. With this purpose, cyclic voltammograms of SPCE, SWSFs, and MWSFs ( $n = 3$ ) were recorded from  $-0.8$  to  $+0.6$  V at different scan rates (from  $v = 0.01$  to  $v = 0.1$  V s $^{-1}$ ) using 1 mM  $[\text{Ru}(\text{NH}_3)_6]\text{Cl}_3$  in 0.5 M  $\text{KNO}_3$  electrolyte (number of transferred electrons = 1 and  $D_o = 7.74 \times 10^{-6}$  cm $^2$  s $^{-1}$  (46)).

#### 2.3.6. X-ray spectroscopy analysis

X-ray photoelectron spectroscopy (XPS) has been used to characterize the chemical composition of the working electrodes. XPS spectra were acquired at normal emission in an UHV chamber with a base pressure of  $10^{-10}$  mbar equipped with a hemispherical electron energy analyzer (SPECS Phoibos 150 spectrometer, Berlin, Germany) and a 2D delay-line detector, using a Mg Al-K $\alpha$  (1253.6 eV) X-ray source. The spectra were analyzed with the CasaXPS program using a Shirley method for background subtraction, for X-ray source satellite removal, and data processing for quantitative XPS analysis. The absolute binding energies of the photoelectron spectra were determined by referencing to the sp $^2$  transition of C $_{1s}$  at 284.6 eV.

For a detailed analysis, C $_{1s}$  high-resolution core level spectra were recorded using an energy step of 0.025 eV and a pass energy of 10 eV in high magnification mode to obtain the narrowest line shape analysis and proper core level fitting. XPS spectra fitting was done by using the deconvolution of several mixed percentage of Gaussian–Lorentzian components, keeping the fwhm and the Gaussian/Lorentzian ratio constant. The energy of the peaks and their relative heights were determined by a least squares method to account for the emission ascribed to the different chemical environment of carbon atoms according to the values reported (47,48).

### 3. Results and discussion

#### 3.1. CNSFs as exclusive electrochemical transducers for AGP-Os(VI) sensing

First of all, the new labeling methodology for AGP (**Figure III.2.2.1 A**), which relies on an exchange of ligands, was evaluated. The obtained AGP-Os(VI) adduct was electrochemically studied using adsorptive transfer stripping square wave voltammetry (AdTSWV) and screen-printed carbon electrodes (SPCEs). **Figure III.2.2.1 B** shows voltammograms of blank (lower black line), AGP (upper black line), and AGP-Os(VI) (red line). Clearly, two peaks at  $-0.90$  V and  $-0.30$  V corresponding to the AGP-Os(VI)TEMED adduct can be observed, which were not found neither unlabeled AGP nor blank. These results demonstrate that this new methodology is valid for the labeling of AGP and it just spends 12 min, reducing the labeling time with respect to our previous work (16 h) (25). This fact reduces dramatically the overall analysis time because labeling is the time-limiting step.

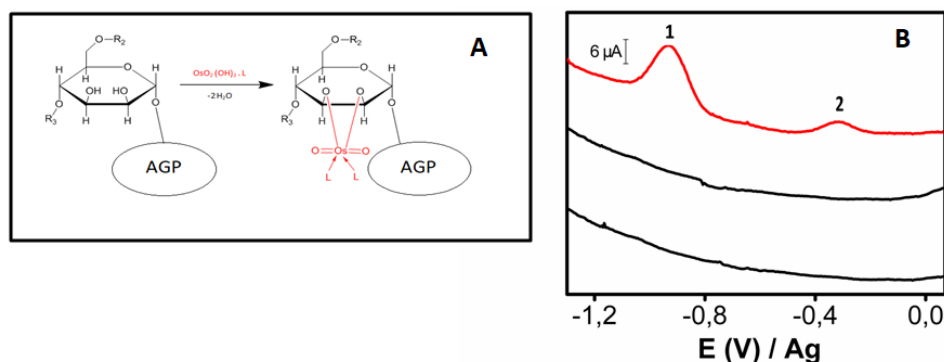


**Figure III.2.2.1.** (A) AGP labeling with Os(VI) complex. (B) Voltammograms obtained by AdTSWV using SPCE for 0.2 M BR buffer at pH 3.0 (blank) (lower black line),  $400 \text{ mg L}^{-1}$  AGP in BR buffer (control) (upper black line) and  $400 \text{ mg L}^{-1}$  AGP-Os(VI) in BR buffer (red line). Conditions: start potential  $-1.4$  V, end potential  $+0.1$  V, step potential 5 mV, amplitude 50 mV, frequency 100 Hz.

### III.2.2. AGP determination using carbon nanomaterial electrodes

As it was aforementioned, the oxidation of proteins on solid electrodes causes electrode passivation. In addition, glycoproteins yield poor sensitivity in direct oxidation. In this sense, the use of CNMs can be a pertinent approach to overcome these problems. Consequently, MWSFs and SWSFs were explored as electrochemical transducers for AGP-Os(VI) detection. In these films, the transduction is exclusively based on the nanomaterial since Teflon filter is a nonconductive substrate (**Figure III.2.2.2 A**).

As can be observed in **Figure III.2.2.2 B**, while that MWSFs and SPCE showed the best analytical responses, surprisingly, the SWSFs showed the poorest performance (peak 1 was selected for electrochemistry follow-up). To understand these differences, it must be taken into account that only adsorbed protein is determined by AdTSWV. Therefore, the active surface of working electrodes and chemical species on the carbon surface will play a prominent role in this case.

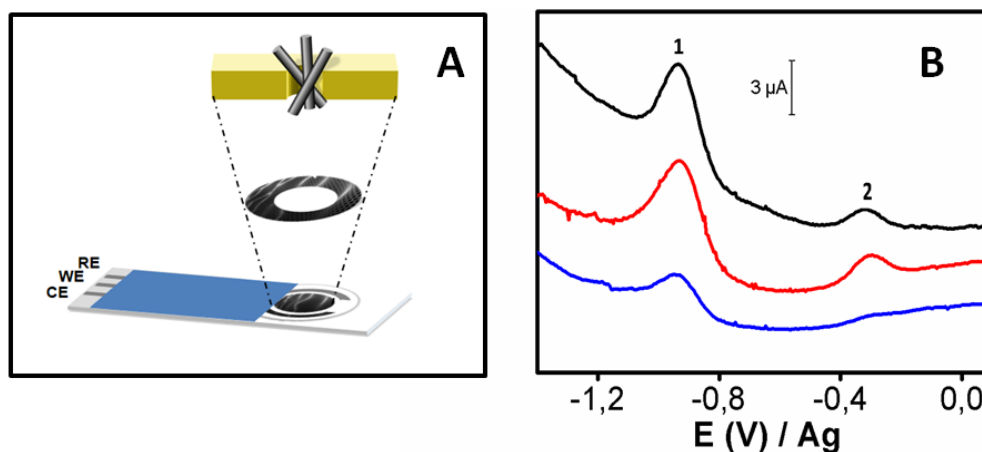


**Figure III.2.2.2.** (A) CNSFs for sensing of AGP-Os(VI). (B) Voltammograms obtained for AGP-Os(VI) (AGP 10 mg L<sup>-1</sup>) in BR buffer pH 3.0. SWSFs (blue line), SPCEs (red line), and MWSFs (black line). Conditions: as in **Figure III.2.2.1**.

Firstly, CNSFs and SPCEs were analyzed by EIS. Based on Nyquist plots (**Figure III.2.2.3**), materials can be sorted according to the charge transfer resistance as follows: SPCEs > MWSFs > SWSFs, revealing the superior conductivity for SWSFs.



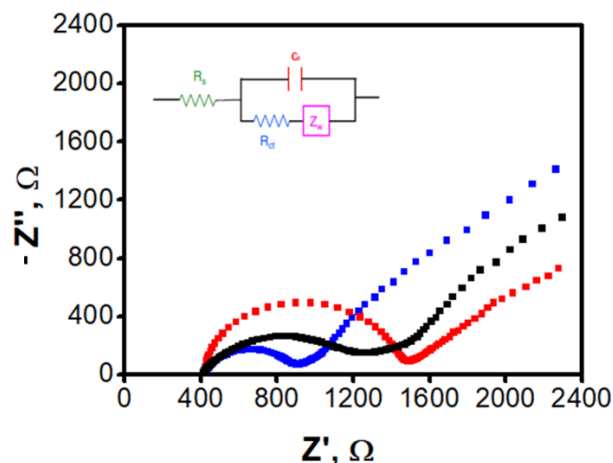


**Figure III.2.2.3.** Nyquist plots corresponding to SWSF (blue color), MWSF (black color), and SPCE (red color). Frequencies ranged from 100,000 to 0.01 Hz using 5 mM  $K_4Fe(CN)_6/K_3Fe(CN)_6$  in 0.1 M KCl electrolyte as redox probe.

As it was aforementioned, AdTSWV measures only adsorbed protein, so the greater the electrode surface, the higher the electrochemical signal. Therefore, the surface of every kind of electrode was electrochemically measured by cyclic voltammetry and using Randles–Sevcik equation. The surface areas of SPCEs, MWSFs, and SWSFs were  $0.091 \pm 0.004 \text{ cm}^2$ ,  $0.110 \pm 0.008 \text{ cm}^2$ , and  $0.11 \pm 0.01 \text{ cm}^2$ , respectively. CNSFs exhibited higher active surface than SPCEs (approx. 20 %). Based on electrochemical characterization, CNM-based films showed the best features; however, specifically, SWSFs showed the lowest sensitivity for AGP sensing. This means that there is another factor controlling the process.

To this end, the surface of all electrodes was analyzed by XPS ( $C_{1s}$  analysis, Electronic Supplementary Material, **Figure III.2.2.S1**). According to these results (**Table III.2.2.1**), SPCE contains more oxygen species, carbons with higher oxidation state, and more defects on its surface than the rest. Furthermore, SWSF is the lowest oxidized one. Although the hydrophobic,  $\pi$ -cation, and  $\pi$ - $\pi$  stacking interactions are the main forces in the protein adsorption on carbon materials (49, 50), hydrophilic interactions cannot be disregarded because of the high glycosylation degree of AGP (40 %  $w/w$ ). We hypothesize that hydrophilic interaction (e.g.,

### III.2.2. AGP determination using carbon nanomaterial electrodes

hydrogen bonding) between carbohydrates from AGP and oxygen containing species from carbon surfaces occurs. This fact could explain why SPCE adsorbs higher amount of AGP than MWSF yielding higher electrochemical signal for AGP despite the lower active surface.

**Table III.2.2.1.** Relative percentage of peak areas for each type of atomic bonding obtained by XPS C<sub>1s</sub> analysis of the studied electrodes.

Functional Group	SPCE	MWSF	SWSF
C-C	59.5	80.0	85.3
C-H or defective graphite	12.4	12.9	7.5
C=O (carbonyl group)	23.6	6.9	7.2
COOR (carboxylic group)	4.5	0.2	0.01

### 3.2. Simplified calibration and sequential determination of AGP in human serum samples

Intra-MWSFs/SPCEs and inter-MWSFs/SPCEs precision was carefully studied. **Figure III.2.2.4** shows intra-MWSFs/SPCEs for AGP-Os(VI) peak area (n = 3): MWSFs (black) and SPCEs (red). In the second measurement (2<sup>nd</sup> in **Figure III.2.2.4**), AGP-Os(VI) signal drops 44 % for SPCE and only 8 % for MWSF. This higher fouling resistance behavior was attributed to the high surface of MWCNTs.

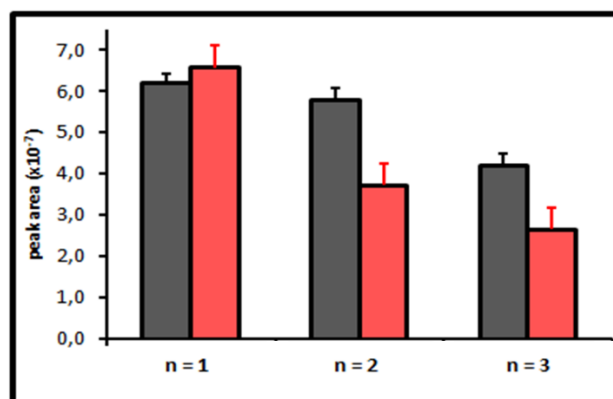


**Figure III.2.2.4.** Peak 1 area variation for three consecutive measurements by AdTSWV using MWSFs (black) and SPCEs (red).

Inter-MWSF/SPCE precision was also carefully studied using an AGP-Os(VI) solution (40 mg L<sup>-1</sup> AGP) prepared in BR buffer at pH 3.0. In SPCEs, RSD = 11 % (n = 4) is obtained using the same batch and employing different SPCEs, whereas in MWSFs, RSD = 5 % (n = 4) was obtained. The origin of this variability using the same batch is mainly due to differences in the electrode active surface. This means that our fabrication protocol is more reproducible than that used for the commercial screen-printed electrodes. Finally, batch-to-batch solutions reproducibility was also evaluated yielding a RSD value of 21 % (n = 4) for SPCEs and 13 % (n = 4) for MWSFs.

Then, MWSF capabilities for determination of AGP in serum samples were carefully evaluated. A good linear correlation coefficient was obtained ( $r = 0.9994$ ) for the concentration range assayed (from 0.8 to 40 mg L<sup>-1</sup> using the peak 1 area) with a slope of  $(7.06 \pm 0.08) \times 10^{-8}$  A L mg<sup>-1</sup> and the intercept  $(1.2 \pm 1.4) \times 10^{-8}$  A (n = 3). The limit of detection (LOD) obtained from the calibration curve was 0.6 mg L<sup>-1</sup> (3 S/N criterion). Interestingly, this LOD was three times lower than that obtained with SPCEs (1.6 mg L<sup>-1</sup>) (25), and it meets the AGP detection requirements in serum samples (AGP concentration in serum is in 0.2-1.0 g L<sup>-1</sup> range).

In addition, because of (i) the demonstrated linearity, (ii) the intercept obtained was zero from a statistical point of view and, (iii) the MWSFs anti-fouling capabilities, and in order to use our approach in extremely simple use as POCT, a simplified calibration and sequential AGP analysis was proposed (namely single-point calibration). The strategy consists of two steps using the same MWSF: first, an AGP standard solution of known concentration is measured (obtaining a single-point calibration curve) and, second, serum sample is quantified.

A certified human serum reference material was analyzed for method validation using both calibration approaches (**Table III.2.2.2**). In the first case, the value obtained was  $505 \pm 20$  mg L<sup>-1</sup> (RSD = 4 %) for AGP (n = 3), whereas the value obtained by single-point calibration was  $498 \pm 7$  mg L<sup>-1</sup> (RSD = 1 %, n = 3). Interestingly, there was no statistical difference (P = 0.05) between both strategies but the precision was improved by using the simplified calibration. Furthermore, this strategy provides a checking of the

### III.2.2. AGP determination using carbon nanomaterial electrodes

MWSF analytical performance for quality control purpose. With respect to method accuracy, the value of the reference material is  $617 \pm 13 \text{ mg L}^{-1}$  so protein recoveries of 82 % and 81 % were obtained for external and single-point calibrations, respectively. These results were similar to those obtained by Stumpe *et al.* (79.1 %) employing the same sample treatment (acidic precipitation) for AGP isolation in plasma samples (45).

**Table III.2.2.2.** Determination of AGP in serum sample using MWSFs.

Calibration Protocol	$\bar{x} \pm s \text{ (mg L}^{-1}\text{)}$	RSD (%)	Recovery (%)
External	$505 \pm 20$	4	82
Simplified	$498 \pm 7$	1	81

## 4. Conclusions

MWSFs exhibited an excellent analytical performance for fast and reliable assessment of AGP in clinical samples. The combination of smart AGP-Os(VI) adduct electrochemistry on board of transducers, exclusively constituted by MWCNTs, in connection with a simplified calibration and analysis route, allowed AGP determination in less than 20 min with good accuracy. MWSFs become a disposable electroanalytical tool for the determination of complex molecules such as glycoproteins, opening the door for future clinical and POCT applications.

### Acknowledgments

This work has been financially supported by the NANOAVANSENS program from the Community of Madrid (S2013/ MIT-3029), the Spanish Ministry of Economy, Industry and Competitiveness (CTQ2017-86441-C2-1-R), and the MINECO (MAT2016-80394-R). T.S. acknowledges the FPI fellowship from the University of Alcalá.

### Associated content

#### Supporting Information

**Figure III.2.2.S1.** XPS spectra of the C<sub>1s</sub> corresponding to the working electrodes (SPCE, MWSFE and SWSFE) together with fit composed of chemically shifted components associated to different C chemical bonding, respectively.

### Author information

#### Corresponding Authors

Alberto Escarpa – Department of Analytical Chemistry, Physical Chemistry and Chemical Engineering, University of Alcalá, Madrid, Spain. Chemical Research Institute “Andrés M. del Río” (IQAR), University of Alcalá, Madrid, Spain; orcid.org/0000-0002-7302-0948; Email: alberto.escarpa@uah.es

Agustín G. Crevillen – Department of Analytical Sciences, Faculty of Sciences, Universidad Nacional de Educación a Distancia (UNED), Madrid, Spain; Email: agustingcrevillen@ccia.uned.es

#### Other Authors

Tania Sierra - Department of Analytical Chemistry, Physical Chemistry and Chemical Engineering, University of Alcalá, Madrid, Spain.

Silvia Dorte - Department of Analytical Chemistry, Physical Chemistry and Chemical Engineering, University of Alcalá, Madrid, Spain.

María Cristina González - Department of Analytical Chemistry, Physical Chemistry and Chemical Engineering, University of Alcalá, Madrid, Spain. Chemical Research Institute “Andrés M. del Río” (IQAR), University of Alcalá, Madrid, Spain.

F. Javier Palomares - Instituto de Ciencia de Materiales de Madrid, CSIC, Madrid, Spain.

#### Authors Contribution

The manuscript was written through contributions of all the authors. All the authors have given approval to the final version of the manuscript.

#### Supplementary Information

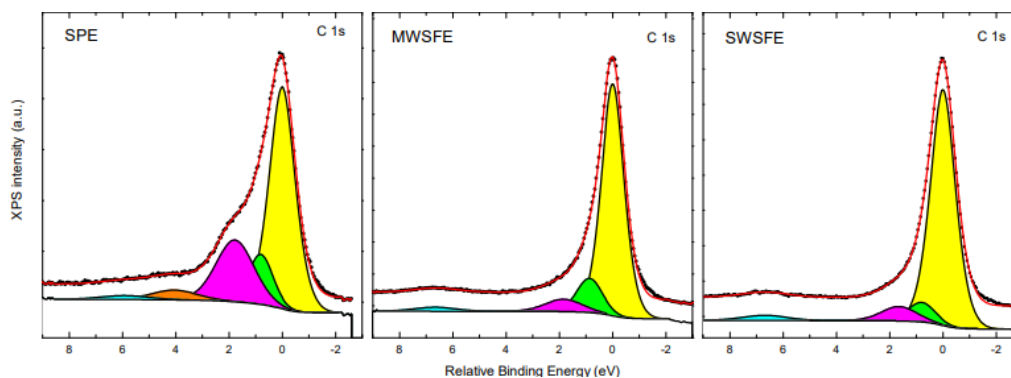


**Figure III.2.2.S1.** XPS spectra of the  $C_{1s}$  corresponding to the working electrodes (SPCE, MWSFE and SWSFE) together with fit composed of chemically shifted components associated to different C chemical bonding, respectively. XPS spectra were normalized to maximum intensity peak in each case for better visual inspection and direct comparison between the samples in order to emphasize subtle line-shape differences, and quantity its contribution for each C environment. Data points in every spectrum are represented as black symbols, and Shirley background and component peaks using solid lines. The fitting curve (red line) resulted from the addition of five contributions belonging to: C=C graphitic structures (yellow), C-H or C-C defective graphitic,  $sp^3$  configurations (green), C-O carbonyl groups (magenta), C=O carboxylic groups (orange), and  $\pi$ - $\pi^*$  transitions coming from graphitic structures (cyan).

#### References

1. Puerta A, Díez-Masa JC, Martín-Álvarez PJ, Martín-Ventura JL, Barbas C, Tuñón J, Egido J, de Frutos M. Study of the capillary electrophoresis profile of intact  $\alpha$ -1-acid glycoprotein isoforms as a biomarker of atherothrombosis. *Analyst*. **2011**,136,816–822.
2. Zhang C, Hage DS. Glycoform analysis of alpha1-acid glycoprotein by capillary electrophoresis. *J Chromatogr A*. **2016**,1475,102–109.
3. Lacunza I, Sanz Perucha J, Díez-Masa JC, de Frutos M. CZE of human alpha-1-acid glycoprotein for qualitative and quantitative comparison of samples from different pathological conditions. *Electrophoresis*. **2006**, 27, 4205–4214.
4. Shiyani SD, Bovin NV. Carbohydrate composition and immunomodulatory activity of different glycoforms of  $\alpha$ 1-acid glycoprotein. *Glycoconj J*. **1997**, 14, 631–638.
5. Beeram S, Bi C, Zheng X, Hage DS. Chromatographic studies of drug interactions with alpha1-acid glycoprotein by ultrafast affinity extraction and peak profiling. *J Chromatogr A*. **2017**, 1497, 92–101.
6. Vermeire S, Van Assche G, Rutgeerts P. Oratory markers in IBD: magic, or unnecessary toys? *Gut*. **2006**, 55, 426–431.
7. Ipek IO, Saracoglu M, Bozaykut A.  $\alpha$ -1-acid glycoprotein for the early diagnosis of neonatal sepsis. *J. Matern. Fetal Neonatal Med*. **2010**, 23, 617–621.
8. Brignola C, Campieri M, Bazzocchi G, Farruggia P, Tragnone A, Lanfranchi GA. A laboratory index for predicting relapse in asymptomatic patients with Crohn's disease. *Gastroenterology*. **1986**, 91, 1490–1494.
9. Miranda-García P, Chaparro M, Gisbert JP. Correlation between serological biomarkers and endoscopic activity in patients with inflammatory bowel disease. *Gastroenterol Hepatol*. **2016**, 39, 508–515.
10. Benitez JM, Meuwis MA, Reenaers C, Van Kemseke C, Meunier P, Louis E. Role of endoscopy, cross-sectional imaging and biomarkers in Crohn's disease monitoring. *Gut*. **2013**, 62, 1806–1816.
11. Suzuki S. Highly sensitive methods using liquid chromatography and capillary electrophoresis for quantitative analysis of glycoprotein glycans. *Chromatography*. **2014**, 35, 1–22.
12. Zhang C, Bi C, Clarke W, Hage DS. Glycoform analysis of alpha1- acid glycoprotein based on capillary electrophoresis and electrophoretic injection. *J Chromatogr A*. **2017**, 1523, 114–122.
13. Yazawa S, Yokobori T, Kaira K, Kuwano H, Asao T. A new enzyme immunoassay for the determination of highly sialylated and fucosylated human  $\alpha$ -1-acid glycoprotein as a biomarker of tumorigenesis. *Clin Chim Acta*. **2018**, 478, 120–128.
14. Christiansen MS, Blirup-Jensen S, Foged L, Larsen M, Magid E. A particle-enhanced turbidimetric immunoassay for quantitative determination of orosomucoid in urine: development, validation and reference values. *Clin Chem Lab Med*. **2004**, 42, 1168–1177.

### III.2.2. AGP determination using carbon nanomaterial electrodes

---

15. Escarpa A. Food electroanalysis: sense and simplicity. *Chem Record*. **2012**, 12, 72–91.
16. Suprun EV, Shumyantseva VV, Archakov AI. Protein electrochemistry: Application in medicine. A review. *Electrochim Acta*. **2014**, 140, 72–82.
17. Paleček E, Tkac J, Bartosik M, Bertok T, Ostatna V, Paleček J. Electrochemistry of nonconjugated Proteins and Glycoproteins. Toward sensors for biomedicine and glycomics. *Chem Rev*. **2015**, 115, 2045–2108.
18. Bertok T, Klukova L, Sediva A, Kasak P, Semak V, Micusik M, Omastiva M, Chovanová L, Vlcek M, Imrich R, Vikartovska A, Tkac J. Ultrasensitive Impedimetric lectin biosensors with efficient antifouling properties applied in glycoprofiling of human serum samples. *Anal Chem*. **2013**, 85, 7324–7332.
19. Yang C, Gu B, Xu C, Xiaoyong X. Self-assembled ZnO quantum dot bioconjugates for direct electrochemical determination of allergen. *J Electroanal Chem*. **2011**, 660, 97–100.
20. Mayorga-Martinez CC, Latiff NM, Sheng Eng AY, Sofer Z, Pumera M. Black phosphorus nanoparticle labels for immunoassays via hydrogen evolution reaction mediation. *Anal Chem*. **2016**, 88, 10074–10079.
21. Toh RJ, Mayorga-Martinez CC, Sofer Z, Pumera M. MoSe<sub>2</sub> nanolabels for electrochemical immunoassays. *Anal Chem*. **2016**, 88, 12204–12209.
22. Trefulka M, Paleček E. Voltammetry of Os(VI)-modified polysaccharides at carbon electrodes. *Electroanalysis*. **2009**, 21, 1763–1766.
23. Trefulka M, Paleček E. Direct chemical modification and voltammetric detection of glycans in glycoproteins. *Electrochem Commun*. **2014**, 48, 52–55.
24. Trefulka M, Paleček E. Modification of poly- and oligosaccharides with Os(VI) pyridine. Voltammetry of the Os(VI) adducts obtained by ligand exchange. *Electroanalysis*. **2013**, 25, 1813–1817.
25. Sierra T, González MC, Moreno B, Crevillen AG, Escarpa A. Total  $\alpha_1$ -acid glycoprotein determination in serum samples using disposable screen-printed electrodes and osmium (VI) as electrochemical tag. *Talanta*. **2018**, 180, 206–210.
26. Martin A, Escarpa A. Graphene: the cutting-edge interaction between chemistry and electrochemistry. *Trends Anal Chem*. **2014**, 56, 13–26.
27. Zhang Q, Wu Z, Li N, Pu Y, Wang B, Zhang T, Tao J. Advanced review of graphene-based nanomaterials in drug delivery systems: synthesis, modification, toxicity and application. *Mat Sci Eng C*. **2017**, 77, 1363–1375.
28. Kuila T, Bose S, Khanra P, Mishra AK, Nam HK, Lee JH. Recent advances in graphene-based biosensors. *Biosens Bioelectron*. **2011**, 26, 4637–4648.
29. Pumera M. Graphene in biosensing. *Mat Today*. **2011**, 14, 308–315.
30. Pumera M, Ambrosi A, Bonanni A, Khim Chng EL, Ling Poh H. Graphene for electrochemical sensing and biosensing. *Trends Anal Chem*. **2010**, 29, 954–965.
31. Power AC, Gorey B, Chandra S, Chapman J. Carbon nanomaterials and their application to electrochemical sensors: a review. *Nanotechnol Rev*. **2017**, 7, 1–48.
32. Agüí L, Yáñez-Sedeño P, Pingarrón JM. Role of carbon nanotubes in electroanalytical chemistry. A review. *Anal Chim Acta*. **2008**, 622, 11–47.



33. Gomez FJ, Martín A, Silva MF, Escarpa A. Screen-printed electrodes modified with carbon nanotubes or graphene for simultaneous determination of melatonin and serotonin. *Microchim Acta*. **2015**, 182, 1925–1931.
34. Merkoçi A, Pumera M, Llopis X, Pérez B, del Valle M, Alegret S. New materials for electrochemical sensing VI: carbon nanotubes. *Trends Anal Chem*. **2005**, 24, 826–838.
35. Wildgoose GG, Banks CE, Leventis HC, Compton RG. Chemically modified carbon nanotubes for use in electroanalysis. *Microchim Acta*. **2006**, 152, 187–214.
36. Baptista FR, Belhout SA, Giordani S, Quinn SJ. Recent developments in carbon nanomaterial sensors. *Chem Soc Rev*. **2015**, 44, 4433–4453.
37. Yang Y, Yang X, Yang Y, Yuan Q. Aptamer-functionalized carbon nanomaterials electrochemical sensors for detecting cancer relevant biomolecules. *Carbon*. **2018**, 129, 380–395.
38. Rivas GA, Rodríguez MC, Rubianes MD, Gutiérrez FA, Eguílaz M, Dalmaso PR, Primo EN, Tettamanti C, Ramírez ML, Montemerlo A, Gallay P, Parrado C. Carbon nanotubes-based electrochemical (bio)sensors for biomarkers. *App. Mat. Today*. **2017**, 9, 566–588.
39. Wang L, Pumera M. Electrochemical catalysis at low dimensional carbons: graphene, carbon nanotubes and beyond – a review. *App Mat Today*. **2016**, 5, 134–141.
40. Gomez FJ, Martín A, Silva MF, Escarpa A. Microchip electrophoresis-single wall carbon nanotube press-transferred electrodes for fast and reliable electrochemical sensing of melatonin and its precursors: nanoanalysis. *Electrophoresis*. **2015**, 36, 1880–1885.
41. Martín A, Vázquez L, Escarpa A. Carbon nanomaterial scaffold films with conductivity at micro and sub-micron levels. *J Mat Chem A*. **2016**, 34, 13142.
42. Pumera M, Escarpa A. Nanomaterials as electrochemical detectors in microfluidics and CE: fundamentals, designs, and applications. *Electrophoresis*. **2009**, 30, 3315–3323.
43. Martín A, Escarpa A. Tailor designed exclusive carbon nanomaterial electrodes for off-chip and on-chip electrochemical detection. *Microchim Acta*. **2017**, 184, 307–313.
44. García-Carmona L, Moreno-Guzmán M, Sierra T, González MC, Escarpa A. Filtered carbon nanotubes-based electrodes for rapid sensing and monitoring of L-tyrosine in plasma and whole blood samples. *Sensors Actuators B Chem*. **2018**, 259, 762–767.
45. Stumpe M, Miller C, Morton N, Bell G, Watson DG. Highperformance liquid chromatography determination of alpha1-acid glycoprotein in small volumes of plasma from neonates. *J Chromatogr*. **2006**, 831, 81–84.
46. Cai Z, Li F, Wu P, Ji L, Zhang H, Cai C, Gervasio DF. Synthesis of nitrogendoped graphene quantum dots at low temperature for electrochemical sensing trinitrotoluene. *Anal Chem*. **2015**, 87, 11803–11811.

### III.2.2. AGP determination using carbon nanomaterial electrodes

---

47. Gutierrez MC, Pico F, Rubio F, Amarilla JM, Palomares FJ, Ferrer ML, del Monte F, Rojo JM. PO15-PEO22-PPO15 block copolymer assisted synthesis of monolithic macro- and microporous carbon aerogels exhibiting high conductivity and remarkable capacitance. *J Mater Chem.* **2009**, 19, 1236–1240.
48. Della Pelle F, Di Battista R, Vázquez L, Palomares FJ, Del Carlo M, Sergi M, Compagnone D, Escarpa A. Press-transferred carbon black nanoparticles for class-selective antioxidant electrochemical detection. *Appl Mat Today.* **2017**, 9, 29–36.
49. Nagy B, Toth A, Savina I, Mikhalovsky S, Mikhalovska L, Geissler E, László K. Double probe approach to protein adsorption on porous carbon surfaces. *Carbon.* **2017**, 112, 103–110.
50. Mahmoodi Y, Mehrnejad F, Khalifeh K. Understanding the interactions of human follicle stimulating hormone with single-walled carbon nanotubes by molecular dynamics simulation and free energy analysis. *Eur Biophys J.* **2018**, 47, 49–57.

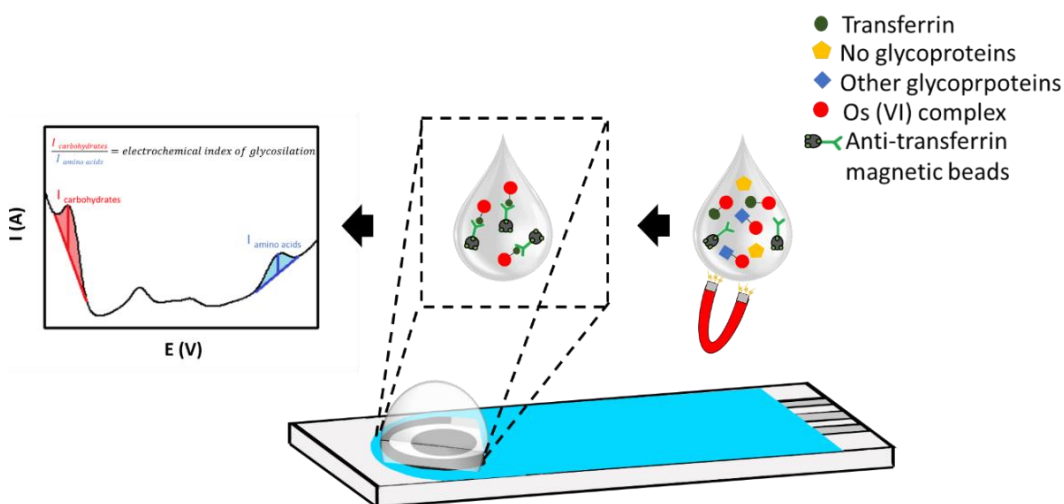


### III.2.3. Article 3: Electrochemical sensor for the assessment of carbohydrate deficient transferrin: application to diagnosis of congenital disorders of glycosylation

Tania Sierra, Agustín G. Crevillén, Alberto Escarpa

Biosensors and Bioelectronics 179 (2021) 113098

**Abstract:** Carbohydrate deficient transferrin (CDT) is used as biomarker of different health problems as, for example, congenital disorders of glycosylation (CDG). We propose a screen-printed-based electrochemical sensor for the determination of carbohydrate deficient transferrin using an Os(VI) tag-based electrochemistry. When transferrin is labeled with Os(VI) complex, it generates two voltammetric signals: one from carbohydrates (electrochemical signal of osmium (VI) complex at -0.9 V/Ag) and one from the amino acids present in glycoprotein (intrinsic electrochemical signal of glycoprotein at +0.8 V/Ag). The relationship between the two analytical signals (carbohydrate signal/protein signal) is an indicator of the degree of glycosylation (electrochemical index of glycosylation), which has shown an excellent correlation ( $r = 0.990$ ) with the official parameter % CDT obtained by CE-UV. The suitability of this approach was demonstrated by analyzing serum samples from CDG patients.





#### 1. Introduction

Transferrin (Tf) is the most important iron transport protein and the most abundant glycoprotein in human serum. It has a molecular weight between 70-95 KDa with an isoelectric point between 5.2-5.6 and consists of a simple polypeptide chain with 679 amino acids. In addition, it has two carbohydrate chains attached to the amino groups of asparagine (Asn in position 413 and 611) (1–3). The main transferrin glycoform contains two N-biantennary glycans with a total number of four sialic acids (tetrasialo-Tf, pI 5.4) but other minority glycoforms with two (disialo-Tf, pI 5.7), three (trisialo-Tf, pI 5.6), five (pentasialo-Tf, pI 5.2) and six (hexasialo-Tf, pI 5.0) sialic acids have been determined in serum (3,4) (**Figure III.2.3.1**).

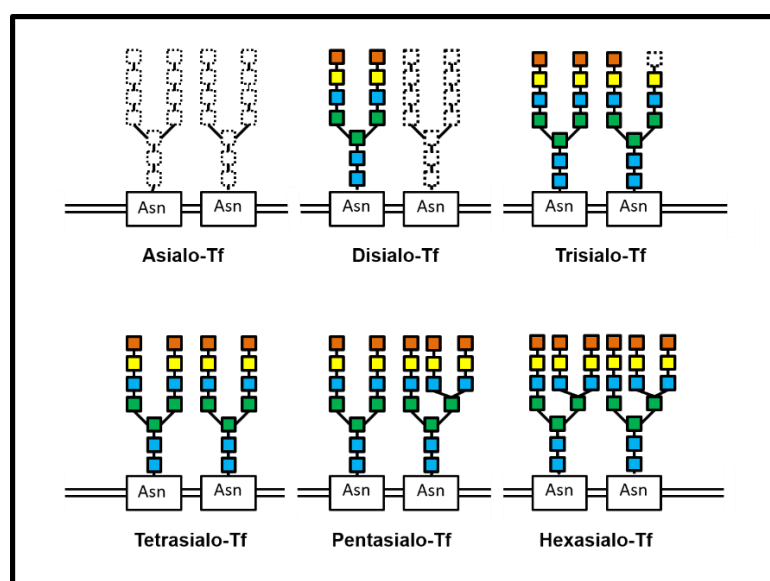


**Figure III.2.3.1.** Different glycoforms of transferrin depending on the number of sialic acids present in the glycoprotein. Asialo-Tf with any sialic acids; diasialo-Tf with two sialic acids; trisialo-Tf with three sialic acids; tetrasialo-Tf with four sialic acids; pentasialo-Tf with five sialic acids; and hexasialo-Tf with six sialic acids.

Under certain pathological states or due to genetic defects, the minority glycoforms of Tf with lower amount of glycans (asialo-, disialo- and trisialo-Tf) are increased respect to the main glycoform (tetrasialo-Tf). This Tf with lower amount of glycans in its structure is called carbohydrate deficient transferrin (CDT). CDT is the clinically used biomarker for the detection of

congenital disorders of glycosylation (CDG) (5–7), chronic alcohol abuse (2,3), and cerebrospinal fluid loss (8,9). In addition, the ratio between two transferrin glycoforms present in cerebrospinal fluid has been recently proposed as a biomarker of neurological diseases (10).

CDG is a kind of rare disease and represents a large family of autosomal recessive, mostly multi-systemic disorders. Clinical features include intellectual disability, seizures, muscle dystrophy, skeletal dysplasia, dysmorphic features, growth retardation, hematological and endocrine abnormalities (7). CDG due to a modification in N-glycosylation are the most abundant and are classified into two types depending on what stage of the glycosylation process the defects occur. CDG-I refers to defects in the assembly of the lipid-bound oligosaccharide chain and their transfer to the protein. CDG-II refers to defects during the subsequent process of binding glycans to the protein that occur in the cytoplasm and Golgi apparatus. CDG-I defects are characterized by unoccupied glycosylation points in proteins, so they are completely free of N-glycans, while CDG-II are characterized in the truncated or incomplete N-glycan chains (5–7,11).

Due to the extremely severe symptoms, CDG must be quickly diagnosed in order to apply as soon as possible a medical treatment (when available) and/or symptomatic support therapy (12), making essential the development of neonatal or even prenatal screening methods. The most commonly used screening method is based on the determination of Tf glycoforms. Patients with CDG show a decrease in glycoform tetrasialo-Tf and an increase in species with fewer sialic groups. Abnormal Tf profiles allow clinicians to classify as CDG type I or type II, depending on whether glycoform asialo- and diasialo-Tf (CDG-I) are increased or if monosialo- and trisialo-Tf (CDG-II) glycoforms are also increased (7,11). In this sense, the most employed analytical methods rely on separation techniques (HPLC and CE) that allow for separating Tf glycoforms and, in consequence, quantifying the loss of carbohydrates (% CDT) (3,11). But expensive instrumentation is needed that is not always available in all analytical laboratories. Immunoassay-based commercial kits have also been developed to determine the percentage of CDTs with different detection methods (turbidimetric, radiometric, and enzymatic) (13). These kits are

### III.2.3. Rapid screening of carbohydrate deficient transferrin

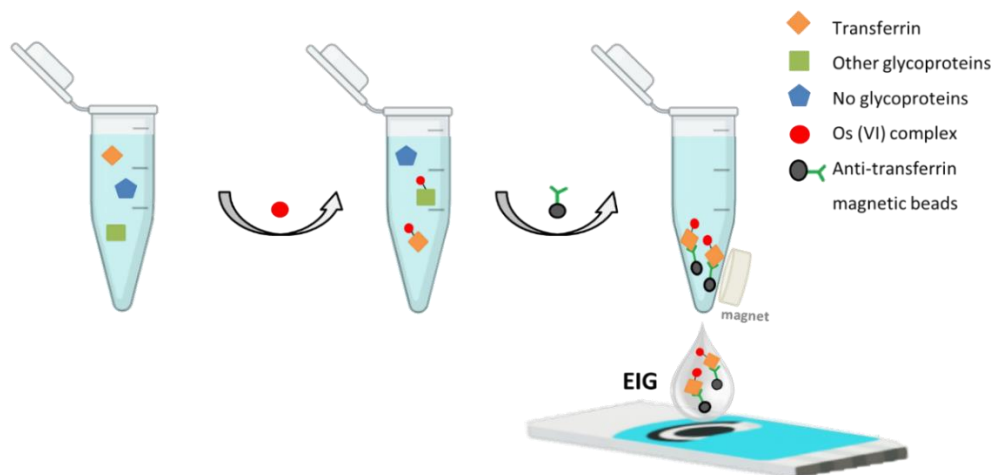
---

fast, do not require the use of complex equipment, and no sample treatment is required. However, their use has not spread too much because they showed low accuracy and gave abnormal results when genetic variants of Tf appeared (14).

On the other hand, screen-printed electrode (SPE) technology (15,16) offers disposable and cheap electrochemical platforms with low sample consumption and it is compatible with *in situ* analysis or point-of-care testing (POCT). Regarding the direct electrochemical sensing of glycoproteins, it must be taking into account that glycoproteins exhibit low sensitivity because their carbohydrate part (glycans) are electrochemically inactive under physiological conditions. However, the use of Os(VI) complexes as electrochemical tags overcame this limitation due to their inherent electroactivity and their ability to bind selectively the glycans of glycoproteins (17–20). In fact, there are several examples of direct electrochemical sensing of glycoproteins by employing SPE technology (18,19).

In this work, Tf was labeled with Os(VI) complex (electrochemical tag) and it generated two signals on screen-printed carbon electrodes (SPCE) by adsorptive transfer stripping square wave voltammetry (AdTSWV): one from the intact protein itself (electroactive amino acids) and another from the electrochemical tag. Regarding this fact, we demonstrated that the amount of Os(VI) complex attached to the Tf is proportional to the amount of glycans that possesses. This allowed us to design and propose a new approach to measure the level of CDT, relied on the Os(VI) signal/protein signal ratio (electrochemical index of glycosylation, (EIG)). This approach is illustrated in **Scheme III.2.3.1**. First, Tf is tagged with Os(VI) complex, then this adduct was isolated from the sample by immunomagnetic beads and, finally, the isolated Tf-Os(VI) complex was analyzed by AdTSWV using a SPCE. EIG showed a high correlation with % CDT measured by CE-UV approach. In addition, the suitability of the proposed electrochemical sensor was evaluated by analyzing serum samples from CDG patients.





**Scheme III.2.3.1.** Strategy to measure the level of CDT by using EIG. Firstly, Tf is labelled with the electrochemical tag (Os(VI) complex) and then it is isolated by immunomagnetic beads. Finally, EIG is measured on a SPCE by AdTSWV.

## 2. Materials and methods

### 2.1. Chemicals

$\alpha_1$ -acid glycoprotein (AGP) ( $\geq 99\%$ ), transferrin (Tf) ( $\geq 98\%$ ), potassium osmate (VI) dihydrate, N,N,N',N'-tetramethylenediamine (TEMED), N-glycosidase F (PNGase F) (REF 11365169001), certified human serum reference material (ERM-DA470 K/IFCC), iron (III) chloride, and 1,4-butanediamine (DAB) were purchased from Sigma–Aldrich (Darmstadt, Germany). Phosphoric acid, hydrochloric acid, acetic acid, disodium hydrogen phosphate, sodium dihydrogen phosphate, sodium borate, and boric acid were purchased from Panreac (Barcelona, Spain). Anti-Transferrin antibody (ab66952) was purchased from Abcam (Cambridge, UK). Boric acid was acquired from Fluka (Darmstadt, Germany).

Anonymized human serum from CDG patients were provided by Centro de Diagnóstico de Enfermedades Moleculares (CEDEM, Madrid, Spain). Samples were collected with the approval of research ethics committee of CEDEM.

Magnetic beads (MBs) functionalized with protein G were acquired from Thermo Fisher Scientific (USA). Before use, MB suspensions were

### III.2.3. Rapid screening of carbohydrate deficient transferrin

---

homogenized and, for each assay, 1  $\mu\text{L}$  was transferred to an Eppendorf tube and washed twice with 100 mL PBS solution pH 7.4.

All solutions were prepared in Milli-Q water (Merck Millipore, Darmstadt, Germany).

#### 2.2. Instrumentation

Potentiostat Autolab PGSTAT204 (Methrom-Autolab, Utrecht, The Netherlands) was used for all electrochemical measurements. This instrument was controlled by the software Nova 1.10.

Screen-printed carbon electrodes (SPCEs) (DRP-110, Dropsens, Oviedo, Spain) were employed. They consist of a carbon working electrode (4 mm diameter), carbon counter electrode, and silver reference electrode. This kind of SPCEs works as an electrochemical cell, which needs a minimum volume of 50  $\mu\text{L}$ .

#### 2.3. Procedures

##### 2.3.1. Preparation of electrochemical tag ( $\text{Os(VI)O}_2(\text{OH})_2\text{TEMED}$ complex)

The preparation of  $\text{Os(VI)O}_2(\text{OH})_2\text{TEMED}$  complex was carried out according to bibliography (21). 18.4 mg of potassium osmate (VI) dihydrate (50  $\mu\text{mols}$ ) were suspended in 1.22 mL of water. Then, 5.8 mg of TEMED (50  $\mu\text{mols}$ ) and 0.41 mL of a 0.2 M sodium phosphate pH 7.0 solution were poured into the previous solution. Finally, 10  $\mu\text{L}$  of 10 M HCl solution were added. The solution was shaken for one hour to allow the formation of  $\text{Os(VI)O}_2(\text{OH})_2\text{TEMED}$  complex and finally, the solution was filtered using a syringe Nylon filter 0.22  $\mu\text{m}$  (Tecno-Air, Barcelona, Spain). The final concentration of Os(VI) complex (electrochemical tag) was 30.3 mM.

##### 2.3.2. Labeling protocol of transferrin with $\text{Os(VI)O}_2(\text{OH})_2\text{TEMED}$ complex

Tf-Os(VI) adducts were prepared as follow: 1.9 mg of Tf ( $2.7 \times 10^{-8}$  mols) were dissolved into 234  $\mu\text{L}$  of 50 mM sodium phosphate buffer at pH 7.0 using a “protein low bind” Eppendorf tube (Hamburg, Germany). Then, 16.5  $\mu\text{L}$  of  $\text{Os(VI)O}_2(\text{OH})_2\text{TEMED}$  solution were added in the previous solution

(mol ratio 1/20 between glycoprotein and Os(VI)) and it was kept under agitation 16 h at 37 °C and 950 r.p.m. using a thermo shaker (Biosan TS-100C, Riga, Latvia).

The labeling protocol of glycoproteins was modified when serum samples were analyzed. The protocol was as follows: 200.5  $\mu\text{L}$  of serum sample were mixed with 49.5  $\mu\text{L}$  of  $\text{Os(VI)O}_2(\text{OH})_2\text{TEMED}$  solution and it was kept under agitation for 16 h at 37 °C and 950 r.p.m. using a thermo shaker (Biosan TS-100C, Riga, Latvia).

#### **2.3.3. Synthesis of carbohydrate deficient transferrin (artificial samples)**

To our best knowledge, there are not commercially available CDT samples, so we prepared CDT with different degrees of glycosylation. These artificial samples were synthesized following a protocol for glycan release. Firstly, 1.9 mg Tf was dissolved in 232  $\mu\text{L}$  of 50 mM sodium phosphate buffer pH 7.0. Then 2  $\mu\text{L}$  PNGase F (2 U) was added to release N-glycans. Afterwards, samples were incubated for different times at 37 °C. Reaction was stopped at 100 °C for 5 min. Then, Tf with different degrees of glycosylation was labeled with  $\text{Os(VI)O}_2(\text{OH})_2\text{TEMED}$  following the above protocol.

#### **2.3.4. Synthesis of anti-transferrin-protein G-MBs (anti-Tf-MBs)**

The optimized conditions for the synthesis of anti-Tf-MBs were as follow: 1  $\mu\text{L}$  of the protein G-MBs suspension was transferred to an Eppendorf tube and resuspended in 50  $\mu\text{L}$  of a 7.46  $\mu\text{g mL}^{-1}$  anti-transferrin solution prepared in PBS solution pH 7.4. After 45 min incubation at 25 °C under stirring, the tube was placed on the magnet holding block for 2 min. Once MBs were deposited on the bottom of the test tube, the supernatant was removed and the beads bearing the antibodies were washed twice with 100  $\mu\text{L}$  of PBS solution pH 7.4. Each washing step consisted on a resuspension of the beads in the washing solution and gentle stirring for 1 min (up to homogenization), followed by separation with the magnet for 2 min to remove the solution.

#### 2.3.5. Immunopurification procedure

When serum samples were analyzed, Tf-Os(VI)TEMED adduct was isolated from the rest of components by immunomagnetic beads. Anti-Tf-MBs were resuspended in 50  $\mu\text{L}$  of Tf-Os(VI)TEMED containing sample. After 45 min incubation at 25  $^{\circ}\text{C}$  under stirring, the tube was placed on the magnet holding block for 2 min. Then, the supernatant was removed, and two washing steps with two 100  $\mu\text{L}$  of PBS solution pH 7.4. Subsequently, the Tf-Os(VI)TEMED-anti-transferrin-protein G-MBs was resuspended in 10  $\mu\text{L}$  of BR buffer at pH 3.0 and transferred onto the surface of SPCE.

#### 2.3.6. Electrochemical sensing and electrochemical index of glycosylation calculation

Electrochemical sensor was based on AdTSWV. In this case, 10  $\mu\text{L}$  of sample were dropped onto the working electrode and, then, the analyte was adsorbed for accumulation time 5 min at open circuit potential. Then, the electrode was washed with water and finally, 50  $\mu\text{L}$  of background electrolyte (0.2 M Britton-Robinson buffer BR pH 3.0) were dropped on the SPCE for voltammogram recording. Square wave voltammetry (SWV) parameters: start potential  $-1.3\text{ V}$ , end potential  $+1.2\text{ V}$ , step potential 5 mV, amplitude 50 mV, and frequency 100 Hz.

Then, to carry out the calculation of EIG, the height value of the electrochemical signal of Os(VI) complex (peak at  $-0.9\text{ V}$ ) is divided by the height of the signal due to amino acid residues (Cys, Trp, Tyr) (peak at  $+0.8\text{ V}$ ) (equation 1).

$$(1) \quad EIG = \frac{\text{height of Os(VI) signal}}{\text{height of amino acid signal}}$$

#### 2.3.7. % CDT measurement by CE-UV

CE-UV analysis was carried out using a Beckman P/ACE MDQ capillary electrophoresis system with a UV diode array detector, controlled by 32 Karat software. New capillaries were conditioned with high-pressure rinses (20 psi) of 1 M NaOH followed by water. The CE-UV procedure for

measuring % CDT was adapted from (22). The method was as follow: 3 min rinse with 0.5 M NaOH, a 6 min rinse with 500 mM borate buffer pH 8.5, a 5 min rinse with the 3 mM DAB solution in 100 mM borate buffer pH 8.5, and sample injection at 0.7 psi for 10 s. Samples were saturated with Fe<sup>3+</sup> to avoid charge variations resulting from a variable degree of Tf iron saturation. Separation was carried out at +30 KV for 30 min, using normal polarity (inlet was the anode), a typical current of approximately 60 μA was observed in all experiments. Capillaries were 80 cm total length (65.5 cm length to detector) x 50 μm i.d and they were maintained at 20 °C during analysis. Transferrin glycoforms were measured by absorption at 200 nm.

The % CDT measurement is calculated following the next equation (equation 2) (23):

$$(2) \quad \% CDT = \frac{\text{area of asialo and disialo glycoform}}{\text{total area of glycoforms}}$$

### 3. Results and Discussion

#### 3.1. Electrochemical behavior of native and labeled transferrin on SPCE

Firstly, native Tf and Tf-Os(VI) adduct were electrochemically studied by using AdTSWV on SPCE employing previously optimized conditions (19). **Figure III.2.3.2** shows voltammograms of BR buffer at pH 3.0 (blank) (black line), Tf (control) (blue line) and Tf-Os(VI) (red line). Clearly, there are differences between labeled and native glycoprotein. In Tf-Os(VI), two peaks rise from the background at -0.9 V (peak 1) and at +0.8 V (peak 2), corresponding to the Tf-Os(VI) signal and the electrochemical oxidation of amino acid residues (Cys, Trp, Tyr) present in the protein, respectively. Whereas there is only the peak at +0.8 V (peak 2) in native glycoprotein.

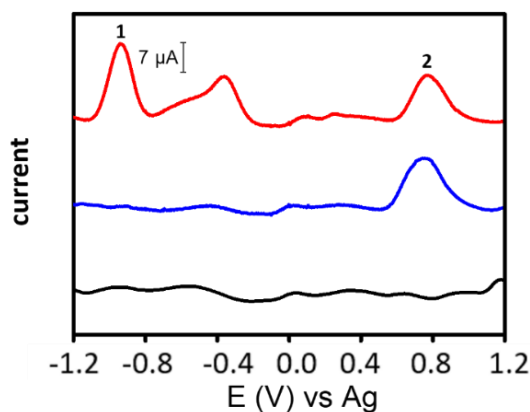


**Figure III.2.3.2.** Voltammograms obtained by AdTSWV of BR buffer at pH 3.0 (blank) (black line), 3800 mg L<sup>-1</sup> Tf (control) (blue line) and 3800 mg L<sup>-1</sup> Tf-Os(VI) (red line). Peak 1: Tf-Os(VI). Peak 2: amino acids residues. Conditions: BR buffer at pH 3.0, start potential -1.3 V, end potential +1.2 V, step potential 5 mV, amplitude 50 mV, frequency 100 Hz. The background signal was linearized.

#### 3.2. Evaluation of immunopurification step

Different experiments were carried out to evaluate the effectiveness of anti-Tf-MBs (supplementary information, SI). Firstly, the unspecific adsorption of Tf-Os(VI)TEMED adduct on protein G-MBs was evaluated and it was below 1 %, considering the signal at -0.9 V (**Figure III.2.3.S1**). In addition, the potential interference of protein G-MBs and anti-Tf-MBs in the signal at +0.8 V was evaluated. Protein G and IgG have electroactive amino acids so that they can yield a signal at this potential. Under our optimized conditions, both kind of MBs yield a signal at +0.8 V corresponding to the 6 % of Tf-Os(VI)TEMED signal, contributing to this peak. This background signal is the same throughout all experiments, because the same amount of MBs is used; therefore, it does not affect significantly to our approach.

On the other hand, anti-Tf-MBs selectivity was checked in the presence of  $\alpha_1$ -acid glycoprotein (AGP), which is the other main glycoprotein in serum. Two concentrations of AGP was analyzed, 400 and 1000 mg L<sup>-1</sup> AGP-Os(VI)TEMED, because AGP concentration in healthy humans ranged between 200–1000 mg L<sup>-1</sup>. There were not significant differences between

the signals of Tf-Os(VI)TEMED obtained in the absence and in the presence of AGP, which demonstrated the excellent selectivity of anti-Tf-MBs (**Figure III.2.3.S2**).

#### **3.3. Analytical performance and validation of electrochemical index of glycosylation for CDT assessment**

Firstly, the analytical performance of the electrochemical sensor for Tf determination was evaluated. Calibration studies were carried out for Tf-Os(VI)TEMED adduct using the peak at -0.9 V (Os(VI) signal) and at +0.8 V (protein signal). In both cases, a good correlation coefficient was obtained from 1000 mg L<sup>-1</sup> to 7600 mg L<sup>-1</sup> ( $r = 0.995$  and  $r = 0.990$ , respectively). The calibration curve slopes were  $(3.0 \pm 0.1) \times 10^{-6}$  A L mg<sup>-1</sup> for the peak at -0.9 V and  $(8.0 \pm 0.6) \times 10^{-7}$  A L mg<sup>-1</sup> for the peak at +0.8 V, and the intercepts were  $(-3.0 \pm 0.6) \times 10^{-6}$  A and  $(-1.0 \pm 0.2) \times 10^{-6}$  A, respectively ( $n = 3$ ) (**Figure III.2.3.3**). The limits of detection (LOD) obtained from the calibration curve were 590 mg L<sup>-1</sup> and 940 mg L<sup>-1</sup> (3 S<sub>a</sub> criterion, where S<sub>a</sub> is the standard deviation of intercept). These LODs were adequate for Tf determination in serum samples, because its concentration in healthy humans ranged between 1700-3700 mg L<sup>-1</sup>. For comparative purposes, the calibration curve for native Tf (without Os(VI) complex) was also built using the signal at +0.8V (**Figure III.2.3.S3**). The slope for native Tf was  $(6.8 \pm 0.5) \times 10^{-7}$  A L mg<sup>-1</sup> and the intercept was  $(-7.0 \pm 0.6) \times 10^{-7}$  A ( $n=3$ ). Native Tf showed lower sensitivity in terms of calibration slope than Tf-Os(VI)TEMED (15 % lower). This is due to Os(VI) complex electrocatalyzes the oxidation of Tf, yielding higher anodic current, as we previously reported (20).

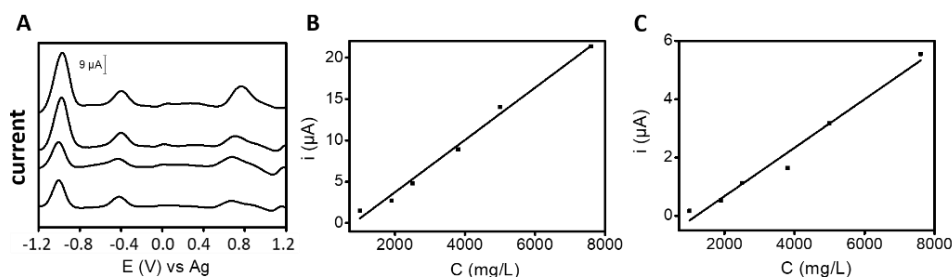


**Figure III.2.3.3.** Analytical calibration. (A) Voltammograms of Tf-Os(VI)TEMED from 1000 to 7600 mg L<sup>-1</sup> (the background signal was linearized). (B) Calibration curve for the peak at -0.9 V. (C) Calibration curve for the peak at +0.8 V. Other conditions as in **Figure III.2.3.2**.

Moreover, a certified human serum reference material ([Tf] = 2360 ± 80 mg L<sup>-1</sup>) was analyzed to evaluate the method accuracy using both calibration curves. In the first case, (calibration curve at -0.9V), the value obtained was 2280 ± 290 mg L<sup>-1</sup>, whereas the value obtained by calibration curve at +0.8 V was 2340 ± 290 mg L<sup>-1</sup>. The method accuracy was excellent ( $E_r \leq 3\%$ ).

Once the good analytical performance of the sensor for Tf determination was demonstrated, we explored its possibilities for CDT assessment. Our hypothesis is that the amount of Os(VI) complex attached to Tf is proportional to the amount of glycans present in Tf. This allow us to propose a new approach to measure the level of CDT, relied on the Os(VI) signal/protein signal ratio, that is named EIG. If Tf is completely deglycosylated, the value of EIG will be zero.

Artificial samples were created to demonstrate our hypothesis. With this purpose, Tf was treated with PNGase enzyme at different times (monitored by CE-UV, **Figure III.2.3.S4**) and then measured by AdTSWV. The longer the time, the lower the amount of carbohydrates. Therefore, EIG should decrease according to equation 1, because a lower signal will be obtained for Os(VI) because this signal is specific for protein carbohydrates. As it is shown in **Table III.2.3.1**, a decrease of Os(VI) signal ( $S_{Os}$ ) is obtained when the PNGase treatment time is increased, while the intrinsic signal of the glycoprotein ( $S_{protein}$ ) remains almost constant, except for 60 min. At this treatment time, the signal at -0.9 V disappears and the  $S_{protein}$  is lower than



### Chapter III. Electrochemical sensors screen-printed based

the other times. This means that Tf is fully deglycosylated and there is not Os(VI) complex to catalyze the oxidation of Tf, as it was aforementioned.

**Table III.2.3.1.** Signals obtained for 3800 mg L<sup>-1</sup> Tf Os(VI) treated with PNGase at different times and their corresponding EIG values (n=3).

PNGase treatment time (min)	S <sub>Os(E=-0.9V)</sub> (μA)	S <sub>protein (E=0.8V)</sub> (μA)	EIG	EIG average ± standard deviation
<b>0</b>	10.12	3.76	2.69	2.9 ± 0.2
	10.52	3.43	3.07	
	10.01	3.48	2.87	
<b>5</b>	8.31	3.23	2.57	2.4 ± 0.2
	8.16	3.68	2.22	
	7.56	3.22	2.35	
<b>10</b>	6.31	3.01	2.06	2.0 ± 0.2
	6.51	3.23	2.01	
	5.62	3.09	1.89	
<b>13</b>	3.86	3.53	1.34	1.5 ± 0.1
	4.77	3.18	1.49	
	4.86	3.15	1.54	
<b>15</b>	2.83	3.17	0.89	0.8 ± 0.1
	2.90	3.89	0.74	
	2.69	3.54	0.76	
<b>60</b>	-	2.45	0	0
	-	2.88	0	
	-	2.77	0	

To validate our proposed EIG, the artificial samples were also analyzed by CE-UV and their corresponding % CDT were calculated according to the literature (3,11). In the case of CE-UV analysis, the peak corresponding to asialo- and disialo-glycoforms grow when the PNGase treatment time is increase (**Figure III.2.3.S4**). Therefore % CDT should increase according to equation 2, since a greater signal will be obtained due to the low-carbohydrate glycoforms of the protein. At 60 min, only a peak corresponding to low glycosylated Tf is observed.

### III.2.3. Rapid screening of carbohydrate deficient transferrin

**Figure III.2.3.4** displays a comparison between the two parameters that measure the glycosylation level of Tf: EIG and % CDT. Both parameters showed an excellent correlation ( $r = 0.990$ ), demonstrating the suitability of EIG for CDT assessment.

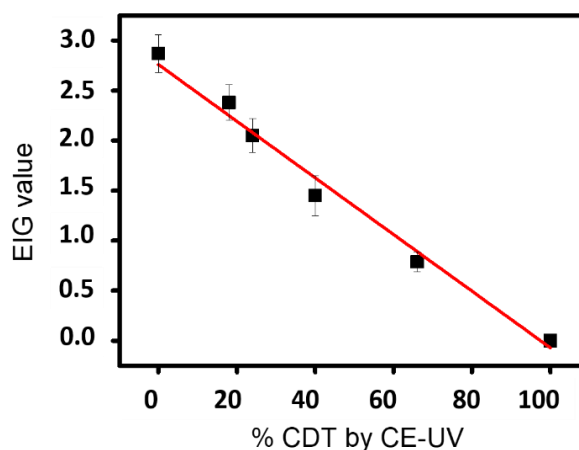


**Figure III.2.3.4.** Correlation between EIG (using an electrochemical sensor) and % CDT (using CE-UV).

### 3.5. Analysis of serum samples from CDG patients

Finally, the screening capabilities of the electrochemical sensor for CDG diagnosis was evaluated.

Two serum samples from CDG-I patients were analyzed, while a commercial serum was used as a control (**Figure III.2.3.S5**). It must be pointed out the difficulties in obtaining these samples because CDG is a rare disease. 10 measurements were made for each sample and the corresponding EIGs were calculated. It was found significant differences between the control sample and CDG samples using a t-test at 95 % confidence level ( $P \leq 0.05$ ) (**Table III.2.3.2**). This means that our sensor was able to discriminate between samples from healthy people and from CDG-I patients, so that it may be used as screening method for diagnosis of CDG.

**Table III.2.3.2.** Comparison between control sample and CDG samples.

	<b>Control serum</b>	<b>CDG Sample 1</b>	<b>CDG Sample 2</b>
EIG $\pm$ standard deviation	2.1 $\pm$ 0.1	1.4 $\pm$ 0.1	1.5 $\pm$ 0.1

#### 4. Conclusions

A disposable screen-printed-based electrochemical sensor was successfully developed to measure CDT in clinical samples. Two voltammetric signals were generated in the sensor by tagged transferrin: one is due to the carbohydrate part (Os(VI) complex) at -0.9 V/Ag and the second is due to the protein part (electroactive amino acids from transferrin) at +0.8 V/Ag. The ratio between both signals (carbohydrate signal/protein signal), called “electrochemical index of glycosylation (EIG)”, is proposed an alternative approach to assess CDT level. In fact, it showed excellent correlation ( $r=0.990$ ) with the official parameter % CDT.

This approach was successfully applied to discriminate between a control serum sample (healthy) and serum samples from CDG-I patients. The combination of SPCE technology (low-cost and disposability) and the proposed “electrochemical index of glycosylation” has an enormous potential to be used as screening method for CDG diagnosis, and even for other diseases such as chronic alcohol abuse, and cerebrospinal fluid loss. However, further experiments with higher number of samples would be necessary to establish cut-off values for this purpose.

#### Acknowledgments

This work has been financially supported by the TRANSNANOAVANSENS program from the Community of Madrid (S2018/NMT-4349), Spanish Ministry of Economy, Industry and Competitiveness (CTQ2017-86441-C2-1-R), MINECO (MAT2016-80394-R), Independent Thinking-Jóvenes Investigadores program from UNED (BICI, nº 34, 17/06/2019) and the Universidad de Alcalá [FPI fellowship (T.S)].

#### Associated content

##### Supporting Information

**Figure III.2.3.S1.** Voltammograms obtained by AdTSWV of 3800 mg L<sup>-1</sup> Tf-Os(VI)TEMED treated with anti-Tf-MBs (red line) and with protein G-MBs without anti-transferrin (black line). Control using only anti-Tf-MBs (green line).

**Figure III.2.3.S2.** Voltammograms obtained by AdTSWV after immunopurification with anti-Tf-MBs for: 3800 mg L<sup>-1</sup> Tf-Os(VI)TEMED (red line), 1000 mg L<sup>-1</sup> AGP-Os(VI)TEMED (black line), 3800 mg L<sup>-1</sup> Tf-Os(VI)TEMED and 400 mg L<sup>-1</sup> AGP-Os(VI)TEMED (green line) and 3800 mg L<sup>-1</sup> Tf-Os(VI)TEMED and 1000 mg L<sup>-1</sup> AGP-Os(VI)TEMED (blue line).

**Figure III.2.3.S3.** Analytical calibration for native Tf (without Os(VI) complex). (A) Voltammograms of native Tf from 1900 to 7600 mg L<sup>-1</sup>. (B) Calibration curve for the peak at +0.8 V.

**Figure III.2.3.S4.** Electropherograms obtained by CE-UV of Tf treated with PNGase enzyme at different times. Peak 1: tetrasialo-Tf. Peak 2: low glycosylated-Tf.

**Figure III.2.3.S5.** Voltammograms obtained by AdTSWV in different samples: control serum (red line), CDG sample 1 (green line) and CDG sample 2 (blue line). BR buffer at pH 3.0 (blank) (black line).

### Author information

#### Corresponding Authors

Alberto Escarpa – Department of Analytical Chemistry, Physical Chemistry and Chemical Engineering, University of Alcalá, Madrid, Spain. Chemical Research Institute “Andrés M. del Río” (IQAR), University of Alcalá, Madrid, Spain; orcid.org/0000-0002-7302-0948; Email: alberto.escarpa@uah.es

Agustín G. Crevillen – Department of Analytical Sciences, Faculty of Sciences, Universidad Nacional de Educación a Distancia (UNED), Madrid, Spain; Email: agustingcrevillen@ccia.uned.es

#### Other Authors

Tania Sierra - Department of Analytical Chemistry, Physical Chemistry and Chemical Engineering, University of Alcalá, Madrid, Spain.

#### Authors Contribution

The manuscript was written through contributions of all the authors. All the authors have given approval to the final version of the manuscript.

Supporting Information

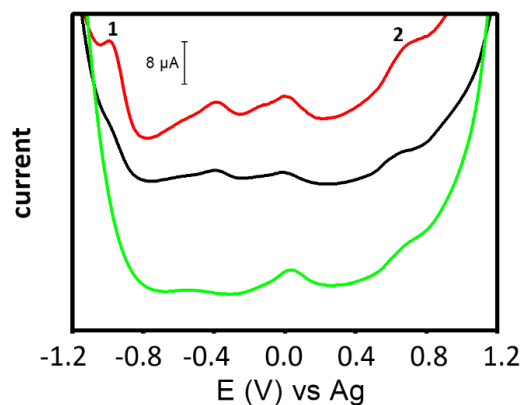


**Figure III.2.3.S1.** Voltammograms obtained by AdTSWV of 3800 mg L<sup>-1</sup> Tf-Os(VI)TEMED treated with anti-Tf-MBs (red line) and with protein G-MBs without anti-transferrin (black line). Control using only anti-Tf-MBs (green line). Conditions: BR buffer at pH 3.0, start potential -1.3 V, end potential +1.2 V, step potential 5 mV, amplitude 50 mV, frequency 100 Hz.

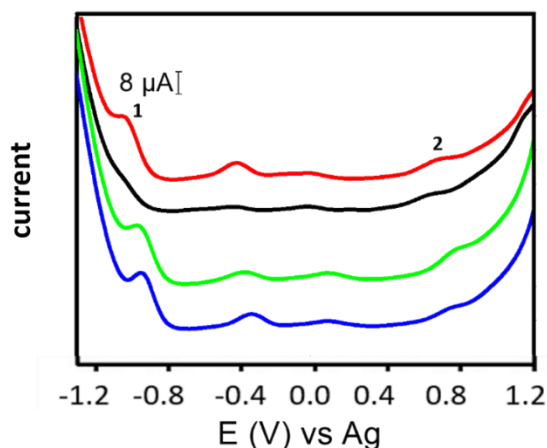


**Figure III.2.3.S2.** Voltammograms obtained by AdTSWV after immunopurification with anti-Tf-MBs for: 3800 mg L<sup>-1</sup> Tf-Os(VI)TEMED (red line), 1000 mg L<sup>-1</sup> AGP-Os(VI)TEMED (black line), 3800 mg L<sup>-1</sup> Tf-Os(VI)TEMED and 400 mg L<sup>-1</sup> AGP-Os(VI)TEMED (green line) and 3800 mg L<sup>-1</sup> Tf-Os(VI)TEMED and 1000 mg L<sup>-1</sup> AGP-Os(VI)TEMED (blue line). Other conditions as in **Figure III.2.3.S1.**

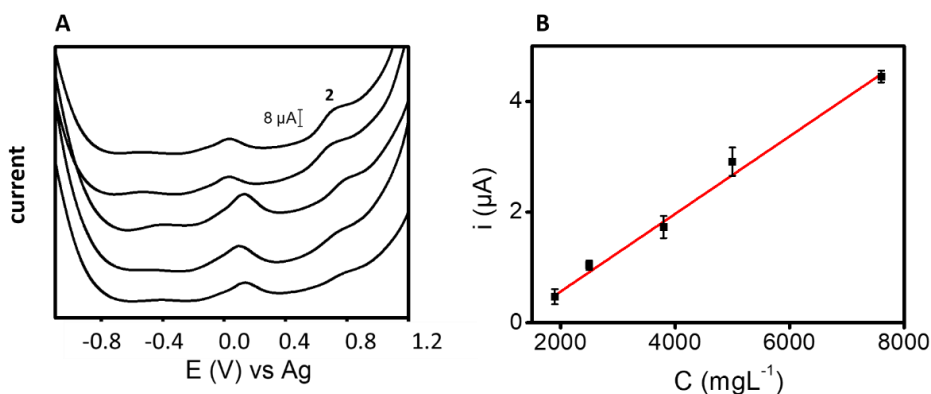


**Figure III.2.3.S3.** Analytical calibration for native Tf (without Os(VI) complex). (A) Voltammograms of native Tf from 1900 to 7600 mg L<sup>-1</sup>. (B) Calibration curve for the peak at +0.8 V. Other conditions as in Figure III.2.3.S1.

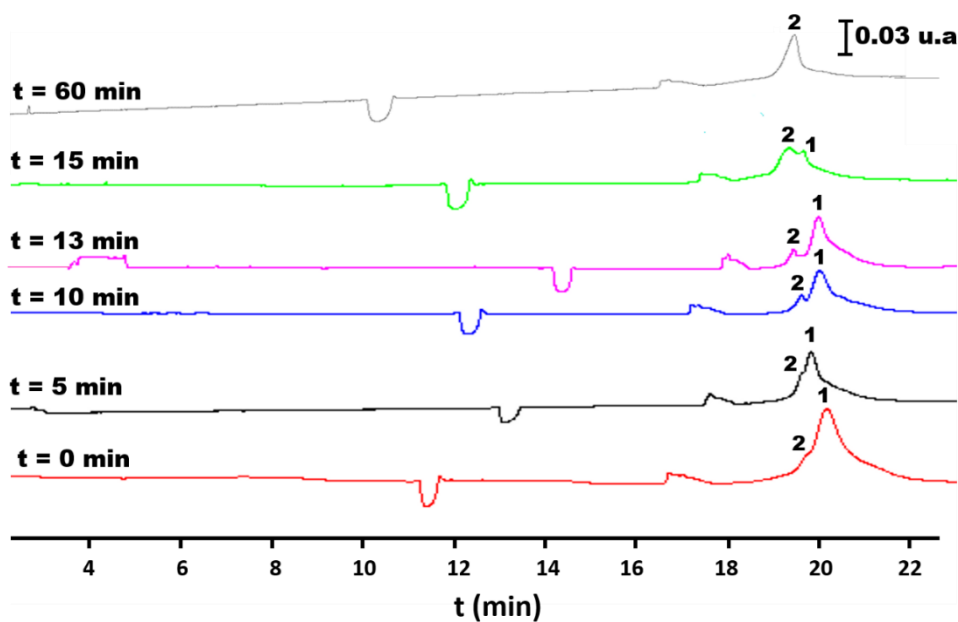


**Figure III.2.3.S4.** Electropherograms obtained by CE-UV of Tf treated with PNGase enzyme at different times. Peak 1: tetrasialo-Tf. Peak 2: low glycosylated-Tf.

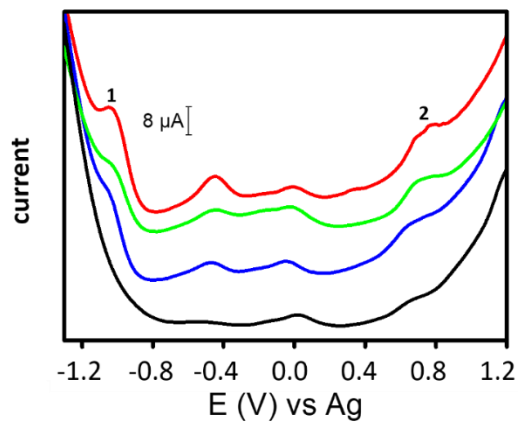


**Figure III.2.3.S5.** Voltammograms obtained by AdTSWV in different samples: control serum (red line), CDG sample 1 (green line) and CDG sample 2 (blue line). BR buffer at pH 3.0 (blank) (black line). Other conditions as in **Figure III.2.3.S1**.



#### References

1. Caslavská J, Thormann W. Monitoring of transferrin isoforms in biological samples by capillary electrophoresis. *J Sep Sci.* **2018**, 41, 303–322.
2. Bortolotti F, Sorio D, Bertaso A, Tagliaro F. Analytical and diagnostic aspects of carbohydrate deficient transferrin (CDT): A critical review over years 2007-2017. *J Pharm Biomed Anal.* **2018**, 147, 2–12.
3. Bortolotti F, Paoli G De, Tagliaro F. Carbohydrate-deficient transferrin (CDT) as a marker of alcohol abuse: A critical review of the literature 2001–2005. *J Chromatogr B.* **2006**, 841, 96–109.
4. Caslavská J, Thormann W. Monitoring of alcohol markers by capillary electrophoresis. *J Sep Sci.* **2013**, 36, 75–95.
5. Freeze HH. Update and perspectives on congenital disorders of glycosylation. *Glycobiology.* **2001**, 11, 129R–143R.
6. Grünewald T, Matthijs G, Jaeken J. Congenital Disorders of Glycosylation: A Review. *Pediatr Res.* **2002**, 52, 618–624.
7. Scherpenzeel M Van, Willems E, Lefeber DJ. Clinical diagnostics and therapy monitoring in the congenital disorders of glycosylation. *Glycoconj J.* **2016**, 33, 345–358.
8. Warnecke A, Averbeck T, Wurster U, Harmening M, Lenarz T, Stover T. Diagnostic Relevance of beta 2 -Transferrin for the Detection of Cerebrospinal Fluid Fistulas. *Arch Otolaryngol neck Surg.* **2004**, 130, 1178–1184.
9. Rudolph P, Meyer JE, Werner JA, Lippert BM, Maune S. Separation of beta2 -Transferrin by Denaturing Gel Electrophoresis to Detect Cerebrospinal Fluid in Ear and Nasal Fluids. *Clin Chem.* **2005**, 51, 1704–1710.
10. Hoshi K, Matsumoto Y, Ito H, Saito K, Honda T. A unique glycan-isoform of transferrin in cerebrospinal fluid: A potential diagnostic marker for neurological diseases. *Biochim Biophys Acta - Gen Subj.* 2017, **1861**, 2473–2478.
11. Albahri Z, Marklová E. Screening and diagnosis of congenital disorders of glycosylation. *Clin Chim Acta.* **2007**, 385, 6–20.
12. Bruneel A, Cholet S, Tran NT, Mai TD, Fenaille F. CDG biochemical screening: Where do we stand? *BBA- Gen Subj.* **2020**, 1864, 129652–12967.
13. Schellenberg F, Mennetrey L, Bacq Y, Pagès JC. Carbohydrate-Deficient Transferrin (CDT) Determination by Nephelometry Using a Commercial Kit. Analytical and Diagnostic Aspects. *Clin Chem Lab Med.* **2001**, 39, 866–871.
14. Bortolotti F, Tagliaro F, Cittadini F, Gottardo R, Trettene M, Marigo M. Determination of CDT, a marker of chronic alcohol abuse, for driving license issuing: immunoassay versus capillary electrophoresis. *Forensic Sci Int.* **2002**, 128, 53–58.
15. Taleat Z, Khoshroo A, Mazloum-Ardakani M. Screen-printed electrodes for biosensing: A review (2008-2013). *Microchim Acta.* **2014**, 181, 865–891.
16. Costa Rama E, Costa-García A. Screen-printed Electrochemical Immunosensors for the Detection of Cancer and Cardiovascular Biomarkers. *Electroanalysis.* **2016**, 28, 1700–1715.

### III.2.3. Rapid screening of carbohydrate deficient transferrin

---

17. Trefulka M, Paleček E. Direct chemical modification and voltammetric detection of glycans in glycoproteins. *Electrochem Commun.* **2014**, 48, 52–55.
18. Sierra T, Cristina M, Moreno B, Crevillen AG. Total  $\alpha_1$ -acid glycoprotein determination in serum samples using disposable screen-printed electrodes and osmium (VI) as electrochemical tag. *Talanta.* **2018**, 180, 206–210.
19. Sierra T, Dorte S, González MC, Palomares FJ, Crevillen AG, Escarpa A. Disposable carbon nanotube scaffold films for fast and reliable assessment of total  $\alpha_1$ -acid glycoprotein in human serum using adsorptive transfer stripping square wave voltammetry. *Anal Bioanal Chem.* **2019**, 411, 1887–1894.
20. Sierra T, Crevillen GA, Escarpa A. Determination of Glycoproteins by Microchip Electrophoresis Using Os(VI)-Based Selective Electrochemical Tag. *Anal Chem.* **2019**, 91, 10245–10250.
21. Trefulka M, Paleček E. Voltammetry of Os(VI)-modified polysaccharides at carbon electrodes. *Electroanalysis.* **2009**, 21, 1763–1766.
22. Giordano BC, Muza M, Trout A, Landers JP. Dynamically-coated capillaries allow for capillary electrophoretic resolution of transferrin sialoforms via direct analysis of human serum. *J Chromatogr B.* **2000**, 742, 79–89.
23. Caslavská J, Schild C, Thormann W. High-resolution capillary zone electrophoresis and mass spectrometry for distinction of undersialylated and hypoglycosylated transferrin glycoforms in body fluids. *J Sep Sci.* **2020**, 43, 241–257.



# CHAPTER IV

## **Microchip electrophoresis with electrochemical detection for analysis of glycoproteins**



## **IV. Microchip electrophoresis with electrochemical detection for analysis of glycoproteins**

### **IV.1. Introduction and objectives**

Microfluidics, which is a technology that facilitates the manipulation of small volumes (lower than  $10^{-6}$  L), was popularized in the early 1990s for applications related to chemical separations (1). However, in recent years it has been applied to an incredible array of applications, such as genomics or synthesis (2).

Microfluidic is most often implemented in planar substrates bearing enclosed channels with lengths, widths, and depths ranging from tens to hundreds of microns. These dimensions result in fluidic phenomena that exhibit increased importance of viscosity, surface tension, and diffusion when it compared to conventional systems.

A particularly attractive vision for the microfluidics community has been the development of integrated "lab-on-a-chip" (LOC) systems that reproduce laboratory-scale processes with reduced cost, less time, and the possibility of development POCT devices (3).

With this idea in mind, the development of microscale analytical systems has experienced an explosive growth during the past decades. Particular attention has been paid to microchip electrophoresis (ME), which represents the first generation of miniaturized electrophoretic devices. Due to their advantages, such as low sample consumption, low-cost, portability, fast analysis, and integration capability, ME has been widely employed for separation of a large number of biochemical species and has been enable in novel investigation in diverse areas, being ME one of the first strides towards a "true" LOC, which integrates all steps of an analytical process on a single compact microfluidics device (4).

## **Chapter IV. Microchip electrophoresis with electrochemical detection**

---

As it is mentioned before, the small volumes used in ME reduce sample and reagent consumption (low to picoliter scale) and, in consequence, the costs. The small dimensions of microchip channels improve heat and mass transfer, minimizing the Joule heating due to the high voltage, and facilitating on-line derivatization reactions. In addition, shorter separation channels decrease analysis time (fast to sub-second), which, along with parallelization, can greatly increase throughput. Finally, applications like POCT can exploit the potential for portability of ME systems (5,6).

Multiple approaches for fluidic transport have been developed, and these fall into two categories: passive (e.g., gravity, surface tension, capillary force) and active (e.g., micropump, electric force, centrifugal force). Among the latter group, electrokinetic flow is particularly advantageous because very little external equipment is required (only a high voltage power supply), but the range of reagents and solvents that can be used is limited. Other forms of fluid manipulation soon followed, including various types of pressure-driven flow controlled by external pumps, centrifugal forces, or on-chip peristaltic pumps (7). The same happen for sample injection, electrokinetically and hydrodynamically are the most used modes. The first is based on the application of voltage, and the second, on pressure (8).

In addition, several materials are available for constructing effective microfluidics-based devices. These materials are classified in three categories: inorganic materials (silicon, glass, and ceramics), polymeric materials (elastomers, thermoplastics) and paper. The choice of material depends on the function(s) that the device will execute, the processing cost, and its compatibility with bulk manufacturing techniques. Each of these materials have a few of advantages. For example, glass or quartz are compatible with the high voltages necessary in many cases. Furthermore, glass have high electrical resistivity, high thermal conductivity, and broad light transmissivity, and its well-known surface chemistry and chemical resistance makes it one of the most widely used materials in these applications, despite the fact that the fabrication is expensive and time-consuming (9,10).

On the other hand, polymer materials that can be molded such as polydimethylsiloxane (PDMS) are straightforward to fabricate but have limited chemical compatibility. Polymethylmethacrylate (PMMA) and cyclic olefin copolymer (COC) are also used in ME (6,11), but polymer microchips exhibit lower electroosmotic flow than those made of glass or quartz. In conclusion, the selection of one material or another depends on the analytical demands.

These microdevices require a miniaturized and sensitive detection system. In proteomics and clinical analysis, laser-induced fluorescence (LIF) is the most used detector coupled to separation techniques (12). LIF detection offers the highest sensitivity but, in general, proteins, peptides, and amino acids are not fluorescents when they are excited in visible or near-infrared region, so it is necessary the use of fluorescence tags (13). Although LIF technique coupled to a separation technique can detect proteins until a concentration of  $10^{-13}$  M, LOD of the overall method is hindered due to the difficulty of labeling analytes at extremely low concentrations (14). Native LIF of proteins at 275 nM has shown to be feasible, but it is difficult to achieve good sensitivity because of the intense background produced by fluorescent impurities that are usually present in real samples (15).

ED is an excellent alternative to LIF because it offers several advantages such as inherent miniaturization, sensitivity, low-cost, portability, short measurement time, and compatibility with microfabrication technologies. In many cases, the electrochemical route allows for on-chip integration of the control instrumentation to produce self-contained truly portable microanalytical systems (16).



## Chapter IV. Microchip electrophoresis with electrochemical detection

The electrochemical detection modes use in ME covers amperometry, potentiometry, and conductimetry. Although in recent years capacitively coupled contactless conductivity detection (C<sup>4</sup>D) (which includes a pair of electrodes that are physically isolated from the solution preventing chemical reactions, contamination, and corrosion) has been extensively applied in ME systems (17), amperometric detection continues being the most used electrochemical method. In this case, a stable voltage is applied to a working electrode relative to a reference electrode, and the current generated from the oxidation or reduction reaction of electroactive species at the working electrode surface is monitored (5,18).

**Figure IV.1.1** shows a typical design of a ME with a single cross injector (similar which is used in this Chapter of the Doctoral Thesis). In a typical configuration, we can find reservoirs for sample input (SR), for separation buffer (RB), and for waste (SW). The reservoirs usually have a capacity between 10-250  $\mu$ L. Platinum electrodes, on which a potential difference is applied by a high voltage source (1-5 KV), are placed in the reservoirs to perform sample injection and electrophoretic separation.

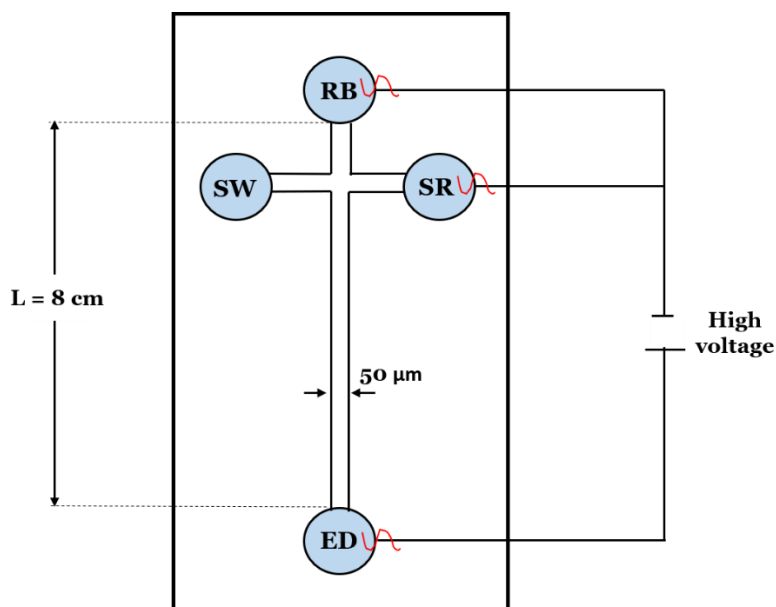


**Figure IV.1.1.** Design and dimensions of the simple cross microchip used in this Doctoral Thesis. The chip holder contained the reservoirs for sample (SR), sample waste (SW) and running buffer (RB), and the electrochemical detection cell (ED).

One of the major considerations in ME is the effect of the separation field and current on the electrochemical response. To minimize the interaction of the two fields, several configurations related to the position of the electrode respect the microchannel have been described. The three major configurations are end-channel, in-channel, and off-channel (**Figure IV.1.2**) (19,20).

The most common configuration is end-channel, in which the working electrode is aligned at the end of the channel separation (**Figure IV.1.2 a**). With this type of configuration, low background noise at the working electrode is exhibited due to its isolation from the separation field. However, the separation voltage can cause a small but significant change in the potential of the working electrode. Therefore, it is necessary to optimize the distance between the electrode and the microchannel outlet. Furthermore, due to the existing distance between the end of the separation channel and the working electrode, a loss of separation efficiency and sensitivity is possible (21,22).

In the case of in-channel configuration, the electrode is set inside the separation channel (**Figure IV.1.2 b**). With this configuration, band broadening is minimized, and higher separation efficiencies and sharper peaks are obtained. However, the separation voltage has a direct effect on the potential of working electrode because the electrode is placed directly in the separation channel. Furthermore, in-channel configuration usually leads to more background noise than end-channel configuration, because, in the first, the fluctuations of the high-voltage power supply affects to the working electrode, worsening the LOD (23).

Off-channel alignment is the third configuration. In this case, a decoupler is placed ahead of the working electrode in the separation channel (**Figure IV.1.2 c**). With this configuration a low background noise is observed. However, if the distance between the decoupler and the working electrode is large, this can lead to significant band broadening, and a loss of resolution (19).

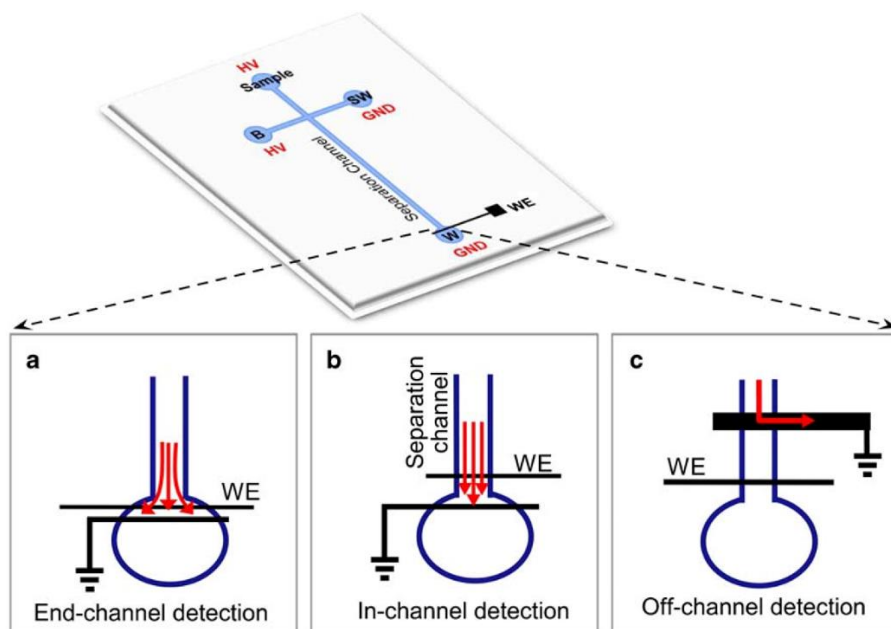


**Figure IV.1.2.** The most electrode alignments used with ME-EC. **(a)** End-channel detection. **(b)** In-channel detection. **(c)** Off-channel detection (19).

Within the end-channel detection protocols, three configurations can be found taking into account the relative position between the working electrode and the flow direction: flow by, the flow direction is parallel to the electrode surface; flow onto, the surface of the electrode is perpendicular to the direction of flow; and flow through where the electrode is placed directly at the outlet of the channel (**Figure IV.1.3**) (22).

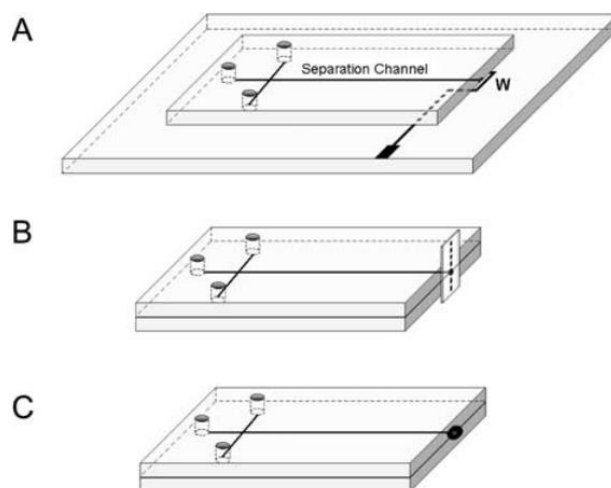


**Figure IV.1.3.** Common configurations of electrochemical detectors for ME depending on the position of the working electrode relative to the flow direction: (A) flow by (using 2 plates); (B) flow onto (with the surface normal to the flow direction); (C) flow through (with the detector placed directly on the channel exit) (22).

One aspect that it is important in ME-ED is that performance and success in these systems are strongly influenced by the material of the working electrode. For that, the selection of the working electrode depends primarily on the redox behavior of the target analytes and the background current. In this sense, there are a lot of examples describing the use of ME with screen-printed electrodes, which are cheap, mass producible, and disposable (25).

Significant developments, particularly the introduction of new modified electrodes, the development of novel derivatization schemes, the integration of additional functional elements (e.g., processes such as clean-up and preconcentration) on a single microchip platform and the coupling on new detection schemes and assays (e.g., immunoassays), are expected to further enhance the power and scope of electrochemical detectors for microscale analytical systems.

Taking into account all the above, this Chapter aims to explore the possibilities of microchip electrophoresis with electrochemical detection (ME-ED) for the separation and detection of two glycoproteins (AGP and Tf).

### IV.1.1. References

1. Whitesides GM. The origins and the future of microfluidics. *Nature*. **2006**, 442, 368–373.
2. Sackmann EK, Fulton AL, Beebe DJ. The present and future role of microfluidics in biomedical research. *Nature*. **2014**, 507, 181–189.
3. Patabadige DEW, Jia S, Sibbitts J, Sadeghi J, Sellens K, Culbertson CT. Micro Total Analysis Systems: Fundamental Advances and Applications. *Anal Chem*. **2016**, 88, 320–338.
4. Maughan N, Nguyen LM, Gamagedara S. Microfluidic Separation and Electrochemical Detection of Serotonin Using a Portable Lab-on-a-Chip Device. *Anal Bioanal Electrochem*. **2015**, 7, 1–11.
5. Ou X, Chen P, Huang X, Shunji L, Liu B. Microfluidic chip electrophoresis for biochemical analysis. *J Sep Sci*. **2020**, 43, 258–270.
6. Castro ER, Manz A. Present state of microchip electrophoresis: State of the art and routine applications. *J Chromatogr A*. **2015**, 1382, 66–85.
7. Rackus DG, Shamsi H, Wheeler AR. Electrochemistry, biosensors and microfluidics: a convergence of fields. *Chem Soc Rev*. **2015**, 44, 5320–5340.
8. Su W, Gao X, Jiang L, Qin J. Microfluidic platform towards point-of-care diagnostics in infectious diseases. *J Chromatogr A*. **2015**, 1377, 13–26.
9. Niculescu AG, Chircov C, Birca AC, Grumezescu, AM. Fabrication and applications of Microfluidic Devices: A review. *Int. J. Mol. Sci*. **2021**, 22, 2011.
10. Dong R, Liu Y, Mou L, Deng J, Jiang X. Microfluidics-Based biomaterials and biodevices. *Adv. Mater*. **2019**, 31, 1805033.
11. Wei Y-C, Fu L-M, Lin C-H. Electrophoresis separation and electrochemical detection on a novel thread-based microfluidic device. *Microfluid Nanofluid*. **2013**, 14, 583–590.
12. Fonslow B, Yates III J. Capillary electrophoresis applied to proteomic analysis. *J Sep Sci*. **2009**, 32, 1175–1188.
13. Sierra T, Crevillen AG, Escarpa A. Derivatization agents for electrochemical detection in amino acid, peptide and protein separations: The hidden electrochemistry? *Electrophoresis*. **2017**, 38, 2695–2703.
14. Wojcik R, Swearingen KE, Dickerson JA, Turner EH, Ramsay LM, Dovichi NJ. Reaction of fluorogenic reagents with proteins I. Mass spectrometric characterization of the reaction with 3-(2-furoyl)quinoline-2-carboxaldehyde, Chromeo P465, and Chromeo P503. *J Chromatogr A*. **2008**, 1194, 243–248.
15. Garrido-Medina R, Puerta A, Rivera-Monroy Z, Frutos M De, Guttman A, Diez-Masa C. Analysis of alpha-1-acid glycoprotein isoforms using CE-LIF with fluorescent thiol derivatization. *Electrophoresis*. **2012**, 33, 1113–1119.
16. Ríos Á, Zougagh M. Modern qualitative analysis by miniaturized and microfluidic systems. *Trends Anal Chem*. **2015**, 69, 105–113.

17. Brito-Neto JGA, Fracassi da Silva JA, Blanes L, Lucio do Lago C. Understanding Capacitively Coupled Contactless Conductivity Detection in Capillary and Microchip Electrophoresis. Part 1. Fundamentals. *Electroanalysis*. **2005**, 17, 1198–1206.
18. Kudr J, Zitka O, Klimanek M, Vrba R, Adam V. Microfluidic electrochemical devices for pollution analysis – A review. *Sensors Actuators B Chem*. **2017**, 246, 578–590.
19. Schilly KM, Gunawardhana SM, Wijesinghe MB, Lunte SM. Biological applications of microchip electrophoresis with amperometric detection: in vivo monitoring and cell analysis. *Anal Bioanal Chem*. **2020**, 412, 6101–6119.
20. Gunasekara DB, Wijesinghe MB, Saylor RA, Lunte SM. Principles and Strategies for Microchip Electrophoresis with Amperometric Detection. In: *Electrochemical Strategies in Detection Science*. **2016**.
21. Matysik F-M. Advances in amperometric and conductometric detection in capillary and chip-based electrophoresis. *Microchim Acta*. **2008**, 160, 1–14.
22. Crevillen AG. Nuevas estrategias electrocinéticas y nuevas aportaciones a la detección electroquímica en microchips de electroforesis capilar basadas en el empleo de nanotubos de carbono y otras nanoestructuras. **2009**.
23. Gunasekara DB, Hulvey MK, Lunte SM. In-channel amperometric detection for microchip electrophoresis using a wireless isolated potentiostat. *Electrophoresis*. **2011**, 32, 832–837.
24. Wang J. Electrochemical Detection for Capillary Electrophoresis Microchips: A Review. *Electroanalysis*. **2005**, 1133–40.
25. Randviir EP, Banks CE. Electrode substrate innovation for electrochemical detection in microchip electrophoresis. *Electrophoresis*. **2015**, 36, 1845–1853.

## **IV.2. Results and discussion**

The combination of microchip electrophoresis and electrochemical detection, in order to develop a separation and determination method for two glycoproteins, AGP and Tf, constitutes the core of this **Chapter IV**.

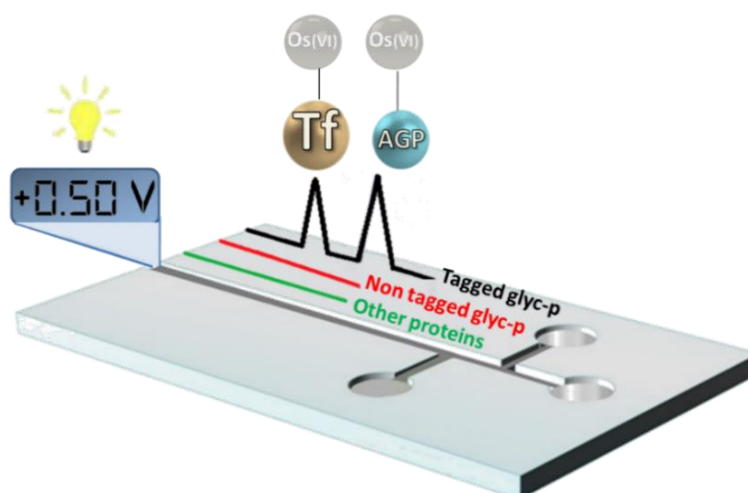
This approach takes a further step towards the development of a point-of-care testing for the simultaneous determination of multiple glycoprotein biomarkers.

## IV.2.1. Article 4: Determination of glycoproteins by microchip electrophoresis using Os(VI)-based selective electrochemical tag

Tania Sierra, Agustín G. Crevillén, Alberto Escarpa

Analytical Chemistry 91 (2019) 10245–10250

**Abstract:** Glycoproteins are excellent biomarkers for diagnosis and prognosis of several illnesses.  $\alpha_1$ -acid glycoprotein (AGP) and transferrin (Tf) are the main glycoproteins present in the serum, whose levels are increased during disease or injury. In this work, a selective detection of these glycoproteins using a microchip electrophoresis with electrochemical detection (ME-ED) platform is proposed for the first time. Because of the reduced sensitivity of glycoproteins, they were labeled with an electrochemical tag (osmium (VI) complex), which binds only to glycans, increasing the amperometric signal. Interestingly, oxidation potential of glycoprotein-Os(VI) adducts started at +0.50 V (*vs* Ag/AgCl) while nontagged glycoproteins started at +0.60 V. So, when the detection potential is set at +0.50 V, only glycoproteins tagged with Os(VI) complex are detected, avoiding the interference of the rest of the proteins. Determination of AGP and Tf was successfully demonstrated in the analysis of a certified human serum reference material yielding excellent accuracy ( $E_r \leq 4\%$ ) in just 400 s. This work offers new possibilities for ED for glycoprotein analysis in microfluidics systems, which has been dominated by fluorescence and MS detection until now. It is worth mentioning that ED has two interesting advantages with respect to others in the point-of-care testing field: easy miniaturization (bedside devices) and low-cost.







### 1. Introduction

Glycosylation is the most common post-translational modification of proteins in nature (it is estimated that over 70 % of all human proteins are glycosylated). Glycoproteins play crucial roles in numerous biological events in living organisms, and the alteration of its glycosylation profile is associated with the occurrence of diverse diseases such as cancer, rheumatoid arthritis, and other kinds of inflammation stages (1,2). In fact, glycoproteins are excellent biomarkers for illness diagnosis and prognosis, so their identification and reliable quantitation has a lot of interest in clinical field (3,4).

Transferrin (Tf) and  $\alpha_1$ -acid glycoprotein (AGP) are the main glycoproteins present in human serum, which have been used as biomarkers and therapeutic targets in clinical diagnosis (5,6). These glycoproteins could provide clinically relevant information for early recognition and monitoring of systemic inflammatory disorders such as Crohn's disease and sepsis because their concentration can increase up to 2–3 times in some of these diseases (7–9).

Regarding chemical structure, AGP is an acute phase glycoprotein with a low isoelectric point ( $pI = 2.8-3.8$ ), a high carbohydrate content (40 % w/w), and 41-43 KDa of molecular mass. In addition, five glycosylation sites are present on this protein (10,11). On the other hand, Tf exhibits only two N-linked disialylated biantennary oligosaccharide chains and an average glycosylation content of about 6 % w/w. Furthermore, its isoelectric point ( $pI = 5.2-5.6$ ) and molecular mass (70-95 KDa) are higher than those of AGP (12).

Many analytical techniques have been currently used for the analysis of glycoprotein biomarkers. There are interesting reviews about the use of liquid chromatography (LC) (13,14), mass spectrometry (MS) (15,16), and capillary electrophoresis (CE) (12,17). Also, glycoproteins determination is carried out by enzyme immunoassays or using lectin arrays (18,19). However, these techniques are time-consuming and/or expensive.

Currently, health care systems are demanding portable, reusable, and effective miniaturized platforms for clinical biomarker testing so that the test or analysis can be performed at or near the site of patient care. These systems are called bedside devices or point-of-care testing (POCT) and they provide physicians with timely diagnostic information, enabling faster, and better-informed decisions for diagnosis and treatment (20,21). In this sense, microfluidics or lab-on-a-chip systems are really an enabling technology for developing new POCT devices (22–24). Within these microfluidics systems, microchip electrophoresis (ME) is one of the earliest and most important examples. This technology offers fast analysis, low reagent and sample consumption, low waste generation (environmentally friendly), high throughput (parallelization), portability (for POCT), and lower cost (even disposability). In addition, ME has been successfully employed in biomedical and clinical analysis (25,26).

The main detection modes applied in ME for protein determination are fluorescence and MS (27,28). Electrochemical detection (ED) has not been explored in spite of its interesting features such as easy miniaturization without losing analytical performance and lower cost, making this detection mode more adequate for developing POCT systems (29,30). Among the reasons, ED has some disadvantages such as it is not as sensitive as fluorescence or MS detection, and not all proteins are electroactive. However, these handicaps could be overcome by labeling the protein with an electroactive tag (in the same way as fluorescence detection) (31). In fact, there are excellent examples in the bibliography for peptide labeling using Biuret reagent (32) and naphthalene-2,3-dicarboxaldehyde (33), among others.

In this sense, Palecek's group published several works in which glycoproteins were detected using an osmium (VI) complex as electrochemical probe (34,35). They demonstrated that this Os(VI) complex specifically links to the carbohydrate part and not to the polypeptide backbone. Specifically, the Os(VI) complexes react with diol groups from saccharides and produce osmate esters, which generate two electrochemical signals in carbon and mercury electrodes at  $-0.70$  and  $-0.25$  V (36,37).

Recently, our group has demonstrated the usefulness of this Os(VI) complex in the off-chip determination of AGP in serum samples (38,39).

In the following sections, we will demonstrate for the first time the analysis of glycoproteins by microchip electrophoresis with amperometric detection (ME-ED) using Os-based electrochemistry, under an oxidation potential so far completely unexplored in the literature.

## 2. Experimental section

### 2.1. Reagents

$\alpha_1$ -acid glycoprotein (AGP) ( $\geq 99\%$ ), transferrin (Tf) ( $\geq 98\%$ ), potassium osmate (VI) dihydrate, N,N,N',N'-tetramethylethylenediamine (TEMED), and certified human serum reference material (ERM-DA470 K/IFCC) were acquired from Sigma-Aldrich (Darmstadt, Germany). Hydrochloric acid, disodium hydrogen phosphate, and sodium dihydrogen phosphate were purchased from Panreac (Barcelona, Spain). Sodium acetate and disodium tetraborate decahydrate were purchased from Merck (Darmstadt, Germany).

All reagents are analytical grade. All solutions were prepared in Milli-Q water (Merck Millipore, Darmstadt, Germany).

### 2.2. Instrumentation

The single-channel glass microchip was used (Micronit, model CH\_X8050, Enschede, The Netherlands). The microchip consisted of a glass plate (90 mm  $\times$  15 mm) with a four-way injection cross, a 80 mm separation channel, and side arms measuring 5 mm. The original waste reservoir was cut-off, leaving the channel outlet at the end of the chip to carry out end-channel amperometric detection. The channels were 50  $\mu\text{m}$  wide and 20  $\mu\text{m}$  deep. The glass chip was set in a homemade Plexiglas holder. The holder contained reservoirs for sample (SR), sample waste (SW), running buffer (RB), and electrochemical detection cell (ED) (**Figure IV.2.1.1 B**).

The end-channel amperometric detector consisted of an Ag/AgCl electrode as a pseudoreference electrode, a platinum wire as counter electrode, and a screen-printed carbon electrode (SPCE) (Dropsens, Spain,

model DRP-C1XX) ( $10 \times 1$  mm) as working electrode. SPCEs are disposable electrodes so they were used only for one analysis, avoiding tedious protocols of electrode cleaning. In addition, other kinds of SPCEs (model DRP-110, Dropsens, Spain) were employed for cyclic voltammetry. They integrated the three electrodes system: carbon working electrode (4 mm diameter), carbon counter electrode, and silver reference electrode.

Amperometric detection and cyclic voltammetry were performed using a Potentiostat Autolab PGSTAT204 (Metrohm-Autolab, Utrecht, The Netherlands). This instrument was controlled by the software Nova 1.10. Voltage was applied using a LabSmith HVS448 high-voltage sequencer with eight independent high-voltage channels and programmable sequencing (LabSmith, Livermore, CA). Microcentrifuge MiniSpin (Eppendorf, Hamburg, Germany) was employed for centrifugation.

Mass spectrometry characterization of labeled glycoproteins were carried out in an UltraflexIII (Bruker, Billerica, MA, USA) using positive linear mode, 2,5-dihydroxyacetophenone (DHAP) as matrix in the presence of ammonium citrate and 2 % trifluoroacetic acid in water.

### 2.3. Procedures

#### 2.3.1. Preparation of Electrochemical Tag ( $\text{Os(VI)-O}_2(\text{OH})_2\text{TEMED Complex}$ )

The preparation of  $\text{Os(VI)O}_2(\text{OH})_2\text{TEMED}$  complex was carried out according to the literature (41). Potassium osmate (VI) dihydrate (18.4 mg, 50  $\mu\text{mol}$ ) were suspended in 1.22 mL of water. Then 5.8 mg of TEMED (50  $\mu\text{mol}$ s) and 0.41 mL of a 0.2 M sodium phosphate pH 7.0 solution were poured into the previous solution. Finally, 10  $\mu\text{L}$  of 10 M HCl solution were added. The solution was shaken for 1 h to allow the formation of  $\text{Os(VI)O}_2(\text{OH})_2\text{TEMED}$  complex, and finally, the solution was filtered using a syringe Nylon filter, 0.22  $\mu\text{m}$  (Tecno-Air, Barcelona, Spain). The final concentration of Os(VI) complex (electrochemical tag) was 30.3 mM.

#### 2.3.2. Glycoprotein-Tag Labeling (with $\text{Os(VI)O}_2(\text{OH})_2\text{TEMED Complex}$ )

Glycoprotein-Os(VI) adducts were prepared as follows: 1.02 mg in the case of AGP ( $2.5 \times 10^{-8}$  mol) and 1.9 mg of Tf ( $2.7 \times 10^{-8}$  mol) were dissolved

into 234  $\mu\text{L}$  of 50 mM sodium phosphate, pH 7.0, buffer using a “protein low bind” Eppendorf tube (Hamburg, Germany). Then 16.5  $\mu\text{L}$  of  $\text{Os(VI)O}_2(\text{OH})_2\text{TEMED}$  solution were added into the previous solution (mole ratio 1/20 between glycoprotein and  $\text{Os(VI)}$ ) and it was kept under agitation for 16 h at 37 °C and 950 r.p.m. using a thermo shaker (Biosan TS-100C, Riga, Latvia). Then these solutions were filtered through Amicon Ultra-0.5 mL centrifugal filters (cut-off 10 KDa) to remove the nonreacted  $\text{Os(VI)O}_2(\text{OH})_2\text{TEMED}$  complex (centrifugal parameters: 20 min at 12 800 r.p.m.). The filters were washed twice with 250  $\mu\text{L}$  of the optimum electrophoresis buffer to ensure the complete removal of  $\text{Os(VI)O}_2(\text{OH})_2\text{TEMED}$  complex. The Amicon filters were inverted and centrifuged (2 min at 5500 r.p.m.) to recover the glycoprotein- $\text{Os(VI)TEMED}$  adduct solution. This solution was diluted until a final volume of 250  $\mu\text{L}$ . Final concentrations were 4000  $\text{mg L}^{-1}$  for AGP and 7600  $\text{mg L}^{-1}$  for Tf (100 and 108  $\mu\text{M}$ , respectively). Finally, working solutions were prepared by dilution of stock solution. The labeling protocol of glycoproteins was modified when serum samples were analyzed because of the high concentration of glucose and other carbohydrates in these samples. The protocol was as follows: 200.5  $\mu\text{L}$  of serum sample was mixed with 49.5  $\mu\text{L}$  of  $\text{Os(VI)O}_2(\text{OH})_2\text{TEMED}$  solution and it was kept under agitation for 16 h at 37 °C and 950 r.p.m. using a thermo shaker (Biosan TS-100C, Riga, Latvia). Then the solution was filtered using Amicon filters for removing not only the excess reagent but also the glucose and other small carbohydrates labeled with  $\text{Os(VI)}$  present in serum.

#### 2.3.3. Microchip Procedure

The glass microchip channels were treated before use and between groups of runs by rinsing them with 0.1 M NaOH for 20 min and then deionized water for 15 min. This procedure was carefully monitored to obtain reproducible results. RB, SW, and ED reservoirs were filled with running buffer (25 mM sodium tetraborate at pH 9.2) and sample reservoir with the sample. Afterward, the separation channel was filled with running buffer applying +3000 V for 5 min to RB reservoir while ED reservoir was grounded.

Sample and standard solutions were prepared in 2.5 mM sodium tetraborate at pH 9.2 (10 times diluted with respect to running buffer) to perform a field-amplified stacking injection. Samples were injected by applying +3000 V for 20 s to SR reservoir while ED reservoir was grounded (unpinched injection).

A wall-jet configuration was used for amperometric detection (end-channel detection). The working electrode was set at +0.50 V during electrophoretic separation. To avoid the coupling of separation electrical field and the detection potential, a spacer (easily removable adhesive tape, 60  $\mu\text{m}$  thick) was placed between the SPCE and the channel outlet.

### 2.3.4. Safety Considerations

The high-voltage supply should be handled with extreme care to avoid electrical shock.

## 3. Results and discussion

### 3.1. Analytical Strategy and Characterization of Glycoprotein-Os(VI) Adduct

First, glycoproteins were selectively labeled with an Os(VI) complex, yielding an adduct that generates an amperometric signal at +0.50 V (*vs* Ag/AgCl) (see **Figure IV.2.1.1 A**). Then glycoproteins were analyzed by ME-ED using a detection potential of +0.50 V, avoiding the interference from other proteins thanks to the selectivity of the electrochemical tag (**Figure IV.2.1.1 B**).

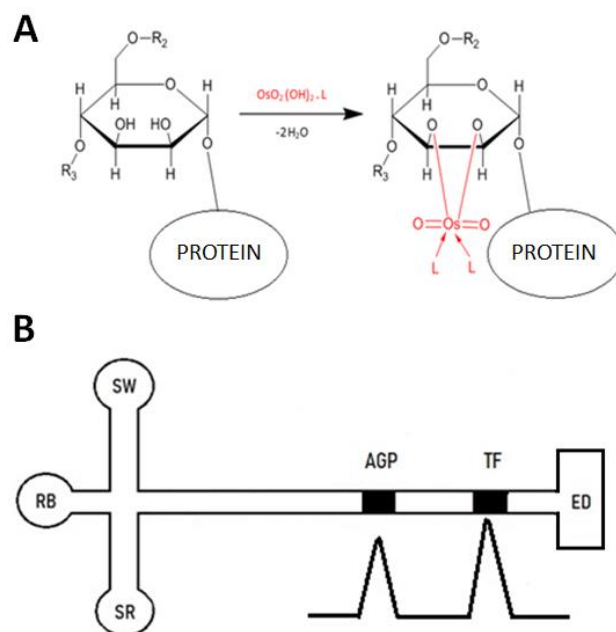


**Figure IV.2.1.1.** (A) Scheme of electrochemical glycoprotein labeling with Os(VI) complex. (B) ME microchip layout used (SR, sample reservoir; RB, running buffer reservoir; SW, sample waste reservoir; ED, end-channel electrochemical detection).

The effectiveness of the label with the Os(VI) complex was verified. As was aforementioned, this electrochemical tag reacts selectively with diols groups from carbohydrates. To prove that Tf was labeled with this tag, MALDI-TOF characterization was carried out. The labeling reaction yielded a Tf mass increase of approximately 1023 Da corresponding to 2.7 molecules of Os(VI) tag ( $M_w [Os(VI)O_2(OH)_2TEMED] = 372.4$  Da) (**Figure IV.2.1.2**). In a similar fashion, AGP labeling with Os(VI) was previously demonstrated and studied by our group (38). In that work, the number of electrochemical tag molecules per AGP molecule was estimated to be around 2, on the basis of mass increasing as measured by MALDI-TOF. This value is similar to Tf labeling in spite of the lower percentage of carbohydrate content of Tf.



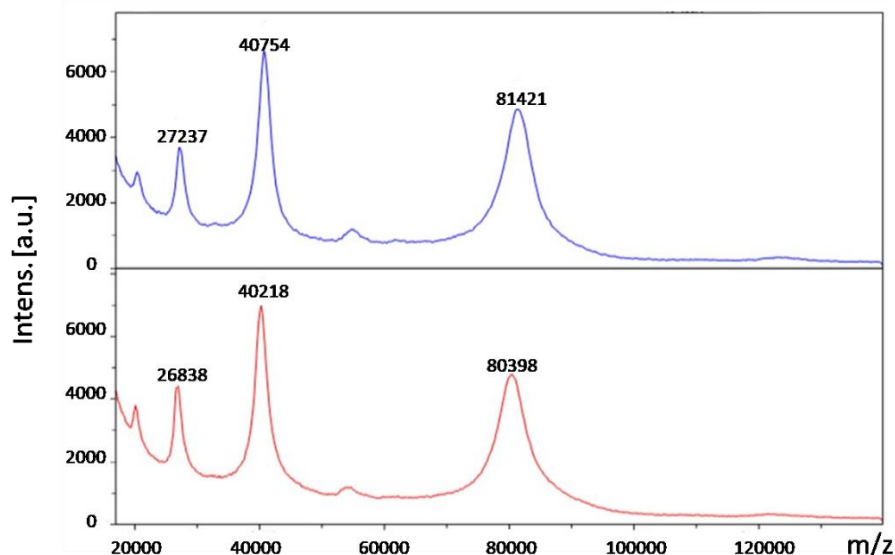


**Figure IV.2.1.2.** MALDI-TOF mass spectra of Tf-Os(VI) adduct (blue line) and intact Tf (red line).

Next the electrochemical behavior of Tf-Os(VI) (**Figure IV.2.1.3 A**) and AGP-Os(VI) adducts (**Figure IV.2.1.3 B**) were evaluated by cyclic voltammetry. As can be observed in **Figure IV.2.1.3**, glycoprotein-Os(VI) adducts (black line) exhibit a completely different behavior than the one obtained in the case of nontagged glycoproteins (red line). Glycoprotein-Os(VI) adducts yield two voltammetric peaks at  $-0.10$  V and at  $+0.80$  V in the anodic sweep, while glycoproteins presented only one well-defined peak at  $+0.80$  V (*vs* Ag). The latter is characteristic of proteins because of the electroactive amino acids present in its structure as Trp and Tyr (40,42). On the other hand, the peak at  $-0.10$  V is due only to the electrochemical tag used (Os(VI) complex). In addition, glycoprotein-Os(VI) adducts yield a cathodic peak at  $-0.20$  V, which forms along with the anodic peak at  $-0.10$  V a quasi-reversible system; surely, it is related to the electrochemistry of Os(VI) cation. Interestingly, glycoprotein-Os(VI) adducts generate higher faradic currents from  $-0.10$  to  $+0.80$  V compared to nontagged glycoproteins.

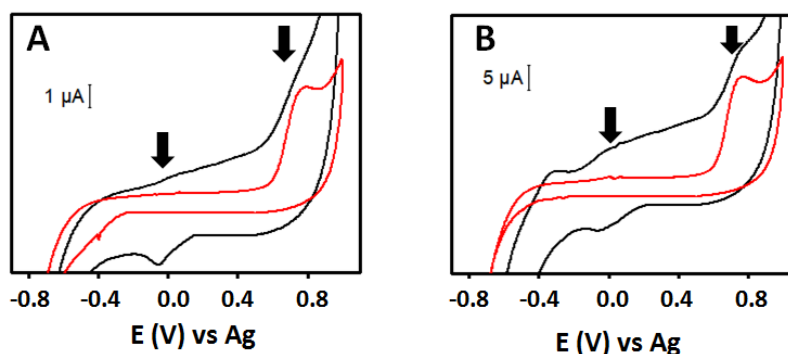


**Figure IV.2.1.3.** Cyclic voltammograms of glycoprotein-Os(VI) adducts and intact glycoproteins. (A) Tf-Os(VI) adduct (black line) and intact Tf (red line). (B) AGP-Os(VI) adduct (black line) and intact AGP (red line). Conditions: buffer Britton-Robinson at pH 3.0, scan rate 1 V/s. All concentrations are 400 mg L<sup>-1</sup>.

### 3.2. Tf and AGP Determination on ME-ED

Hydrodynamic voltammograms (HDV) for each glycoprotein were built to select the optimal detection potential (see **Figure IV.2.1.4**).

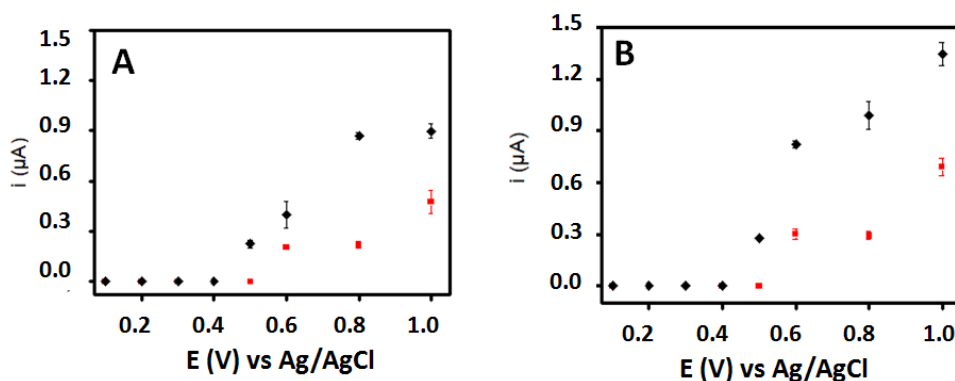


**Figure IV.2.1.4.** Hydrodynamic voltammograms of glycoprotein-Os(VI) adducts and intact glycoproteins. Hydrodynamic voltammograms were performed in 25 mM sodium tetraborate, pH 9.2; separation voltage +3.00 KV; injection voltage = +3.00 KV for 20.0 s. (A) 7600 mg L<sup>-1</sup> Tf-Os(VI) adduct (black line) and 7600 mg L<sup>-1</sup> intact Tf (red line). (B) 4000 mg L<sup>-1</sup> AGP-Os(VI) adduct (black line) and 4000 mg L<sup>-1</sup> intact AGP (red line).

Interestingly, oxidation potential of glycoproteins started at +0.60 V while glycoprotein-Os(VI) adducts started at +0.50 V (*vs* Ag/AgCl).

Furthermore, the electrochemical tag increased the anodic signal and, therefore, the method sensitivity. These results revealed that, at +0.50 V, only glycoproteins tagged with Os(VI) complex are detected, avoiding the interference of the rest of the proteins, even with higher sensitivity.

The difference found in the HDV between the starting oxidation potential of glycoproteins-Os(VI) adduct and that of intact glycoprotein is not noticeable in the cyclic voltammograms shown in **Figure IV.2.1.3**. Surely, this is due to the broad oxidation peak of electroactive amino acids from glycoproteins (+0.80 V) covering the selective signal of electrochemical tag.

To deepen this finding, glucose was selected as electrochemical probe because it is not electroactive in carbon electrodes, so the signal due to Os(VI) tag should be clearer. Os(VI) complex alone and tagged and nontagged glucose were characterized by cyclic voltammetry using the labeling reaction buffer for simplicity. As can be observed in **Figure IV.2.1.5**, there is no peak for nontagged glucose (red line). Os(VI) complex yields a small peak around +0.7 V (green line). However, when glucose is tagged with the Os(VI) complex, the corresponding adduct yields a high and well-defined peak around +0.40 (black line). This demonstrates that the reaction of Os(VI) tag with glucose is responsible for the appearance of this new peak in tagged glucose CV and, indeed, for the oxidation potential at +0.50 V in glycoprotein-Os(VI) adduct HDVs, so far completely unexplored in the literature. This interesting finding opens new directions for sugar electrochemical detection.

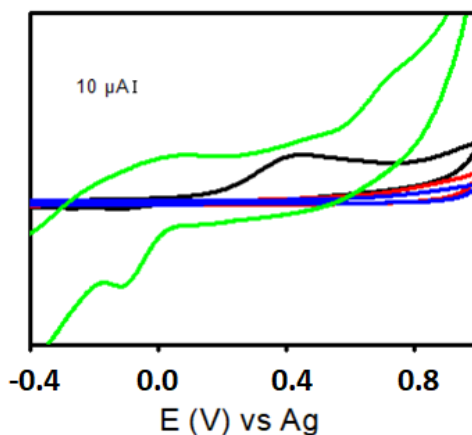


**Figure IV.2.1.5.** Cyclic voltammograms of 30.3 mM Os(VI) complex (green line), 4000 mg L<sup>-1</sup> glucose-Os(VI) adduct (black line), 4000 mg L<sup>-1</sup> glucose (red line), and 50 mM sodium phosphate buffer, pH 7.0 (blue line).

On the other hand, injection time, separation voltage, and injection voltage were also studied to obtain the best glycoproteins separation. At the optimal conditions (25 mM sodium tetraborate, pH 9.2, separation voltage +3000 V, injection at +3000 V for 20 s), AGP and Tf were well separated in less than 400 s with a baseline resolution ( $R_{Tf-AGP} = 1.3$ ) at +0.50 V as detection potential.

According to the HDVs, it is possible to develop two different approaches: one in which sensitivity is prioritized (detection potential at +1.00 V), and another in which selectivity is prioritized (+0.50 V). **Figure IV.2.1.6** reports both approaches. At +1.00 V detection potential (**Figure IV.2.1.6 A**), glycoproteins-Os(VI) adducts (black line) yield higher signals than nontagged glycoproteins (red line), improving the sensitivity. At +0.50 V (**Figure IV.2.1.6 B**), only glycoproteins tagged with Os(VI) complex are detected. In both cases, electrophoretic peaks show tailing. This is common in microfluidics systems with end-channel detection. Slow heterogeneous electron-transfer rate causes peak broadening of the analyte zone within the detector because the detector volume is significantly larger than the volume of injected sample (43) and this may be our case. This problem can be solved using other kinds of electrode materials.

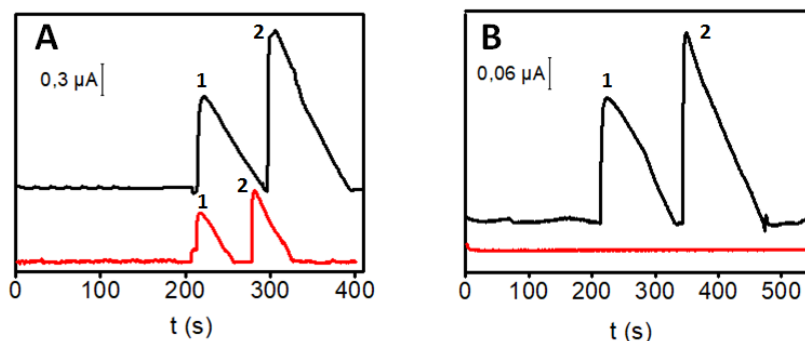


**Figure IV.2.1.6.** ME-ED detection of Tf (peak 1) and AGP (peak 2) at (A) +1.0 V and (B) +0.50 V. Protein-Os(VI) adducts (black line) and intact proteins (red line). Conditions: as in **Figure IV.2.1.4**. Tf: 7600 mg L<sup>-1</sup>. AGP: 4000 mg L<sup>-1</sup>.

### 3.3. Analytical Performance and Serum Analysis

The capability of our method for determination of Tf and AGP in serum samples was carefully evaluated. In this sense, a detection potential of +0.50 V was chosen for the rest of the experiments because of the complexity of serum, which contains a lot of proteins. External calibration parameters are reported in **Table IV.2.1.1**. The resulting calibration plots were linear ( $r^2 > 0.97$ ) in the concentration range assayed. The LOD and LOQ obtained (3  $S_a/N$  and 10  $S_a/N$  criterion, respectively) were adequate for Tf and AGP determination in serum samples because concentration ranges in healthy humans are between 1700 and 3700 mg L<sup>-1</sup> for Tf and 200–1000 mg L<sup>-1</sup> for AGP.

**Table IV.2.1.1.** Analytical features of the ME-ED approach for glycoproteins determination.

Glycoprotein	IL (mgL <sup>-1</sup> )	Intercept	Slope	$r^2$	LOD (mgL <sup>-1</sup> )	LQ (mgL <sup>-1</sup> )
		$a \pm s_a$ ( $\times 10^{-8}$ ) (A)	$b \pm s_b$ ( $\times 10^{-8}$ ) (ALmg <sup>-1</sup> )			
Tf	760-7600	-1,5 ± 1,1	0,003 ± 0,002	0,98	310	1031
AGP	400-4000	-1,8 ± 1,9	0,009 ± 0,008	0,97	126	422

#### IV.2.1. Determination of glycoproteins by ME-ED

Method reproducibility (intermediate precision) was also evaluated by analyzing a solution containing 7600 mg L<sup>-1</sup> Tf and 4000 mg L<sup>-1</sup> AGP on different days (see **Table IV.2.1.2**).

**Table IV.2.1.2.** Reproducibility of the method in different days (n=3).

Glycoprotein	Migration time (s)	RSD (%)	Peak height (x10 <sup>-7</sup> A)	RSD (%)
Tf	201 ± 25	12	3,5 ± 0,3	9
AGP	277 ± 32	12	4,9 ± 0,6	11

Although the peak height precision was not good (RSD ≤ 11 %), these values are typical for methods in which disposable electrodes are employed because of the variation between each SPCE. Considering migration times, it is worth mentioning that uncoated channels were used because of its simplicity but, as counterbalance, protein adsorption on surface channels may happen, affecting the migration time reproducibility. Anyway, RSDs were acceptable (≤ 12 %) for analyte identification and quantification.

Finally, a certified human serum reference material (CRM) was analyzed to evaluate the method accuracy. As is shown in **Table IV.2.1.3**, the method accuracy was excellent, obtaining relative errors ≤ 4 %.

**Table IV.2.1.3.** Analysis of a human serum certified reference material (CRM) (n=3).

Glycoprotein	C <sub>M</sub> (mg L <sup>-1</sup> )	C <sub>R</sub> (mg L <sup>-1</sup> )	E <sub>r</sub> (%)
Tf	2452 ± 314	2360 ± 80	4
AGP	604 ± 75	617 ± 13	2

**Figure IV.2.1.7** shows electropherograms corresponding to the serum analyzed at two different detection potentials. Interestingly, and as expected, a different profile was observed in the analysis of the certified human serum when the analysis was done at +0.50 V (black line) and at +1.00 V (red line). In the case of the profile at +1.00 V, other peaks occur in the electropherogram, interfering with AGP and Tf peaks because of the lack

of selectivity at this potential. However, at +0.50 V only glycoproteins labeled with Os(VI) show signals, demonstrating the selectivity of our approach.

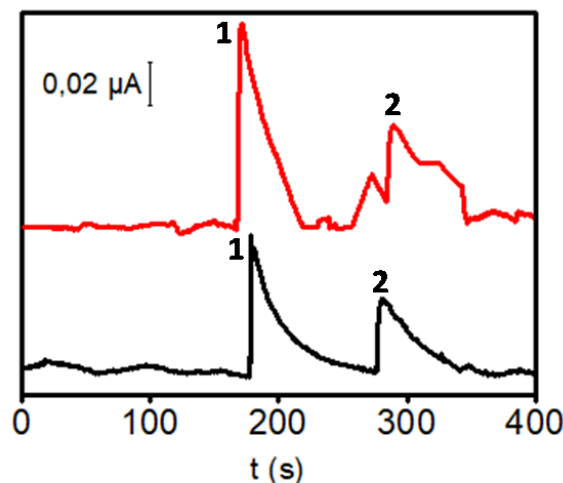


**Figure IV.2.1.7.** Microchip electrochemical detection of AGP and Tf in a human serum certified reference material at +0.50 V (black line) and at +1.0 V (red line). Conditions: as in **Figure IV.2.1.6**.

### 4. Conclusions

For the first time, glycoproteins were separated and detected by ME, using a Os(VI) complex tag-based electrochemistry. This tag binds selectively to glycans present in glycoproteins and the corresponding synthesized adduct yields an anodic signal at +0.50 V. At this so far completely unexplored detection potential, there is no interference from other proteins.

Our approach was evaluated by analyzing Tf and AGP glycoproteins in serum CRM. Both glycoproteins were determined with excellent accuracy ( $E_r \leq 4\%$ ) in less than 400 s.

This work opens the door to ME-ED for glycoprotein analysis which seemed to be reserved only for fluorescence and MS detection, exploiting the specific advantages of ED for POCT and bedside devices such as easy miniaturization and low-cost.

### **Acknowledgments**

This work has been financially supported by the TRANSNANOAVANSENS program from the Community of Madrid (P2018/NMT-4349), Spanish Ministry of Economy, Industry and Competitiveness (CTQ2017-86441-C2-1-R), and MINECO (MAT2016-80394-R). T.S. acknowledges the FPI fellowship from the University of Alcalá.

### **Author information**

#### **Corresponding Authors**

Alberto Escarpa – Department of Analytical Chemistry, Physical Chemistry and Chemical Engineering, University of Alcalá, Madrid, Spain. Chemical Research Institute “Andrés M. del Río” (IQAR), University of Alcalá, Madrid, Spain; [orcid.org/0000-0002-7302-0948](https://orcid.org/0000-0002-7302-0948); Email: [alberto.escarpa@uah.es](mailto:alberto.escarpa@uah.es)

Agustín G. Crevillen – Department of Analytical Sciences, Faculty of Sciences, Universidad Nacional de Educación a Distancia (UNED), Madrid, Spain; Email: [agustingcrevillen@ccia.uned.es](mailto:agustingcrevillen@ccia.uned.es)

#### **Other Authors**

Tania Sierra - Department of Analytical Chemistry, Physical Chemistry and Chemical Engineering, University of Alcalá, Madrid, Spain.

### **Authors Contribution**

The manuscript was written through contributions of all the authors. All the authors have given approval to the final version of the manuscript.



### References

1. Hayes AJ, Melrose J. Glycans and glycosaminoglycans in neurobiology: key regulators of neuronal cell function and fate. *Biochem. J.* **2018**, 475, 2511–2545.
2. Kolarich D, Lepenies B, Seeberger PH. Glycomics, glycoproteomics and the immune system. *Curr. Opin. Chem. Biol.* **2012**, 16, 214–220.
3. Kirwan A, Utratna M, O'Dwyer ME, Joshi L, Kilcoyne M. Glycosylation-based serum biomarkers for cancer diagnostics and prognostics. *Biomed Res. Int.* **2015**, 2015, 1–16.
4. Adameczyk B, Tharmalingam T, Rudd PM. Glycans as cancer biomarkers. *Biochim. Biophys. Acta - Gen. Subj.* **2012**, 1820, 1347–1353.
5. Smith KD, Behan J, Matthews-Smith G, Magliocco AM. Alpha-1-acid glycoprotein (AGP) as a potential biomarker for breast cancer. *Glycosylation.* **2012**, 201–222.
6. Szőke D, Panteghini M. Diagnostic value of transferrin. *Clin. Chim. Acta.* **2012**, 413, 1184–1189.
7. Makszin L, Szirmay B, Páger C, Mező E, Kalács KI, Pászthy V, Györgyi E, Kilar F, Ludány A, Köszegi T. Microchip gel electrophoretic analysis of perchloric acid-soluble serum proteins in systemic inflammatory disorders. *Electrophoresis.* **2019**, 40, 447–454.
8. Ipek İÖ, Saracoglu M, Bozaykut AJ.  $\alpha$ -Acid glycoprotein for the early diagnosis of neonatal sepsis. *Matern. Fetal & Neonatal Med.* **2010**, 23, 617–621.
9. Miranda-García P, Chaparro M, Gisbert JP. Correlation between serological biomarkers and endoscopic activity in patients with inflammatory bowel disease. *Gastroenterol. Hepatol.* **2016**, 39, 508–515.
10. Puerta A, Díez-Masa JC, Martín-Álvarez PJ, Martín-Ventura JL, Barbas C, Tuñón J, Egido J, de Frutos M. Study of the capillary electrophoresis profile of intact  $\alpha$ -1-acid glycoprotein isoforms as a biomarker of atherothrombosis. *Analyst.* **2011**, 136, 816–822.
11. Zhang C, Hage DS. Glycoform analysis of alpha1-acid glycoprotein by capillary electrophoresis. *J. Chromatogr. A.* **2016**, 1475, 102–109.
12. Alhazmi HA, Al Bratty M, Javed SA, Lalitha KG. Investigation of transferrin interaction with medicinally important noble metal ions using affinity capillary electrophoresis. *Pharmazie.* **2017**, 72, 243–248.
13. Suzuki S. Highly sensitive methods using liquid chromatography and capillary electrophoresis for quantitative analysis of glycoprotein glycans. *Chromatography.* **2014**, 35, 1–22.
14. Rowe L, Burkhart G. Analyzing protein glycosylation using UHPLC: a review. *Bioanalysis.* **2018**, 10, 1691–1703.
15. Veillon L, Huang Y, Peng W, Dong X, Cho BG, Mechref Y. Characterization of isomeric glycan structures by LC-MS/MS. *Electrophoresis.* **2017**, 38, 2100–2114.
16. Budnik BA, Lee RS, Steen JA. Global methods for protein glycosylation analysis by mass spectrometry. *J. Biochim. Biophys. Acta, Proteins Proteomics.* **2006**, 1764, 1870–1880.

17. Banazadeh A, Veillon L, Wooding KM, Zabetmoghaddam M, Mechref Y. Recent advances in mass spectrometric analysis of glycoproteins. *Electrophoresis*. **2017**, *38*, 162–189.
18. Pires F, Arcos-Martinez MJ, Dias-Cabral AC, Vidal JC, Castillo JR. A rapid magnetic particle-based enzyme immunoassay for human cytomegalovirus glycoprotein B quantification. *J. Pharm. Biomed. Anal.* **2018**, *156*, 372–378.
19. Yazawa S, Yokobori T, Kaira K, Kuwano H, Asao T. A new enzyme immunoassay for the determination of highly sialylated and fucosylated human  $\alpha$ 1-acid glycoprotein as a biomarker of tumorigenesis. *Clin. Chim. Acta.* **2018**, *478*, 120–128.
20. McPartlin DA, O 'Kennedy R. Point-of-care diagnostics, a major opportunity for change in traditional diagnostic approaches: potential and limitations. *J. Expert Rev. Mol. Diagn.* **2014**, *14*, 979–998.
21. Gomez FA. The future of microfluidic point-of-care diagnostic devices. *Bioanalysis*. **2013**, *5*, 1–3.
22. Nayak S, Blumenfeld NR, Laksanasopin T, Sia SK. Point-of-care diagnostics: recent developments in a connected age. *Anal. Chem.* **2017**, *89*, 102–123.
23. Jung W, Han J, Choi J, Ahn CH. Point-of-care testing (POCT) diagnostic systems using microfluidic lab-on-a-chip technologies. *Microelectron. Eng.* **2015**, *132*, 46–57.
24. Syedmoradi L, Daneshpour M, Alvandipour M, Gomez FA, Hajghassem H, Omidfar K. Point of care testing: The impact of nanotechnology. *Biosens. Bioelectron.* **2017**, *87*, 373–387.
25. Pagaduan JV, Sahore V, Woolley AT. Applications of microfluidics and microchip electrophoresis for potential clinical biomarker analysis. *Anal. Bioanal. Chem.* **2015**, *407*, 6911–6922.
26. Nuchtavorn N, Suntornsuk W, Lunte SM, Suntornsuk L. Recent applications of microchip electrophoresis to biomedical analysis. *J. Pharm. Biomed. Anal.* **2015**, *113*, 72–96.
27. Dawod M, Arvin NE, Kennedy RT. Recent advances in protein analysis by capillary and microchip electrophoresis. *Analyst*. **2017**, *142*, 1847–1866.
28. Štěpařová S, Kasička V. Recent developments and applications of capillary and microchip electrophoresis in proteomics and peptidomics (2015–mid 2018). *J. Sep. Sci.* **2019**, *42*, 398.
29. Nyholm L. Electrochemical techniques for lab-on-a-chip applications. *Analyst*. **2005**, *130*, 599–605.
30. Gencoglu A, Minerick AR. Electrochemical detection techniques in micro-and nanofluidic devices. *Microfluid. Nanofluid.* **2014**, *17*, 781–807.
31. Sierra T, Crevillen AG, Escarpa A. *Derivatization agents for electrochemical detection in amino acid, peptide and protein separations: The hidden electrochemistry?* *Electrophoresis*. **2017**, *38*, 2695–2703.
32. Warner AM, Weber SG. Electrochemical detection of peptides. *Anal. Chem.* **1989**, *61*, 2664–2668.

33. Faure M, Pallandre A, Chebol S, Le Potier I, Taverna M, Tribollet B, Desloius C, Haghiri-Gosnet AM, Gamby J. Improved electrochemical detection of a transthyretin synthetic peptide in the nanomolar range with a two-electrode system integrated in a glass/PDMS microchip. *Lab Chip*. **2014**, 14, 2800–2805.
34. Trefulka M, Paleček E. Direct chemical modification and voltammetric detection of glycans in glycoproteins. *Electrochem. Commun.* **2014**, 48, 52–55.
35. Trefulka M, Dorcak V, Krenkova J, Foret F, Paleček E. Electrochemical analysis of Os(VI)-modified glycoproteins and label-free glycoprotein detection eluted from lectin capillary column. *Electrochim. Acta*. **2017**, 239, 10–15.
36. Paleček E, Trefulka M. Electrocatalytic detection of polysaccharides at picomolar concentrations. *Analyst*. **2011**, 136, 321–326.
37. Billova S, Kizek R, Paleček E. Differential pulse adsorptive stripping voltammetry of osmium-modified peptides. *Bioelectrochemistry*. **2002**, 56, 63–66.
38. Sierra T, González MC, Moreno B, Crevillen AG, Escarpa A. Total  $\alpha$ 1-acid glycoprotein determination in serum samples using disposable screen-printed electrodes and osmium (VI) as electrochemical tag. *Talanta*. **2018**, 180, 206–210.
39. Sierra T, Dorte S, González MC, Palomares FJ, Crevillen AG, Escarpa A. Disposable carbon nanotube scaffold films for fast and reliable assessment of total  $\alpha$ 1-acid glycoprotein in human serum using adsorptive transfer stripping square wave voltammetry. *Anal. Bioanal. Chem.* **2019**, 411, 1887–1894.
40. Suprun EV, Zharkova MS, Morozovich GE, Veselovsk AV, Shumyantseva VV, Archakov AI. Analysis of redox activity of proteins on the carbon screen printed electrodes. *Electroanalysis*. **2013**, 25, 2109–2116.
41. Trefulka M, Paleček E. Voltammetry of Os(VI)-Modified Polysaccharides at Carbon Electrodes. *Electroanalysis*. **2009**, 21, 1763–1766.
42. Suprun EV, Shumyantseva VV, Archakov AI. Protein electrochemistry: application in medicine. A review. *Electrochim. Acta*. **2014**, 140, 72–82.
43. Wang J, Tian B, Prakash Chatrathim M, Escarpa A, Pumera M. Effects of heterogeneous electron-transfer rate on the resolution of electrophoretic separations based on microfluidics with end-column electrochemical detection. *Electrophoresis*. **2009**, 30, 3334–3338.





# CHAPTER V

**Capillary-driven  
electrochemical  
microfluidics  
for analysis of  
glycoproteins**



# V. Capillary driven electrochemical microfluidics for analysis of glycoproteins

## V.1. Introduction and objectives

In recent years, researchers have taken a further step in finding new methods and techniques that allow the determination of biomarkers in a faster, more accurate, and cheaper way. In this aspect, materials like paper or polymers, which were already used extensively in analytical and clinical chemistry (for example in paper chromatography, to separate and identify mixtures of small molecules, amino acids, proteins and/or antibodies) have become a good alternative to fabricate new microfluidics devices.

The first functional paper device, which performed a glucose assay, was created by the Whitesides' Group at Harvard University in 2007 (1). Since this moment and due to its biocompatible properties with various substrates, lightweight, flexibility, low-cost, hydrophilic nature, ease-to-use, and availability (2), paper has become a popular substrate for both two-dimensional (2D) and three-dimensional (3D) microfluidics paper-based analytical devices ( $\mu$ PADs) (3,4) (**Figure V.1.1**). The latter, obtained by stacking layers of the 2D patterned paper, offers potential advantages for multiplexing. Other fabrication strategies for 3D  $\mu$ PADs are spray adhesives, thermal adhesives (toner), cutting and lamination, and origami (5). In general, these  $\mu$ PADs provide cost-effective solutions for POCT diagnostics.

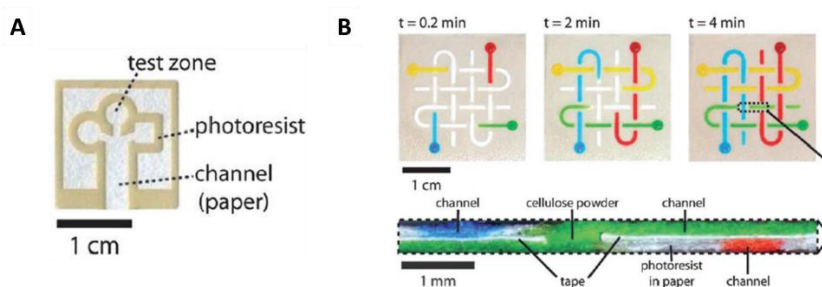


**Figure V.1.1.** (A) An example of two-dimensional (2D)  $\mu$ PAD (6) (B) Three-dimensional (3D)  $\mu$ PAD (4).



Unlike conventional microfluidics devices, the spontaneous liquid flow on  $\mu$ PADs is driven by capillary action in the presence of the cellulose matrix, and it avoids the use of any pumping equipment or external power supply. Furthermore, paper has other advantages such as: (i) it is thin, lightweight ( $\sim 10 \text{ mg cm}^{-2}$ ), available in a wide range of thicknesses (0.07-1 mm), and easy-to-stack, store, and transport; (ii) paper is compatible with biological samples due to it is typically made of cellulose or cellulose-polymer blends; (iii) paper can be easily chemically modified to incorporate a wide variety of functional groups, which can be covalently bound to proteins, DNA, or small molecules (7); (iv) paper is usually white and is a good medium for colorimetric tests because it provides strong contrast with a colored substrate; (v) paper is flexible and compatible with a host of existing printing technologies that could, in principle, be used to fabricate  $\mu$ PADs; and (vi) paper is available in a wide range of highly engineered forms with a very wide range of properties (6).

There are various proposed approaches to create channels and barriers in paper and fabricate these microfluidics devices, including cutting, photolithography, plotting, inkjet etching, plasma etching, was printing, among others (3,6,8). In addition, there are several substrates for PADs such as filter paper, chromatography paper, nitrocellulose membrane, and paper/polymer or paper/nanomaterial composites (5).

As for the detection methods used in these types of devices, it is found that two techniques are the most used: colorimetric and electrochemical. For the first, most chemical reactions with color change can be achieved on paper, such as acid-alkali reaction, precipitation reaction, redox reaction, enzymation reaction, etc. For qualitative detection, colorimetric changes in paper-based diagnostic assays can be visualized by the naked eye to yield a yes/no answer. In contrast, analysis by a handheld reader or a cell phone (by comparing the color change to a predetermined score) is used to report quantitative analysis. However, both qualitative and quantitative colorimetric strategies suffer in many cases low sensitivity and poor accuracy (3). In this aspect, paper-based electrochemical devices (ePAD) offer higher sensitivity and selectivity, more quantitative capability and faster response time, and they have attracted increasing attention among

other lab-on-a-chip systems to detect and quantify a wide variety of analytes from proteins and metabolites to nucleic acids and metal ions (9–11). For example, Whitesides *et al.* coupled simple ePAD with a commercial glucose meter to rapidly quantify the number of compounds relevant to human health (glucose, cholesterol, lactate and alcohol, in blood and urine) (12).

In these devices, the electrodes are prepared from conducting inks (carbon or metal) by screen-printing, inkjet-printing, or pencil-drawing on paper or plastic (**Figure V.1.2**).

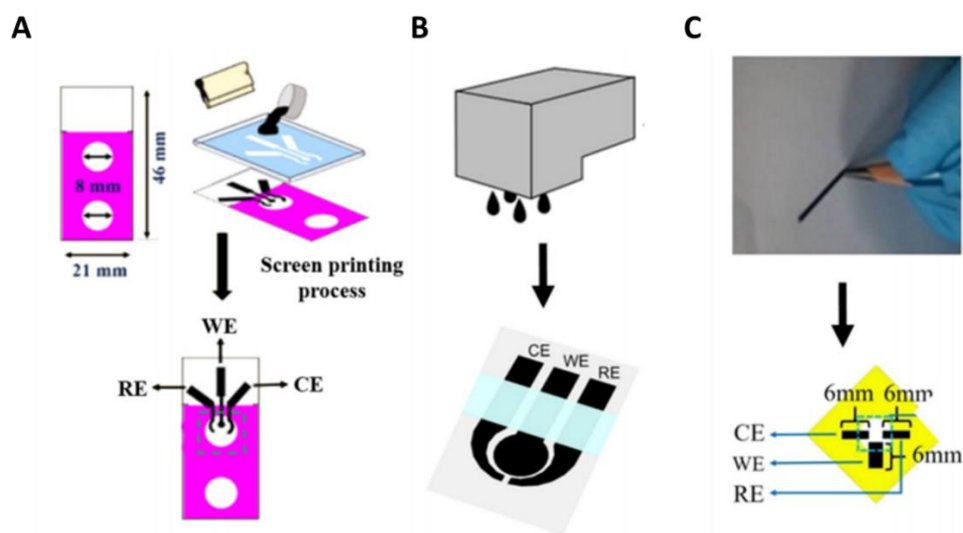


**Figure V.1.2.** Fabrication technologies of paper-based electrochemical devices. (A) Screen-printing. Three-electrode system was screen-printed on the detection zone of paper substrate using carbon ink. (B) Inkjet-printing. Mixing of carbon nanotube ink in deionized water, followed by inkjet-printing the carbon nanotube ink. (C) Writing. Three-electrode system was drawn on the working zone using a commercial graphite pencil (10).

However, paper has disadvantages in terms of its practical applicability for diagnostic applications, such as the porosity, and optical properties. So, although PADs have shown promise as diagnostic tools, the porous material has limitations in particle and reagent transport, low flow rate, and non-uniform flow (13).

Lamination-based devices have been recently introduced to overcome the limitations of conventional porous-based devices. In this approach, the

fabrication method is based on stacking multiple layers of pre-cut paper or polymeric film to form microfluidics channels. The channel geometry is defined on each layer and all layers are bonded by using adhesive, plasma bonding, or toner (13). Among several bonding approaches, double-sided adhesive (DSA) is a common material for the fabrication of lamination-based microfluidics channels because using a cutting process it is possible generated the hollow channel at a direct way (13,14). Like porous-based devices, the flow is driven by capillary action in lamination-based devices. However, the fluid mixing in the latter is faster than in the former (15,16), as we will discuss below.

In microfluidics devices, the flow is laminar and there is lack of turbulence, which makes molecular diffusion the primary mechanism for mixing. High mixing efficiency cannot be achieved with the help of only diffusion and can be one of the most difficult-to-achieve situations because the development of efficient mixing schemes is essential to increase the throughput of microfluidics systems and realizing the concept of micro-total-analysis systems and LOC devices (17,18).

In conventional microfluidics devices, mixing can be achieved using physical forces (pressure, magnetic, etc.) or through electrical forces (19,20). In the capillary-driven microfluidics devices, also called passive devices, instead of using an external pump to induce flow, utilize the surface tension of a fluid acting on the channel wall (or fibers in the case of paper) to drive flow. This reduces operational complexity at the point-of-use (21).

In passive micromixers, the mixing performance is improved by increasing the interface area of the different liquids or by manipulating the laminar flow within the microchannel using serpentine or herringbone structures (14,22). Among passive mixing systems (3D serpentine structure, embedded barriers, surface-chemistry...), lamination-based micromixers are one of the most used. In these types of microfluidics devices, the mixing mechanism relies on overlapping channels to increase the interface area of two or more fluids (23,24). As can be seen in **Figure V.1.3** depending on the geometry of these layers, the complete mixture could be obtained or not.

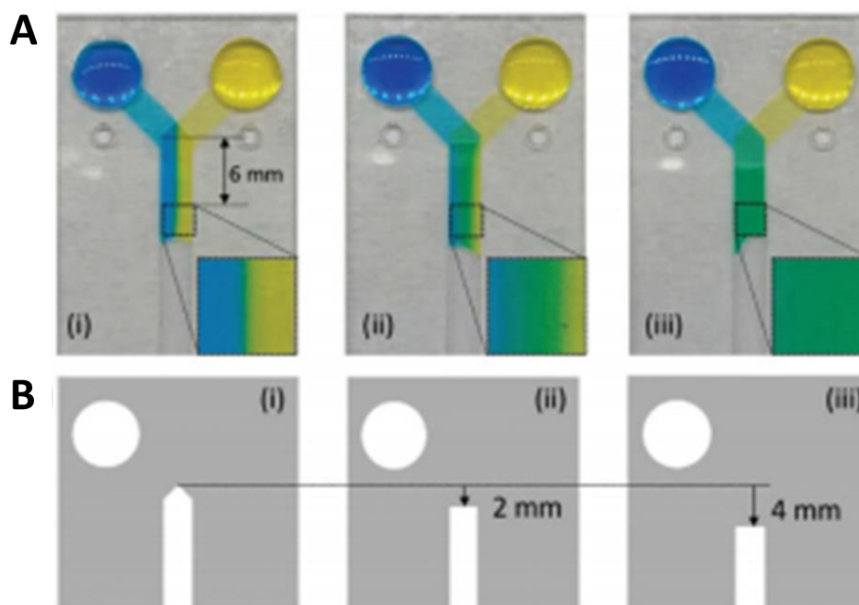


**Figure V.1.3.** (A) Three types of the Y-shaped device generating (i) non mixing, (ii) a concentration gradient, (iii) fully mixing concentration profile. (B) Different geometries of the middle transparency layers (13).

In this aspect, passive microfluidics devices have been used in many applications, including the detection of drugs, viruses, or cancer biomarkers, among others. But the potential of these microfluidics devices is not only limited to healthcare; devices developed for environmental safety, detecting water, soil or air contamination, and for food and beverage control are also available (25,26).

A recent laminated microfluidics device composed of transparency films and DSA showed for the first time that capillary-driven flow and rapid mixing could be achieved without porous media (**Figure V.1.4**). In this type of device, non-uniform flow and flow resistance caused by cellulose fibers is reduced, and accurate and rapid flow functionality can be realized. The hollow channel in this device was also made with transparent film so direct visualization of particles and flow is possible.

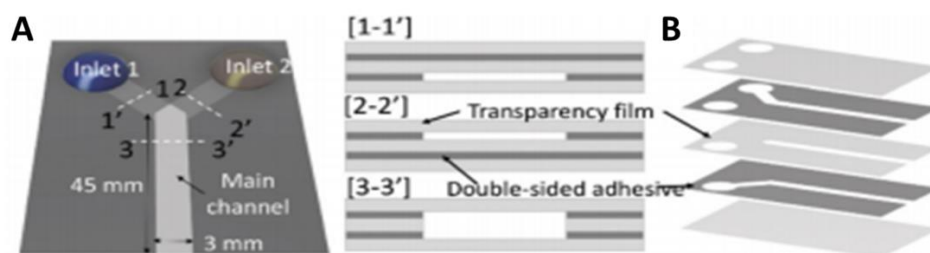


**Figure V.1.4.** Schematics of the passive device fabricated by lamination of double-sided adhesive and transparency film. **(A)** In this case consist in Y-shape device with two inlet channels placed in the different vertical positions. **(B)** Channel geometries of the Y-shape device defined on each layer (13).

The main objective of the works presented in this Chapter is the design and development of low-cost microfluidics devices based on capillary-driven flow for glycoprotein analysis. This approach allows us to carry out more analytical tasks (analyte labelling and detection) inside the microdevice, getting closer to a complete point-of-care testing system. The microfluidics devices used in these studies were fabricated using double-sided adhesive (DSA) and transparency film layers and they were composed of multi-layered channels.

### V.1.1. References

1. Martinez AW, Phillips ST, Butte MJ, Whitesides GM. Patterned Paper as a Platform for Inexpensive, Low-Volume, Portable Bioassays. *Angew Chem Int Ed.* **2007**, 46, 1318–1320.
2. Sachdeva S, Davis RW, Saha AK. Microfluidic Point-of-Care Testing: Commercial Landscape and Future Directions. *Front Bioeng Biotechnol.* **2021**, 8, 1–14.
3. Hu J, Wang S, Wang L, Li F, Pingguan-Murphy B, Jian Lu T, Xu F. Advances in paper-based point-of-care diagnostics. *Biosens Bioelectron.* **2014**, 54, 585–597.
4. Martinez AW, Phillips ST, Whitesides GM. Three-dimensional microfluidic devices fabricated in layered paper and tape. *PNAS.* **2008**, 105, 19606 – 19611.
5. Vashist SK, Lippa PB, Yeo LY, Ozcan A, Luong JHT. Emerging Technologies for Next-Generation Point-of-Care Testing. *Trends Biotechnol.* **2015**, 33, 692–705.
6. Martinez AW, Phillips ST, Whitesides GM. Diagnostics for the Developing World: Microfluidic Paper-Based Analytical Devices. *Anal Chem.* **2010**, 82, 3–10.
7. Sicard C, Brennan JD. Bioactive paper: Biomolecule immobilization methods and applications in environmental monitoring. *MRS Bull.* **2013**, 38, 331–334.
8. Dungchai W, Chailapakul O, Henry CS. A low-cost, simple, and rapid fabrication method for paper-based microfluidics using wax screen-printing. *Analyst.* **2011**, 136, 77–82.
9. Pal A, Cuellar HE, Kuang R, Caurin HFN, Goswami D, Martínez R V. Self-Powered , Paper-Based Electrochemical Devices for Sensitive Point-of-Care Testing. *Adv Mater Technol.* **2017**, 2, 1700130–1700140.
10. Li Y, He R, Niu Y, Li F. Paper-Based Electrochemical Biosensors for Point-of-Care Testing of Neurotransmitters. *J Anal Test.* **2019**, 3, 19–36.
11. Wang Y, Luo J, Liu J, Li X, Kong Z, Jin H, Cai X. Electrochemical integrated paper-based immunosensor modified with multi-walled carbon nanotubes nanocomposites for point-of-care testing of 17  $\beta$ -estradiol. *Biosens Bioelectron.* **2018**, 107, 47–53.
12. Nie Z, Liu X, Akbulut O, Whitesides GM. Integration of paper-based microfluidic devices with commercial electrochemical readers. *Lab Chip.* **2010**, 10, 3163–3169.
13. Jang I, Kang H, Song S, Dandy DS, Geiss BJ, Henry CS. Flow control in a laminate capillary-driven microfluidic device. *Analyst.* **2021**, 6, 1932–1939.
14. Jang I, Carrao D, Menger R, Rodrigo A, Oliveira M De, Henry CS. Pump-Free Microfluidic Rapid Mixer Combined with a Paper-Based Channel. *ACS Sensors.* **2020**, 5, 2230–2238.
15. Shi H, Nie K, Dong B, Long M, Xu H, Liu Z. Recent progress of micro fluidic reactors for biomedical applications. *Chem Eng J.* **2019**, 361, 635–650.

16. Lee C, Wang W, Liu C, Fu L. Passive mixers in microfluidic systems: A review. *Chem Eng J.* **2016**, 288, 146–160.
17. Moghimi M, Jalali N. Design and fabrication of an effective micromixer through passive method. *J Comput Appl Res Mech Eng.* **2019**, 9, 371–383.
18. Samae M, Ritmetee P, Chirasatitsin S, Kojić S, Kojić T, Jevremov J. Precise Manufacturing and Performance Validation of Paper-Based Passive Microfluidic Micromixers. *Int J Precis Eng Manuf.* **2020**, 21, 499–508.
19. Wu J, Xia H, Zhang Y, Zhao S, Zhu P, Wang Z. An efficient micromixer combining oscillatory flow and divergent circular chambers. *Microsyst Technol.* **2019**, 7, 2741–2750.
20. Zhao W, Yang F, Wang K, Bai J, Wang G. Rapid mixing by turbulent-like electrokinetic microflow. *Chem Eng Sci.* **2017**, 165, 113–121.
21. Bayareh M, Ashani MN, Usefian A. Active and passive micromixers: A comprehensive review. *Chem Eng Process Process Intensif.* **2020**, 147, 1–19.
22. Jang I, Berg KE, Henry CS. Viscosity measurements utilizing a fast-flow microfluidic paper-based device. *Sensors Actuators B Chem.* **2020**, 319, 128240.
23. Rappa K, Samargia J, Sher M, Pino JS, Rodriguez HF, Asghar W. Quantitative analysis of sperm rheotaxis using a microfluidic device. *Microfluid Nanofluidics.* **2018**, 22, 1–11.
24. Cassano CL, Fan ZH. Laminated paper-based analytical devices (LPAD): fabrication, characterization, and assays. *Microfluid Nanofluid.* **2013**, 15, 173–181.
25. Ozer T, McMahon C, Henry CS. Advances in Paper-Based Analytical Devices. *Annu Rev Anal Chem.* **2020**, 13, 85–109.
26. Pol R, Céspedes F, Gabriel D, Baeza M. Microfluidic lab-on-a-chip platforms for environmental monitoring. *Trends Anal Chem.* **2017**, 95, 62–68.

## V.2. Results and discussion

In the search for a point of care testing device that allows the determination of glycoproteins by electrochemical methods, this **Chapter V** has been focused on a new technology: capillary-driven microfluidics devices with electrochemical detection.

We report a new, cheap, and pump-free microfluidics mixer with electrochemical detection for the determination of  $\alpha_1$ -acid glycoprotein (AGP) (**V.2.1**) and transferrin (Tf) (**V.2.2**).

The passive mixer was fabricated by laminating transparency film and double-sided adhesive to form overlapping inlets. With the proposed geometry, we can carry out all the steps inside the device: labeling (with Os(VI) complex), washing, and detection by adsorptive transfer stripping square wave voltammetry.



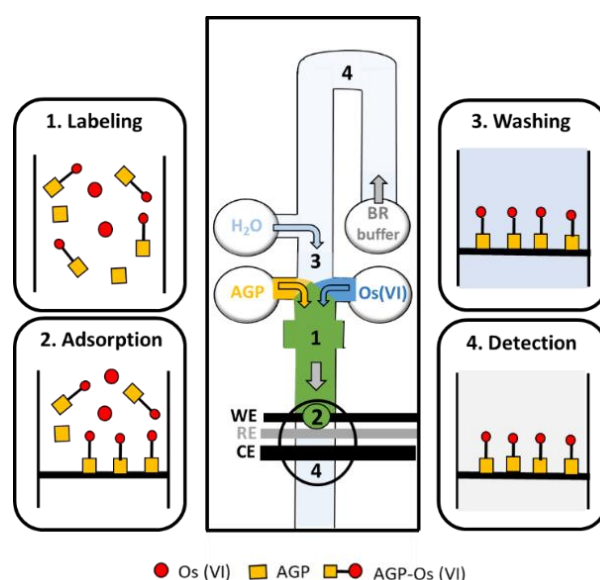


# V.2.1. Article 5: Pump-free microfluidic device for the electrochemical detection of $\alpha_1$ -acid glycoprotein

Tania Sierra, Ilhoon Jang, Eka Noviana, Agustín G. Crevillen, Alberto Escarpa, Charles S. Henry

ACS Sensors

**Abstract:**  $\alpha_1$ -acid glycoprotein (AGP) is a glycoprotein present in serum, which is associated with the modulation of the immune system in response to stress or injuries and a biomarker for inflammatory diseases and cancers. Here, we propose a pump-free microfluidics device for the electrochemical determination of AGP. The microfluidics device utilizes capillary-driven flow and a passive mixing system to label the AGP with Os(VI) complex (an electrochemical tag) inside the main channel, before delivering the products to the electrode surface. Furthermore, thanks to the resulting geometry, all the analytical steps can be carried out inside the device: labeling, washing, and detection by adsorptive transfer stripping square wave voltammetry. The microfluidics device exhibited a linear range from 500 to 2000 mg L<sup>-1</sup> ( $R^2 = 0.990$ ) and adequate limit of detection ( $LOD = 231$  mg L<sup>-1</sup>). Commercial serum samples were analyzed to demonstrate the success of the method, yielding recoveries around 83%. Due to its simplicity, low sample consumption, low-cost, short analysis time, disposability, and portability, the proposed method can serve as a point-of-care/need testing device for AGP.





### 1. Introduction

Glycoproteins play crucial roles in biological processes, such as the growth control, division and signaling of cells, protein-protein interactions, cellular differentiation, and cell migration (1–3). Almost 70 % of all proteins in the human body are glycosylated, having great structural diversity, and many of them have some specificity towards specific diseases (4,5). For that reason, the identification and quantification of glycoproteins are of significant interest in clinical chemistry.  $\alpha_1$ -acid glycoprotein (AGP) or also known as orosomucoid, is a serum glycosylated protein with an isoelectric point range from 2.8 to 3.8 and a range between 41–43 KDa as molecular weight (6). It is a glycoprotein that is considered to have a high carbohydrate percentage (40 % w/w). AGP is a perfect example of glycoprotein that can be used as a biomarker due to its relationship with inflammatory diseases where its concentration can increase by two to three times in the disease state (7). Furthermore, AGP was studied as potential biomarker for the diagnosis of neonatal sepsis in the early stages of the disease (8).

There are many techniques used for glycoprotein analysis, including separation techniques (9–11) and enzyme immunoassays (12,13). In addition, glycoproteins such as AGP have been analyzed by separation methods, which include capillary electrophoresis (CE) and high-performance liquid chromatography (HPLC). For example, Zhang *et al.* were able to analyze nine AGP glycoforms within 20 min via CE by considering factors such as the pH, various techniques for preventing protein adsorption onto the capillary, and the use of a non-ionic surfactant in the running buffer (6). The same group was also able to detect up to eleven glycoforms using reversed polarity mode CE and a coated capillary with a low electroosmotic flow (14). In this case, the total analysis time is 40 min (acid precipitation plus electrophoretic injection and separation). Glycan-based antibodies and lectins have also been developed as analytical reagents for the detection and quantification of AGP. For example, Yazawa *et al.* developed an enzyme immunoassay (EIA) bearing an anti-AGP antibody and a fucose-binding lectin to detect AGP in samples from patients with cancer and healthy controls (13). The times used in this type of method are very long

(some stages need overnight). However, these techniques not only are expensive and/or time-consuming but also require trained personnel and specialized laboratories to perform the measurements.

Unlike the centralization in laboratory diagnostics, today there is a trend towards a more decentralized analysis, known as point-of-care testing (POCT), also described as bedside, near-patient, remote, and decentralized laboratory testing (15–17). Ideally, only using a simple protocol (one or two steps) POCT device must provide accurate results using whole blood, urine, or other biological samples. The number of analytes which can be detected by POCT is substantial (e.g., metabolites, proteins, microorganisms, physical and chemical parameters), and in many cases can improve response time in diagnosing diseases and the overall level of care.

Electrochemical detection is highly suitable for the POCT of glycoproteins because of the low-cost and ease-to-miniaturization without losing analytical performance. However, direct oxidation of glycoproteins is not simple because, under near-physiological states, the carbohydrate part of the glycoprotein (glycans) is inactive. To overcome this limitation, Palecek's group proposed the use of six-valent osmium complexes with nitrogenous ligands [Os(VI)L] as an electrochemical probe (18,19). The Os(VI) complex reacts with diol groups of the glycan and forms an osmate ester. This adduct generates two signals on carbon electrodes.

Escarpa's group developed simple and inexpensive electrochemical methods for glycoprotein determination (20,21). In the first example (20), glycoprotein was labeled off-chip with Os(VI)TEMED complex. Quantification of AGP was carried out applying the method with successful results. However, the protocol to label the glycoprotein was too long (16 h), which complicates its implementation as POCT. In the second example (21), they took the advantage of the favorable kinetics of a chemical approach based in an exchange of ligands to achieve high stability of the products (AGP-Os(VI)TEMED), allowing a dramatic reduction in labeling time to 12 min (off-chip).

Microfluidics have emerged as a solid tool with demand in many fields (22–24) due to their advantages including reduced sample consumption, minimal waste generation, short analysis time, high throughput, and portability (25,26). These microfluidics devices also allow for chemical reactions, such as biomolecule labeling to run more efficiently than those in macroscale reactors and thus, are potential for on-chip labeling in an integrated electrochemical detection system. Furthermore, capillary-driven microfluidics devices can be applied to reduce operational complexity. In these devices, the surface tension of a fluid acting on the porous material such as paper and nitrocellulose membrane, and the hydrophilic channel wall is used to drive the flow.

Rapid mixing is an important step in many microfluidics applications in biology, chemistry, biomedicine, and the food industry (27–30). Several microfluidics devices have demonstrated the importance of mixing tools in the detection of drugs, viruses, and cancer biomarkers (31–36). For instance, Wu *et al.* developed a three-dimensional (3D) printed clear plastic microfluidics device for the detection of albumin in urine as an indicator of kidney damage in chronic kidney disease (37). The potential of these microfluidic devices is not only limited to healthcare, but also to environmental safety, water, soil, and air contamination, or for food and beverage control (38–41).

In microfluidics devices, where the flow is typically laminar making molecular diffusion the primary mechanism for mixing. Several studies have been conducted to enhance the mixing in the microfluidics channel. They can be divided into active and passive methods depending on whether additional equipment is used. For example, the active methods employ physical (pressure, magnetic, etc.) (42–44) or electrical forces (45–48) to improve the mixing. In contrast, passive mixing methods increase the contact surface between the fluids and reduce the mixing path (49,50) to promote mixing without any external force. Integrating a passive mixing mechanism into the capillary-driven microfluidics device can yield a simple, yet functional platform for on-chip processing (such as labeling) and detection of target analytes at the point-of-care/need.

Among the passive mixing methods, the lamination method is one of the most used due to its simplicity. In this method, each channel layer was formed bonding with each other by toner or double-sided adhesive (DSA). These overlapping channels increment the interface area between the two fluids (51–55).

In this work, we report a new, inexpensive, and pump-free microfluidics mixer with electrochemical detection for the determination of AGP, which is used to demonstrate its application as a universal method for glycoproteins. The passive mixer was formed by overlapping method using transparency film and double-sided adhesive and is based on previously published work by Jang *et al.* (52). However, it is the first time that a glycoprotein, in this case AGP, was labeled with the electrochemical tag within the channel and the labeled product was then adsorbed on the working electrode. Finally, AGP was determined by AdTSWV. This novelty makes it possible to take a great step towards the development of POCT devices that allow *in situ* analysis of glycoproteins and therefore help in the diagnosis or monitoring of diseases related to these macromolecules.

### 2. Material and methods

$\alpha_1$ -acid glycoprotein (AGP) ( $\geq 99$  %), potassium osmate (VI) dihydrate, silver paint, hexaammineruthenium (III) chloride, and sodium hydroxide were purchased from Sigma Aldrich (St. Louis, Missouri, USA). Hydrochloric acid, phosphoric acid, acetic acid, boric acid, disodium hydrogen phosphate, sodium dihydrogen phosphate, N,N,N',N'-tetramethylenediamine (TEMED), and boric acid were purchased from Fisher (New Jersey, USA). The synthesis of ferrocenylmethyl trimethylammonium hexafluorophosphate (FcTMA<sup>+</sup>) was carried out according to published bibliography (56).

Polymethylmethacrylate (PMMA) was obtained from Plaskolite Inc. (Ohio, USA). Polycaprolactone (PCL) was purchased from ThermoMorph® (Ohio, USA). Graphite (GR, MFG-15-99-500) was purchased from Graphene Supermarket. Double-walled carbon nanotube (DWCNT). Commercial carbon ink (E3178) was purchased from Ercon Incorporated

(Massachusetts, USA). Serum samples (Control-II) were purchased from Pointe Scientific (Michigan, USA). Ultrapure water ( $R \geq 18.2 \text{ M}\Omega \text{ cm}^{-1}$  at 25 °C, Milli-Q, Millipore) was used for preparing all solutions.

### 2.1. Procedures

#### 2.1.1. Preparation of Os(VI)O<sub>2</sub>(OH)<sub>2</sub>TEMED complex

Based on the bibliography (57), the preparation of the Os(VI)O<sub>2</sub>(OH)<sub>2</sub>TEMED complex was carried out as follows. Firstly, potassium osmate (VI) dihydrate was suspended in water (18.4 mg in 1.22 mL). 50 μmols TEMED and 0.41 ml of a 0.2 M sodium phosphate buffer (pH = 7.0) were added into the suspension. Then, 10 μl of HCl with a concentration of 10 M was poured into the previous solution. This mix was shaken for 1 h to form the Os(VI)O<sub>2</sub>(OH)<sub>2</sub>TEMED complex. After this time, a syringe Nylon filter of 0.22 μm was used to filter the solution. 30.3 mM was the final concentration obtained for Os (VI) complex.

#### 2.1.2. Acidic precipitation

Due to the presence of other glycoproteins in the serum samples, an off-channel pre-treatment was needed. A selective acidic precipitation was used to separate AGP from other proteins. 100 μl of perchloric acid with a concentration of 0.5 M and 50 μl of serum were mixed in a “protein low bind” microtube (20 s). Then, this acidified serum was centrifuged with the follow conditions: 7400 rpm for 20 min at room temperature. Finally, phosphate buffer (50 mM at pH 7) was used to re-dilute the supernatant.

#### 2.1.3. Device fabrication

Capillary-driven microfluidics device is composed by four inlets, four microfluidics channels that ultimately merge into a single channel, and one outlet united to a rectangular-shaped paper layer. 9 layers composed the mixing device, which was fabricated by laminating method using double-sided adhesive (467MP, 3M) and transparency film (Samsill) (**Figure V.2.1.1**). While the channel area is covered by the top and bottom transparence layers, the middle layers define the height and channel geometry. For example, DSA layers 2 and 3 (each layer was 50 μm thick)



were used to form a 100  $\mu\text{m}$  height channel between layers 1 and 4, while layer 5 formed a 50  $\mu\text{m}$  channel between layers 4 and 6. The channel areas were sketched out using CorelDRAW X4 (Corel), which is a graphic design software. Then, they were cut using a laser cutter (Zing 10000, Epilog Laser). Furthermore, the top layer contains electrodes for electrochemical detection. A rectangular-shaped paper (3 mm x 2 mm) was inserted at the outlet of the mixing device after assembling the DSA and transparency film layers to start the fluid flow.

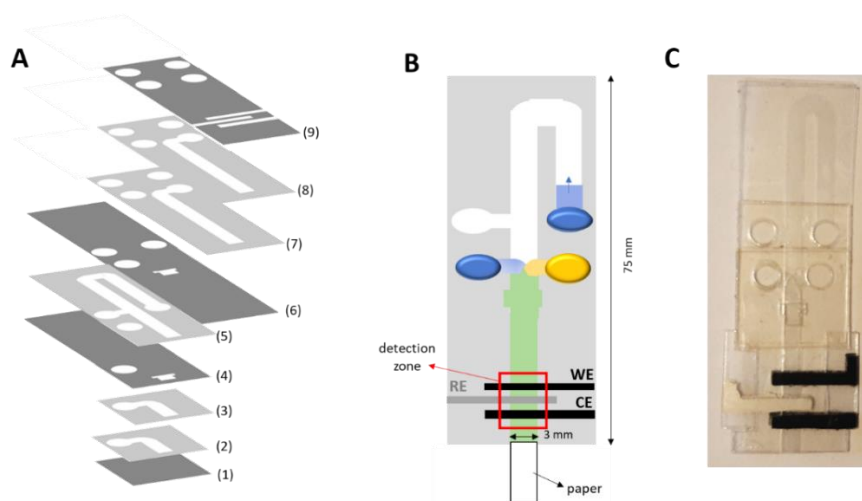


**Figure V.2.1.1.** Schematic representation of the capillary-driven microfluidics analytical device. **(A)** The geometry of double-sided adhesives and transparency films: layers 1, 4, 6, and 9 consist of transparency film (dark grey) while layers 2, 3, 5, 7, and 8 are made of double-sided adhesive (light grey). **(B)** Assembled mixing device with the integrated electrochemical detector: working electrode (WE), reference electrode (RE), and counter electrode (CE). **(C)** Image of the microfluidics analytical device.

### 2.1.4. Fabrication of electrodes

Corel Draw software (Ontario, Canada) was used to design the electrode geometry on the top layer of the device. A stencil was created using a transfer tape to serve as the electrode template in which the dimensions of working electrode (WE) and pseudo-reference electrode (RE) were 1.37 mm x 3 mm. They are separated 1 mm each other. The dimensions of counter electrode

(CE) was 2.5 mm x 3 mm and was also 1 mm apart from the adjacent electrode. Both WE and CE were carbon electrodes, whereas Ag/AgCl ink painted on carbon was used as the RE.

The fabrication of the electrodes was as follows: commercial carbon ink (Ercon) and carbon materials (1.0 g ink : 0.5 g graphite or DWCNT) was hand mixed and was patterned on the surface of the transparency film (top layer) using the stencil. Then the electrodes were cured at 60 °C for ~10 min. These electrodes are referred to as GPE (graphite electrode) and DWE (DWCNT electrode) in the next sections. DWCNT shows an increase in the heterogeneous charge rate, the mechanical strength, thermal stability (DWCNTs are stable even at 2000 °C in a vacuum, and 800 °C in air), and chemical stability over that of single-walled carbon nanotubes (SWCNTs). Additionally, DWCNTs enable a combination of solubility and functionality (which is not possible with SWCNTs) (59-61).

Finally, we painted the reference electrode with Ag/AgCl ink and cured the electrode again at 60 °C for ~10 min.

In addition to stencil-printed electrodes, we also investigated the use of thermoplastic electrodes (TPEs) for the detection. A previously reported fabrication protocol was used to create the electrodes (62). The process began dissolving polycaprolactone (PCL) in dichloromethane. Once the PCL was dissolved, it joined graphite powder (1:2). The mixture was poured onto a non-stick surface (Si wafer) and dried in a fume hood. The dried composite was heated above the melting point of PCL (70–85 °C) and then pressed into a PMMA mold using a hydraulic press (~50 psi). Once cooled, razor blade was used to remove excess material from the surface, followed by sandpaper.

### 2.1.5. Electrochemical electrode characterization and determination of AGP

Electrodes were characterized using FcTMA<sup>+</sup> as a redox probe. The electrochemical detection was performed using square wave voltammetry (SWV). SWV starts at – 0.2 V and finishes at + 1.0 V (other parameters: amplitude 50 mV, frequency 5 Hz and step potential 5 mV).

To determine the electrode active surface, Randles–Sevcik Equation (at 25 °C) was used:

$$I_p = 2.69 \times 10^5 n^{\frac{3}{2}} A C_o D_o^{\frac{1}{2}} \nu^{\frac{1}{2}}$$

In this equation,  $I_p$  is the anodic peak current;  $A$  is the electrode surface area;  $D_o$  is the diffusion coefficient of redox probe;  $n$  is the electron transfer number;  $C_o$  is the concentration of redox probe, and finally,  $\nu$  is the scan rate. Calculating the slope of  $I_p$  vs  $\nu^{1/2}$  plot using a reversible redox probe, it is possible to determine the electrode surface area. With this objective, different cyclic voltammograms were carried out at different scan rates (from  $\nu = 0.01$  to  $\nu = 0.1$  V s<sup>-1</sup>) and using 1 mM [Ru(NH<sub>3</sub>)<sub>6</sub>]Cl<sub>3</sub> in 0.5 M KNO<sub>3</sub> electrolyte ( $n = 1$  and  $D_o = 7.74 \times 10^{-6}$  cm<sup>2</sup> s<sup>-1</sup>). CHI1242B potentiostat (CH Instruments, Texas, USA) was used for all electrochemical measurements.

Determination of AGP-Os(VI)TEMED was carried out by employing adsorptive transfer square wave voltammetry (AdTSWV). In this case, AGP and Os(VI) complex were allowed to mix for 30 min and the labeled analyte was adsorbed onto the WE. Next the electrode was rinsed with water. Finally, the main channel was filled with background electrolyte (0.2 M BR buffer pH 3) and the electrochemical detection was carried out. SWV parameters: start potential – 1.5 V, end potential + 0.0 V, amplitude 50 mV, frequency 2 Hz and step potential 5 mV

### 3. Results and discussion

#### 3.1. Mixing experiments

First the geometry of the analytical device was optimized. It consisted of four inlets, four microfluidics channels, and one outlet connected to a rectangular-shaped paper layer. With this geometry, we can perform all steps in the same device (labeling, washing, and measuring). **Figure V.2.1.2** shows sequential images to understand the flow inside the device.

First, deionized water (15  $\mu\text{L}$ ) for the washing step was added to the upper left inlet reservoir and filled the main channel area placed on the 5<sup>th</sup> layer (**Figure V.2.1.2 a**). To ensure mixing, there are systems where two fluids should enter the main channel area at the same time. However, the arrival of fluids at different times can cause air entrapment problems and lead to flow inconsistency. To solve this problem, we used a burst valve at the junction of three microfluidics channels (52). The water will stop at the valve area until both blue and yellow dye solutions arrive at the valve through each channel. Despite the two fluids being added at the same time (10  $\mu\text{L}$ ) onto their respective inlets, one fluid may arrive at the valve first (i.e., the blue solution). However, the solution cannot continue to flow into the main channel due to surface tension at the junction. When the yellow solution arrives at the valve, the solutions will combine at the junction, and open the burst valve, allowing all three fluids to start flowing into the detection zone (**Figure V.2.1.2 b** and **c**) while mixing due to the short vertical mixing path and gravitational force. The two dyes were model solutions for two reagents that would be mixed/reacted within the channel. Finally, another blue dye solution (30  $\mu\text{L}$ ) was added onto the upper right inlet reservoir (**Figure V.2.1.2 d**). This blue dye solution was a model for buffered solution that would be used as supporting electrolyte for the electrochemical measurement. Since all channels were filled by solutions added in advance, the blue dye added last did not enter the channel immediately.

The use of a rectangular-shaped paper as a capillary pump in laminate devices was introduced by Jang *et al.* (51). Here, we utilized the paper pump in a slightly different way. As the mixed solution of water and dyes stopped

flowing upon arrival at the end of the device (outlet), the incubation/mixing time could be controlled. After a designated incubation time, the paper pump could be inserted at the outlet to pull the solution out of the laminated channel, allowing the water (for the washing step) and the lastly added blue dye solution to flow sequentially through the channel (**Figure V.2.1.2 e**). When the blue dye filled the detection zone, we then removed the paper pump to stop the flow (**Figure V.2.1.2 f**). This process allows us to carry out the electrochemical measurement with optimized reaction times.

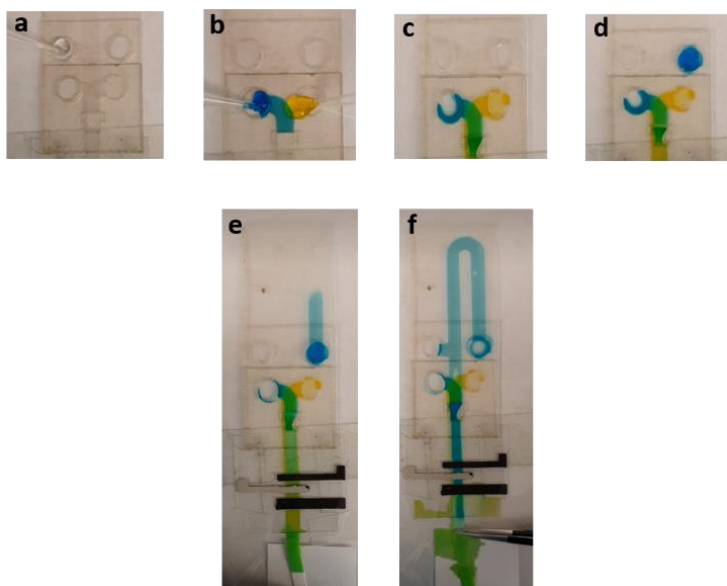


**Figure V.2.1.2.** Sequential images showing the moments of: **(a)** water (wash solution) injection, **(b)** the injected first reagent (blue dye) flows first and stops at the valve, **(c)** the injected second reagent (yellow dye) arrives and opens the valve, allowing the two solutions to mix to produce green color in the main channel, **(d)** flow stops until the rectangular-shaped paper is inserted to the outlet of the main channel, **(e)** flow starts when the rectangular-shaped paper is inserted to the outlet, and **(f)** blue dye from the top reservoir arrives at the main channel.

### 3.2. Electrode characterization

The carbon electrodes were characterized by electrochemical techniques, allowing us to choose the best material between GPE, DWE, and TPE, for subsequent measurements. GPE and TPE are based on graphite but DWE is

made of a carbon nanomaterial. This kind of nanomaterials (SWCNT and MWCNT) showed excellent analytical performance for electrochemical detection of glycoproteins (21). For this reason, we explored other type of carbon nanomaterial (DWCNT). **Figure V.2.1.3 A** shows the square wave voltammograms corresponding to the different electrodes using 1 mM FcTMA<sup>+</sup> as the redox probe. All the electrodes showed similar current signals. The peak height (at +0.4 V) of GPE, DWE, and TPE were  $6.6 \pm 0.4 \mu\text{A}$ ,  $6.1 \pm 0.3 \mu\text{A}$ , and  $5.3 \pm 0.8 \mu\text{A}$ , respectively.

The detection of AGP-Os(VI) adduct (target glycoprotein) was also studied with the three different electrode materials using AdTSWV. In **Figure V.2.1.3 B**, we can see the signals obtained from AGP-Os(VI) adduct ( $2000 \text{ mg L}^{-1}$  labeled off-device (20)) in BR buffer pH 3.0 using DWE (blue line), TPE (red line) and GPE (black line). A peak appears at  $-1.1 \text{ V}$ , which is corresponded to the AGP-Os(VI) signal. This result agrees with previous works on the characterization of this tag (20,21). DWE showed the best analytical response, and TPE showed the poorest performance.

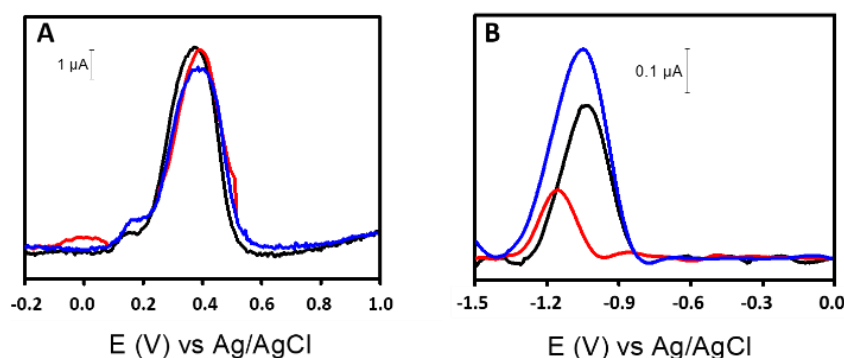


**Figure V.2.1.3.** (A) Voltammograms obtained by SWV using 1 mM FcTMA<sup>+</sup> in 50 mM phosphate buffer at pH 7. DWE (blue line), TPE (red line) and GPE (black line). Conditions: start potential  $-0.2 \text{ V}$ , end potential  $+1.0 \text{ V}$ , amplitude  $50 \text{ mV}$ , frequency  $5 \text{ Hz}$  and step potential  $5 \text{ mV}$ . (B) Voltammograms obtained for  $2000 \text{ mg L}^{-1}$  of AGP-Os(VI) in BR buffer at pH 3.0 using AdTSWV. DWE (blue line), TPE (red line) and GPE (black line). SWV parameters: step potential  $5 \text{ mV}$ , amplitude  $50 \text{ mV}$ , and frequency  $2 \text{ Hz}$  (electrochemical signals were baseline corrected and smoothed out).

To explain the different behavior on the electrodes, it must be understood that only AGP adsorbed on the electrode produces a signal in AdTSWV. Taking this into account, it seems clear that the active surface of electrodes plays a prominent role. For this reason, the surface area of each electrode was electrochemically determined by cyclic voltammetry using the Randles-Sevcik equation. The larger the surface area of the electrode, the greater signal would be produced. The surface areas of GPE, DWE and TPE were  $9.7 \pm 0.8 \text{ mm}^2$ ,  $9.3 \pm 0.9 \text{ mm}^2$  and  $6.7 \pm 0.3 \text{ mm}^2$ , respectively. The surface area increased in GPE, DWE, and TPE in comparison to electrodes made of carbon ink only ( $4.5 \pm 0.4 \text{ mm}^2$ ). GPE and DWE had larger active surfaces, enabling more AGP molecules to adsorb and produce higher electrochemical signals.

As DWE exhibited the best response for AGP-Os(VI) by AdTSWV, it was chosen for the following experiments.

### 3.3. Method optimization and analytical performance for AGP determination

The microfluidics device was designed to perform the following sequential steps: (i) labeling of AGP with the Os(VI) complex through the mixing of the reagents inside the channel, (ii) incubation of the labeled product (AGP-Os(VI)) to allow the product to be adsorbed on the electrode surface, (iii) wash step with water to remove the non-adsorbed product, and (iv) electrochemical determination of the AGP-Os(VI) adduct in the presence of BR buffer. The methodology was as follows: first, water (15  $\mu\text{L}$ ) was added to the upper left inlet ( $\text{H}_2\text{O}$  reservoir in **Figure V.2.1.4 A**). After filling the main channel area placed on the 5<sup>th</sup> layer, water would stop at the valve. Second, AGP and Os(VI)O<sub>2</sub>(OH)<sub>2</sub>TEMED complex were added (10  $\mu\text{L}$ ) to separate reservoirs/inlets and arrived at the valve. Once all reached the valve, the three fluids started flowing to the main channel outlet. Finally, the BR buffer (30  $\mu\text{L}$ ) was added at the upper right inlet reservoir (BR reservoir in **Figure V.2.1.4 A**) and the paper pump was connected to resume the flow inside the microfluidics device. The BR buffer was used as the electrolyte for AdTSWV measurements.

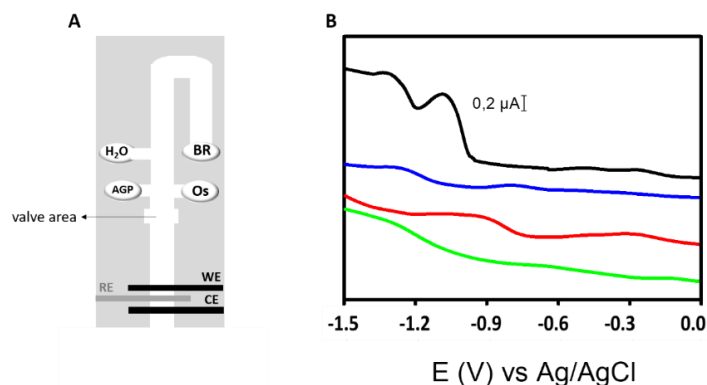


**Figure V.2.1.4.** (A) Schematic of mixing device with the integrated electrochemical detector. H<sub>2</sub>O, BR, AGP, and Os represents inlets for water, BR buffer, AGP and Os(VI) complex, respectively (B) Voltammograms obtained using AdTSWV with 30 min incubation time for 0.2 M BR buffer at pH 3.0 (blank) (green line), 15.15 mM Os(VI) complex (control) (red line), 2000 mg L<sup>-1</sup> AGP (control) (blue line), and 2000 mg L<sup>-1</sup> AGP-Os(VI) (black line). Conditions: as in **Figure V.2.1.3 B**.

The labeling of AGP with the Os(VI) complex occurs in the main channel. As aforementioned, AdTSWV measures only adsorbed protein. Thus, a sufficient incubation period is required to allow not only the AGP to be labeled with the Os(VI) complex, but also the AGP-Os(VI) adduct to be adsorbed onto the WE. When the incubation time is finished, the non-adsorbed Os(VI)O<sub>2</sub>(OH)<sub>2</sub>TEMED complex is then removed by a washing step. It is only after the paper pump is connected at the outlet that the flow inside the microfluidics device restarts. The mixed solution flows followed by water (washing step) and BR buffer sequentially. When paper was removed, the flow stops and then the electrochemical detection of the adsorbed AGP-Os(VI) is performed.

**Figure V.2.1.4 B** shows voltammograms of blank (green line), Os(VI) complex (red line), AGP (blue line), and AGP-Os(VI) (black line) using our approach. Clearly, a peak at -1.1 V, which is corresponded to the AGP-Os(VI)TEMED adduct can be noticed. Unlike this, unlabeled AGP, Os(VI) complex and blank not present this peak. These results demonstrated that this approach works for labeling and detecting AGP inside the device.



To optimize the incubation time, 2000 mg L<sup>-1</sup> AGP-Os(VI) was measured at different incubation times ranging from 0 and 30 min (**Figure V.2.1.S1** in Electronic Supplementary Material, ESM). From a practical point of view, it was not considered useful to study longer times. The signal at -1.1 V increased as a function of time, indicating that more AGP was labeled with the Os(VI) complex and adsorbed onto the WE. 30 min was selected as the best incubation time.

Inter-day precision of measurements on DWE was also studied using two concentrations of AGP-Os(VI) (2000 and 500 mg L<sup>-1</sup> AGP). RSDs of 12 % and 7 % were obtained from 3 days measurements (3 electrodes per day, n = 9), for 2000 and 500 mg L<sup>-1</sup> AGP, respectively (**Figure V.2.1.S2** in Electronic Supplementary Material, ESM). This level of reproducibility is sufficient for this assay.

Calibration was performed at the previously optimized experimental conditions. Using the peak intensity, a good linear correlation was obtained from 500 mg L<sup>-1</sup> to 2000 mg L<sup>-1</sup> with a correlation coefficient of R<sup>2</sup> = 0.990 (**Figure V.2.1.5**). A good correlation coefficient was obtained (r<sup>2</sup> = 0.990). The calibration curve slope was (1.03 ± 0.06) × 10<sup>-10</sup> A L mg<sup>-1</sup> and the intercept was (4.6 ± 0.8) × 10<sup>-8</sup> A (n = 3). The LOD was 231 mg L<sup>-1</sup> using the 3 S/N criterion. In previous works (20,21,63), lower LODs were obtained; however, in those works the labeling step was not integrated in the microfluidics device and the incubation time was longer (16 h).

The analytical characteristics show that AdTSWV method is adequate for AGP determination in serum samples, because AGP concentration in healthy humans ranged between 200 and 1000 mg L<sup>-1</sup> and the concentrations are higher in patients with inflammatory and other related diseases.

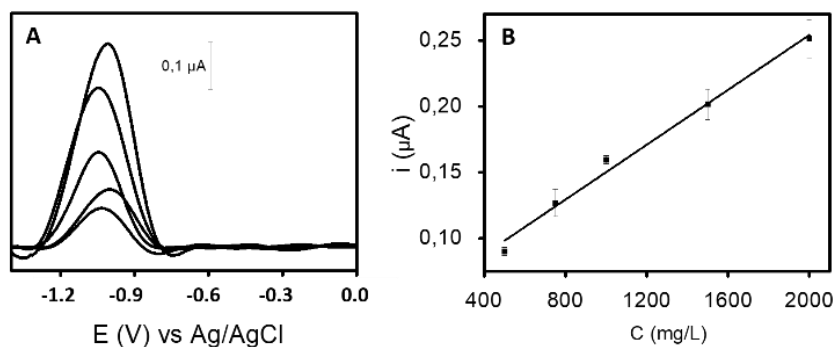


**Figure V.2.1.5.** (A) Voltammograms corresponding to AGP at different concentrations using the pump-free microfluidics device (electrochemical signals were baseline corrected and smoothed out). (B) Calibration curve ( $n = 3$ ). Conditions: as in **Figure V.2.1.3 B**.

### 3.4. Determination of AGP in human serum samples

Finally, AGP was determined in serum samples to evaluate the capability of the method for real samples. A serum sample was diluted 1:4 in 50 mM phosphate buffer pH 7 to reduce the signal due to endogenous AGP and next a learned concentration of AGP was added.

First, the selectivity of the method was checked using a sample serum containing 2000 mg L<sup>-1</sup> of AGP and 1000 mg L<sup>-1</sup> of glucose (potential interference). Glucose was selected because it is not eliminated by acidic precipitation, it is at high concentration in serum and it can be labeled with Os(VI) complex. The sample was treated using the acidic precipitation protocol and then it was analyzed by AdTSWV. Using an external calibration, a recovery of  $81 \pm 7\%$  ( $n = 3$ ) was obtained. A similar result was reported by Stumpe *et al.* (79.1%) when they employed the acidic precipitation in plasma samples (58). This means that glucose does not interfere in the AGP analysis, probably because it is not adsorbed or is weakly adsorbed on electrode surface, so it is removed during washing step. We also tested the integration of the acidic precipitation inside the device. However, there were a lot of components that precipitated inside the channel, hindering the flow of AGP and Os(VI) complex solutions.

Finally, a commercial serum sample was analyzed (spiked with 1000 mg L<sup>-1</sup> of AGP). The recovery was 83 ± 11 % (n = 3). (Table V.2.1.1). This low value is due to some AGP molecules are swept away by the precipitation of the other glycoproteins. Anyway, these results indicate that the overall assay has the basic performance needed for analysis of clinical samples.

**Table V.2.1.1.** Study of recoveries using a serum sample (n=3).

$C_{AGP\ ADD}$ (mg L <sup>-1</sup> )	$I_{SERUM+AGP}$ (A)x10 <sup>-7</sup>	$C_{SERUM+AGP}$ (mg L <sup>-1</sup> )	Recoveries (%)
1000	1.3 ± 0.2	830 ± 119	83 ± 11

## 4. Conclusions

In this work, we propose a pump-free microfluidics device for the electrochemical detection of AGP. The device was fabricated by a lamination method and consisted of a passive mixer and an integrated electrochemical detection.

All steps necessary for the quantification of AGP (labeling with Os(VI) complex and electrochemical detection) were successfully carried out in 30 min using a microfluidics device without an external pumping system. The feasibility of this approach for the determination of AGP in serum samples has been demonstrated and this approach can be extended to other glycoprotein biomarkers.

The proposed platform (pump-free microfluidics device with integrated electrochemical detectors) can serve as POCT devices for clinical analysis with attractive features such as simplicity, low sample consumption, low-cost, short analysis time, disposability, and portability.

### Acknowledgments

This work has been financially supported by the US National Science Foundation (CHEM-1710222), by the TRANSNANOAVANSENS program from the Community of Madrid (S2018/NMT-4349), and Spanish Ministry of Economy, Industry and Competitiveness (CTQ2017-86441-C2-1-R).

### Associated content

#### Supporting Information

**Figure V.2.1.S1.** Voltammograms of 2000 mgL<sup>-1</sup> AGP-Os(VI) by AdTSWV using different incubation times.

**Figure V.2.1.S2.** Voltammograms of (A) 2000 mgL<sup>-1</sup> AGP-Os(VI) and (B) 500 mgL<sup>-1</sup> of AGP-Os(VI) by AdTSWV obtained from 3 days measurements (3 electrodes per day, n = 9).

### Author information

#### Corresponding Authors

Charles S. Henry - Department of Chemistry, Colorado State University, Fort Collins, CO, 80526, USA, E-mail: Chuck.Henry@colostate.edu

#### Other Authors

Tania Sierra - Department of Chemistry, Colorado State University, Fort Collins, USA. Department of Analytical Chemistry, Physical Chemistry and Chemical Engineering, University of Alcalá, Madrid, Spain.

Ilhoon Jang - Department of Chemistry, Colorado State University, Fort Collins, USA. Institute of Nano Science and Technology, Hanyang University, Seoul, Korea

Eka Noviana - Department of Chemistry, Colorado State University, Fort Collins, USA. Department of Pharmaceutical Chemistry, Faculty of Pharmacy, Universitas Gadjah Mada, Yogyakarta, Indonesia

Agustín G. Crevillen – Department of Analytical Sciences, Faculty of Sciences, Universidad Nacional de Educación a Distancia (UNED), Madrid, Spain.

Alberto Escarpa – Department of Analytical Chemistry, Physical Chemistry and Chemical Engineering, University of Alcalá, Madrid, Spain. Chemical Research Institute “Andrés M. del Río” (IQAR), University of Alcalá, Madrid, Spain.

### Authors Contribution

The manuscript was written through contributions of all the authors. All the authors have given approval to the final version of the manuscript.

## Supporting Information

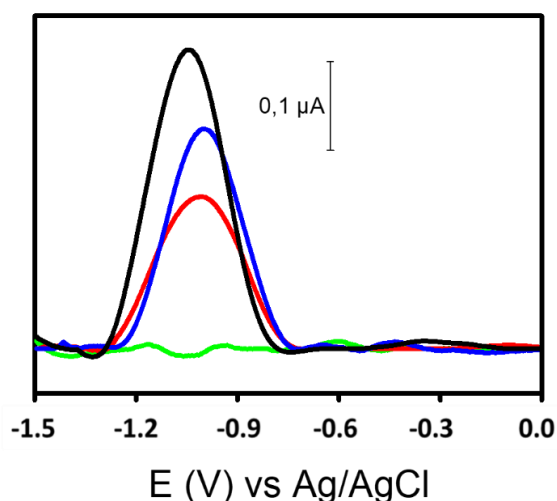


**Figure V.2.1.S1.** Voltammograms of  $2000 \text{ mgL}^{-1}$  AGP-Os(VI) by AdTSWV using different incubation times. Green line: 0 min; red line: 10 min; blue line: 20 min and black line: 30 min. SWV parameters: start potential  $-1.5 \text{ V}$ , end potential  $+0.0 \text{ V}$ , step potential  $5 \text{ mV}$ , amplitude  $50 \text{ mV}$ , and frequency  $2 \text{ Hz}$  (electrochemical signals were baseline corrected and smoothed out).

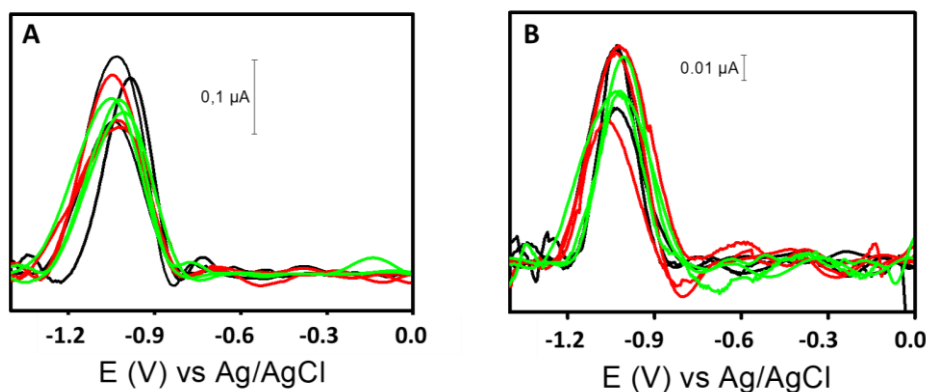


**Figure V.2.1.S2.** Voltammograms of (A)  $2000 \text{ mgL}^{-1}$  AGP-Os(VI) and (B)  $500 \text{ mgL}^{-1}$  of AGP-Os(VI) by AdTSWV obtained from 3 days measurements (3 electrodes per day,  $n = 9$ ). Green line: 3 measurements day 1; red line: 3 measurements day 2; and black line: 3 measurements day 3 (electrochemical signals were baseline corrected and smoothed out). Conditions: as in **Figure V.2.1.S1**.

### References

1. Li Y, Tran AH, Danishefsky SJ, Tan Z. Chemical biology of glycoproteins: From chemical synthesis to biological impact. *1st ed. Vol. 621, Chemical and Synthetic Biology Approaches To Understand Cellular Functions - Part A*. Elsevier Inc. **2019**, 213–229.
2. Hayes AJ, Melrose J. Glycans and glycosaminoglycans in neurobiology: key regulators of neuronal cell function and fate. *Biochem J.* **2018**,475,2511–2545.
3. Sun F, Suttapitugsakul S, Wu R. Enzymatic Tagging of Glycoproteins on the Cell Surface for Their Global and Site-Specific Analysis with Mass Spectrometry. *Anal Chem.* **2019**,91,4195–4203.
4. Connelly MA, Gruppen EG, Otvos JD, Dullaart RPF. Inflammatory glycoproteins in cardiometabolic disorders, autoimmune diseases and cancer. *Clin Chim Acta.* **2016**,459,177–186.
5. Kailemia MJ, Park D, Lebrilla CB. Glycans and glycoproteins as specific biomarkers for cancer. *Anal Bioanal Chem.* **2017**,409,395–410.
6. Zhang C, Hage DS. Glycoform analysis of alpha1-acid glycoprotein by capillary electrophoresis. *J Chromatogr A.* **2016**,1475,102–109.
7. Beeram S, Bi C, Zheng X, Hage DS. Chromatographic studies of drug interactions with alpha1-acid glycoprotein by ultrafast affinity extraction and peak profiling. *J Chromatogr A.* **2017**,1497,92–101.
8. İpek İÖ, Saracoglu M, Bozaykut A.  $\alpha_1$  -Acid glycoprotein for the early diagnosis of neonatal sepsis. *J Matern Neonatal Med.* **2010**,23,617–621.
9. Rowe L, Burkhart G. Analyzing protein glycosylation using UHPLC: a review. *Bioanalysis.* **2018**,10,1691–1703.
10. Veillon L, Huang Y, Peng W, Dong X, Cho BG, Mechref Y. Characterization of Isomeric Glycan Structures by LC-MS / MS. *Electrophoresis.* **2017**,38,2100–2114.
11. Banazadeh A, Veillon L, Wooding KM, Zabet-Moghaddam M, Mechref Y. Recent Advances in Mass Spectrometric Analysis of Glycoproteins. *Electrophoresis.* **2017**,38,162–189.
12. Pires F, Arcos-Martinez MJ, Dias-Cabral AC, Vidal JC, Castillo JR. A rapid magnetic particle-based enzyme immunoassay for human cytomegalovirus glycoprotein B quantification. *J Pharm Biomed Anal.* **2018**,156,372–378.
13. Yazawa S, Yokobori T, Kaira K, Kuwano H, Asao T. A new enzyme immunoassay for the determination of highly sialylated and fucosylated human  $\alpha_1$ -acid glycoprotein as a biomarker of tumorigenesis. *Clin Chim Acta.* **2018**,478,120–128.
14. Zhang C, Bi C, Clarke W, Hage DS. Glycoform analysis of alpha1-acid glycoprotein based on capillary electrophoresis and electrophoretic injection. *J Chromatogr A.* **2017**,1523,114–122.
15. Jung W, Han J, Choi J, Ahn CH. Point-of-care testing (POCT) diagnostic systems using microfluidic lab-on-a-chip technologies. *Microelectron Eng.* **2015**,132,46–57.

16. Nichols JH. Point-of-care testing. *Contemporary Practice in Clinical Chemistry. INC.* **2020**, 323–336.
17. Hernandez-Rodriguez JF, Rojas D, Escarpa A. Electrochemical Sensing Directions for Next-Generation Healthcare: Trends, Challenges, and Frontiers. *Anal Chem.* **2021**,93,167–183.
18. Trefulka M, Paleček E. Modification of poly- and oligosaccharides with Os(VI)pyridine. Voltammetry of the Os(VI) adducts obtained by ligand exchange. *Electroanalysis.* **2013**,25,1813–1817.
19. Trefulka M, Paleček E. Direct chemical modification and voltammetric detection of glycans in glycoproteins. *Electrochem commun.* **2014**,48,52–55.
20. Sierra T, González MC, Moreno B, Crevillen AG, Escarpa A. Total  $\alpha$ 1-acid glycoprotein determination in serum samples using disposable screen-printed electrodes and osmium (VI) as electrochemical tag. *Talanta.* **2018**,180,206–210.
21. Sierra T, Dorte S, González MC, Palomares FJ, Crevillen AG, Escarpa A. Disposable carbon nanotube scaffold films for fast and reliable assessment of total  $\alpha$  1 -acid glycoprotein in human serum using adsorptive transfer stripping square wave voltammetry. *Anal Bioanal Chem.* **2019**,411,1887–1894.
22. Weng X, Kang Y, Guo Q, Peng B, Jiang H. Recent advances in thread-based microfluidics for diagnostic applications. *Biosens Bioelectron.* **2019**,132,171–185.
23. Fallahi H, Zhang J, Phan H, Nguyen N. Flexible Microfluidics: Fundamentals, Recent Developments, and Applications. *Micromachines.* **2019**,10,830.
24. Dong R, Liu Y, Mou L, Deng J, Jiang X. Microfluidics-Based Biomaterials and Biodevices. *Adv Mater.* **2019**,31,1805033.
25. Ríos Á, Zougagh M, Avila M. Miniaturization through lab-on-a-chip: Utopia or reality for routine laboratories? A review. *Anal Chim Acta.* **2012**,740,1–11.
26. Vyawahare S, Griffiths AD, Merten CA. Miniaturization and Parallelization of Biological and Chemical Assays in Microfluidic Devices. *Chem Biol.* **2010**,17,1052–1065.
27. Suh YK, Kang S. A Review on Mixing in Microfluidics. *Micromachines.* **2010**,1,82–111.
28. Lee C, Chang C, Wang Y, Fu L. Microfluidic Mixing: A Review. *Int J Mol Sci.* **2011**,12,3263–3287.
29. Lee C, Wang W, Liu C, Fu L. Passive mixers in microfluidic systems: A review. *Chem Eng J.* **2016**,288,146–160.
30. Shi H, Nie K, Dong B, Long M, Xu H, Liu Z. Recent progress of micro fluidic reactors for biomedical applications. *Chem Eng J.* **2019**,361,635–650.
31. Damiati S, Kompella UB, Damiati SA, Kodzius R. Microfluidic Devices for Drug Delivery Systems and Drug Screening. *Genes (Basel).* **2018**,9,103.
32. Tang CK, Vaze A, Rusling JF. Automated 3D-printed unibody immunoarray for chemiluminescence detection of cancer biomarker proteins. *Lab Chip.* **2017**,17,484–489.

33. Soum V, Park S, Brilian AI, Kwon OS, Shin K. Programmable Paper-Based Microfluidic Devices for Biomarker Detections. *Micromachines*. **2019**,10,516.
34. Chen H, Chen C, Bai S, Gao Y, Metcalfe G, Cheng W, Zhu Y. Multiplexed detection of cancer biomarkers using a microfluidic platform integrating single bead trapping and acoustic mixing techniques. *Nanoscale*. **2018**,10,20196–20206.
35. Natsuhara D, Takishita K, Tanaka K, Kage A, Suzuki R, Mizukami Y, Saka N, Nagai M, Shibata T. A Microfluidic Diagnostic Device Capable of Autonomous Sample Mixing and Dispensing for the Simultaneous Genetic Detection of Multiple Plant Viruses. *Micromachines*. **2020**,11,540.
36. Noviana E, Blascke Carrao D, Pratiwi R, Henry CS. Emerging applications of paper-based analytical devices for drug analysis: A review. *Anal Chim Acta*. **2020**,1116,70–90.
37. Wu J, Tomsa D, Zhang M, Komenda P, Tangri N, Rigatto C, Lin F. A Passive Mixing Microfluidic Urinary Albumin Chip for Chronic Kidney Disease Assessment. *ACS Sensors*. **2018**,3,2191–2197.
38. Ozer T, McMahon C, Henry CS. Advances in Paper-Based Analytical Devices. *Annu Rev Anal Chem*. **2020**,13,85–109.
39. Pol R, Céspedes F, Gabriel D, Baeza M. Microfluidic lab-on-a-chip platforms for environmental monitoring. *Trends Anal Chem*. **2017**,95,62–68.
40. Weng X, Neethirajan S. Ensuring food safety: Quality monitoring using microfluidics. *Trends Food Sci Technol*. **2017**,65,10–22.
41. Zhang X, Wang X, Chen K, Cheng J, Xian N, Ni Z. Passive flow regulator for precise high-throughput flow rate control in microfluidic environment. *RSC Adv*. **2016**,6,31639–31646.
42. Wu J, Xia H, Zhang Y, Zhao S, Zhu P, Wang Z. An efficient micromixer combining oscillatory flow and divergent circular chambers. *Microsyst Technol*. **2019**,7,2741–2750.
43. Zhang M, Zhang W, Wu Z, Shen Y, Chen Y, Lan C, Li F, Cai W. Comparison of Micro-Mixing in Time Pulsed Newtonian Fluid and Viscoelastic Fluid. *Micromachines*. **2019**,10,262.
44. Lee KY, Park S, Lee YR, Chung SK. Magnetic droplet microfluidic system incorporated with acoustic excitation for mixing enhancement. *Sensors Actuators A Phys*. **2016**,243,59–65.
45. Ober TJ, Foresti D, Lewis JA. Active mixing of complex fluids at the microscale. *PNAS*. **2015**,112,2–7.
46. Shanko E, Burgt Y Van De, Anderson PD, Toonder JMJ Den. Microfluidic Magnetic Mixing at Low Reynolds Numbers and in Stagnant Fluids. *Micromachines*. **2019**,10,731.
47. Ebrahimi S, Hasanzadeh-Barforoushi A, Nejat A, Kowsary F. Numerical study of mixing and heat transfer in mixed electroosmotic / pressure driven flow through T-shaped microchannels. *Int J Heat Mass Transf*. **2014**,75,565–580.
48. Zhao W, Yang F, Wang K, Bai J, Wang G. Rapid mixing by turbulent-like electrokinetic microflow. *Chem Eng Sci*. **2017**,165,113–121.



## Chapter V. Capillary-driven electrochemical microfluidics

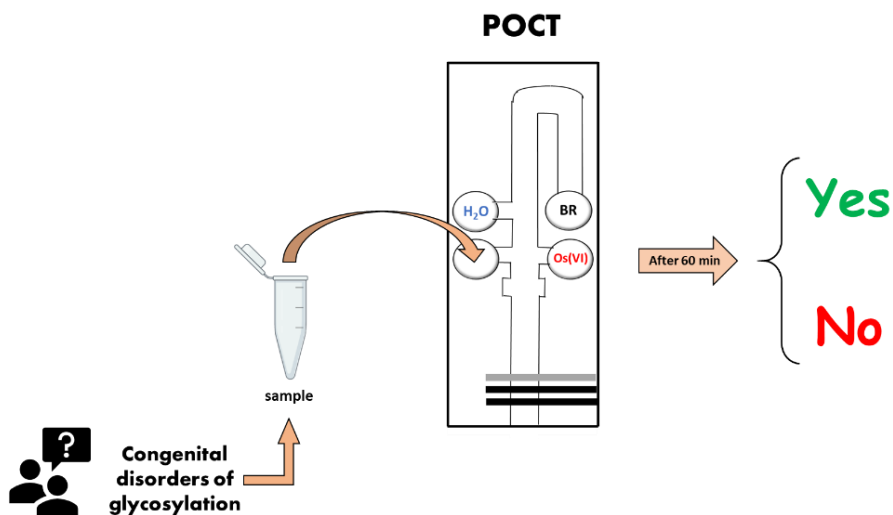
---

49. Hessel V, Löwe H, Schönfeld F. Micromixers – a review on passive and active mixing principles. *Chem Eng Sci.* **2005**,60,2479–2501.
50. Bayareh M, Ashani MN, Usefian A. Active and passive micromixers: A comprehensive review. *Chem Eng Process Process Intensif.* **2020**,147,1–19.
51. Jang I, Blascke Carrao D, Menger R, Rodrigo A, Oliveira M De, Henry CS. Pump-Free Microfluidic Rapid Mixer Combined with a Paper-Based Channel. *ACS Sensors.* **2020**,5,2230–2238.
52. Jang I, Kang H, Song S, Dandy DS, Geiss BJ, Henry CS. Flow control in a laminate capillary-driven microfluidic device. *Analyst.* **2021**,146,1932–1939.
53. Jang I, Berg KE, Henry CS. Viscosity measurements utilizing a fast-flow microfluidic paper-based device. *Sensors Actuators B Chem.* **2020**,319,128240.
54. Rappa K, Samargia J, Sher M, Pino JS, Rodriguez HF, Asghar W. Quantitative analysis of sperm rheotaxis using a microfluidic device. *Microfluid Nanofluidics.* **2018**,22,1–11.
55. Hernandez-Rodriguez JF, Rojas D, Escarpa A. Rapid and cost-effective benchtop microfabrication of disposable carbon-based electrochemical microfluidic devices. *Sensors Actuators B Chem.* **2020**,324,128679.
56. Lemay SG, Broek DM Van Den, Storm AJ, Krapf D, Smeets RMM, Heering HA, Dekker C. Lithographically Fabricated Nanopore-Based Electrodes for Electrochemistry. *Anal Chem.* **2005**,77,3824–3828.
57. Trefulka M, Paleček E. Voltammetry of Os(VI)-Modified Polysaccharides at Carbon Electrodes. *Electroanalysis.* **2009**,21,1763–1766.
58. Stumpe M, Miller C, Morton NS, Bell G, Watson DG. High-performance liquid chromatography determination of  $\alpha$ 1-acid glycoprotein in small volumes of plasma from neonates. *J Chromatogr B Anal Technol Biomed Life Sci.* **2006**,831,81–84.
59. Shen C, Brozena AH, Wang Y. Double-walled carbon nanotubes: Challenges and opportunities. *Nanoscale.* **2011**,3,503–518.
60. Green AA, Hersam MC. Properties and Application of Double-Walled Carbon Nanotubes Sorted by Outer-Wall Electronic Type. *ACS Nano.* **2011**,5,1459–1467.
61. Moore KE, Flavel BS, Ellis AV, Shapter JG. Comparison of double-walled with single-walled carbon nanotube electrodes by electrochemistry. *Carbon.* **2011**,49,2639–2647.
62. Klunder KJ, Clark KM, Mccord C, Berg KE, Minteer SD, Henry CS. Polycaprolactone-enabled sealing and carbon composite electrode integration into electrochemical microfluidics. *Lab Chip.* **2019**,19,2589–2597.
63. Sierra T, Crevillen AG, Escarpa A. Determination of Glycoproteins by Microchip Electrophoresis Using Os(VI)-Based Selective Electrochemical Tag. *Anal Chem.* **2019**,91,10245–10250.

## V.2.2. Article 6: Low-cost and passive electrochemical microfluidic device for diagnosis of congenital disorders of glycosylation

Tania Sierra, Charles S. Henry, Agustín G. Crevillen, Alberto Escarpa

**Abstract:** Here, a pump-free microfluidics device coupled with electrochemical made by using a multilayer lamination technique is proposed for detection of glycosylation disorders. Thanks to the stacking of PET films and double adhesive layers, it is possible to create a geometry that allows the filling of the tailored channels in a determined/fixed time. In the main channel of this passive microfluidics device, the necessary steps to perform the electrochemical determination of transferrin are performed: labeling of the protein with Os(VI) complex (electrochemical tag), washing with water of the osmium residues, and electrochemical detection by adsorptive transfer stripping square wave voltammetry. Electrochemical detection released two electrochemical signals: one from Os(VI) complex due to carbohydrates at  $-0.9\text{V}$  and other from the intrinsic electrochemical signal of glycoprotein due to the amino acids at  $+0.8\text{V}$ . The ratio between them (carbohydrate signal/protein signal) establishes an indicator of the degree of glycosylation (called electrochemical index of glycosylation). The method was applied to the analysis of clinical samples from patients with congenital disorders of glycosylation.





### 1. Introduction

In recent years, the trend towards decentralization of clinical analysis is growing (1,2). In comparison with traditional clinical analysis performed in centralized clinical laboratories, analysis that provides more immediacy and efficiency are highly desired to improve patient care (3,4). For this reason, the development of point-of-care testing (POCT), also called point-of-need or bedside testing, has targeted a paradigm shift, making this technology very useful in decision-making with relation to patient health (5,6).

To be useful, a POCT must be low-cost, easy-to-use, and miniaturized device in which the analysis can be carried out by non-trained people in a hospital, emergency department, or at home while also providing accurate results (7,8). Ideally, POCT devices must provide results in a few minutes and using a simple protocol with one or two steps in different biological fluids, such as whole blood, urine, or other easily obtained biological samples (9,10). These devices have the potential to provide a faster result making a tremendous positive impact. Furthermore, they offer the advantages of minimal sample volume consumption, which in many cases, such as newborn tests, is critical (11,12). Therefore, there is a growing tendency to develop new point-of-care platforms that show real advantages over laboratory pre-existing methods. In this sense, the guidelines provided by The World Health Organization (WHO) are very clear and they are called as ASSURED, in which the acronym ASSURED stands for affordable, sensitive, specific, user-friendly, rapid/robust, equipment-free or minimal, and deliverable to end users (13,14). Recently, an extended criteria was proposed: real-time connectivity and ease of sample collection (REASSURED) were added (1). With these indications, the number of analytes (e.g., metabolites, microorganisms, proteins, chemical and physical parameters) which can be detected by POCT is enormous (15–18).

Although there are many POCT devices based on colorimetric detection (19,20), electrochemical devices have traditionally received a significant share of the attention in (bio)-sensor development. Electrochemical detection produces simple and yet accurate and sensitive platforms for patient diagnosis and has been a promising approach for POCT diagnosis.

The primary advantages are high sensitivity, inexpensive instrumentation, easy miniaturization, and integration in compact analytical devices (21–23).

Microfluidics, due to its inherent advantages (low sample and reagent volume, minimal waste generation, short analysis time, high throughput, and portability) has emerged as a powerful tool with applications in many fields, specially, in the development of integrated lab-on-a-chip systems that reproduce laboratory-scale processes on a miniaturized format (24–27). In this sense, it is still difficult to find devices that perform complicated sample preparation steps such as mixing of reagents, separation/isolation of the target sample, and effective reaction between reagents and samples. For that reason, many innovative and creative methods have been and continue to be proposed (9,28,29). One promising approach is the use of capillary-driven microfluidics, also named passive methods. In these systems, fluids autonomously move along a channel without external force by the capillary effect (30–33), unlike traditional microfluidics devices, which use external forces such as pressure, magnetic, electrical, etc. (34,35). Capillary-driven flow is quite robust and easy-to-use, and it does not require any moving components or external power (36). Furthermore, in these types of devices paper can be act as a capillary pump (37). Interestingly, we recently developed a pump-free microfluidic device for the labeling and electrochemical detection of  $\alpha$ 1- acid glycoprotein in serum samples.

Glycoproteins, which represents almost the 70 % of proteins in the human body, are the focus of intensive research because can reveal the presence of certain diseases (38,39) such as congenital disorders of glycosylation (CDG). This is a rare disease, which is formed by large family of autosomal recessive and mostly multi-systemic disorders. There are not unique and precise symptoms which can be relate with CDG diseases (40). Most CDG patients have dysmorphic facial features, variable coagulation and endocrine defects, and abnormal fat distribution. In other patients, it can be found neurologic, cardiac, gastrointestinal, hepatic, renal, hematologic and/or immunologic problems (41,42). However, it seems clear that, due to the extremely severe symptoms, and for timely implementation of appropriate therapies and improving clinical outcomes, an early and accurate diagnosis of CDG is crucial (43,44).

One of the biomarkers used for the detection of this disease is carbohydrate deficient transferrin (CDT) which is defined as the ratio between the amount of transferrin (Tf) glycoforms with lower glycosylation (asialo-, disialo- and trisialo-Tf) and the total amount of glycoforms (aforementioned glycoforms plus tetrasialo-, pentasialo- and hexasialo-Tf) (45–47). In CDG patients, glycoforms asialo-, disialo- and trisialo-Tf, which are those with lower amount of glycans are increased respect to the main glycoform (tetrasialo-Tf), so their CDT values are high (47).

The most employed analytical methods (HPLC and CE) are based on separation techniques for separating transferrin glycoforms and, in consequence, quantifying the loss of carbohydrates (% CDT) (48,49). However, in these methods, expensive instrumentation, which not in all laboratories is available, is needed and prevents diagnosis at the point of care. In consequence, POCT is a pertinent approach, because it would facilitate the early diagnosis of CDG (it commonly happens after disregarding other diseases) and also the extension of its diagnosis to developing countries.

In this sense, our group have recently proposed a new parameter to measure the glycosylation level of Tf, called “electrochemical index of glycosylation (EIG)” (50). This parameter showed an excellent correlation with the official parameter % CDT and it can be easily measured by a simple screen-printed carbon electrode. In addition, this methodology was able to differentiate between serum from CDG patients and healthy people. The method uses an Os(VI) complex, which selectively reacts with glycans, as electrochemical tag for Tf. This adduct (Tf-Os(VI) complex) yields two peaks in square wave voltammetry (SWV): one from the carbohydrate component (Os(VI) complex) at  $-0.9\text{ V vs Ag/AgCl}$  and the other from protein component (electroactive amino acids from transferrin) at  $+0.8\text{ V vs Ag/AgCl}$ . The ratio between these two signals (carbohydrate signal/protein signal) is the EIG parameter. The main limitation of this approach was the long reaction time of labelling step (16 h) that was performed manually.

In this work, we explored the use of capillary-driven microfluidics for developing a passive and low-cost microfluidics electrochemical device for CDG diagnosis. The lamination method, in which the channel geometry of

each layer (PET films and double-sided adhesive (DSA)) was formed before aligning and bonding with each other, was used to create the device. The steps necessary for the measurement of EIG value for Tf were carried out in the main channel of the device without external pumps. These steps include the labeling of Tf with Os(VI) complex (which acts as electrochemical probe), the adsorption of the formed adduct on the working electrode, the washing step with water to remove the excess of complex, and finally the electrochemical detection (EIG measurement).

## 2. Material and methods

### 2.1. Materials

Adhesive vinyl sheets (Tavolozza), transparency film (Avery Zweckform), and double-sided adhesive paper (Klebefolie) for the fabrication of the devices were obtained from a local store. Carbon ink (C2000802P2, Gwent Group) was employed to form the electrodes (working and counter) and Ag/AgCl paste (C2130809D5, SunChemical) was used to reference electrode.

Transferrin (Tf) ( $\geq 98\%$ ), potassium osmate (VI) dihydrate and N,N,N',N'-tetramethylenediamine (TEMED) were purchased from Sigma–Aldrich (Darmstadt, Germany). Phosphoric acid, hydrochloric acid, acetic acid, disodium hydrogen phosphate and sodium dihydrogen phosphate were purchased from Panreac (Barcelona, Spain). Anti-Transferrin antibody (ab66952) was purchased from Abcam (Cambridge, UK).

Centro de Diagnostico de Enfermedades Moleculares (CEDEM, Madrid, Spain) donated us serum samples from patients diagnosed with CDG. These samples were previously anonymized (approved by research ethic committee of CEDEM).

Protein G was used to functionalize magnetic beads (MBs), which were acquired from Thermo Fisher Scientific (USA). Before use, to homogenize MB suspensions, 1  $\mu\text{L}$  was added to a microtube and rinsed twice with 100 mL PBS solution pH 7.4.

Ultrapure water was used for preparing all solutions (Merck Millipore, Darmstadt, Germany).

### 2.2. Instrumentation

A multi potentiostat/galvanostat  $\mu$ STAT 8000 (DropSens, Oviedo, Spain) was used for all electrochemical measurements. This potentiostat incorporates “DropView 8400”, which was the software used for electrochemical measurements.

AutoCAD 2018 (Autodesk, Student Version) was used to design the stencil with the geometry of electrodes and this stencil was cut using a desktop cutting plotter (Silhouette Cameo 3, Silhouette). In this work, a three-electrode configuration was used. The steps to fabricate these electrodes are shown in **Figure V.2.2.1**. First, it was used a template of adhesive vinyl in which pseudo-reference electrode (RE), working electrode (WE) and counter electrode (CE) were constructed in dimensions of 1.34 mm x 3 mm and are 1.25 mm apart from each other. From upstream to downstream electrodes were placed as follows: RE, WE and CE. Then, it was used carbon ink to drop on the transparency film surface of WE and CE using the template and the electrodes were cured at 50 °C for ~10 min. Finally, it was used the template to cover the RE with Ag/AgCl paste and it was cured again at 50 °C for ~10 min.

Before to electrochemical experiments, WE were electrochemically pretreated in BR buffer solution by carrying out cyclic voltammetry (1 cycle) from  $-1.0$  V to  $+1.0$  V (scan rate =  $0.05$  V s<sup>-1</sup>).



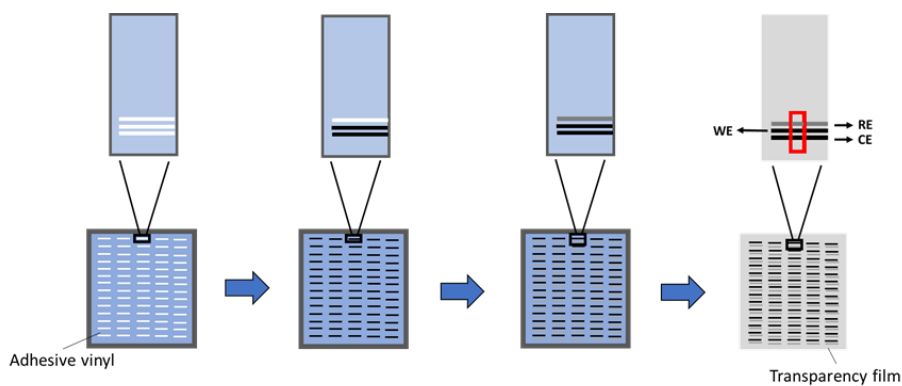


**Figure V.2.2.1.** Fabrication scheme of electrodes using screen - printing technology. Three-electrode system was screen-printed on the detection zone of transparency film substrate (6<sup>th</sup> layer) using carbon ink for working electrode (WE) and counter electrode (CE); and Ag/AgCl paste for reference electrode (RE).

### 2.3. Immunopurification procedure

Tf needed to be isolated from the rest of components when serum samples were analyzed using immunomagnetic beads. The synthesis of anti-transferrin-protein G-MBs (anti-Tf-MBs) was previously reported (50).

The immunopurification procedure was as follows: 1  $\mu\text{L}$  of anti-Tf-MBs were mixed with 100  $\mu\text{L}$  of serum sample in a microtube. This suspension was incubated for 45 min under soft shaking at 25  $^{\circ}\text{C}$ . Then the microtube was set on the magnet holding block (2 min) and the supernatant was removed. Tf-anti-Tf-MBs were washed twice with PBS pH 7.4 and, finally, resuspended in 20  $\mu\text{L}$  of PBS pH 7.0 and transferred into the device to be labeled with Os(VI) complex.

### 2.4. Device fabrication and operation

A capillary-driven microfluidics device was fabricated by laminating double-sided adhesive (DSA) and PET film as shown in **Figure V.2.2.2**. In this case, the device was composed of 9 layers of DSA and transparency film whose thickness is 50 and 100  $\mu\text{m}$ , respectively. All layer designs were devised using AutoCAD 2018 (Autodesk, Student Version) and cut with a desktop cutting plotter (Silhouette Cameo 3, Silhouette).

The device consists of four inlet channels (the two bottom inlets have 100  $\mu\text{m}$  height, while the two top inlets have 50  $\mu\text{m}$  height) that eventually connect to a main channel (100  $\mu\text{m}$  height and 3 mm width) (**Figure V.2.2.2 A**). As shown in the cross-sectional view (**Figure V.2.2.2 B**), each inlet channel was placed in a different vertical position to control the flow, and the main channel was formed between the top and bottom PET film layers.

**Figure V.2.2.2 C** shows all geometries of the transparency film and DSA layers for the microfluidics device. The device operation consists of the following steps:

- 1) 30  $\mu\text{L}$  of water was added in the upper left inlet (**a** in **Figure V.2.2.2 A**), filling the channel of 5<sup>th</sup> layer, until the valve area.

- 2) 20  $\mu\text{L}$  of different fluids was added in the lower left and right inlets (**b** and **c** in **Figure V.2.2.2 A**), filling channels of 3<sup>rd</sup> and 8<sup>th</sup> layers. Although these two fluids are pipetted at the same time, the speed of the flow through the inlet channel prevents both fluids arrive simultaneously, so one fluid arrives at the junction first. Air to be trapped within the channel and/or inconsistent flows may be caused by this difference in arrival times. To avoid these problems, the microfluidics device has a valve, which is called burst valve because it bursts only when the second fluid arrives (valve opening). So, the fluid that arrives first cannot continue to flow into the main channel, due to the junction (burst valve) formed in the middle layer. The fluid meniscus loses contact with the transparency surface on one side and it is only when second fluid reaches the junction and creates a combined meniscus in the main channel, that both fluids start flowing into the main channel.

- 3) There was an incubation time to allow the mix between fluids (labelling reaction) and the adsorption on the WE.

- 4) 90  $\mu\text{L}$  of buffer was added in the upper right inlet (**d** in **Figure V.2.2.2 A**). As all channels are filled, there is not flow by capillarity. So, a piece of paper (paper pump) is connected in the outlet to start the flow inside the microfluidics device, replacing the liquid in the channel of 5<sup>th</sup>

layer by buffer. Finally, this buffer, which acts as electrolyte, arrives to detection zone, and electrochemical detection is carried out.

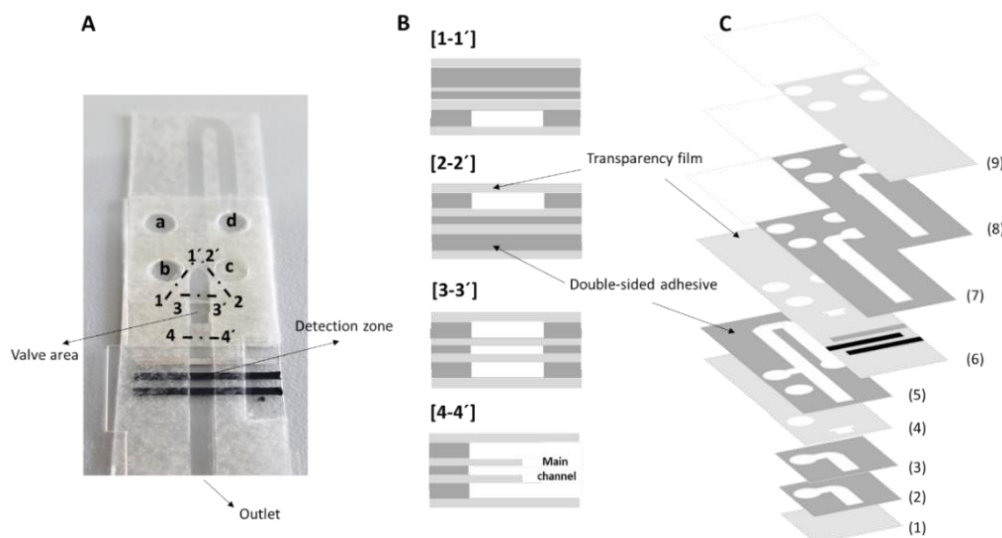


**Figure V.2.2.2.** Schematics of the microfluidics device. (A) The microfluidics electrochemical device consisted of four inlet channels, one main channel, a valve and three electrodes (detection zone). (B) Channels are placed in different vertical positions, as shown in the cross-sectional view of [1-1'], [2-2'], [3-3'] and [4-4']. (C) Channel geometries of the microfluidics device defined on each layer. 1, 4, 6 and 9 consist of transparency film (light grey) while layers 2, 3, 5, 7 and 8 are made of double-sided adhesive (dark grey).

### 2.5. Electrochemical measurements

The determination of Tf-Os(VI)TEMED was carried out employing adsorptive transfer square wave voltammetry (AdTSWV). In this case, the mixture of Tf and Os(VI) complex was incubated during 60 min and the analyte was adsorbed onto the WE. Next, the electrode was rinsed with water and then with 0.2 M BR buffer pH 3 (background electrolyte for electrochemical detection). Square wave voltammetry (SWV) parameters: start potential  $-1.2$  V, end potential  $+1.2$  V, frequency 100 Hz, amplitude 50 mV, and step potential 5 mV.

The calculation of EIG was carried out following the equation (1), in which the peak height of Os(VI) complex signal (at  $-0.9$  V) is divided by the peak height of amino acid residues (Cys, Trp, Tyr) signal (at  $+0.8$  V) (50).

$$(1) \quad \text{EIG} = \frac{\text{height of Os(VI)signal (at } -0.9\text{V)}}{\text{height of amino acid signal (at } 0.8\text{V)}}$$

### 3. Results and discussion

#### 3.1. Optimization of labeling and detection of transferrin inside the microfluidic device

A 30 mM Os(VI)O<sub>2</sub>(OH)<sub>2</sub>TEMED complex in 0.2 M sodium phosphate pH = 7.0 solution was used as labeling solution. It was prepared according to the bibliography (50,51). The proposed microfluidics device must not only perform the labeling of Tf with Os(VI) complex inside the main channel, but also it must carry out the electrochemical detection of Tf-Os(VI) adduct. Firstly, the main channel placed on the 5<sup>th</sup> layer was filled with water (30  $\mu$ L was added to the upper left reservoir) (**Figure V.2.2.3 A a**). Then, Tf and Os(VI)O<sub>2</sub>(OH)<sub>2</sub>TEMED complex solutions were added (20  $\mu$ L) to reservoirs (see **Figure V.2.2.3 A b** and **c**) and arrived at the valve, which is formed downstream the junction of three microfluidics channels. With this valve, the fluids enter the main channel at the same time to ensure mixing as shown previously (33). Once this happens, the three fluids (water, Tf and Os(VI) complex solutions) flow to the main channel outlet. At this point, the labeling reaction began (Tf-Os(VI) adduct formation), so an incubation period was required. When the Tf-Os(VI) adduct arrived at the detection zone, it was adsorbed onto the working electrode.

Finally, BR buffer (90  $\mu$ L) was added at the upper right reservoir and the paper pump was connected to restart the flow inside the microfluidics device (**Figure V.2.2.3 A d**). The mixed solution begins to flow, followed by water and BR buffer, sequentially (**Figure V.2.2.3 A e**). When this buffer, which acts as the electrolyte for electrochemical measurements, fills the detection zone, the paper pump was removed to stop flow and the electrochemical measurement performed with the optimized reaction times.

The non-reacted Os(VI)O<sub>2</sub>(OH)<sub>2</sub>TEMED complex is removed by a washing step (water) and only adsorbed protein was measured by AdTSWV.

First, the new approach for labeling and detecting Tf inside the devices was evaluated. **Figure V.2.2.3 B** shows voltammograms of BR buffer (black line), Os(VI) complex (green line), Tf (blue line) and Tf-Os(VI) (red line). Clearly, two peaks at  $-0.90$  V (peak 1) and  $+0.8$  V (peak 2) were observed when Tf was labelled with the Os(VI)TEMED complex. These same peaks, were not found for the Os(VI) complex or the blank (buffer). First correspond to the Tf-Os (VI) signal, while the second correspond to the oxidation of electroactive amino acid (Cys, Trp, Tyr) from Tf. In the native glycoprotein, there is only the peak at  $+0.8$  V. These results demonstrate that this new methodology is valid for labeling and detecting Tf.

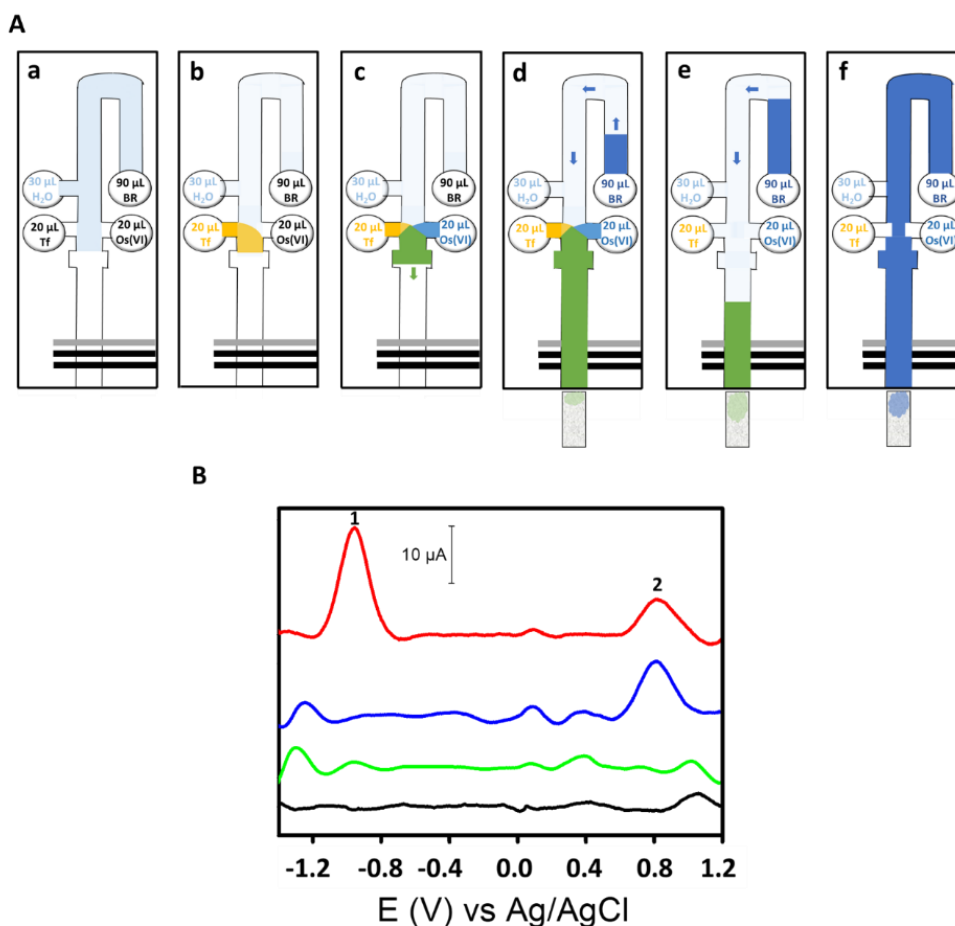


**Figure V.2.2.3.** (A) Sequential steps showing the moments of: (a) water injecting, (b) Tf flows first and stops at the valve, (c)  $\text{Os(VI)}$  complex arrives and valve release and producing the mix in the main channel, (d) and (e) flow starts when rectangular-shaped paper was put in outlet part, and (f) BR buffer arrive at the main channel. (B) Voltammograms obtained using AdTSWV with 60 min incubation time for 0.2 M BR buffer at pH 3.0 (blank) (black line), 7.58 mM  $\text{Os(VI)}$  complex (control) (green line), 9.4  $\text{mg mL}^{-1}$  Tf (blue line) and 9.4  $\text{mg mL}^{-1}$  Tf- $\text{Os(VI)}$  (red line). Peak 1: Tf- $\text{Os(VI)}$ . Peak 2: amino acids residues. SWV parameters: start potential  $-1.2$  V, end potential  $+1.2$  V, frequency 100 Hz, amplitude 50 mV. and step potential 5 mV (the background signal was linearized).

As mentioned before, an incubation time was required for labeling and adsorption of adduct Tf- $\text{Os(VI)}$  complex, as key parameter. In this case, 9.4  $\text{mg mL}^{-1}$  Tf- $\text{Os(VI)}$  was measured by AdTSWV using different incubation times (from 5 to 120 min) (Figure V.2.2.S1 in Electronic Supplementary Material, ESM). As is shown in Figure V.2.2.S1, between 5 and 60 min,

longer times increased signal, indicating that more Tf was labeled with the Os(VI) complex and absorbed onto the WE. However, after 60 min the signal does not increase as the adsorption time increases, indicating that at 60 min the maximum of Tf labeled with Os(VI) complex was achieved. For this reason, 60 min was selected as the best incubation time and used in the following experiments. In our previous work (50), the labeling of transferrin with Os(VI) complex to carry out the EIG measurements involved a time of 16 hours, besides this step was not integrated into the analytical device.

### 3.2. Analytical performance of the method for EIG determination

Once the methodology was proven to be valid for labeling and detecting inside the microfluidics device, the electrochemical sensor was evaluated for Tf determination. First, the method calibration was performed for Tf-Os(VI)TEMED adduct using both peaks (peak 1 at -0.9 and peak 2 at +0.8 V). Good linear correlation coefficient was obtained for both peaks (peak 1,  $r = 0.980$ ; and peak 2,  $r = 0.990$ , respectively) in the concentration range assayed (from  $3.8 \text{ mg mL}^{-1}$  to  $11.6 \text{ mg mL}^{-1}$ ). The calibration curve slopes were  $(1.4 \pm 0.1) \mu\text{A mL mg}^{-1}$  for the peak at -0.9 V and  $(0.35 \pm 0.02) \mu\text{A mL mg}^{-1}$  for the peak at +0.8 V, and the intercepts were  $(-1.6 \pm 0.9) \mu\text{A}$  and  $(-0.4 \pm 0.2) \mu\text{A}$ , respectively ( $n = 3$ ) (**Figure V.2.2.4**). The limits of detection (LOD) were  $2.04 \text{ mg mL}^{-1}$  and  $1.56 \text{ mg mL}^{-1}$  (3Sa criterion, where Sa is the standard deviation of intercept). The concentration of Tf in serum from healthy humans ranged between  $2.1$  and  $3.7 \text{ mg mL}^{-1}$ , so this method is suitable (52).

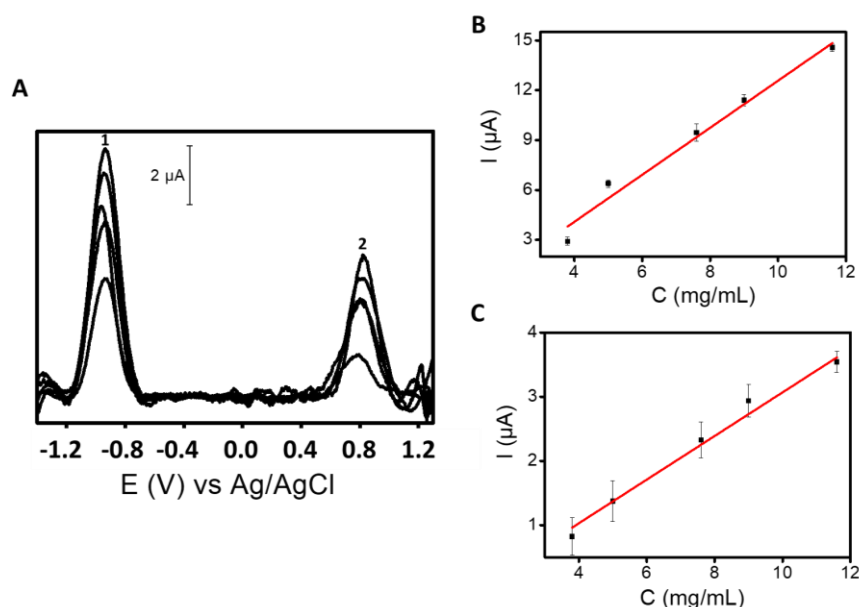


**Figure V.2.2.4.** (A) Voltammograms corresponding to Tf-Os(VI) at different concentrations using the pump-free microfluidics device (the background signal was linearized). (B) Calibration curve for peak 1 (−0.9 V). (C) Calibration curve for peak 2 (+0.8 V). Conditions: as in **Figure V.2.2.3 B**.

As it was previously demonstrated (50), the greater the amount of glycans in Tf, the higher the number of Os (VI) complex molecules bound to Tf. This allowed us to propose a new approach to measure the level of CDT, based on the ratio generated by the relation between Os (VI) signal and protein signal (EIG). This parameter must be constant because it only depends on the glycosylation of Tf and not on the concentration. Only under some pathological states such as CDG, the glycosylation of Tf is lower so that, in these cases, the Os (VI) signal decreases and, in consequence, the EIG parameter too.

### 3.3. Application to diagnosis of CDG I in serum samples

When analyzing serum samples, an immunopurification process is necessary to isolate Tf from the rest of components in the sample (see **Section 2.3**). In this step, Tf was captured by anti-Tf-MBs, resuspended in 20 μL PBS pH 7.0 and, finally, transferred into the device to be labeled with Os(VI) complex. However, antibodies are glycoproteins that have a group of



carbohydrates to which the Os(VI) complex could bind and increase the signal.

For this reason, it is necessary to perform a control experiment in which, the magnetic particles with the Tf antibody, without Tf, were transferred into the device and labeled with Os(VI) complex with 60 min of incubation time.

As can be seen in **Figure V.2.2.S2 A**, the signal obtained for the concentration used for antibody is negligible (represents less than 2 % of the signal) compared to the signal obtained by Tf-Os(VI)TEMED adduct. So, it is possible to use these magnetic beads in the immunoassay. However, it was necessary to use a magnet to lead them to the detection zone and to prevent their deposition on the reservoir and main channel bottom (in **Figure V.2.2.S2 B**)

Finally, the methodology was tested in serum samples using this microfluidics device as electrochemical sensor for CDG diagnosis. Firstly, commercial serum was analyzed as a control sample. Next, a serum sample from CDG-I patient was analyzed (**Figure V.2.2.5**). **Table V.2.2.1** shows the main results obtained. Using a t-test at 95% confidence level ( $P \leq 0.05$ ), it was found significant differences between the control sample and CDG sample, demonstrating that with this approach it was possible to distinguish between healthy people and CDG I patients.

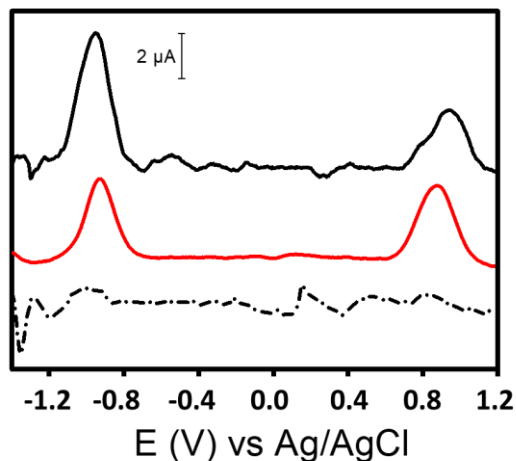


**Figure V.2.2.5.** Voltammograms obtained by AdTSWV in different samples using the pump-free microfluidics device (the background signal was linearized): BR buffer at pH 3.0 (blank) (dot line), CDG sample (red line) and control serum (black line). Other conditions as in **Figure V.2.2.3 B**.

**Table V.2.2.1.** Comparison between EIG values obtained in control sample and CDG sample (n = 3).

	Control serum	CDG-I sample
<b>EIG ± standard deviation</b>	2.58 ± 0.4	1.13 ± 0.2

### 4. Conclusions

A low-cost and passive electrochemical microfluidics device has been fabricated by lamination method and it was applied to measure the glycosylation degree of Tf (EIG). This device enables performance of several assay steps with minimal user intervention: transferrin labeling with Os(VI) complex, washing, and electrochemical detection. Moreover, the microfluidics approach enables to reduce the labelling reaction time (60 min) respect previous reported works (16 h).

The microfluidics device was applied to analyze serum samples using immunomagnetic beads for Tf isolation. The approach enabled to discriminate between serum samples from healthy person and from CDG patients, being a further step towards the creation of a truly POCT device for CDG diagnosis.

### Acknowledgments

This work has been financially supported by the TRANSNANOAVANSENS program from the Community of Madrid (S2018/NMT-4349), Spanish Ministry of Economy, Industry and Competitiveness (CTQ2017-86441-C2-1-R), MINECO (MAT2016-80394-R), Independent Thinking-Jóvenes Investigadores program from UNED (BICI, n° 34, 17/06/2019) and the Universidad de Alcalá [FPI fellowship (T.S)]. We are grateful for the donation of CDG sample by Centro de Diagnostico de Enfermedades Moleculares (CEDEM, Madrid, Spain). CSH was supported through grants from the National Institutes of Health (R21EBEB030349) and the National Science Foundation (CHE-1710222).

### Associated content

#### Supporting Information

**Figure V.2.2.S1.** Voltammograms of  $9.4 \text{ mg mL}^{-1}$  Tf-Os(VI) by AdTSWV using different incubation times. **(a)** 5 min; **(b)** 10 min; **(c)** 20min; **(d)** 40 min; **(e)** 60 min; **(f)** 90 min; **(g)** 120 min. SWV parameters: start potential -1.2 V, end potential +1.2 V, step potential 5 mV, amplitude 50 mV, and frequency 100 Hz (the background signal was linearized).

**Figure V.2.2.S2.** **(A)** Voltammograms obtained by AdTSWV with 60 min incubation time for 0.2 M BR buffer at pH 3.0 (blank) (black line), antiTf-MB-Os(VI) (control) (blue line) and  $9.4 \text{ mg mL}^{-1}$  Tf-antiTf-MB-Os(VI) (red line) (the background signal was linearized). **(B)** The microfluidics analytical device with antiTf-MBs deposited on the reservoir and main channel bottom (no magnet).

### Author information

#### Corresponding Authors

Alberto Escarpa – Department of Analytical Chemistry, Physical Chemistry and Chemical Engineering, University of Alcalá, Madrid, Spain. Chemical Research Institute “Andrés M. del Río” (IQAR), University of Alcalá, Madrid, Spain; [orcid.org/0000-0002-7302-0948](https://orcid.org/0000-0002-7302-0948); Email: [alberto.escarpa@uah.es](mailto:alberto.escarpa@uah.es)

Agustín G. Crevillen – Department of Analytical Sciences, Faculty of Sciences, Universidad Nacional de Educación a Distancia (UNED), Madrid, Spain; Email: [agustingcrevillen@ccia.uned.es](mailto:agustingcrevillen@ccia.uned.es)

#### Other Authors

Tania Sierra - Department of Analytical Chemistry, Physical Chemistry and Chemical Engineering, University of Alcalá, Madrid, Spain.

Charles S. Henry - Department of Chemistry, Colorado State University, Fort Collins, CO, USA.

### Authors Contribution

The manuscript was written through contributions of all the authors. All the authors have given approval to the final version of the manuscript.

## Supporting Information

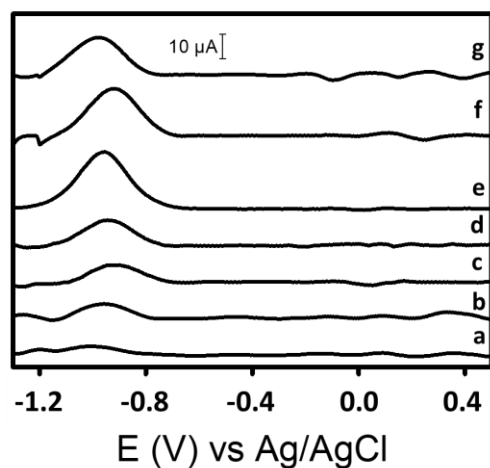


**Figure V.2.2.S1.** Voltammograms of  $9.4 \text{ mg mL}^{-1}$  Tf-Os(VI) by AdTSWV using different incubation times. (a) 5 min; (b) 10 min; (c) 20 min; (d) 40 min; (e) 60 min; (f) 90 min; (g) 120 min. SWV parameters: start potential  $-1.2 \text{ V}$ , end potential  $+1.2 \text{ V}$ , step potential  $5 \text{ mV}$ , amplitude  $50 \text{ mV}$ , and frequency  $100 \text{ Hz}$  (the background signal was linearized).

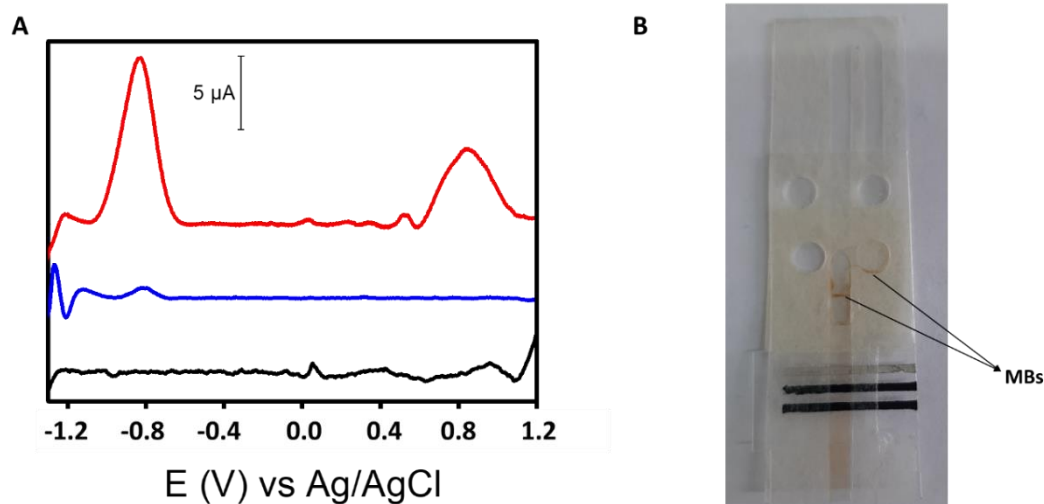


**Figure V.2.2.S2.** (A) Voltammograms obtained by AdTSWV with 60 min incubation time for  $0.2 \text{ M}$  BR buffer at  $\text{pH } 3.0$  (blank) (black line), antiTf-MB-Os(VI) (control) (blue line) and  $9.4 \text{ mg mL}^{-1}$  Tf-antiTf-MB-Os(VI) (red line) (the background signal was linearized). Conditions: as in **Figure V.2.2.S1**. (B) The microfluidics analytical device with antiTf-MBs deposited on the reservoir and main channel bottom (no magnet).

### References

1. Hernandez-Rodriguez JF, Rojas D, Escarpa A. Electrochemical Sensing Directions for Next-Generation Healthcare: Trends, Challenges, and Frontiers. *Anal Chem.* **2021**, 93, 167–183.
2. John AS, Price CP. Existing and Emerging Technologies for Point-of-Care Testing. *Clin Biochem Rev.* **2014**, 35, 155–167.
3. Song Q, Sun X, Dai Z, Gao Y, Gong X, Zhou B, Wu J, Wen W. Point-of-care testing detection methods for COVID-19. *Lab Chip.* **2021**, 21, 1634–1660.
4. Dohla M, Boesecke C, Schulte B, Diegmann C, Sib E, Richter E, Eschbach-Bludau M, Aldabbagh S, Marx B, Eis-Hübinger AM, Schimithausen RM, Streeck H. Rapid point-of-care testing for SARS-CoV-2 in a community screening setting shows low sensitivity. *Public Health.* **2020**, 182, 170–172.
5. Jung W, Han J, Choi J, Ahn CH. Point-of-care testing (POCT) diagnostic systems using microfluidic lab-on-a-chip technologies. *Microelectron Eng.* **2015**, 132, 46–57.
6. Nichols JH. Point-of-care testing. Contemporary Practice in Clinical Chemistry. *INC.* **2020**, 323–336.
7. Shrivastava S, Trung TQ, Lee N. Recent progress, challenges, and prospects of fully integrated mobile and wearable point-of-care testing systems for self-testing. *Chem Soc Rev.* **2020**, 49, 1812–1866.
8. Abel G. Current status and future prospects of point-of-care testing around the globe. *Expert Rev Mol Diagn.* **2015**, 15, 853–855.
9. Park J, Han DH, Park J. Towards practical sample preparation in point-of-care testing: user-friendly microfluidic. *Lab Chip.* **2020**, 20, 1191.
10. Khan RS, Khurshid Z. Advancing Point-of-Care (PoC) Testing Using Human Saliva as Liquid Biopsy. *Diagnostics.* **2017**, 7, 39.
11. Vashist SK, Lippa PB, Yeo LY, Ozcan A, Luong JHT. Emerging Technologies for Next-Generation Point-of-Care testing. *Trends Biotechnol.* **2015**, 33, 692–705.
12. Liu J, Geng Z, Fan Z, Liu J, Chen H. Point-of-care testing based on smartphone: The current state-of-the-art (2017–2018). *Biosens Bioelectron.* **2019**, 132, 17–37.
13. Lippa PB, Bietenbeck A, Beaudoin C, Giannetti A. Clinically relevant analytical techniques, organizational concepts for application and future perspectives of point-of-care testing. *Biotechnology Adv.* **2016**, 34, 139–160.
14. Kosack C, Page A, Klatser P. A guide to aid the selection of diagnostic test. *Bull World Heal Organ.* **2017**, 95, 639–645.
15. Yang J, Wang K, Xu H, Yan W, Jin Q, Cui D. Detection platforms for point-of-care testing based on colorimetric, luminescent, and magnetic assays: A review. *Talanta.* **2019**, 202, 96–110.
16. Noah NM, Ndongili PM. Current Trends of Nanobiosensors for Point-of-Care Diagnostics. *J Anal Methods Chem.* **2019**, 2019, 1–16.
17. Chen H, Liu K, Li Z, Wang P. Point of care testing for infectious diseases. *Clin Chim Acta.* **2019**, 493, 138–147.

18. Dincer C, Bruch R, Kling A, Dittrich S, Urban GA. Multiplexed Point-of-Care Testing – xPOCT. *Trends Biotechnol.* **2017**, 35, 728–742.
19. Coleman B, Coarsey C, Kabir M, Asghar W. Point-of-care colorimetric analysis through smartphone video. *Sensors Actuators B Chem.* **2019**, 282, 225–231.
20. Coleman B, Coarsey C, Asghar W. Cell phone based colorimetric analysis for point-of-care settings. *Analyst.* **2019**, 144, 1935–1947.
21. Gao H, Wen L, Tian J, Wu Y, Liu F, Lin Y, Hua W, Wu G. A portable electrochemical immunosensor for highly sensitive point-of-care testing of genetically modified crops. *Biosens Bioelectron.* **2019**, 142, 111504.
22. Dai Y, Liu CC. Recent Advances on Electrochemical Biosensing Strategies toward Universal Point-of-Care Systems. *Angew Chem.* **2019**, 131, 12483–12496.
23. Li Y, He R, Niu Y, Li F. Paper-Based Electrochemical Biosensors for Point-of-Care Testing of Neurotransmitters. *J Anal Test.* **2019**, 3, 19–36.
24. Fallahi H, Zhang J, Phan H, Nguyen N. Flexible Microfluidics: Fundamentals, Recent Developments, and Applications. *Micromachines.* **2019**, 10, 830.
25. Chaudhuri P, Warkiani M, Jing T, Kenry, Lim C. Microfluidics for Research and Applications in Oncology. *Analyst.* **2016**, 141, 504–524.
26. Dong R, Liu Y, Mou L, Deng J, Jiang X. Microfluidics-Based Biomaterials and Biodevices. *Adv Mater.* **2019**, 31, 1805033.
27. Nasserri B, Soleimani N, Rabiee N, Kalbasi A, Karimi M, Hamblin MR. Point-of-care microfluidic devices for pathogen detection. *Biosens Bioelectron.* **2018**, 117, 112–128.
28. Chen C, Mehl BT, Munshi AS, Townsend AD, Spence DM, Martin RS. 3D-printed microfluidic devices: fabrication, advantages, and limitations—a mini review. *Anal Methods.* **2016**, 8, 6005–6012.
29. Islam M, Natu R, Martinez-Duarte R. A study on the limits and advantages of using a desktop cutter plotter to fabricate microfluidic networks. *Microfluid Nanofluidics.* **2015**, 19, 973–985.
30. Lee C, Wang W, Liu C, Fu L. Passive mixers in microfluidic systems: A review. *Chem Eng J.* **2016**, 288, 146–160.
31. Wu J, Tomsa D, Zhang M, Komenda P, Tangri N, Rigatto C, Lin F. A Passive Mixing Microfluidic Urinary Albumin Chip for Chronic Kidney Disease Assessment. *ACS Sensors.* **2018**, 3, 2191–2197.
32. Narayanamurthy V, Jeroish ZE, Bhuvaneshwari KS, Bayat P, Premkumar R, Samsuri F, Yusoff MM. Advances in passively driven microfluidics and lab-on-chip devices: a comprehensive literature review and patent analysis. *RSC Adv.* **2020**, 10, 11652–11680.
33. Jang I, Kang H, Song S, Dandy DS, Geiss BJ, Henry CS. Flow control in a laminate capillary-driven microfluidic device. *Analyst.* **2021**, 146, 1932–1939.
34. Huang PH, Nama N, Mao Z, Li P, Rufo J, Chen Y, Xie Y, Wei CH, Wang L, Huang TJ. A reliable and program mable acoustofluidic pump powered by oscillating sharp-edge structures. *Lab Chip.* **2014**, 14, 4319.

35. Byun CK, Abi-Samra K, Cho Y, Takayama S. Pumps for microfluidic cell culture. *Electrophoresis*. **2014**, 35, 245–257.
36. Xu L, Wang A, Li X, Oh KW. Passive micropumping in microfluidics for point-of-care testing. *Biomicrofluidics*. **2020**, 14, 031503.
37. Jang I, Carrao D, Menger R, Rodrigo A, Oliveira M De, Henry CS. Pump-Free Microfluidic Rapid Mixer Combined with a Paper-Based Channel. *ACS Sensors*. **2020**, 5, 2230–2238.
38. Kailemia MJ, Park D, Lebrilla CB. Glycans and glycoproteins as specific biomarkers for cancer. *Anal Bioanal Chem*. **2017**, 409, 395–410.
39. Connelly MA, Gruppen EG, Otvos JD, Dullaart RPF. Inflammatory glycoproteins in cardiometabolic disorders, autoimmune diseases, and cancer. *Clin Chim Acta*. **2016**, 459, 177–186.
40. Chang IJ, He M, Lam CT. Congenital disorders of glycosylation. *Ann Transl Med*. **2018**, 6, 1–13.
41. Verheijen J, Tahata S, Kozicz T, Witters P, Morava E. Therapeutic approaches in Congenital Disorders of Glycosylation (CDG) involving N-linked glycosylation: an update. *Genet Med*. **2020**, 22, 268–279.
42. Scherpenzeel M Van, Willems E, Lefeber DJ. Clinical diagnostics and therapy monitoring in the congenital disorders of glycosylation. *Glycoconj J*. **2016**, 33, 345–358.
43. Wolthuis DFGJ, Janssen MC, Cassiman D, Lefeber DJ, Morava-Kozicz E. Defining the phenotype and diagnostic considerations in adults with congenital disorders of N-linked glycosylation. *Expert Rev Mol Diagn*. **2014**, 14, 217–224.
44. Teneiji A Al, Bruun TUJ, Sidky S, Cordeiro D, Cohn RD, Mendoza-Londono R, Moharir M, Raiman J, Siriwardena K, Kyriakopoulou L, Mercimek-Mahmutoglu S. Phenotypic and genotypic spectrum of congenital disorders of glycosylation type I and type II. *Mol Genet Metab*. **2017**, 120, 235–242.
45. Bortolotti F, Sorio D, Bertaso A, Tagliaro F. Analytical and diagnostic aspects of carbohydrate deficient transferrin (CDT): A critical review over years 2007 – 2017. *J Pharm Biomed Anal*. **2018**, 147, 2–12.
46. Ordonez YN, Anton F, Davis WC. Quantification of total serum transferrin and transferrin sialoforms in human serum; an alternative method for the determination of carbohydrate-deficient transferrin in clinical samples. *Anal Methods*. **2014**, 6, 3967–3974.
47. Chen J, Li X, Edmondson A, Meyers GD, Izumi K, Ackermann AM, Morava E, Ficicioglu C, Bennett MJ, He M. Increased Clinical Sensitivity and Specificity of Plasma Protein N -Glycan Profiling for Diagnosing Congenital Disorders of Glycosylation by Use of Flow Injection – Electrospray Ionization – Quadrupole Time-of-Flight Mass Spectrometry. *Clin Chem*. **2019**, 663, 653–663.
48. Dave MB, Dherai AJ, Udani VP, Hegde AU, Desai NA, Ashavaid TF. Comparison of transferrin isoform analysis by capillary electrophoresis and HPLC for screening congenital disorders of glycosylation. *J Clin Lab Anal*. **2018**, 32, 1–8.



49. Yoo G, Kim J, Joon K, Lee YL. The characteristics of transferrin variants by carbohydrate- deficient transferrin tests using capillary zone electrophoresis. *J Clin Lab Anal.* **2018**, 32, 1–4.
50. Sierra T, Crevillen AG, Escarpa A. Electrochemical sensor for the assessment of carbohydrate deficient transferrin: Application to diagnosis of congenital disorders of glycosilation. *Biosens Bioelectron.* **2021**, 179, 113098.
51. Trefulka M, Paleček E. Voltammetry of Os(VI)-modified polysaccharides at carbon electrodes. *Electroanalysis.* **2009**, 21, 1763–1766.
52. M.A. Connelly, E. G. Gruppen, J.D. Otvos, R. P. F. Inflammatory glycoproteins in cardiometabolic disorders, autoimmune diseases and cancer. *Clin. Chim. Acta.* **2016**, 459, 177-186.





# CHAPTER VI

**General  
conclusions**



## VI. General conclusions

The suitability of electrochemical detection coupled to different point-of-care testing approaches (electrochemical sensors screen-printed based, microchip electrophoresis, and capillary-driven electrochemical microfluidics devices) in the field of disease diagnosis based on glycoprotein biomarkers, has been revealed from this Doctoral Thesis.

The main objective of this Doctoral Thesis has been reached. On one hand, several methodologies for the determination of glycoprotein biomarkers related with important diseases have been proposed, trying to satisfy a medical and social demand such as early diagnosis. On the other hand, new miniaturized analytical technologies, and their potential to fulfill this demand were explored. These technologies have in common their potential miniaturization, automatization, portability, and easy-to-use, therefore they meet the POCT requirements.

The electrochemical detection has constituted the basis of the methodologies developed in this Doctoral Thesis. In this sense, the use of six-valent osmium complex was the decisive step to be able to carry out the measurements of these glycoprotein biomarkers.

Firstly, electrochemical sensors based on screen-printed electrodes (SPEs) were developed for the individual determination of two glycoprotein biomarkers:  $\alpha_1$ -acid glycoprotein (AGP) level and carbohydrate deficient transferrin (CDT). The results demonstrated their suitability for fast, sensitive, and accurate determination of both biomarkers in serum samples.

Microfluidics technology since it allowed the integration of additional steps required to perform the analysis. In this aspect, firstly, microchip electrophoresis in combination with electrochemical detection (ME-ED) was used for the separation and detection of AGP and Tf using a single-channel glass microchip with a screen-printed carbon electrode (SPCE).

Secondly, capillary-driven microfluidics devices were developed. These devices were composed of multiple layers made by different materials including double-sided adhesive (DSA) and transparent plastic. The proper design of these layers provided device with multiple channels and microfluidics components (reservoirs, valves...), which allows to carry out all the necessary steps inside the device (labeling, washing, and detection) for the electrochemical determination of the AGP and Tf. No external pump was needed.

These electrochemical microfluidics systems allowed to perform fast and accurate analysis using very low sample and reagents and minimizing human intervention, making them valuable devices for POCT.

Overall, it can be concluded that these miniaturized, portable, and potentially automatable approaches proved to be an added value to the analytical performance of routine glycoprotein biomarkers analysis. The additional analytical benefits such as simplicity, minimal use of reagents and samples, speed, and cost reduction, make them serious candidates for POCT, so we envision their use in the doctor's office or at patient's bedside in the near future.

Once these reflections have been made, it has been considered appropriate to summarize the main conclusions of each chapter:

1. A simple and cheap electrochemical method (AdTSWV) has demonstrated to be useful for the determination of AGP in serum samples using an electrochemical sensor screen-printed based. The use of Os(VI) complexes as electrochemical tags was fundamental for glycoprotein sensing in terms of sensitivity and selectivity. The advantages of SPCE technology such as low sample consumption, low-cost, and portability make this methodology very attractive in point-of-care testing field. These benefits were achieved without detriment to other analytical characteristics, where an adequate accuracy (recovery 81 %) and a good sensitivity (LOD = 1.6 mg L<sup>-1</sup>) were obtained.

**2.** The use of multi-walled carbon nanotubes scaffold films (MWSFs) as electroodic material for AGP determination allowed us to improve the sensitivity ( $\text{LOD} = 0.6 \text{ mg L}^{-1}$ ) and reproducibility ( $\text{RSD} < 1 \%$ ) of the aforementioned sensor. This is due to the high active surface and high fouling resistance of this carbon nanomaterial. MWSFs become a disposable electroanalytical tool for the determination of complex molecules such as glycoproteins. In addition, the time of labelling reaction with Os(VI) complex was dramatically reduced to 15 min by an exchange ligand step, opening the door for future clinical and POCT applications.

**3.** The disposable screen-printed based electrochemical sensor combined with immunomagnetic beads has demonstrated to be successful in the measurement of carbohydrate deficient transferrin (CDT) in clinical samples. Two voltammetric signals were generated in the sensor by tagged transferrin: one was due to the carbohydrate part (Os(VI) complex) ( $E_{\text{Os(VI) complex}} = -0.9 \text{ V/Ag}$ ) and the second was due to the protein part (electroactive amino acids from transferrin) ( $E_{\text{amino acids}} = +0.8 \text{ V/Ag}$ ). The ratio between both signals (carbohydrate signal/protein signal), called “electrochemical index of glycosylation (EIG)”, showed excellent correlation ( $R = 0.990$ ) with the official parameter % CDT. Furthermore, its applicability has been assessed through the analysis of serum samples from congenital disorders of glycosylation (CDG) patients, getting satisfactory results and being able to discriminate between healthy and CDG patients.

**4.** The simultaneous determination of two glycoproteins (AGP and Tf) in serum samples was achieved in less than 400 s by microchip electrophoresis with electrochemical detection. Furthermore, the use of Os(VI) complex tag allowed us to set a selective detection potential at  $+0.50 \text{ V/Ag}$ . At this potential, the synthesized glycoprotein-Os(VI) adducts yielded an anodic signal, but not the rest of proteins, avoiding their interference. The approach showed an excellent accuracy ( $E_r \leq 4 \%$ ) in the analysis of a certified human serum reference material.



5. A pump-free microfluidics device, which was fabricated by a lamination method, has demonstrated to be successful in the electrochemical detection of AGP. The microfluidics device uses capillary-driven flow and a passive mixing system to label the AGP with Os(VI) complex inside the main channel. So, all steps necessary for the determination of AGP (labeling with Os(VI) complex, washing with water, and electrochemical detection) were successfully carried out in 30 min inside the microfluidics device without an external pumping system. The optimized method showed a good linear correlation ( $R^2 = 0.990$ ) and an acceptable limit of detection ( $LOD = 231 \text{ mg L}^{-1}$ ). The feasibility of this approach for the determination of AGP in commercial serum samples was demonstrated.

6. Using the aforementioned approach, a low-cost and passive microfluidics device was successfully developed for the diagnosis of CDG. Tf was isolated from serum samples by using immunomagnetic beads and then, it was analyzed in the microfluidics device, assessing its EIG, which is indicator of the degree of glycosylation and its potential utility for CDG diagnosis was previously reported by us. The overall methodology took about 60 min with minimal analyst intervention, requiring low volume of sample (100  $\mu\text{L}$ ) and reagents. Finally, it was able to discriminate between serum samples from a healthy person and those from CDG patients.





# CHAPTER VII

## **Appendices**



---

## VII. Appendices

### Acronyms

<b>AdTSWV</b>	Adsorptive transfer stripping square wave voltammetry
<b>AGP</b>	$\alpha_1$ -acid glycoprotein
<b>BR</b>	Britton-Robinson buffer
<b>CDG</b>	Congenital disorders of glycosylation
<b>CDT</b>	Carbohydrate deficient transferrin
<b>CE</b>	Capillary electrophoresis
<b>CE</b>	Counter electrode
<b>CRP</b>	C-Reactive protein
<b>CVD</b>	Cardiovascular disease
<b>CNM</b>	Carbon nanomaterial
<b>CNSF</b>	Carbon nanotube scaffold film
<b>CNT</b>	Carbon nanotubes
<b>DSA</b>	Double-sided adhesive
<b>ED</b>	Electrochemical detection
<b>EIG</b>	Electrochemical index of glycosylation
<b>EIS</b>	Electrochemical impedance spectroscopy
<b>ER</b>	Endoplasmic reticulum
<b>FDA</b>	Food and Drug Administration
<b>HPLC</b>	High-performance liquid chromatography
<b>LAC</b>	Lectin affinity chromatography
<b>LC</b>	Liquid chromatography
<b>LIF</b>	Laser-induced fluorescence detection

<b>LOC</b>	Lab-on-a-chip
<b>LOD</b>	Limit of detection
<b>LOQ</b>	Limit of quantification
<b>MB</b>	Magnetic beads
<b>ME</b>	Microchip electrophoresis
<b>MS</b>	Mass spectrometry
<b>MWCNTs</b>	Multi-walled carbon nanotubes
<b>MWSF</b>	Multi-walled scaffold film
<b>Os</b>	Osmium
<b>ePAD</b>	Paper-based electrochemical device
<b>μPAD</b>	Microfluidics paper-based analytical device
<b>pI</b>	Isoelectric point
<b>PNGase F</b>	N-glycosidase F
<b>POCT</b>	Point-of-care testing
<b>PTMs</b>	Post-translational modifications
<b>Py</b>	Pyridine
<b>RE</b>	Reference electrode
<b>SPEs</b>	Screen-printed electrodes
<b>SPCEs</b>	Screen-printed carbon electrodes
<b>SWCNTs</b>	Single-walled carbon nanotubes
<b>SWSF</b>	Single-walled scaffold film
<b>Tf</b>	Transferrin
<b>Trp</b>	Tryptophan
<b>Tyr</b>	Tyrosine
<b>TEMED</b>	N,N,N',N'-tetramethylethylenediamine
<b>WE</b>	Working electrode
<b>WHO</b>	World Health Organization

# List of figures

## Chapter I

<b>Scheme I.1.</b>	Schematics to achieve the central objective of this Doctoral Thesis	7
--------------------	---	---

## Chapter II

<b>Figure II.1.1.</b>	Different protein post-translational modifications	12
<b>Figure II.1.2.</b>	Summary of the top experimental Post-Translational Modification	12
<b>Figure II.1.3.</b>	Different types of glycoproteins	13
<b>Figure II.1.4.</b>	Glycoconjugate biosynthesis process and cell surface recognition	14
<b>Figure II.1.5.</b>	Crystal structure of human AGP at 1.8 Å resolution	22
<b>Figure II.1.6.</b>	Crystal structure of transferrin	23
<b>Figure II.1.7.</b>	Different isoforms of transferrin	25
<b>Figure II.2.1.</b>	Schematic representation showing mechanism of glycan release from proteins of N-glycans by PNGase F	30
<b>Figure II.2.2.</b>	Schematic showing the most common types of electrochemical biosensors for glycan analysis: (A) electron impedance spectroscopy-(EIS) based assay; (B) a lectin biosensor sandwich assay; (C) surface cell carbohydrate assay using a binding lectin/enzyme conjugate to provide the electrochemical signature	35
<b>Figure II.2.3.</b>	Schemes of electrochemical oxidation of tyrosine (Tyr) and tryptophan (Trp)	38
<b>Figure II.2.4.</b>	Reactions of electrochemical derivatization reagents with amino acids	39
<b>Figure II.2.5.</b>	Reaction of electrochemical derivatization reagents with proteins (A) and glycoproteins (B)	40
<b>Figure II.2.6.</b>	Types of nanomaterials depending on their geometric shape (A) nanoparticles; (B) nanowires; (C) nanotubes; (D) nanorods	45
<b>Figure II.2.7.</b>	Types of carbon nanotubes (A) SWCNT; (B) MWCNT	45
<b>Figure II.2.8.</b>	Ven diagram: electrochemistry, biosensors, and microfluidics (A) electrochemistry & microfluidics; (B) electrochemical biosensing; (C) microfluidics biosensing; (D) microfluidics electrochemical biosensing	53



## Chapter III

<b>Figure III.1.1.</b>	(A) Manufacturing process of SPEs. (B) Commercial SPEs used for microchip electrophoresis in this Thesis. (C) Commercial SPEs with working, counter and reference electrodes and minimal cell volume (50 $\mu$ L)	73
<b>Figure III.1.2.</b>	Strategy to make carbon nanotubes scaffold films (CNSFs)	75
<b>Figure III.1.3.</b>	Analysis by the AdTSV technique using a SPEs	76

### III.2.1. Article 1: Total $\alpha_1$ -acid glycoprotein determination in serum samples using disposable screen-printed electrodes and osmium (VI) as electrochemical tag

<b>Figure III.2.1.1.</b>	Cyclic voltammogram of 10 mM Os(VI)O <sub>2</sub> (OH) <sub>2</sub> TEMED complex in 50 mM phosphate buffer pH 7. Scan rate 1 V/s	88
<b>Figure III.2.1.2.</b>	Voltammograms obtained by AdTSWV of 50 mM phosphate buffer at pH 7.0 (blank) (red line), 400 mg L <sup>-1</sup> AGP in phosphate buffer (control) (blue line) and 400 mgL <sup>-1</sup> AGP-Os(VI) in phosphate buffer (blackline). Conditions: start potential -1.4 V, end potential +0.1 V, step potential 5 mV, amplitude 50 mV, frequency 100 Hz, accumulation time 1 min	89
<b>Figure III.2.1.3.</b>	Voltammograms obtained for AGP-Os(VI) (AGP 400 mg L <sup>-1</sup> ) in BR buffer at different pHs; 9 (a), 7 (b), 5 (c), 3 (d) and 2 (e). Peaks 1 and 2 belong to AGP-Os(VI) adduct	91
<b>Figure III.2.1.4.</b>	Voltammograms obtained by AdTSWV of AGP solution labeled and analyzed at concentration 1.6 mg L <sup>-1</sup> . Conditions: BR buffer pH 3, start potential -1.4 V, end potential +0.1 V, step potential 5 mV, amplitude 50 mV, frequency 100 Hz, accumulation time 5 min. Peak 2 belongs to AGP-Os(VI) adduct	92

### Supporting Information

<b>Figure III.2.1.S1.</b>	MALDI-TOF mass spectra of unlabeled AGP (red line) and AGP-Os(VI) adduct (blue line)	97
---------------------------	--	----

---

**III.2.2. Article 2: Disposable carbon nanotube scaffold films for fast and reliable assessment of  $\alpha_1$ -acid glycoprotein in human serum using adsorptive transfer stripping square wave voltammetry**

<b>Figure III.2.2.1.</b>	(A) AGP labeling with Os(VI) complex. (B) Voltammograms obtained by AdTSWV using SPCE for 0.2 M BR buffer at pH 3.0 (blank) (lower black line), 400 mg L <sup>-1</sup> AGP in BR buffer (control) (upper black line) and 400 mg L <sup>-1</sup> AGP-Os(VI) in BR buffer (red line). Conditions: start potential - 1.4 V, end potential + 0.1 V, step potential 5 mV, amplitude 50 mV, frequency 100 Hz	110
<b>Figure III.2.2.2.</b>	(A) CNSF for sensing of AGP-Os(VI). (B) Voltammograms obtained for AGP-Os(VI) (AGP 10 mg L <sup>-1</sup> ) in BR buffer pH 3.0. SWSFs (blue line), SPCEs (red line), and MWSFs (black line)	111
<b>Figure III.2.2.3.</b>	Nyquist plots corresponding to SWSF (blue color), MWSF (black color), and SPCE (red color). Frequencies ranged from 100,000 to 0.01 Hz using 5 mM K <sub>4</sub> Fe(CN) <sub>6</sub> /K <sub>3</sub> Fe(CN) <sub>6</sub> in 0.1 M KCl electrolyte as redox probe	112
<b>Figure III.2.2.4.</b>	Peak 1 area variation for three consecutive measurements by AdTSWV using MWSFs (black) and SPCEs (red)	113

**Supporting Information**

<b>Figure III.2.2. S1.</b>	XPS spectra of the C <sub>1s</sub> corresponding to the working electrodes (SPE, MWSFE and SWSFE) together with fit composed of chemically shifted components associated to different C chemical bonding, respectively. XPS spectra were normalized to maximum intensity peak in each case for better visual inspection and direct comparison between the samples in order to emphasize subtle line-shape differences, and quantify its contribution for each C environment	117
----------------------------	---	-----

**III.2.3. Article 3: Electrochemical sensor for the assessment of carbohydrate deficient transferrin: application to diagnosis of congenital disorders of glycosylation**

<b>Figure III.2.3.1.</b>	Different isoforms of transferrin depending the number of sialic acids present in the glycoprotein. Asialo-Tf with any sialic acids; diasialo-Tf with two sialic acids; trisialo-Tf with three sialic acids; tetrasialo-Tf with four sialic acids; pentasialo-Tf with five sialic acids; and hexasialo-Tf with six sialic acids	125
<b>Scheme III.2.3.1.</b>	Strategy to measure the level of CDT by using EIG. Firstly, Tf is labelled with the electrochemical tag (Os(VI) complex) and then it is isolated by immunomagnetic beads. Finally, EIG is measured on a SPCE by AdTSWV	128
<b>Figure III.2.3.2.</b>	Voltammograms obtained by AdTSWV of BR buffer at pH 3.0 (blank) (black line), 3800 mg L <sup>-1</sup> Tf (control) (blue line) and 3800 mg L <sup>-1</sup> Tf-Os(VI) TEMED (red line). Peak 1: Tf-Os(VI). Peak 2: amino acids residues. Conditions: BR buffer at pH 3.0, start potential -1.3 V, end potential +1.2 V, step potential 5 mV, amplitude 50 mV, frequency 100 Hz. The background signal was subtracted	133
<b>Figure III.2.3.3.</b>	Analytical calibration. (A) Voltammograms of Tf-Os(VI)TEMED from 1000 to 7600 mg L <sup>-1</sup> (the background signal was subtracted). (B) Calibration curve for the peak at -0.9 V. (C) Calibration curve for the peak at +0.8 V	135
<b>Figure III.2.3.4.</b>	Correlation between EIG (using an electrochemical sensor) and %CDT (using CE-UV)	137

**Supporting Information**

<b>Figure III.2.3.S1.</b>	Voltammograms obtained by AdTSWV of 3800 mg L <sup>-1</sup> Tf-Os(VI)TEMED treated with anti-Tf-MBs (red line) and with protein G-MBs without anti-transferrin (black line). Control using only anti-Tf-MBs (green line)	141
<b>Figure III.2.3.S2.</b>	Voltammograms obtained by AdTSWV after immunopurification with anti-Tf-MBs for: 3800 mg L <sup>-1</sup> Tf-Os(VI)TEMED (red line), 1000 mg L <sup>-1</sup> AGP-Os(VI)TEMED (black line), 3800 mg L <sup>-1</sup> Tf-Os(VI)TEMED and 400 mg L <sup>-1</sup> AGP-Os(VI)TEMED (green line) and 3800 mg L <sup>-1</sup> Tf Os(VI)TEMED and 1000 mg L <sup>-1</sup> AGP-Os(VI)TEMED (blue line)	141
<b>Figure III.2.3.S3.</b>	Analytical calibration for native Tf (without Os(VI) complex). (A) Voltammograms of native Tf from 1900 to 7600 mg L <sup>-1</sup> . (B) Calibration curve for the peak at +0.8 V	142
<b>Figure III.2.3.S4.</b>	Electropherograms obtained by CE-UV of Tf treated with PNGase enzyme at different times. Peak 1: tetrasialo-Tf. Peak 2: low glycosylated-Tf	142

<b>Figure III.2.3.S5.</b>	Voltammograms obtained by AdTSWV in different samples: control serum (red line), CDG sample 1 (green line) and CDG sample 2 (blue line). BR buffer at pH 3.0 (blank) (black line)	143
---------------------------	---	-----

## Chapter IV

<b>Figure IV.1.1.</b>	Design and the dimensions of the simple cross microchip used in this Thesis. The chip holder contained the reservoirs for sample (SR), sample waste (SW) and running buffer (RB), and the electrochemical detection cell (ED).	152
<b>Figure IV.1.2.</b>	The most electrode alignments used with ME-EC. (a) End-channel detection. (b) In-channel detection. (c) Off-channel detection	154
<b>Figure IV.1.3.</b>	Common configurations of electrochemical detectors for ME depending on the position of the working electrode relative to the flow direction: (A) flow by (using 2 plates); (B) flow onto (with the surface normal to the flow direction); (C) flow through (with the detector placed directly on the channel exit)	155

### IV.2.1. Article 4: Determination of glycoproteins by microchip electrophoresis using Os(VI)-based selective electrochemical tag

<b>Figure IV.2.1.1.</b>	(A) Scheme of electrochemical glycoprotein labeling with Os(VI) complex. (B) ME microchip layout used (SR, sample reservoir; RB, running buffer reservoir; SW, sample waste reservoir; ED, end-channel electrochemical detection)	167
<b>Figure IV.2.1.2.</b>	MALDI-TOF mass spectra of Tf-Os(VI) adduct (blue line) and intact Tf (red line)	168
<b>Figure IV.2.1.3.</b>	Cyclic voltammograms of glycoprotein-Os(VI) adducts and intact glycoproteins. (A) Tf-Os(VI) adduct (black line) and intact Tf (red line). (B) AGP-Os(VI) adduct (black line) and intact AGP (red line). Conditions: buffer Britton-Robinson at pH 3.0, scan rate 1 V/s. All concentrations are 400 mg L <sup>-1</sup>	169
<b>Figure IV.2.1.4.</b>	Hydrodynamic voltammograms of glycoprotein-Os(VI) adducts and intact glycoproteins. Hydrodynamic voltammograms were performed in 25 mM sodium tetraborate, pH 9.2; separation voltage +3.00 kV; injection voltage = +3.00 kV for 20.0 s. (A) 7600 mg L <sup>-1</sup> Tf-Os(VI) adduct (black line) and 7600 mg L <sup>-1</sup> intact Tf (red line). (B) 4000 mg L <sup>-1</sup> AGP-Os(VI) adduct (black line) and 4000 mg L <sup>-1</sup> intact AGP (red line)	169
<b>Figure IV.2.1.5.</b>	Cyclic voltammograms of 30.3 mM Os(VI) complex (green line), 4000 mg L <sup>-1</sup> glucose-Os(VI) adduct (black line), 4000 mg L <sup>-1</sup> glucose (red line), and 50 mM sodium phosphate buffer, pH 7.0 (blue line)	171

- Figure IV.2.1.6.** ME-ED detection of Tf (peak 1) and AGP (peak 2) at **(A)** +1.0 V and **(B)** +0.50 V. Protein-Os(VI) adducts (black line) and intact proteins (red line). Conditions: as in Figure 4. Tf: 7600 mg L<sup>-1</sup>. AGP: 4000 mg L<sup>-1</sup> 172
- Figure IV.2.1.7.** Microchip electrochemical detection of AGP and Tf in a human serum certified reference material at +0.50 V (black line) and at +1.0 V (red line) 174

## Chapter V

- Figure V.1.1.** **(A)** A typical two-dimensional (2D)  $\mu$ PAD **(B)** A typical three-dimensional (3D)  $\mu$ PAD 183
- Figure V.1.2.** Fabrication technologies of paper-based electrochemical devices. **(A)** Screen printing. Three-electrode system was screen printed on the detection zone of paper substrate using carbon ink. **(B)** Inkjet printing. Mixing of carbon nanotube ink in deionized water, followed by inkjet printing the carbon nanotube ink. **(C)** Writing. Three-electrode system was drawn on the working zone using a commercial graphite pencil 185
- Figure V.1.3.** **(A)** Three types of the Y-shaped device generating **(i)** non mixing, **(ii)** a concentration gradient, **(iii)** fully mixing concentration profile. **(B)** Different geometries of the middle transparency layers 187
- Figure V.1.4.** Schematics of the passive device fabricated by lamination of double-sided adhesive (DSA) and transparency film. **(A)** In this case consist in Y-shape device with two inlet channels placed in the different vertical positions. **(B)** Channel geometries of the Y-shape device defined on each layer 188

### V.2.1. Article 5: Pump-free microfluidic device for the electrochemical detection of $\alpha_1$ -acid glycoprotein

- Figure V.2.1.1.** Schematic representation of the capillary-driven microfluidics analytical device. **(A)** The geometry of double-sided adhesives and transparency films: layers 1, 4, 6, and 9 consist of transparency film (dark grey) while layers 2, 3, 5, 7, and 8 are made of double-sided adhesive (light grey). **(B)** Assembled mixing device with the integrated electrochemical detector: working electrode (WE), reference electrode (RE), and counter electrode (CE). **(C)** Image of the microfluidics analytical device 200

<b>Figure V.2.1.2.</b>	Sequential images showing the moments of: <b>(a)</b> water (wash solution) injection, <b>(b)</b> the injected first reagent (blue dye) flows first and stops at the valve, <b>(c)</b> the injected second reagent (yellow dye) arrives and opens the valve, allowing the two solutions to mix to produce green color in the main channel, <b>(d)</b> flow stops until the rectangular-shaped paper is inserted to the outlet of the main channel, <b>(e)</b> flow starts when the rectangular-shaped paper is inserted to the outlet, and <b>(f)</b> blue dye from the top reservoir arrives at the main channel	204
<b>Figure V.2.1.3.</b>	<b>(A)</b> Voltammograms obtained by SWV using 1 mM FcTMA <sup>+</sup> in 50 mM phosphate buffer at pH 7. DWE (blue line), TPE (red line) and GPE (black line). Conditions: start potential – 0.2 V, end potential + 1.0 V, step potential 5 mV, amplitude 50 mV, frequency 5 Hz. <b>(B)</b> Voltammograms obtained for AGP-Os(VI) (2000 mg L <sup>-1</sup> ) in BR buffer pH 3.0 by AdTSWV. DWE (blue line), TPE (red line) and GPE (black line). SWV parameters: start potential – 1.5 V, end potential + 0.0 V, step potential 5 mV, amplitude 50 mV, and frequency 2 Hz (electrochemical signals were baseline corrected and smoothed out)	205
<b>Figure V.2.1.4.</b>	<b>(A)</b> Schematic of mixing device with the integrated electrochemical detector. H <sub>2</sub> O, BR, AGP, and Os represents inlets for water, BR buffer, AGP and Os(VI) complex, respectively <b>(B)</b> Voltammograms obtained using AdTSWV with 30 min incubation time for 0.2 M BR buffer at pH 3.0 (blank) (green line), 15.15 mM Os(VI) complex (control) (red line), 2000 mg L <sup>-1</sup> AGP (control) (blue line), and 2000 mg L <sup>-1</sup> AGP-Os(VI) (black line)	207
<b>Figure V.2.1.5.</b>	<b>(A)</b> Voltammograms corresponding to AGP at different concentrations using the pump-free microfluidics device (electrochemical signals were baseline corrected and smoothed out). <b>(B)</b> Calibration curve (n = 3)	209

## Supporting Information

<b>Figure V.2.1.S1.</b>	Voltammograms of 2000 mgL <sup>-1</sup> AGP-Os(VI) by AdTSWV using different incubation times. Green line: 0 min; red line: 10 min; blue line: 20 min and black line: 30 min. SWV parameters: start potential – 1.5 V, end potential + 0.0 V, step potential 5 mV, amplitude 50 mV, and frequency 2 Hz (electrochemical signals were baseline corrected and smoothed out)	212
<b>Figure V.2.1.S2.</b>	Voltammograms of <b>(A)</b> 2000 mgL <sup>-1</sup> AGP-Os(VI) and <b>(B)</b> 500 mgL <sup>-1</sup> of AGP-Os(VI) by AdTSWV obtained from 3 days measurements (3 electrodes per day, n = 9). Green line: 3 measurements day 1; red line: 3 measurements day 2; and black line: 3 measurements day 3 (electrochemical signals were baseline corrected and smoothed out).	212

**V.2.2. Article 6: Low-cost and passive electrochemical microfluidic device for diagnosis of congenital disorders of glycosylation**

- Figure V.2.2.1.** Fabrication scheme of electrodes using screen printing technology. Three-electrode system was screen printed on the detection zone of transparency film substrate (6<sup>th</sup> layer) using carbon ink for working electrode (WE) and counter electrode (CE); and Ag/AgCl paste for reference electrode (RE) 224
- Figure V.2.2.2.** Schematics of the microfluidics device. (A) The microfluidics electrochemical device consisted of four inlet channels, one main channel, a valve and three electrodes (detection zone). (B) Channels are placed in different vertical positions, as shown in the cross-sectional view of [1-1'], [2-2'], [3-3'] and [4-4']. (C) Channel geometries of the microfluidics device defined on each layer. 1, 4, 6 and 9 consist of transparency film (light grey) while layers 2, 3, 5, 7 and 8 are made of double-sided adhesive (dark grey) 226
- Figure V.2.2.3.** (A) Sequential steps showing the moments of: (a) water injecting, (b) Tf flows first and stops at the valve, (c) Os(VI) complex arrives and valve release and producing the mix in the main channel, (d) (e) flow starts when rectangular-shaped paper was put in outlet part, and (f) BR buffer arrive at the main channel. (B) Voltammograms obtained using AdTSWV with 60 min incubation time for 0.2 M BR buffer at pH 3.0 (blank) (black line), 7.58 mM Os(VI) complex (control) (green line), 9.4 mg mL<sup>-1</sup> Tf (blue line) and 9.4 mg mL<sup>-1</sup> Tf-Os(VI) (red line). Peak 1: Tf-Os(VI). Peak 2: amino acids residues. SWV parameters: start potential -1.2 V, end potential +1.2 V, step potential 5 mV, amplitude 50 mV, and frequency 100 Hz (the background signal was linearized). 229
- Figure V.2.2.4.** (A) Voltammograms corresponding to Tf-Os(VI) at different concentrations using the pump-free microfluidics device (the background signal was linearized). (B) Calibration curve of peak at -0.9 V. (C) Calibration curve of peak at +0.8 V 231
- Figure V.2.2.5.** Voltammograms obtained by AdTSWV in different samples using the pump-free microfluidics device (the background signal was linearized): BR buffer at pH 3.0 (blank) (dot line), CDG sample (red line) and control serum (black line). 233

---

**Supporting Information**

- Figure V.2.2.S1.** Voltammograms of  $9.4 \text{ mg mL}^{-1}$  Tf-Os(VI) by AdTSWV using different incubation times. **(a)** 5 min; **(b)** 10 min; **(c)** 20 min; **(d)** 40 min; **(e)** 60 min; **(f)** 90 min; **(g)** 120 min. SWV parameters: start potential  $-1.2 \text{ V}$ , end potential  $+1.2 \text{ V}$ , step potential  $5 \text{ mV}$ , amplitude  $50 \text{ mV}$ , and frequency  $100 \text{ Hz}$  (the background signal was linearized) 236
- Figure V.2.2.S2.** **(A)** Voltammograms obtained by AdTSWV with 60 min incubation time for  $0.2 \text{ M}$  BR buffer at pH 3.0 (blank) (black line), antiTf-MB-Os(VI) (control) (blue line) and  $9.4 \text{ mg mL}^{-1}$  Tf-antiTf-MB-Os(VI) (red line) (the background signal was linearized). **(B)** The microfluidics analytical device with antiTf-MBs deposited on the reservoir and main channel bottom (no magnet) 236



## List of tables

### Chapter II

<b>Table II.1.1.</b>	Examples of glycosylation studies for various clinically relevant biological fluids	18
<b>Table II.1.2.</b>	Human inflammatory glycoproteins modified during an acute phase response	20
<b>Table II.2.1.</b>	Nitrogenous ligands (L) applied in Os(VI)L complexes	42
<b>Table II.2.2.</b>	Comparison of laboratory-based blood testing and point-of-care system	47
<b>Table II.2.3.</b>	Advantages and disadvantages of point-of-care testing	49

### Chapter III

#### **III.2.1. Article 1: Total $\alpha_1$ -acid glycoprotein determination in serum samples using disposable screen-printed electrodes and osmium (VI) as electrochemical tag**

<b>Table III.2.1.1.</b>	Comparison between cleaning methodologies in serum samples	94
-------------------------	--	----

#### **III.2.2. Article 2: Disposable carbon nanotube scaffold films for fast and reliable assessment of $\alpha_1$ -acid glycoprotein in human serum using adsorptive transfer stripping square wave voltammetry**

<b>Table III.2.2.1.</b>	Relative percentage of peak areas for each type of atomic bonding obtained by XPS C1s analysis of the studied electrodes	113
<b>Table III.2.2.2.</b>	Determination of AGP in serum sample using MWSFs	115

**III.2.3. Article 3: Electrochemical sensor for the assessment of carbohydrate deficient transferrin: application to diagnosis of congenital disorders of glycosylation**

<b>Table III.2.3.1.</b>	Signals obtained for 3800 mg L <sup>-1</sup> Tf Os(VI) treated with PNGase at different times and their corresponding EIG values (n=3)	136
<b>Table III.2.3.2.</b>	Comparison between control sample and CDG samples	138

## Chapter IV

**IV.2.1. Article 4: Determination of glycoproteins by microchip electrophoresis using Os(VI)-based selective electrochemical tag**

<b>Table IV.2.1.1.</b>	Analytical features of the ME-ED approach for glycoproteins determination	172
<b>Table IV.2.1.2.</b>	Reproducibility of the method in different days (n=3)	173
<b>Table IV.2.1.3.</b>	Analysis of a human serum certified reference material (CRM) (n=3)	173

## Chapter V

**V.2.1. Article 5: Pump-free microfluidic device for the electrochemical detection of  $\alpha_1$ -acid glycoprotein**

<b>Table V.2.1.1.</b>	Study of recoveries using a serum sample (n=3)	210
-----------------------	--	-----

**V.2.2. Article 6: Low-cost and passive electrochemical microfluidic device for diagnosis of congenital disorders of glycosylation**

<b>Table V.2.2.1.</b>	Comparison between EIG values obtained in control sample and CDG sample (n=3)	233
-----------------------	---	-----



# CHAPTER VIII

**Publications,  
patents, and  
conferences**



## VIII. Publications, patents, and conferences

### International publications

- 1. T. Sierra**, A.G. Crevillen, A. Escarpa. Derivatization agents for electrochemical detection in amino acid, peptide, and protein separations: The hidden electrochemistry (Review). *Electrophoresis*, 38 (2017), 2695-2703, DOI: 10.1002/elps.201700167 (**In Chapter II**).
- 2. T. Sierra**, M.C. González, B. Moreno, A.G. Crevillen, A. Escarpa. Total  $\alpha$ 1-acid glycoprotein determination in serum samples using disposable screen-printed electrodes and osmium (VI) as electrochemical tag. *Talanta*, 180 (2018), 206-210, DOI: 10.1016/j.talanta.2017.12.018 (**In Chapter III.2.1**).
- 3. T. Sierra**, A.G. Crevillen, A. Escarpa. Electrochemical detection based on nanomaterials in CE and microfluidic systems (Review). *Electrophoresis*, 40 (2019), 113-123, DOI: 10.1002/elps.201800281 (**In Chapter II**).
- 4. T. Sierra**, S. Dorte, M.C. González, F.J. Palomares, A.G. Crevillén, A. Escarpa. Disposable carbon nanotube scaffold films for fast and reliable assesment of total  $\alpha$ 1-acid glycoprotein in human serum using adsorptive transfer stripping square wave voltammetry. *Analytical and Bioanalytical Chemistry*, 411 (2019), 1887-1894, DOI: 10.1007/s00216-018-1419-6 (**In Chapter III.2.2**).
- 5. T. Sierra**, A.G. Crevillén, A. Escarpa. Determination of Glycoproteins by Microchip Electrophoresis Using Os(VI)-Based Selective Electrochemical Tag. *Analytical Chemistry*, 91 (2019), 10245-10250 DOI: 10.1021/acs.analchem.9b02375 (**In Chapter IV.2.1**).
- 6. A.S. Lorenzetti, T. Sierra**, C.E. Domini, A.G. Lista, A. González-Crevillén, A. Escarpa. Electrochemically Reduced Graphene Oxide-Based Screen-Printed Electrodes for Total Tetracycline Determination by Adsorptive Transfer Stripping Differential Pulse Voltammetry. *Sensors*, 20 (2020). DOI: doi:10.3390/s20010076

7. S. Dorte, **T. Sierra**, A.G. Crevillén, A. Escarpa. CE/microchip electrophoresis of Carbohydrates and Glycoconjugates with Electrochemical Detection. (Book Chapter) Ed. Elsevier (**2021**).

8. **T. Sierra**, S. Dorte, A.G. Crevillén, A. Escarpa. Food Analysis by Microchip Electrophoresis. (Book Chapter) Ed. Bentham Science, Singapur (**2021**).

9. **T. Sierra**, A.G. Crevillén, A. Escarpa. Electrochemical sensor for the assessment of carbohydrate deficient transferrin: application to diagnosis of congenital disorders of glycosilation. Biosensors and Bioelectronics, 179 (**2021**), 113098 DOI: 10.1016/j.bios.2021.113098 (**In Chapter III.2.3**).

10. **T. Sierra**, I. Jang, E. Noviana, A.G. Crevillén, A. Escarpa, C.S. Henry. Pump-free microfluidic device for the electrochemical detection of  $\alpha_1$ - acid glycoprotein. ACS Sensors, (**2021**), (**In Chapter V.2.1**).

11. **T. Sierra**, C.S. Henry, A.G. Crevillén, A. Escarpa. Low-cost and passive electrochemical microfluidic device for diagnosis of congenital disorders of glycosylation. (**2021**), (**In Chapter V.2.2**).

## Patents

1. Inventors: **T. Sierra**, A.G. Crevillen, A. Escarpa. Title: Procedimiento para determinar el grado de glicosilación de la transferrina y equipo electroquímico para llevar a cabo dicho procedimiento. Reference: 202030806 Universidad de Alcalá, Spain.

## Poster presentations

1. **T. Sierra**, M. C. González, A. G. Crevillén, A. Escarpa. Filtered multi-walled carbon nanotubesbased electrodes for total  $\alpha$ 1–acid glycoprotein determination in serum samples. NanoSpain 2018, Bilbao, Spain, 2018.

## Oral communications

1. A. G. Crevillén, **T. Sierra**, A. Escarpa. Determination of glycoproteins by microchip electrophoresis with electrochemical detection. 25th Latin-American Symposium on Biotechnology, Biomedical, Biopharmaceutical and Industrial Applications of Capillary Electrophoresis and Microchip Technology. Alcalá de Henares, Spain, 2019.





